



**Biochemical Characterisation of the *Escherichia coli*
Haemolysin A Type I Secretion System**

Inaugural-Dissertation

zur Erlangung des Doktorgrades
der Mathematisch-Naturwissenschaftlichen Fakultät der
Heinrich Heine Universität Düsseldorf

vorgelegt von
Kerstin Kanonenberg
aus Köln

Düsseldorf, Oktober 2018

aus dem Institut für Biochemie
der Heinrich Heine Universität Düsseldorf

Gedruckt mit der Genehmigung der
Mathematisch-Naturwissenschaftlichen Fakultät der
Heinrich Heine Universität Düsseldorf

Berichterstatter:

1. Prof. Dr. Lutz Schmitt

2. Prof. Dr. Andreas P. M. Weber

Tag der mündlichen Prüfung: 19.11.2018

„[...] Daneben aber gibt es auch das Häuflein derer, die frühzeitig erkennen, dass die schönsten Dinge, die ein Mensch erleben kann, nicht von außen kommen, sondern an die Entwicklung der Fähigkeiten des eigenen Fühlens, Denkens und Gestaltens geknüpft sind. Alle wirklichen Künstler, Forscher und Denker waren von dieser Art. So unscheinbar das Leben dieser Art Menschen zunächst verläuft, so sind doch die Früchte ihres Strebens das Wertvollste, was eine Generation den späteren Generationen zu geben hat. [...]“

Albert Einstein (1879 - 1955), aus dem Nachruf
auf Emmy Noether (1882 – 1935)

Abstract

Type I secretion systems (T1SS) are ubiquitous transport machineries in Gram-negative bacteria. The translocon is of a relatively simple assembly and comprises an ABC transporter, a membrane fusion protein (MFP) and a TolC-like outer membrane porin (OMP). While the ABC transporter and the MFP likely form a constantly assembled complex in the inner membrane, the OMP is only recruited upon substrate recognition in the cytosol. The assembled complex mediates the secretion of its dedicated substrate in one step, without periplasmic intermediate, C-terminus first, across both membranes to the extracellular space.

The substrates of T1SS are of remarkable variability in terms of size and function, ranging from 5 to more than 800 kDa and display functions as bacteriocins, haemolytic exotoxins, proteases, lipases, iron scavenger proteins or adhesins. Different types of accessory domains on the transporter subunits and accessory domains within the operons are involved in mediating the secretion process.

In this thesis, the haemolysin A T1SS from *Escherichia coli* was studied. The ABC transporter subunit HlyB, which comprises a C39 peptidase-like domain at its N-terminus, was purified, reconstituted in saposin-A nanoparticles and functionally characterised in a detergent-free environment. These studies revealed a strong influence of free detergent micelles on the functional properties of the ABC transporter.

Furthermore, the overexpression by fed-batch fermentation of the assembled inner membrane complex, the ABC transporter HlyB and the MFP HlyD, and its subsequent purification were established. Initial structural studies were performed by negative-stain electron microscopy. To reduce impurities and to overall facilitate the overexpression of membrane proteins the new expression strain C41(DE3) $\Delta ompF\Delta acrAB$ was developed. The strain was found to increase yield, purity and stability of integral membrane proteins and provided protection from degradation.

Finally, this thesis was completed by bioinformatic studies that aimed at classifying the different T1SS and identifying conserved secretion motifs in the substrates. An initial study was solely based on the accessory domains of the cognate ABC transporters and was later on extended to include also operon organisation, potential secretion signals and accessory proteins. This resulted in overall five different classes of T1SS and a conserved motif was identified in the C-termini of RTX toxins.

Zusammenfassung

Typ I Sekretionssysteme (T1SS) sind in Gram-negativen Bakterien allgegenwärtige Transportmaschinerien. Das Translokon ist von relativ simpler Bauweise und besteht aus einem ABC Transporter, einem Membranfusionsprotein (MFP) und einem TolC-artigen Porin in der äußeren Membran (OMP). Während der ABC Transporter und das MFP wahrscheinlich einen konstant assemblierten Komplex in der inneren Membran bilden, wird das OMP nur nach Interaktion mit dem Substrat im Cytosol rekrutiert. Der assemblierte Komplex sekretiert sein dediziertes Substrat in einem Schritt und ohne periplasmatische Intermediate, mit dem C-Terminus voran, über beide Membranen in den extrazellulären Raum.

Die Substrate von T1SS sind von bemerkenswerter Variabilität bezüglich ihrer Größe und Funktion. Sie haben eine Größe von 5 bis über 800 kDa und beinhalten Bakteriocine, hämolytische Exotoxine, Proteasen, Lipasen, Hämophore oder Adhesine. Verschiedene zusätzliche Domänen an den Transporter-Untereinheiten und zusätzliche Proteine in den Operons sind im Sekretionsprozess involviert.

In der vorliegenden Arbeit wurde das Hämolysin A T1SS aus *Escherichia coli* untersucht. Die ABC Transporter-Untereinheit HlyB, die eine C39 Peptidase-ähnliche Domäne (CLD) an ihrem N-Terminus beinhaltet, wurde gereinigt, in Saposin-A Nanopartikel rekonstituiert und in einer detergentfreien Umgebung funktionell charakterisiert. Diese Studien zeigten einen starken Einfluss von freien Detergenzmizellen auf die funktionellen Eigenschaften des ABC Transporters.

Weiterhin wurde die Überexpression des assemblierten inneren Membrankomplexes, bestehend aus dem ABC Transporter HlyB und des MFPs HlyD, mithilfe eines Zulaufprozesses im Bioreaktor sowie die nachfolgende Reinigung etabliert. Initiale Strukturstudien wurden mittels Negativfärbung-Elektronenmikroskopie durchgeführt. Um Verunreinigungen zu reduzieren und insgesamt die Überexpression von Membranproteinen zu vereinfachen, wurde der neue Expressionsstamm C41(DE3) $\Delta ompF\Delta acrAB$ entwickelt. Der Stamm zeigte einen höheren Ertrag und verbesserte Reinheit und Stabilität von integralen Membranproteinen und verhinderte deren Abbau.

Abschließend wurde die Dissertation mit bioinformatischen Studien komplettiert, die zum Ziel hatten, die verschiedenen T1SS zu klassifizieren und konservierte Sekretionsmotive in den Substraten zu identifizieren. Eine initiale Studie beschränkte sich hierbei auf die

zusätzlichen Domänen der ABC Transporter, die später erweitert wurde, um auch Operonaufbau, potenzielle Sekretionssignale und zusätzliche Proteine zu berücksichtigen. Dies ergab insgesamt fünf verschiedene Klassen von T1SS und ein konserviertes Motiv wurde in den C-Termini von RTX Toxinen identifiziert.

Table of Contents

ABSTRACT	IV
ZUSAMMENFASSUNG	V
LIST OF FIGURES.....	IX
LIST OF TABLES	X
LIST OF ABBREVIATIONS	XI
1. INTRODUCTION.....	1
1.1 THE IMPORTANCE OF MEMBRANES	1
1.2 TRANSPORT ACROSS MEMBRANES.....	1
1.2.1 ABC Transporters	2
1.3 MECHANISMS OF TRANSPORT OF ABC TRANSPORTERS	4
1.3.1 The Switch Model.....	5
1.3.2 The Constant Contact Model.....	6
1.4 BACTERIAL SECRETION SYSTEMS	7
1.4.1 Secretion into a Target Cell without Periplasmic Intermediates	8
1.4.2 Secretion to the Extracellular Space without Periplasmic Intermediates.....	9
1.5 TYPE I SECRETION SYSTEMS.....	9
1.5.1 Substrates of Type I Secretion Systems	10
1.5.2 ABC Transporters of Type I Secretion Systems	11
1.5.3 Membrane Fusion Proteins of Type I Secretion Systems	12
1.5.4 The Outer Membrane Porin of Type I Secretion Systems	14
1.6 THE HAEMOLYSIN A TYPE I SECRETION SYSTEM FROM <i>ESCHERICHIA COLI</i>	15
1.6.1 Structural Studies and Assembly of the HlyA-Type I Secretion System.....	16
1.6.2 The ABC Transporter HlyB	17
1.6.3 The Membrane Fusion Protein HlyD	18
1.6.4 Functional studies of the HlyA-T1SS.....	18
2. AIMS	20
3. PUBLICATIONS	21
3.1 CHAPTER I – CLASSIFICATION OF ABC TRANSPORTERS OF TYPE I SECRETION SYSTEMS	21
3.2 CHAPTER II – MECHANISTIC VARIABILITY OF TYPE I SECRETION SYSTEMS.....	31
3.3 CHAPTER III – TYPE I SECRETION SYSTEMS – RECENT FINDINGS.....	78
3.4 CHAPTER IV – FUNCTIONAL CHARACTERISATION OF RECONSTITUTED HLYB	89
3.5 CHAPTER V – A NEW EXPRESSION STRAIN FOR MEMBRANE PROTEINS.....	119

3.6 CHAPTER VI – IDENTIFYING A SECRETION SIGNAL IN RTX TOXINS.....	149
3.7 CHAPTER VII – STUDYING THE ASSEMBLED INNER MEMBRANE COMPLEX OF THE HLYA-T1SS .	167
4. DISCUSSION	187
4.1 BACTERIOCIN-SECRETING T1SS	188
4.1.1 <i>The Bacteriocin-T1SS ABC Transporter</i>	<i>190</i>
4.1.2 <i>The Substrates of Bacteriocin-T1SS</i>	<i>190</i>
4.2 LARGE RTX TOXIN-T1SS	191
4.2.1 <i>The Substrates of Large RTX Toxin-T1SS.....</i>	<i>192</i>
4.2.2 <i>ABC Transporters of Large RTX Toxin-T1SS.....</i>	<i>193</i>
4.2.3 <i>Large RTX Toxin-T1SS Membrane Fusion Proteins.....</i>	<i>193</i>
4.3 SMALL RTX PROTEIN-T1SS	195
4.3.1 <i>The Small RTX Protein Substrates – Serralysins, Proteases.....</i>	<i>197</i>
4.3.2 <i>The Small RTX Protein Substrates – Haemophores.....</i>	<i>197</i>
4.3.3 <i>The Small RTX Protein Substrates – Lipases</i>	<i>198</i>
4.3.4 <i>The Small RTX Protein Substrates – Surface Layer Proteins.....</i>	<i>198</i>
4.3.5 <i>The Small RTX Protein Substrates – Haem Peroxidases.....</i>	<i>198</i>
4.4 “LAPA-LIKE” T1SS.....	198
4.4.1 <i>The LapA-like T1SS ABC Transporter</i>	<i>200</i>
4.5 SII-E-LIKE T1SS	201
4.6 SUMMARY	202
4.7 EXCEPTIONS AND “INCOMPLETE” OPERONS.....	205
4.8 CHARACTERISATION OF THE HAEMOLYSIN A T1SS FROM <i>ESCHERICHIA COLI</i>	205
4.8.1 <i>Improving Membrane Protein Overexpression by Modifying the Membrane Environment</i>	<i>206</i>
4.8.2 <i>Functional Reconstitution of HlyB and the Detrimental Effects of Free Detergent Micelles.....</i>	<i>208</i>
4.8.3 <i>Studying the Assembled Inner Membrane Complex</i>	<i>210</i>
5. REFERENCES.....	211
5. CURRICULUM VITAE	224
6. ACKNOWLEDGEMENTS.....	227
7. DECLARATION	231

List of Figures

Figure 1: Mechanisms of membrane transport.....	2
Figure 2: Schematic representation of an ABC transporter (exporter) and the (simplified) allosteric access model	3
Figure 3: Schematic representation of the switch model	6
Figure 4: Schematic representation of the constant contact model	7
Figure 5: Overview of the different secretion systems and their components without a periplasmic transport intermediate in Gram-negative bacteria	8
Figure 6: Three-dimensional structures of two ABC transporters.....	12
Figure 7: Structural build of a T1SS-MFP.....	13
Figure 8: Crystal structure of the OMP TolC from <i>E. coli</i>	15
Figure 9: Summary of the HlyA-T1SS.....	16
Figure 10: Homology model of HlyB.....	17
Figure 11: Schematic overview of the coding regions of class II microcin-secreting T1SS	190
Figure 12: Alignment of the N-termini of selected T1SS-secreted bacteriocins.....	191
Figure 13: Variable operon organisation of Large RTX toxin-T1SS.....	192
Figure 14: Alignment of the N-terminal domain of MFPs from RTX-toxin T1SS.....	194
Figure 15: Possible operon organisations of “serralyisin-like” T1SS.....	195
Figure 16: Alignment of the C-terminal 100 amino acids of small RTX proteins	196
Figure 17: Operon organisation of LapA-like T1SS	199
Figure 18: Homology models of a LapB-like CLD.....	200
Figure 19: Operon organisation of SiiE-like operons.....	201
Figure 20: Sequence alignment of HlyB-CLD and SiiF-like CLD	201
Figure 21: Structural alignment of a SiiF-like CLD	202
Figure 22: Crystal Structures of AcrB and OmpF.....	207
Figure 23: Overexpression of ABC transporters in C43(DE3) $\Delta ompF\Delta acrAB$	208
Figure 24: Room occupancy of lysolipids and lipids.	209

List of Tables

Table 1: Classification of T1SS based on their operons and accessory domains and proteins	
.....	204

List of Abbreviations

Å	Ångstrom
ABC transporter	ATP-binding cassette transporter
ACP	acyl carrier protein
ADP	adenosine-5-diphosphate
ATP	adenosine-5-triphosphate
<i>B. pertussis</i>	<i>Bordetella pertussis</i>
Ca	calcium
CBB	coomassie brilliant blue
CLD	C39 peptidase-like domain
cmc	critical micellar concentration
CyaA	adenylate cyclase toxin-haemolysin
DDM	n-dodecyl- β -D-maltsoside
DNA	deoxyribonucleic acid
EDTA	ethylenediaminetetraacetic acid
<i>E. coli</i>	<i>Escherichia coli</i>
e.g.	exempli gratia
FC-14	fos-choline 14
FC-16	fos-choline 16
GFP	green fluorescent protein
HlyA	haemolysin A
HlyB	haemolysin B
HlyC	haemolysin C
HlyD	haemolysin D
IMAC	immobilised metal affinity chromatography
K _d	dissociation constant
kDa	kilodalton
LMNG	lauryl maltose neopentyl glycol
LPS	lipopolysaccharide
MALS	multi-angle light scattering
MARTX	multifunctional autoprocessing RTX toxins
MFP	membrane fusion protein

mg	milligram
mM	millimolar
NBD	nucleotide binding domain
Ni	nickel
nM	nanomolar
nm	nanometre
NTA	nitrilotriacetic acid
OMP	outer membrane porin
PCC	<i>trans</i> -4-(<i>trans</i> -4'-propylcyclohexyl)- α -D-maltoside
pdb	protein database
PE	phosphatidylethanolamine
PG	phosphatidylglycerol
pmf	proton motive force
proHlyA	preprotein of HlyA
PS	phosphatidylserine
RTX	repeats-in-toxin
Sec	general secretory
SEC	size exclusion chromatography
SDS	sodium dodecyl sulphate
TXSS	type X secretion system
TMD	transmembrane domain
μ M	micromolar

Amino Acid	Three letter code	One letter code
Alanine	Ala	A
Arginine	Arg	R
Asparagine	Asn	N
Aspartic Acid	Asp	D
Cysteine	Cys	C
Glutamic Acid	Glu	E
Glutamine	Gln	Q
Glycine	Gly	G
Histidine	His	H
Isoleucine	Ile	I
Leucine	Leu	L
Lysine	Lys	K
Methionine	Met	M
Phenylalanine	Phe	F
Proline	Pro	P
Serine	Ser	S
Threonine	Thr	T
Tryptophan	Trp	W
Tyrosine	Tyr	Y
Valine	Val	V

1. Introduction

1.1 The Importance of Membranes

Membranes are a universal and key feature of all living organisms on Earth. It is the membrane that defines the three-dimensional space of a cell or an organelle, and separates the cytosol from the extracellular space. Any biochemical process taking place within a cell would not be possible without this defining edge, keeping all cell components within close proximity and ensuring constant chemical conditions. Most biological membranes are composed of lipid bilayers that, due to their amphiphilic nature, are composed of a hydrophobic interior made up of the fatty acid tails of lipid molecules, and a hydrophilic exterior, composed of the lipid molecules' head groups. This build allows the strict separation of a water-filled cytoplasm from a hydrophilic exterior.

Transport across membranes is the key feature in order to ensure a cell's survival and interaction with its environment. As only small and uncharged molecules can pass biological membranes by passive diffusion, nature has evolved a fascinating range of membrane proteins, which are integrated into cellular membranes and tightly control the influx and efflux of any kind of molecule and ion into and out of a cell.

Even though many proteins have been identified so far that are responsible for membrane trafficking, the mechanistic details underlying the transport processes are often not completely understood.

1.2 Transport Across Membranes

Transport processes across biological membranes can be divided into passive and active transport (1-3). Passive transport, also called facilitated diffusion, is the selective passage of molecules via membrane proteins using an electrochemical or concentration gradient and therefore does not require the input of metabolic energy. Proteins facilitating this type of transport are called channels or uniporters. A gating mechanism ensures selectivity, and a regulatory module may also control the opening and closure of the protein.

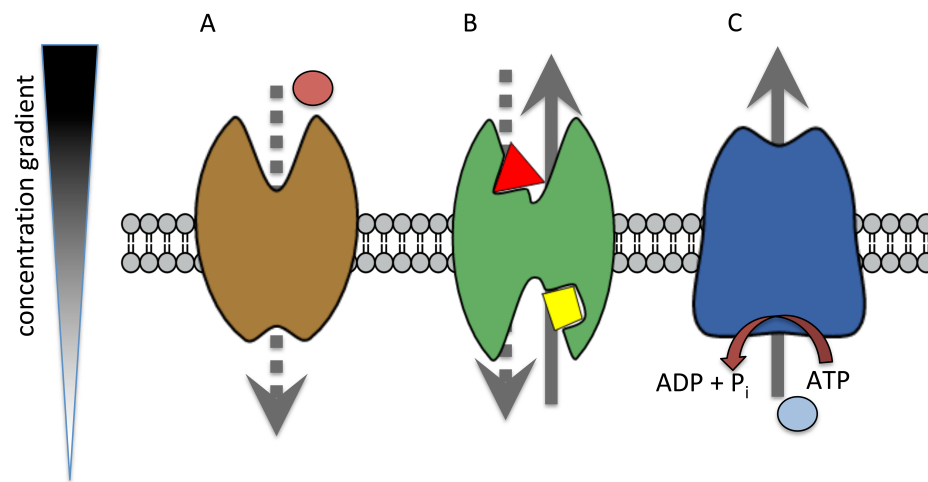


Figure 1: Mechanisms of membrane transport. Dotted lines represent transport down the concentration gradient (no input of metabolic energy); straight lines up the concentration gradient (metabolic energy required). (A) – Facilitated diffusion, (B) – secondary active transport, (C) – primary active transport with for example ATP as the source of energy shown here as an example.

Active transport always requires the input of some sort of energy. Secondary active transporters couple the transport of a substrate to the symport or antiport of a second substrate with its previously established concentration- or electrochemical gradient. Primary active transport, on the other hand, is characterised by actively pumping the substrate across the membrane, usually at the expense of ATP. The different mechanisms of membrane transport are summarised in Figure 1.

The study of membrane proteins has always been of particular difficulty. Due to their embedment into a membrane their extraction is achieved by detergents, which are often harmful to a protein's conformation and can distort their original fold.

1.2.1 ABC Transporters

ABC transporters are primary active pumps that usually (but not exclusively) translocate their substrate across a membrane up a concentration gradient (see Figure 1). ABC transporters can be found in all kingdoms of life and comprise a basically conserved, overall structure, composed of four canonical domains. Two nucleotide-binding domains (NBDs) are responsible for nucleotide binding and hydrolysis, while two transmembrane domains (TMDs) span the lipid bilayer and build up the substrate cavity that is responsible for the

translocation process (Figure 2A) (4). In some cases, ABC transporters may contain additional accessory domains that, for example, modify a substrate prior to or are a prerequisite for transport (5,6).

Despite their overall similar build, the nature of substrates is immensely diverse, ranging from small molecules and ions to peptides and even large proteins. Also, the substrate specificity ranges from narrow, with only one dedicated substrate, to wide, where a whole battery of substrates, structurally very diverse and with no apparent homology, are exported. In eukaryotes, ABC transporters are usually “full-size” transporters, meaning that all functional units are present on one single polypeptide chain, even though their order may vary. Some ABC transporters are so-called “half-size” transporters, where one TMD and one NBD are fused. This organisation allows for the formation of homo- or heterodimeric ABC transporters (4).

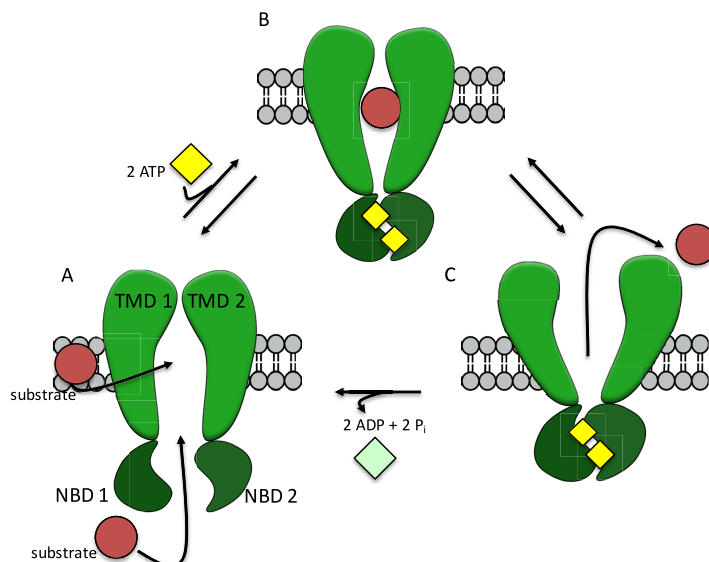


Figure 2: Schematic representation of an ABC transporter (exporter) and the (simplified) allosteric access model (7). TMD – transmembrane domain, NBD – nucleotide binding domain. (A) – inward-open conformation, the substrate enters the cavity either from the membrane or from the cytosol. (B) – occluded state, two ATP molecules are bound to the NBDs and the substrate is trapped in the transmembrane region. (C) – outward-open state, the substrate leaves the cavity. Hydrolysis of two ATPs releases two phosphate molecules and two ADPs and the transporter returns to the inward-open state.

In prokaryotes, ABC transporters reflect a higher variability in domain organisation. Here, no full-size ABC transporters have been reported so far but instead, apart from homo- and heterodimers, also each NBD and TMD can correspond to an individual, non-fused unit (5,8). A well-characterised example is the maltose importer, where MalF and MalG represent the TMDs, while MalK is the NBD. The functional unit of the protein is MalFGK₂ (9).

ABC transporters are either exporters or importers, the latter only being found (apart from exceptions in, for example, plants) in prokaryotes. Additionally to the canonical built, importers require an accessory unit, the substrate-binding protein that delivers the dedicated substrate to the transporter. ABC exporters recruit their substrates from the (cytosolic) lumen, or directly from the lipid bilayer. ABC transporters can also be found as components of large secretory complexes, where they fuel secretion in complex with other membrane proteins. Prominent examples are the type 1 secretion systems in Gram-negative bacteria as well as the MacA-MacB-TolC multidrug export machinery (10,11).

1.3 Mechanisms of Transport of ABC Transporters

To date, no common mechanism of transport has been described for all ABC exporters. It remains questionable whether one general mechanism is applicable to all systems considering the vast variety in translocated substrates. Nevertheless, many mechanisms have been proposed over time, based on the allosteric access model that was originally developed for P-type ATPases (Figure 2) (7).

In principle, the allosteric access model suggests a conformational change from an “inward-open” state to an “outward-open” state, releasing the substrate on the other side of the membrane. In the inward-open conformation, no substrate is bound to the ABC transporter. As observed in many crystal structures, the two NBDs might even be physically separated from each other (Figure 2A). Upon substrate- and ATP-binding, the transporter switches into an intermediate, the “occluded” state (Figure 2B). The substrate may be recruited either from the cytosolic lumen or from the membrane bilayer. The substrate-binding cavity is closed from both sides, and the NBDs, having two molecules of ATP bound, are in close physical proximity. The protein’s conformation subsequently changes to the outward-open state (Figure 2C), the affinity for the substrate changes and, as a consequence, it is released from the substrate-binding cavity. Hydrolysis of ATP to ADP and the release of two phosphate molecules and two ADPs move the system back into the inward-open state (Figure 2A).

The detailed mechanism of transport, especially the order of substrate and ATP binding, ATP hydrolysis and ADP and substrate release, is still under debate. Several models have

been proposed of which the most prominent ones are the “Switch Model” (12) and the “Constant Contact Model” (13), which are both described in greater detail below. However, it needs to be noted that one model is not necessarily valid for all ABC transporters and that these models provide only theoretical explanations for the scientific data that is available to date.

1.3.1 The Switch Model

The Switch Model, originally proposed by Higgins and Linton in 2004, describes how the binding and hydrolysis of nucleotides in the NBDs of an ABC transporter are possibly linked to the movement of the TMDs from inward- to outward-facing conformations and vice-versa (12,14).

In principle, the Switch Model is based on two conformational states of the NBD dimer: an open conformation in the ADP-bound or nucleotide-free state, in which the dimers might even be physically separated from each other, and a closed conformation, with two ATP molecules bound at the dimer interface that act like a molecular glue (Figure 3, steps I and II). Binding of ATP provides the power stroke that is needed to change the conformation of the TMDs from the inward- to the outward-facing conformation (Figure 3, step III). Sequential hydrolysis of the ATP molecules causes the system to move back into the inward-facing conformation and the NBDs disengage (Figure 3, steps IV-VII) (12,14).

To date, all structural data available for ABC transporters can be explained by the switch model. Further evidence was provided by studies exploring the conformational landscapes of homo- and heterodimeric ABC transporters, which, even though revealing differences in the rate-limiting steps of the transport cycles, are coherent with the proposed model (15-17).

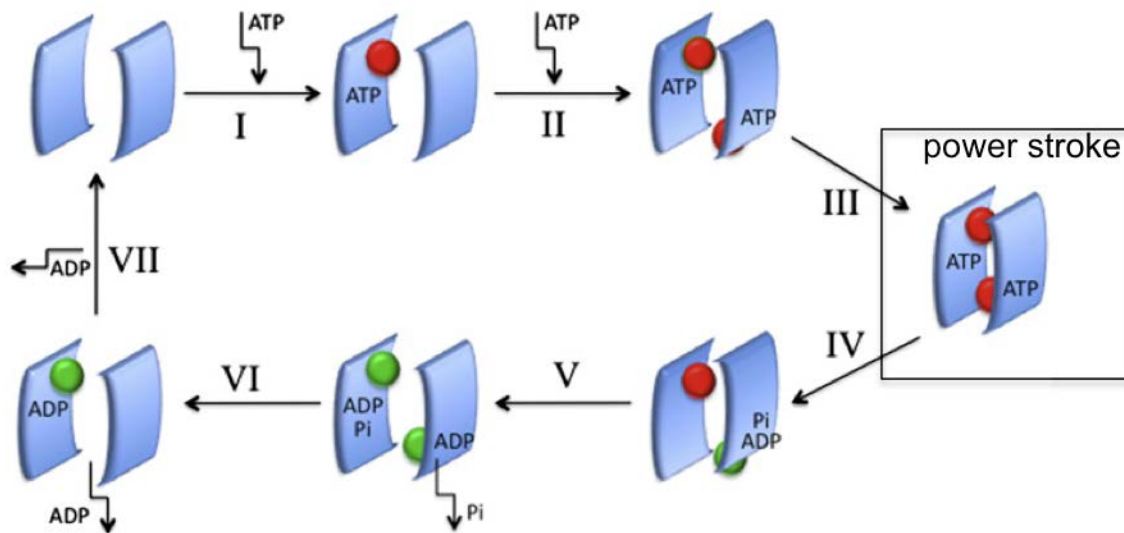


Figure 3: Schematic representation of the switch model (adapted from George and Jones, 2012) (18). Steps I and II: ATP is binding sequentially to the two nucleotide binding sites of the NBDs. This causes the dimerisation of the two NBDs, which provides the power stroke to change the conformation of the TMDs from the inward-facing to the outward-facing conformation (step III). Sequential hydrolysis of ATP to ADP (steps IV and V) results in separation of the NBD dimers and moves the system back into the inward-facing state. Sequential release of ADP+P_i (Steps VI and VII) returns the system to the initial apo-state.

1.3.2 The Constant Contact Model

The constant contact model assumes that the NBDs do not disengage after ATP hydrolysis as proposed by the switch model, but remain in constant contact by alternating ATP hydrolysis in the two nucleotide binding sites (13). It is based on the assumption that the nucleotide-free apo states, as observed in many crystal structures, are physiologically irrelevant as the intracellular ATP concentration greatly exceeds the K_d of ATP-binding to the NBDs (13).

The sequential binding and hydrolysis of ATP and release of ADP and P_i is depicted in Figure 4. The two NBDs function 180° out of phase, thus providing a constant physical contact during the whole cycle (13,18). However, it has not clearly been defined which steps provide the power stroke for the conformational changes in the TMDs (13).

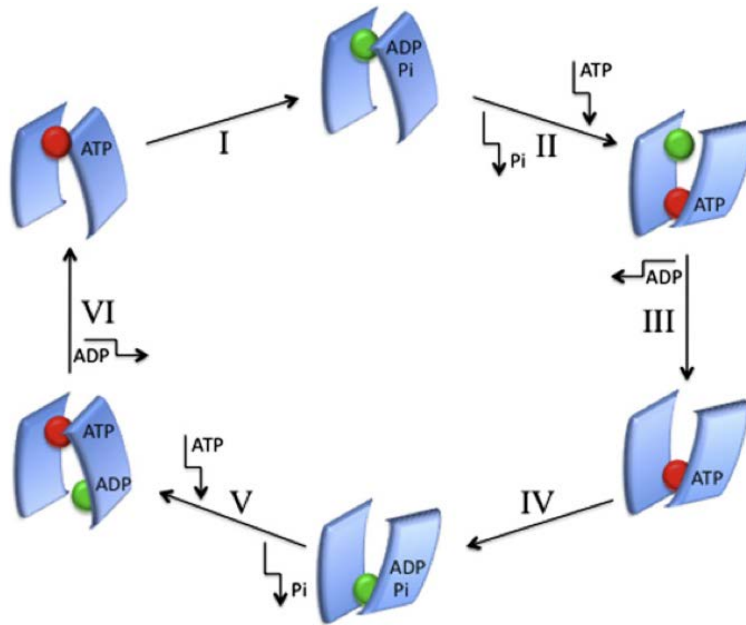


Figure 4: Schematic representation of the constant contact model (adapted from George and Jones, 2012) (18). The model is based on a constant physical contact between the two NBD monomers, provided by sequential hydrolysis of ATP and release of ADP + P_i , 180° out of phase, of the two nucleotide binding sites (13). Step I: ATP bound to binding site 1 is hydrolysed to ADP + P_i . Step II: P_i is released from binding site 1 and ATP is binding to binding site 2. Step III: ADP is released from binding site 1. Step IV: ATP bound to binding site 2 is hydrolysed to ADP + P_i . Step V: P_i is released from binding site 2 and ATP binds to binding site 1. Step VI: ADP is released from binding site 2.

The constant contact model is mainly supported by molecular simulations experiments, which have for example been performed on the NBD of HlyB (19). Structural support is provided by the crystal structure of the inward facing heterodimeric ABC transporter TM287/288 from *Thermotoga maritima*, where the NBDs do not have ATP bound but remain in physical contact (20).

1.4 Bacterial Secretion Systems

The secretion of proteins and other molecules to the extracellular space is widespread amongst bacteria. Secreted proteins are functionally diverse and involved in many processes like nutrient acquisition, biofilm formation or host invasion.

Depending on the definition, a minimum of 15 different secretion systems have been identified so far in Gram-negative bacteria, where the presence of the outer membrane imposes a particular challenge to the secretion process (21). They can be divided into two

subgroups based on the presence or absence of a periplasmic transport intermediate (22). Figure 5 summarises the secretion systems without periplasmic transport intermediates.

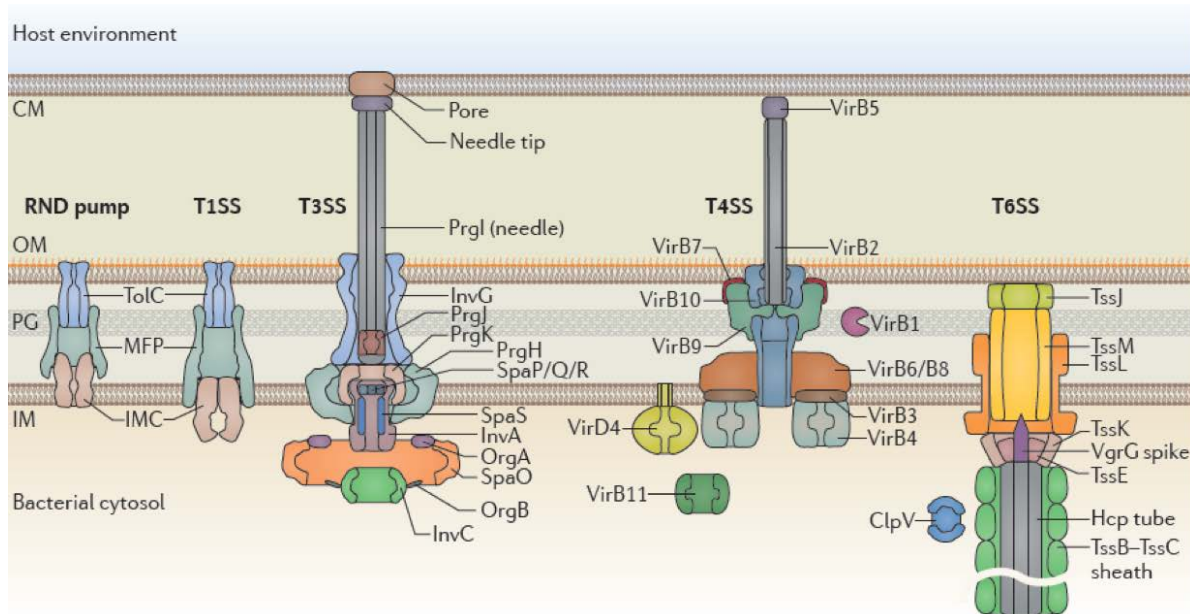


Figure 5: Overview of the different secretion systems and their components without a periplasmic transport intermediate in Gram-negative bacteria (adapted from Costa et al. 2015 (21)). T3SS and T4SS span a total of three membranes, as they inject their substrate directly into the cytosol of the target cell.

RND pumps, Type I, III, IV and VI secretion systems traverse both membranes of the secreting organism. While most secretion systems release their substrate into the extracellular space, Type III, IV and VI secretion systems deliver their substrates directly into the cytosol of a target cell, thus traversing three membranes in total. The secretion apparatuses are composed of a tunnel-shaped protein complex, which is composed out of three to up to more than ten membrane-localised proteins (Figure 5) (21-23).

1.4.1 Secretion into a Target Cell without Periplasmic Intermediates

Type III, IV and VI secretion systems not only traverse the two membranes of Gram-negative organisms without the occurrence of periplasmic intermediates, they also deliver their substrates directly to the membrane or cytosol of a eukaryotic or prokaryotic target cell, thus mediate the crossing of three to four membranes in total.

Type III secretion systems can be found mainly in pathogenic and enteropathogenic organisms. Bacterial effector proteins are injected directly into a target eukaryotic cell (24).

The secretion apparatus can be divided into the base and the needle, and is composed out of up to 16 different proteins (Figure 5) (25).

Type IV secretion systems are the most ubiquitous secretion system and present in Gram-negative as well as Gram-positive prokaryotes (26). They are capable of transporting DNA as well as proteins into prokaryotic or eukaryotic cells and mediate the conjugation of plasmid DNA (27,28). The secretion apparatus is made up of 12 different proteins and can be divided into the translocon and the pilus (Figure 5).

Type VI secretion systems deliver mainly lethal effectors to their eukaryotic or prokaryotic target cells. The apparatus forms a contractile nanomachine made up of the membrane-embedded complex and the tail complex containing the puncturing device (29-31). Contraction of sheaths propels effectors across membranes (32). The whole complex is made up of a minimum of 13 different proteins (Figure 5) (33).

1.4.2 Secretion to the Extracellular Space without Periplasmic Intermediates

RND pumps and Type I secretion systems cross both membranes of their Gram-negative host to secrete their substrates into the extracellular medium.

RND pumps are relatively simple structures and are composed of only three proteins (Figure 5). These complexes are mainly linked to multidrug resistance; however, they are capable of transporting a wide spectrum of substances. Prominent members of this group are for example the AcrAB-TolC (34,35) and the MexAB-OprM drug efflux systems (36,37).

Type I secretion systems transport small peptides and proteins of up to 900 kDa in size and comprise a similar build to RND pumps out of three membrane-localised proteins. Their structural and functional features are discussed in more detail below.

1.5 Type I Secretion Systems

Compared to other secretion systems, type I secretion complexes comprise a relatively simple basic build of only three membrane proteins (Figure 5) (11,38-40). An ABC transporter and a membrane fusion protein (MFP) form a constantly assembled complex in

the inner membrane, while the outer membrane porin (OMP), a TolC-like protein, is recruited once the dedicated substrate interacts with the cytosolic part of the secretion complex (Figure 5) (41,42).

1.5.1 Substrates of Type I Secretion Systems

The substrates of type I secretion systems (T1SS) are of wide functional diversity. Examples are the iron scavenger protein HasA from *Serratia marcescens* (43), class II microcins like ColV from *Escherichia coli* (44), lipases like LipA from *Pseudomonas brassicacearum* and TliA from *Pseudomonas fluorescens* (45-47), proteases, such as AprA from *Pseudomonas aeruginosa* or PrtA from *Erwinia chrysanthemi* (48-50), exotoxins like HlyA from *Escherichia coli* or LktA from *Mannheimia haemolytica* (51,52), adenylate cyclases such as CyaA from *Bordetella pertussis* (53) or adhesins, such as SiiE from *Salmonella enterica* (54). Their sizes range from only 5-6 kDa (class II microcins) to up to 900 kDa (MARTX proteins).

Many of the T1SS substrates are members of the protein family of RTX (“repeats in toxin”) proteins (55). Even though structurally and functionally very diverse, they all contain the common nonapeptide consensus sequence GGxGxDxUx (x: any amino acid, U: large hydrophobic amino acid), which was termed “GG-repeats” or “RTX-domains” (56,57). RTX proteins bind calcium ions via these RTX domains in the high micromolar range, which induces folding of the entire protein (58-62). A free cytosolic calcium ion concentration in the nanomolar range prevents folding of the substrate prior to secretion (63).

After the translocation is finished, RTX proteins adopt their tertiary structure in the extracellular space, triggered by a calcium ion concentration of up to 10 mM. The number of RTX domains correlates to some extent with the molecular weight of the protein (56).

The secretion signal of RTX proteins is located within the last 50 to 100 C-terminal amino acids, while the N-terminal moieties of the proteins encode for their functionality (56,64-66). Unlike during many other secretion processes, the secretion signal is not cleaved prior to or during secretion (67).

1.5.2 ABC Transporters of Type I Secretion Systems

In principle, the ABC transporters of T1SS can be divided into three subgroups, depending on the presence or absence and the nature of an N-terminal appendix (11), thus deviating from the canonical build of ABC transporters. In the case of ABC transporters involved in the export of class II microcins, this domain functions as a C39 peptidase domain, which cleaves an N-terminal signal peptide prior to secretion (44,68). This domain can also be found in bacteriocin-secreting ABC transporters in Gram-positive bacteria (Figure 6) (68,69). However, in many T1SS-ABC transporters the catalytic triad of the domain is corrupted by a cysteine-tyrosine replacement, leaving the domain with an identical tertiary structure compared to C39 peptidase domains but no proteolytic activity (Figure 6) (6,70). Thus, these domains were named “C39 peptidase-like domains”, or CLD (6).

As for HlyB and HlyA it was shown that the CLD interacts with the unfolded substrate, it is suggested that the CLD is needed as a receptor that ensures correct positioning of the substrate for subsequent transport (6). This interaction was confirmed by functional studies with the purified full-length ABC transporter (71). Furthermore, it is speculated whether the CLDs play a role in keeping the substrates unfolded in the cytosol and preventing their degradation until the secretion process is initiated (11,22).

To date, structural information of full-length T1SS or related ABC transporters is limited to the structure of a PrtD homologue from *Aquifex aeolicus* (72) and the structure of PCAT1, a bacteriocin secreting ABC transporter from the Gram-positive organism *Clostridium thermocellum* (Figure 6) (68). Even though the latter ABC transporter is not part of a T1SS, it shows the possible arrangement of the N-terminal accessory domain within a fully assembled ABC transporter (Figure 6A).

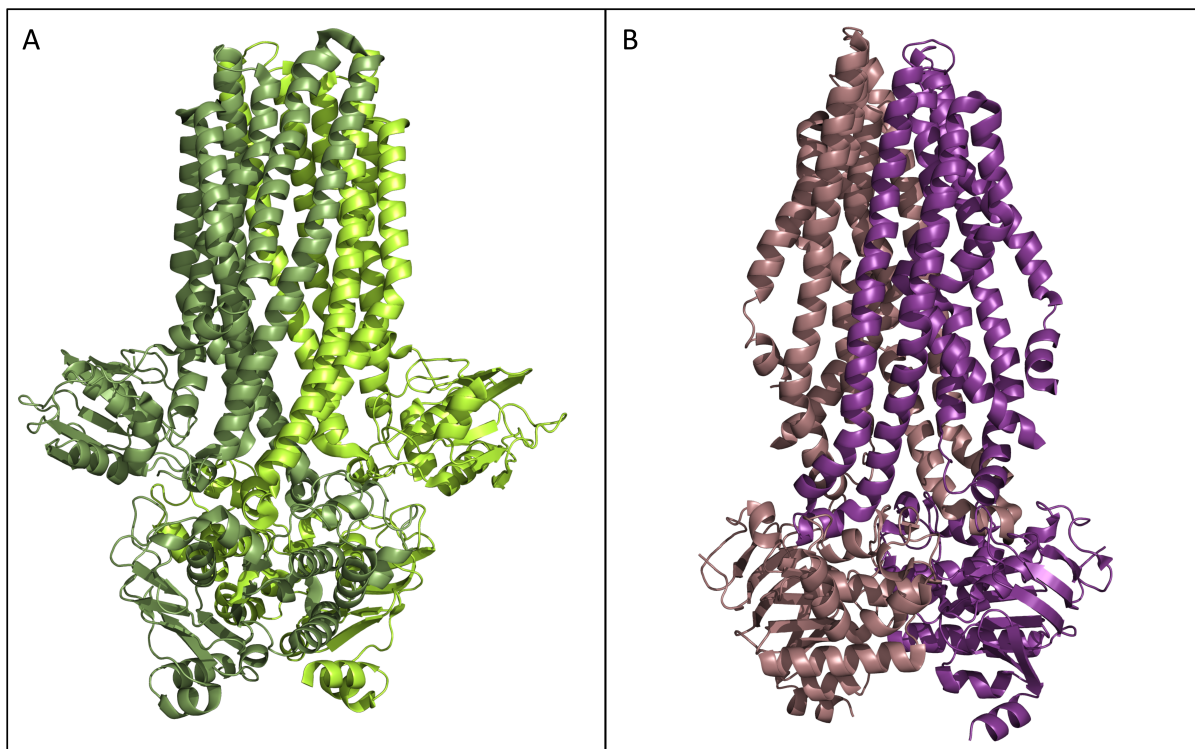


Figure 6: Three-dimensional structures of two ABC transporters, both obtained by X-ray crystallography. Structures were visualised using the software Pymol. (A) – Structure of PCAT1, a bacteriocin secreting and processing ABC transporter from the Gram-positive bacterium *Clostridium thermocellum* (68). PCAT1 contains an N-terminal C39-peptidase domain that processes the polypeptide prior to secretion (pdb: 4RY2). (B) – Structure of AaPrtD from the Gram-negative bacterium *Aquifex aeolicus* (72). AaPrtD is a homologue to PrtD from *Dickeya dadantii*, an ABC transporter that is part of a type I secretion system (73). PrtD does not contain an N-terminal accessory domain.

Some ABC transporters involved in type I secretion do not contain an additional domain. Examples are HasB, the ABC transporter involved in the secretion of the iron scavenger protein HasA in *Serratia marcescens* or PrtD from *Dickeya dadantii*, which is part of a T1SS secreting a range of proteases (Figure 6B) (73). Remarkably, it was shown that SecB is involved in the transport process of HasA by preventing its folding prior to secretion (74).

1.5.3 Membrane Fusion Proteins of Type I Secretion Systems

Proteins belonging to the family of membrane fusion proteins (MFP) are involved in a large number of export processes that cover a wide range of physiological functions, i.e. protection against toxic compounds, export of metabolites or secretion of virulence factors (75). As

such, they are part of tripartite efflux pumps like AcrAB-TolC (35) or MacAB-TolC (10) and T1SS (67).

In principle, within these systems the MFP is required to bridge the physical space across the periplasm between the inner-membrane component (e.g. an ABC transporter or secondary active transporter) and the OMP. Furthermore, within the HlyA-T1SS it has been shown that the MFP HlyD holds a function required for the correct folding of the substrate (76).

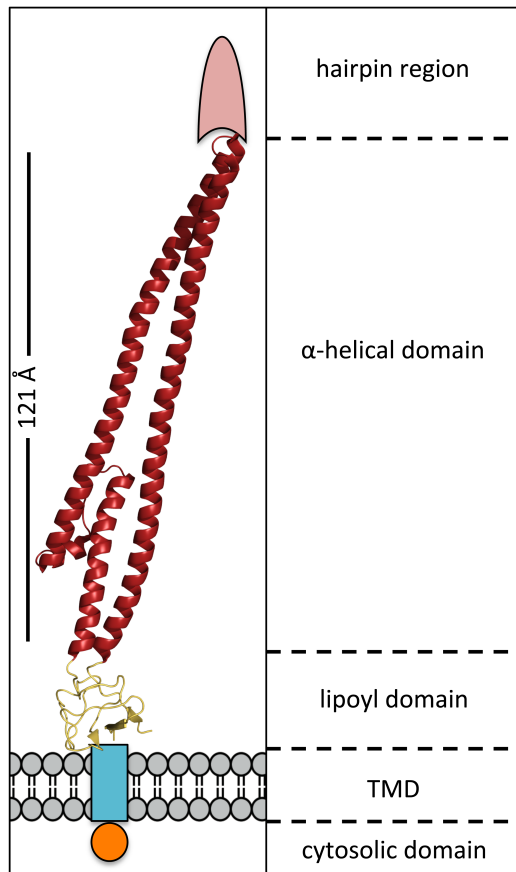


Figure 7: Structural build of a T1SS-MFP, exemplified by the structural information available for LipC from *Serratia marcescens*. The crystal structure of a soluble fragment of LipC covers the lipoyl domain and the α-helical domain (pdb: 5NEN) (77). Missing domains, namely the hairpin region at the C-terminus and the TMD and cytosolic domain at the N-terminus, are added as schematic representations.

MFPs comprise an overall similar build of up to four domains. Common features are the periplasmatically localised α-helical and lipoyl domains. Additionally, they may contain a membrane anchor or a TMD, followed by a small cytosolic domain (Figure 7).

The structural information on T1SS-MFPs is very limited and currently restricted to soluble fragments of HlyD from *Escherichia coli* and LipC from *Serratia marcescens*, both covering the α-helical domains and the lipoyl domains but lacking the TMDs and the cytosolic domains as well as the membrane proximal domains, which include the hairpin region (Figure 7) (77,78).

The α-helical domains of T1SS-MFPs contain a helical hairpin at the C-terminus, which has not been structurally resolved (Figure 7) (77,78). The hairpin-region is of functional

importance as it has been shown to be the site of interaction with the outer membrane porin (78-80). In LipC, the α -helical domain has a length of 121 Å, which was shown to be similar for HlyD. They both contain three α -helices, which might be a common feature for T1SS-MFPs (77,78).

The exact function of the lipoyl domain is still unknown. It is thought to act as a stabilising factor for the assembly of the complex, forming the central shaft of the periplasmic part of the secretion complex (81,82).

In analogy to the MacAB-TolC complex in *E. coli*, where MacB also is a dimeric ABC transporter, it is assumed that LipC forms a hexamer within the type I secretion complex (77).

1.5.4 The Outer Membrane Porin of Type I Secretion Systems

In order to traverse the outer membrane of Gram-negative bacteria, T1SS contain a specific outer membrane porin (OMP). Members of this family are for example TolC, PrtF, CyaE and LipD (40).

The best-characterised OMP is TolC from *E. coli*, whose structure has been determined by X-ray crystallography in two conformations (83,84). It is a ubiquitous outer membrane protein and involved in several export processes, namely as a member of multidrug efflux systems such as AcrA-AcrB-TolC (35) or MacA-MacB-TolC (10) but also in T1SS, like the HlyA-T1SS or the ColV-T1SS (85,86).

TolC is a homotrimer and has a total length of 140 Å, spanning the outer membrane and protruding far into the periplasm (Figure 8A) (83). The interior of the tunnel-shaped protein is a water-filled pore with a diameter of 20 Å (Figure 8B) (83). To open the channel for export, an iris-like movement has been proposed (Figure 8C, D) (87).

It has been shown that the OMP interacts directly with its corresponding MFP (41,88). For this purpose, a binding groove is present in TolC, identified by direct interaction of TolC with the MFP AcrA (84,89). However, this interaction was not confirmed by the structural studies on the ArcAB-TolC complex (35). Furthermore, TolC seems to play a role in the correct folding of HlyA (90) and a direct interaction between both proteins during the secretion process seems likely (40).

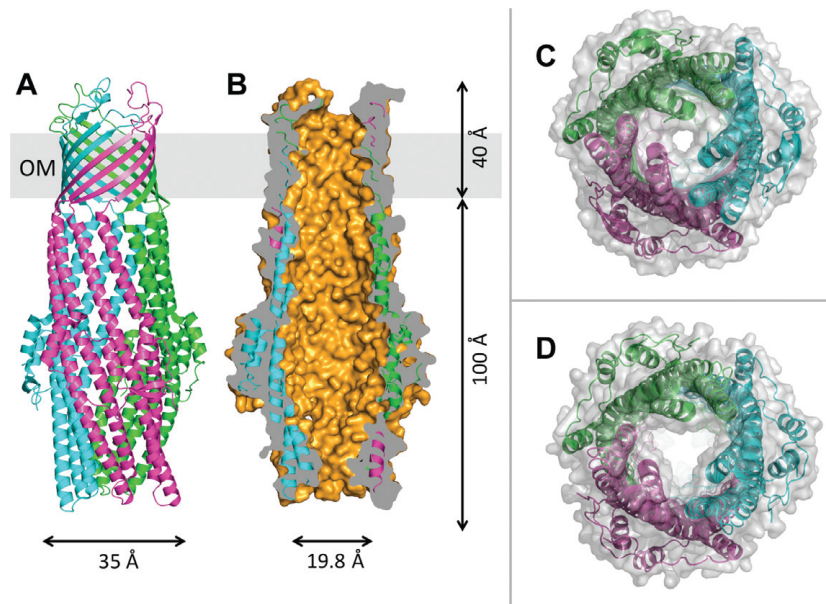


Figure 8: (A) – Crystal structure of the OMP TolC from *E. coli* in a closed conformation, each monomer is represented in a different colour (pdb: 1EK7) (83). (B) – Cross-sectional side view of TolC, highlighting the continuous channel through the protein. (C)– Closed (pdb: 1EK9) and (D) open pore (pdb: 2XMN) of TolC from the periplasmic side of the protein. For better illustration, the shape of the surface is shown in grey (figure taken from Lenders et al. 2013) (91).

1.6 The Haemolysin A Type I Secretion System from *Escherichia coli*

The haemolysin A (HlyA) Type I secretion system from *E. coli* was the first T1SS to be discovered (92) and has set many paradigms for the mechanism of Type I-mediated transport. The RTX protein haemolysin A is a lytically active toxin that is secreted by several uropathogenic *E. coli* strains (3,93). The secretion complex is composed out of the ABC transporter HlyB, the membrane fusion protein HlyD and the outer membrane porin TolC (Figure 9). HlyB, HlyD and the substrate HlyA are located on the same *hly*-operon (94). Additionally to the substrate and the membrane-localised proteins, the operon contains a component that is not directly involved and not necessary for the secretion process, the cytosolic acyltransferase HlyC (94,95). HlyC is responsible for the activation of proHlyA prior to secretion by acylating two internal lysine residues of the unfolded polypeptide, leaving lytically active HlyA to be secreted into the extracellular space (96-99).

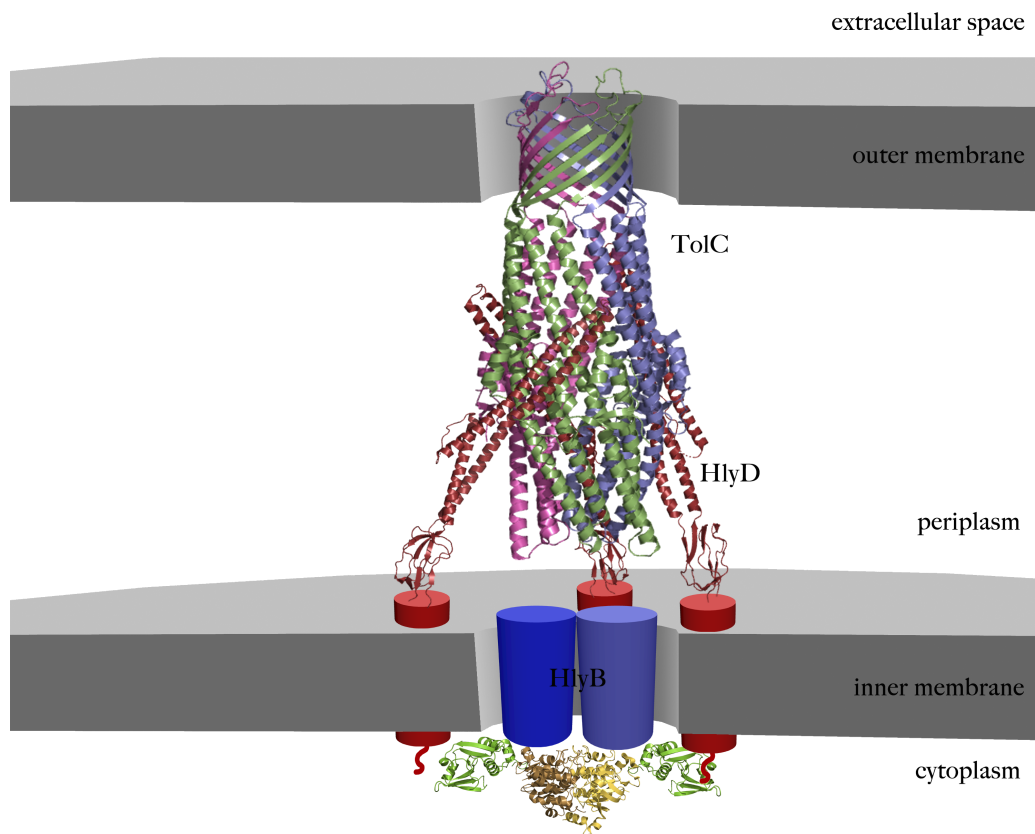


Figure 9: Summary of the HlyA-T1SS including all the structural information available to date. The NMR structure of the CLD (pdb: 3ZUA) (6) and the crystal structure of the NBD (pdb: 1XEF) (100) are shown in green and yellow, respectively. The TMDs of HlyB are shown as blue cylinders. The crystal structure of the soluble fragment of HlyD is shown in red (pdb: 5C21), with the TMDs represented as red cylinders which have the small cytosolic domain attached (78). The three monomers of TolC (pdb: 1EK9) are represented in pink, green and blue, respectively (83). The trimeric arrangement of HlyD is based on the crosslinking studies performed by Thanabalu et al. 1998 (41).

1.6.1 Structural Studies and Assembly of the HlyA-Type I Secretion System

The stoichiometry of T1SS is still under debate. Following general knowledge, the ABC transporter in the T1SS forms a dimer and TolC is known to be of trimeric build. However, a trimeric as well as a hexameric state was proposed for the MFP, pointing out the necessity for further investigation (41,78).

A putative assembly of the HlyA-T1SS including all the structural information available to date is depicted in Figure 9. The trimeric arrangement of HlyD is based on the crosslinking

studies performed by Thanabalu et al. (41). The inner membrane components of the HlyA-T1SS are described in further detail below.

1.6.2 The ABC Transporter HlyB

HlyB is a half-size ABC transporter that contains a CLD as an accessory domain at its N-terminus (6). The dimer contains a putative number of ten transmembrane helices. Functional studies have been performed with detergent-purified HlyB, revealing a modulating activity of the CLD on the ATPase activity in presence and absence of the substrate (71).



Figure 10: Homology model of HlyB, created with phyre2 (101) and Pymol, based on the three-dimensional structure of PCAT1 (pdb: 4RY2) (68) obtained by X-ray crystallography.

The three dimensional structure of full-length HlyB is not yet known. However, the structures of the NBD as well as the CLD of HlyB have been determined by X-ray crystallography and NMR, respectively, providing insights into functional details of both domains (6,102). Figure 10 shows a homology model of HlyB based on the crystal structure of PCAT1 (68). This shows a possible arrangement of the different domains within the protein.

1.6.3 The Membrane Fusion Protein HlyD

The structural information available for HlyD is currently restricted to a soluble fragment that comprises the α -helical domain and the lipoyl domain (Figure 9) (78). The structure resembles the structure of LipC, with an α -helical domain of slightly shorter length (115 Å). The small cytosolic domain that is present in HlyD is essential for the recruitment of TolC into the secretion complex, which is triggered by an interaction with the substrate HlyA (42). The hairpin region of HlyD has been shown to be the interaction site with the outer membrane porin TolC (78-80).

The oligomeric state of HlyD is still under debate. Despite crosslinking studies that propose a trimeric assembly of HlyD (41), a hexameric assembly within T1SS seems more likely and would fit the hexameric nature of other MFPs (10,35). In the model proposed by Kim et al. (78) HlyD adopts a hexameric, doughnut-like assembly that would fit with the multiplicity of the dimeric ABC transporter HlyB and the trimeric nature of the OMP TolC.

1.6.4 Functional studies of the HlyA-T1SS

Several functional studies of the HlyA-T1SS have been performed *in vivo*. With the secretion signal at the C-terminus of the substrate, the directionality of transport has long been under debate. By stalling the assembled HlyA secretion process *in vivo* by the use of a GFP-tagged substrate, the directionality of secretion was shown to be C-terminus first (103). The same concept was used to address the secretion rate, which was determined to be 16 amino acids per second per transporter, meaning that a total of 90 seconds is needed for the secretion of one HlyA molecule (104).

The secretion rate of HlyA is within the ribosomal rate of protein synthesis (10 to 20 amino acids per second) and approximately 10 to 15-fold lower than the SecA-dependent protein translocation rate (152 to 228 amino acids per second) (105,106). Opposing studies on CyaA, where the presence of Ca^{2+} in the extracellular medium has a positive influence on the secretion efficiency, the secretion rate of HlyA is not influenced by varying Ca^{2+} concentrations (104,107). These differences suggest similar, but not necessarily identical secretion mechanisms across the RTX type I secretion substrates, which follow rather a

Brownian ratchet mechanism than the alternating access model, considering the length of the substrates of up to 9000 amino acids (104,107).

2. Aims

The overall aim of this thesis was to provide a deeper understanding of the underlying molecular mechanism(s) of type I secretion. To achieve this aim, the HlyA-T1SS from *E. coli* was chosen, as it is one of the best-studied T1SS and to a limited extent, structural data is available (6,78,100,102,108,109).

Overall, the detailed secretion mechanism of T1SS is not very well understood. The vast size of many T1SS substrates suggests a novel export mechanism for the cognate ABC transporter that differs largely from the generally accepted allosteric two-side access model (7).

For the HlyA-T1SS, the substrate has been shown to interact with the ABC transporter HlyB via its accessory domain, a C39 peptidase like domain (CLD) (6) as well as its NBD (110). Another interaction takes place at the cytosolic domain of the MFP HlyD (41,42). The functions of these interactions during the secretion process are not fully understood and are further examined upon the unusual directionality of transport, C-terminus first, of the substrate HlyA (103).

To provide an understanding of the ABC transporter HlyB and its accessory domain, the first aim was its overexpression, purification and reconstitution in an artificial bilayer system, such as saposin-A (111) or nanodiscs (112). In contrast to detergent-solubilised protein, this offers the possibility of studying a membrane protein within a more native-like lipid environment. Subsequently, the second aim was to establish the overexpression and purification of the assembled inner membrane complex for functional and structural characterisation.

It was aimed to address the optimisation of expression and purification conditions by on one hand trying different expression strains and expression conditions and on the other hand, by modifying the purification conditions, e.g. by varying the detergents used for solubilisation and subsequent purification procedures.

Furthermore, it was aimed to support functional studies with bioinformatic analyses and to classify T1SS into different groups, based on similarities within their operon organisations, accessory domains and proteins and potential secretion signals in the substrates.

3. Publications

3.1 Chapter I – Classification of ABC Transporters of Type I Secretion Systems

Title:	Type I secretion systems – a story of appendices
Authors:	Kerstin Kanonenberg, Christian K. W. Schwarz, Lutz Schmitt
Published in:	<i>Research in Microbiology</i> (2013)
Impact Factor:	2.372
Own Work:	70 % Bioinformatic/ phylogenetic analyses Writing of the manuscript



Research in Microbiology 164 (2013) 596–604



www.elsevier.com/locate/resmic

Type I secretion systems – a story of appendices

Kerstin Kanonenberg, Christian K.W. Schwarz, Lutz Schmitt*

Institute of Biochemistry, Heinrich Heine University Düsseldorf, Universitätsstrasse 1, 40225 Düsseldorf, Germany

Received 20 November 2012; accepted 13 March 2013

Available online 26 March 2013

Abstract

Secretion is an essential task for prokaryotic organisms to interact with their surrounding environment. In particular, the production of extracellular proteins and peptides is important for many aspects of an organism's survival and adaptation to its ecological niche. In Gram-negative bacteria, six different protein secretion systems have been identified so far, named Type I to Type VI; differing greatly in their composition and mechanism of action (Economou et al., 2006). The two membranes present in Gram-negative bacteria are negotiated either by one-step transport mechanisms (Type I and Type III), where the unfolded substrate is translocated directly into the extracellular space, without any periplasmic intermediates, or by two-step mechanisms (Type II and Type V), where the substrate is first transported into the periplasm to allow folding before a second transport step across the outer membrane occurs. Here we focus on Type I secretion systems and summarise our current knowledge of these one-step transport machineries with emphasis on the N-terminal extensions found in many Type I-specific ABC transporters. ABC transporters containing an N-terminal C39 peptidase domain cut off a leader peptide present in the substrate prior to secretion. The function of the second type of appendix, the C39 peptidase-like domain (CLD), is not yet completely understood. Recent results have shown that it is nonetheless essential for secretion and interacts specifically with the substrate of the transporter. The third group present does not contain any appendix. In light of this difference we compare the function of the appendix and the differences that might exist among the three families of T1SS.

© 2013 Institut Pasteur. Published by Elsevier Masson SAS. All rights reserved.

Keywords: ABC transporters; C39 peptidase domain; Haemolysin; Type I secretion systems

1. Introduction to Type I secretion systems (T1SS)

In 1985, Nicaud et al. (Nicaud et al., 1985) identified two membrane proteins of the inner membrane of *Escherichia coli* (*E. coli*), haemolysin (Hly) B and HlyD, to be essential for the secretion of the toxin HlyA, a member of the repeats-in-toxins (RTX) family (Linhartova et al., 2010). A one-step translocation process was proposed by the same group also in 1985 (Mackman et al., 1985), when they described the translocation of HlyA across the membranes of the Gram-negative bacteria *E. coli* as a single-step mechanism without the occurrence of periplasmic intermediates.

Nowadays we know that proteins secreted via the T1SS vary greatly in size and function, for example, the bacteriocin colicin V or Mcc V with a size of 5.8 kDa, as well as large

RTX or MARTX proteins whose molecular weight can be up to 900 kDa (Gilson et al., 1990; Linhartova et al., 2010; Satchell, 2011).

Many proteins secreted via the T1SS, such as haemolysins and leukotoxins, are of great importance for the pathogenesis in the host organism or, like some bacteriocins, for antibacterial activity (Bleves et al., 2010; Dirix et al., 2004). Other proteins secreted by T1SS are involved in nutrient acquisition. Examples are extracellular proteases and lipases or the well-characterised iron scavenger protein HasA (Akatsuka et al., 1995; Duong et al., 1992; Létoffé et al., 1994). A brief summary of substrates of T1SS is provided in Table 1.

It is now commonly accepted that T1SS are composed of three indispensable membrane proteins (Fig. 1), an ABC transporter, a membrane fusion protein (MFP) and an outer membrane protein or factor (OMF). Furthermore, all substrates contain a Sec-system independent secretion sequence. This sequence is either located at the N-terminus (bacteriocins or colicins) or at the C-terminus (all other systems) of the substrate.

* Corresponding author. Tel.: +49 (0)211 81 10773; fax: +49 (0)211 81 15310.

E-mail address: lutz.schmitt@hhu.de (L. Schmitt).

Table 1
Examples of substrates of T1SS and their dedicated transport components.

Type of protein	Example of the secreted protein	Secretion apparatus ABC/MFP/OMF	Reference
Bacteriocin	ColicinV/MccV	CvaB/CvaA/TolC	(Fath et al., 1994; Gilson et al., 1987, 1990)
Adhesin	LapA	unknown	(Espinosa-Urgel et al., 2000; Hinsä et al., 2003)
Lipase	LipA	LipB/LipC/LipD	(Akatsuka et al., 1995)
Protease	Alkaline protease	AprD/AprE/AprF	(Guzzo et al., 1991)
Iron scavenger protein	HasA	HasD/HasE/HasF	(Letoffe et al., 1996)
S-layer protein	RsaA	RsaD/RsaE/RsaF(&RsaF _b)	(Awram and Smit, 1998; Smit et al., 1992)
RTX toxin	HlyA	HlyB/HlyD/TolC	(Wandersman and Deleplaire, 1990; Koronakis et al., 2000; Holland et al., 2005)

In this review, the T1SS will be discussed with regard to the different types of ABC transporters, which constitute part of the secretion apparatus. Such a classification distinguishes three different groups of transport proteins, which differ in their N-terminal domains as well as in the kind of substrates being translocated.

2. General structure of the T1SS

The best-studied T1SS are the HasA secretion system from *Serratia marcescens* (*S. marcescens*) (Letoffe et al., 1996) and the HlyA secretion machinery from *E. coli* (Holland et al., 2005).

Each substrate or allocrite of a T1SS is secreted by its dedicated and relatively simple secretion apparatus, which

consists of only three proteins (Fig. 1). They form a tunnel-like structure to transfer the substrate directly from the cytosol to the extracellular space. The currently accepted molecular blueprint of T1SS assumes that an ABC transporter provides a transport pathway across the inner membrane and the energy required via binding and hydrolysis of ATP, while an OMF forms a pore through the outer membrane. Finally, an inner membrane-anchored MFP completes the machinery by spanning the periplasm and connecting the large periplasmic domain of the OMF and the ABC transporter (Holland et al., 2005).

The HasA and the HlyA T1SS are composed of the ABC transporters, MFPs and OMFs, HasD/HasE/HasF, and HlyB/HlyD/TolC, respectively (Binet and Wandersman, 1996; Koronakis et al., 2000; Letoffe et al., 1990). Whereas the inner

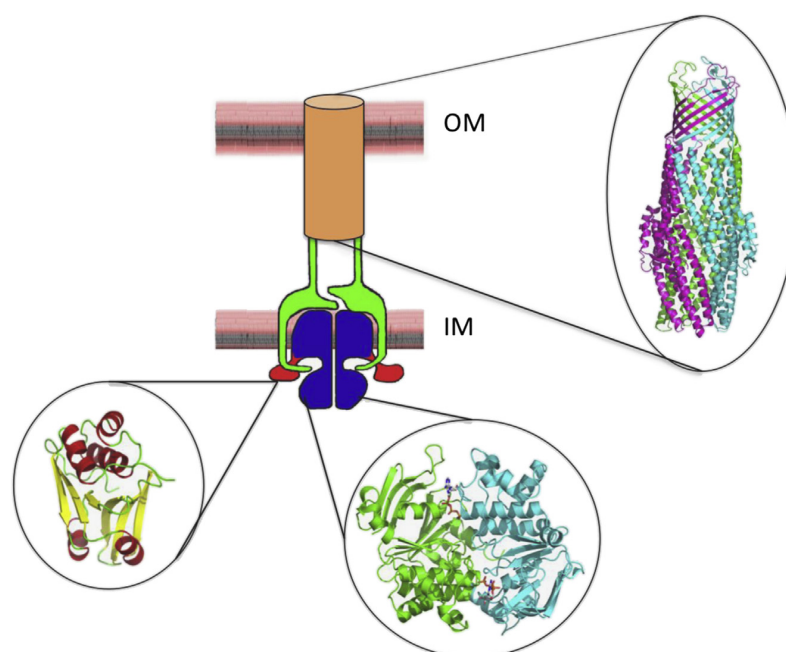


Fig. 1. Schematic summary of the general architecture of a T1SS involved in secretion of an RTX protein, for example HlyA. The ABC transporter is shown in blue with the CLD highlighted in red, the MFP in green and the OMF in orange. Structures of components of T1SS are also included. The structures of the ATP-bound dimer of HlyB (Zaitseva et al., 2005), the CLD of HlyB (Lecher et al., 2012) and TolC (Koronakis et al., 2000) are shown in cartoon representation. The currently known crystal structures of substrates of T1SS (Arnoux et al., 1999; Baumann et al., 1993) have not been included for simplicity. Please note that the functional unit of the ABC transporter is a dimer and the oligomeric state of the OMF is trimeric (each chain of the TolC structure is coloured differently). This would generate a symmetry break that might be resolved by the MFP, which has been drawn arbitrarily as a dimer. The described crystal structures of MFPs not involved in T1SS did not resolve this issue (Akama et al., 2004; Higgins et al., 2004; Mikolosko et al., 2006). Only recently, the crystal structure of CusB (Su et al., 2011; Su et al., 2009), the MFP of a Cu⁺/Ag⁺ export systems (non ABC) revealed a hexameric state, which would be a solution to cope with the apparent symmetry mismatch between ABC transporter and OMF.

membrane components display a very high degree of specificity for their substrates, the OMFs are also involved in multiple export processes. For example, the OMF TolC of *E. coli* is involved in HlyA secretion (Mackman et al., 1985) but also the secretion of colicin V of Mcc V (Gilson et al., 1987), and the extrusion of cytotoxic compounds (Nakashima et al., 2011), to confer drug resistance in bacteria (Pos, 2009). In all of these cases, TolC interacts with different sets of proteins of the inner membrane. In T1SS, there are always MFPs and ABC transporters (Delepelaire, 2004; Holland et al., 2005), while in drug transport processes the coupling occurs mainly but not exclusively with an MFP and a member of the RND (resistance–nodulation–drug resistance) family of secondary transporters (Pos, 2009).

Apart from connecting the other two components of the secretion machinery, the MFP seems to play an important role in substrate recognition, mediated by its N-terminal, cytoplasmic part. Deletion of this domain in HlyD, which is located on the cytosolic side of the membrane, abolishes HlyA secretion (Balakrishnan et al., 2001; Pimenta et al., 1999). Nonetheless, the secretion complex is still found to be assembled; thereby bridging the two membranes of *E. coli*. However, it is important to realise that T1SS do not exist as permanently associated, static complexes (Fig. 2). This was already suggested by the multiple tasks accomplished by TolC (see above). While the ABC transporter and the MFP always form a complex in the inner membrane as shown by cross-linking studies, the entire

complex only assembles upon interaction of the substrate with the ABC transporter and/or the MFP (Balakrishnan et al., 2001; Benabdelhak et al., 2003; Letoffe et al., 1996; Thanabalu et al., 1998). The components of T1SS and their specific interactions with their substrates are described in greater detail in the following sections.

3. ABC transporters

The basic structure of an ABC transporter consists of four modules; two so-called transmembrane domains (TMDs) and two nucleotide-binding domains (NBDs) (Davidson et al., 2008; Jones et al., 2009) that can be arranged in any possible combination. In bacteria, these four modules are mostly encoded by separate genes (Davidson et al., 2008). Interestingly, ABC transporters of T1SS form an exception because here, one NBD and one TMD are encoded by a single gene (so-called ‘half-size transporter’) and the functional unit of these transporters is thought to correspond to the dimer. The transmembrane helices of the TMDs form the translocation pathway for the substrate across the membrane (Hollenstein et al., 2007), while the NBDs are responsible for energy supply through nucleotide binding and hydrolysis and the coordination of the cofactor (e.g. Mg^{2+}) (Oswald et al., 2006). In the functionally active state of the ABC transporter, the two NBDs face each other in a head-to-tail manner so that the

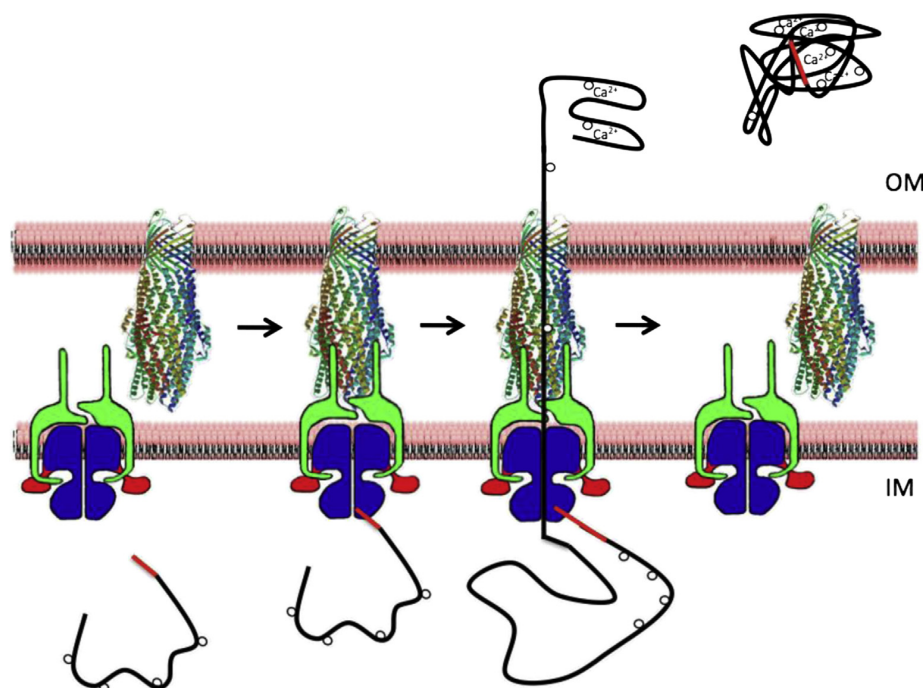


Fig. 2. Current model of the coordination of a T1SS specific for RTX proteins in time and space. Colour coding is identical to Fig. 1. The substrate is shown in black in the unfolded state in the cytosol. The secretion sequence is highlighted in red and the Ca^{2+} -binding sites within the RTX domain are presented as circles. Step 1: The ABC transporter and the MFP form a static complex in the inner membrane in the absence of the substrate. Step 2: The secretion sequence of the substrate located in the extreme C-terminus interacts with the NBDs of the ABC transporter and/or MFP and triggers engagement of the OMF and formation of the channel-tunnel through the periplasm. Step 3: Stepwise translocation of the substrate in the unfolded state. Direct experimental evidence for transport of the substrate in the unfolded state was only recently provided (Bakkes et al., 2010). Step 5: Ca^{2+} -induced refolding of the substrate in the extracellular space and resetting of the T1SS.

nucleotide is sandwiched between the Walker A motif of the one and the C-loop of the other domain (Chen et al., 2003; Smith et al., 2002; Zaitseva et al., 2005).

While more sequence variability is found amongst the TMDs, which is likely due to their involvement in substrate binding and transport, the NBDs show high sequence homology due to their function as power plants. The translocation of a substrate across the membrane involves conformational changes of the ABC transporter that likely follow the ‘two-site access’ model (Jardetzky, 1966). Interaction of the substrate with the transporter in the presence of ATP triggers the formation of dimeric NBDs and opens the transporter’s cavity on the substrate-binding side of the membrane. It is hypothesised that the hydrolysis of ATP destabilises the dimeric NBDs, triggering the transporter to return into its original conformational state and releasing the substrate on the substrate delivery side (Hollenstein et al., 2007; Jones et al., 2009). In light of the size of T1SS substrates, a sequential transport mechanism, i.e. a stepwise substrate translocation is hard to imagine, because the substrate would be located within the translocation pathway interfering with the conformational changes postulated to occur within the “two-site access model”. If this model applied also for ABC transporters involved in T1SS, only one hydrolysis cycle of ATP per transported substrate would be required, which is intuitively hard to imagine.

All ABC transporters, which have been described so far and which are involved in Type I secretion, contain the four canonical domains; two TMDs and two NBDs. However, many of these deviate from this basic blueprint as they feature additional domains located at the cytosolic N-termini of the transporters. These N-terminal extensions allow a differentiation into three distinct groups of ABC transporters involved in T1SS.

4. Group 1: C39-containing ABC transporters

Many secreted proteins are targeted to their specific transporting units by a specific peptide, the N-terminal signal sequence that is cleaved during translation, e.g. the Sec-translocation pathway (for recent reviews see (du Plessis et al., 2011; Lycklama and Driessen, 2012)). Generally, the T1SS has been described as being “signal peptide-independent” but nonetheless, one group of T1SS secreting peptides contains an N-terminal leader peptide. These are small bacteriocins or microcins; secreted by Gram-negative bacteria (Duquesne et al., 2007a,b).

Being normally a feature of Gram-positive bacteria, the secretion of small antimicrobial peptides is not commonly found amongst Gram-negative bacteria (Gebhard, 2012). The microcins secreted by T1SS of Gram-negative bacteria all belong to the Class II subfamily of microcins with a low molecular weight (<10 kDa) and are hence the smallest substrates for T1SS known so far (Duquesne et al., 2007a,b). The corresponding ABC transporters contain an additional domain at their N-terminus, which exhibits Ca^{2+} -dependent proteolytic activity (Wu and Tai, 2004). The structure and primary

sequence of this domain resembles a C39 peptidase (Havarstein et al., 1995), which is a member of the papain-superfamily. They cleave polypeptides C-terminal to a canonical double glycine (GG) motif. This particular motif is present in Class II microcins, at the C-terminus of the N-terminal leader peptide (Duquesne et al., 2007a,b). Upon interaction of the leader peptide with the C39 domain, subsequent cleavage occurs at the C-terminal site of the GG motif and the mature protein is secreted into the extracellular space via the cognate T1SS (Havarstein et al., 1995). One well-characterised member of this family is colicin V or Mcc V from *E. coli* (ColV), with a secretion apparatus consisting of the ABC transporter CvaB, the MFP CvaA and the OMF TolC. Once secreted, ColV inserts into the membrane of other prokaryotic cells to form a pore, leading to lysis and cell death (Fath et al., 1994; Gilson et al., 1987, 1990).

Conserved histidine and cysteine residues in the C39 peptidase domain were shown to be crucial for proteolytic activity and secretion (Wu and Tai, 2004). Recently, further functional analysis revealed an aspartate residue as the third member of the catalytic triad in CvaB (Wu et al., 2012). In the same study, other residues adjacent to the active site have been identified to be essential for functional secretion. Thus, the C39 domain not only cleaves off the leader peptide of the substrate, but is also essential for the translocation activity of these ABC transporters.

In general, leader sequences have been found to be important for the stability of the corresponding mRNA (Xu et al., 1995) or recognition by the export machinery (Huber et al., 1990). For the case of T1SS, the precise role of the leader peptide still remains unclear. Considering the size of T1SS substrates and that no chaperone has yet been found to be involved in the export process of C39 ABC transporter T1SS, it seems likely that the interaction of the leader peptide with the C39 domains keeps the substrate in an unfolded state until the secretion process occurs.

5. Group 2: CLD-containing ABC transporters

Some T1SS ABC transporters contain an N-terminal domain whose primary sequence as well as the three-dimensional structure strongly resembles a C39 peptidase domain (Ishii et al., 2010; Lecher et al., 2012). Interestingly, the domain, however, does not have any proteolytic activity due to the absence of the catalytic essential cysteine in the active centre (Lecher et al., 2012). Hence, these degenerated domains are called C39-like domains (CLD). Furthermore and most importantly, the substrates of these ABC transporters do not contain the N-terminal leader peptide, which is found amongst the class II microcins.

Finally, we have nevertheless shown that the CLD is essential for secretion in the haemolysin secretion, Type I system (Lecher et al., 2012; Mackman et al., 1985). Moreover, our studies showed that the isolated CLD interacts specifically with the unfolded C-terminal fragment of HlyA containing the 3 RTX repeats. However, the secretion signal in the terminal 60 amino acids was not required.

Being the first protein shown to be secreted by a T1SS, the HlyA secretion system (Welch et al., 1981) often serves as a paradigm for Type I secretion. The secretion apparatus consists of the ABC transporter HlyB, the MFP HlyD and the OMF TolC (Holland et al., 2003, 2005; Wandersman and Delepelaire, 1990). The secreted protein, HlyA, has a molecular weight of 110 kDa and is composed of 1024 amino acids, thus differing greatly in size from the previously described microcins.

All information that is required and necessary to target the substrate HlyA to the secretion machinery composed of HlyB/HlyD/TolC, the so-called secretion signal (Gray et al., 1989), is located in the last 50 to 60 C-terminal amino acids (Kenny et al., 1994). Sequence analyses combined with mutational studies have demonstrated that no highly conserved motifs or hardly any conserved individual amino acids are present within the secretion sequence (Chervaux and Holland, 1996; Kenny et al., 1992, 1994). The proposal that secondary structure elements rather than conserved amino acids govern the recognition process were also not sustained because the isolated secretion sequence only adopted a helical conformation in the presence of trifluoro-ethanol, which is one if not the strongest helical promoting agent (Sheps et al., 1995; Yin et al., 1995). Hence, the interaction and recognition of the substrate by the secretion system is not yet completely understood (Holland et al., 2005).

HlyA is an exotoxin formed and released by some pathogenic *E. coli* strains (Welch et al., 1981, 2001). It is thought to insert into the membranes of a wide range of eukaryotic cells (e.g. red blood cells), either dependent on a specific receptor or receptor independent, where it forms a pore resulting in cell death (Linhartova et al., 2010) and references therein). HlyA belongs to the family of RTX (repeats-in-toxins) proteins characterised by the presence of numerous RTX domains. These are glycine- and aspartate-rich nonapeptide repeats with the consensus sequence $^N\text{GGXGXDXUX}^C$, where X can be any amino acid and U is a large, hydrophobic residue (Welch, 2001). The number of repeats may vary from less than 10 to more than 40 per protein, depending on its total length. Nowadays, it is assumed that all RTX proteins are secreted by T1SS (Linhartova et al., 2010). RTX domains are able to bind free Ca^{2+} -ions as demonstrated by the crystal structure of the alkaline protease from *Pseudomonas aeruginosa* (Baumann et al., 1993). In the case of RTX toxins, binding of Ca^{2+} is thought to be essential for the folding of the mature protein. Since the calcium ion concentration in the cytoplasm is extremely low (300–500 nM), in contrast, usually to a mM range in the extracellular space (Jones et al., 1999) this is a simple but very efficient mechanism to prevent folding of the polypeptide inside the cell, whilst promoting folding once the protein has left the secretion apparatus (Sotomayor-Perez et al., 2011).

6. Structural analysis of the HlyB-CLD

The first crystal structure of an isolated C39 domain of the ABC transporter ComA (ComA-PEP), which translocates the

bacteriocin ComC, was reported in 2010 (Ishii et al., 2010). Two more crystal structures of C39 domains have been deposited in the pdb (www.rcsb.org), but not yet published. The structure of ComA-PEP revealed the basic architecture of a C39 peptidase and the arrangement of the catalytic triad; composed of the expected cysteine, histidine and aspartate residues. Based on this structure, the authors generated a model of the ComA-PEP/substrate complex and identified residues within ComA-PEP important for recognition of the consensus sequence N-LSXXELXXIXGG-C, where X can be any amino acid (Dirix et al., 2004; Havarstein et al., 1995). This model was verified by site-directed mutagenesis and biochemical assays (Ishii et al., 2010). Thus, we have now a rather detailed picture of how a C39 domain recognises conserved residues of the leader sequence located N-terminal to the GG motif and the nature of the catalytic mechanism that cleaves C-terminal to the highly conserved GG motif.

The solution structure of the isolated CLD of the ABC transporter HlyB (HlyB-CLD) revealed overall a three-dimensional structure very similar to that of ComA-PEP (Lecher et al., 2012). As expected from the sequence analysis of HlyB-CLD, a tyrosine residue (Tyr⁹) replaces the catalytically essential cysteine residue. While the aspartate residue of the catalytic triad was conserved in space, the histidine forming the proton relay system was flipped out of the active site through π – π stacking with a tryptophane residue. This interaction removes the histidine from the active site and a simple re-introduction of a cysteine residue at position 9 of the HlyB-CLD did not restore proteolytic activity, a result that could not be explained in the absence of the structure. Furthermore, a phylogenetic analysis revealed that the tryptophane residue is always conserved in CLDs, but absent in C39 domains (Lecher et al., 2012). This arrangement, His–no Cys and Trp (CLD) versus His–Cys and no Trp (C39 domain) might serve as a diagnostic tool in the future to identify the substrate of an ABC transporter involved in Type I secretion.

Importantly, NMR experiments combined with site-directed mutagenesis and functional studies (i.e. secretion efficiency) revealed that in the CLD the substrate-binding region (Lecher et al., 2012) is positioned on the opposite side of the domain relative to the peptide-binding site of the C39 domain (Ishii et al., 2010). Moreover, as indicated above, C39 domains recognise the consensus sequence N-LSXXELXXIXGG-C within the leader peptide of the substrate (Dirix et al., 2004; Havarstein et al., 1995). Such a recognition motif is apparently absent in RTX domains. Rather, the only detectable conserved motif is located C-terminal to the GG-pairs, the Ca^{2+} -binding motif N-GGXGXDXUX-C (Welch, 2001). Consequently, even though the C39 domain and the CLD show high structural homology, the CLD does not bind to GG motifs and furthermore, the binding site for peptides in the classical C39 domain is not involved in binding the HlyA molecule.

Lecher et al. specified that the ABC transporters, which are dedicated to the transport of RTX toxins, all contain a CLD (Lecher et al., 2012). RTX proteins are rather large, greater than 50 kDa in size, and frequently more than 1000 kDa. This raises the question, how a protein of such size remains

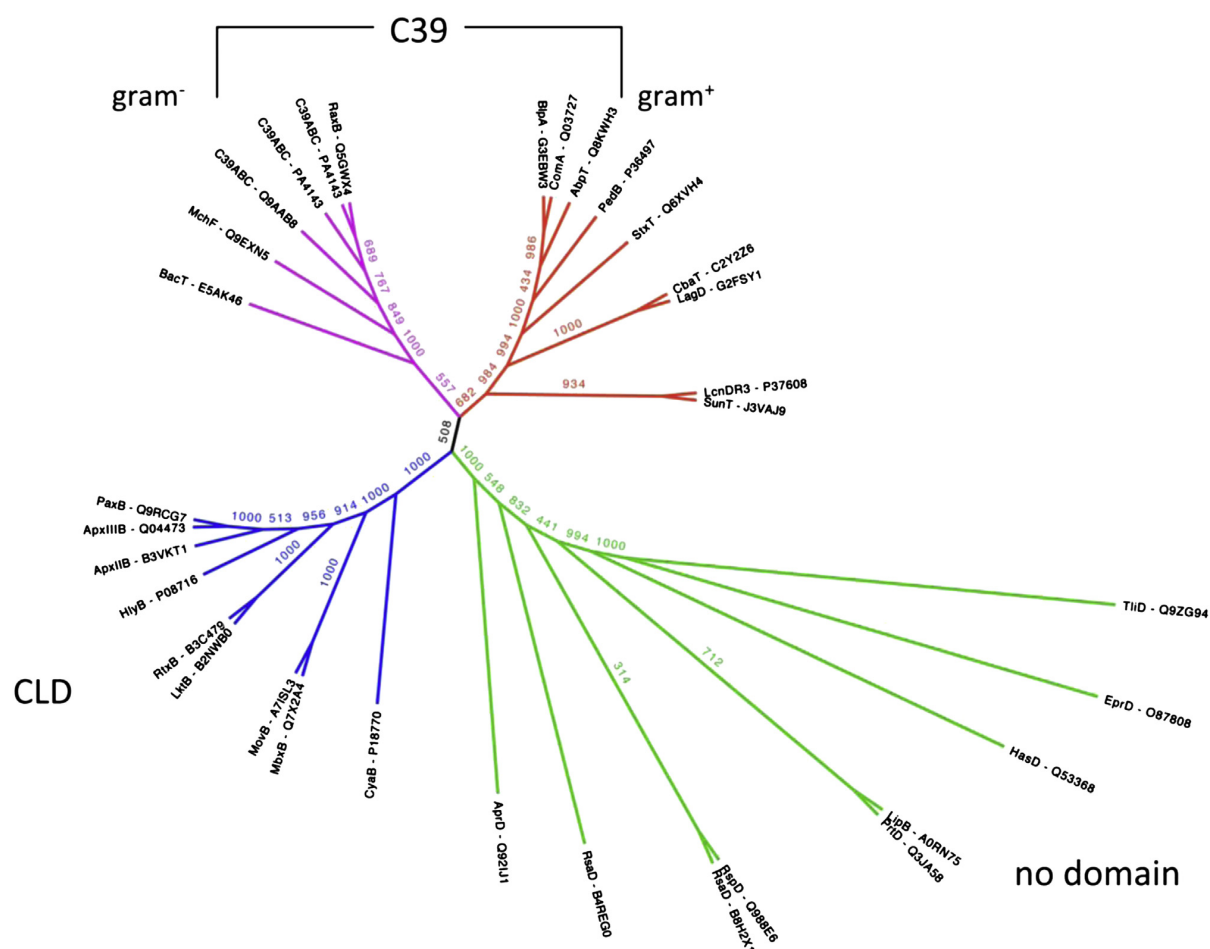


Fig. 3. Phylogenetic analysis of ABC transporters involved in TISS. Sequences were aligned using MAFFT (Kato and Toh, 2008) using the default parameters. A phylogenetic tree was reconstructed with PhyML3 (Guindon et al., 2010) using the best fit model as inferred with ProtTest3 (Darriba et al., 2011) by the AIC measure. A bootstrap analysis was performed with 1000 repeats, values are given on the branches. Further details are provided in the text.

unfolded and without aggregation in the cytoplasm, until its C-terminal secretion signal is synthesised on the ribosome. The intervention of a dedicated “chaperone molecule” has never been shown but the interaction of the N-terminal part of the substrate with the CLD suggests that this role is taken over by the CLD to prevent the protein’s aggregation or degradation in the cytosol (Lecher et al., 2012). This would explain why a degenerated appendix (CLD versus C39) of an ABC transporter has been retained during evolution.

7. Group 3: ABC transporters without appendix

Some TISS ABC transporters are composed simply of the canonical domains generally described for ABC transporters. These ABC transporters do not contain any additional N-terminal domains and their substrates may contain RTX repeats but no N-terminal leader peptide. Most peptides secreted by this group of ABC transporters are rather small in size (compared to RTX proteins) and exhibit a hydrolytic activity, for example, proteases or lipases (Delepelaire, 2004; Holland et al., 2003).

A very well-characterised example in this group is the secretion system of HasA, a 19 kDa iron scavenger protein secreted by *S. marcescens* under iron starving conditions. The active haemophore binds free or haeme-bound iron in the extracellular space and delivers it to specific receptors on the host cell’s surface (Létoffé et al., 1994). The whole secretion system consists of the ABC transporter HasD, the MFP HasE and the OMF HasF, a TolC analogue found in *S. marcescens* (Binet and Wandersman, 1996).

As mentioned above, HasA does not belong to the RTX family, since it does not contain any RTX domains. However, like RTX protein exporting systems, the secretion signal is located in the C-terminal moiety of the protein (Delepelaire, 2004). The last 29 residues of PrtG, a protease secreted by a TISS, are sufficient to promote its secretion (Sapriel et al., 2002). On the other hand, Masi et al. demonstrated in an elegant set of experiments (Masi and Wandersman, 2010), that HasA contains additional regions, so-called “primary anchor sites” that are required for interaction with the ABC transporter and necessary for efficient secretion. This strongly suggests that even Type I ABC transporters such as HasD,

lacking an N-terminal appendix (C39 or CLD), still interact with their substrates independently of the secretion signal. However, the exact regions within HasA that interact with the ABC transporter have not yet been identified.

A striking difference of the HasA secretion system compared to other TISS described so far is the requirement for the general chaperone SecB (Delepelaire and Wandersman, 1998). SecB interacts with the N-terminal portion of the translated HasA in the cytoplasm and prevents folding of the peptide, a state which was shown to be incompatible with secretion (Sapriel et al., 2002, 2003). In the absence of SecB secretion of HasA is completely abolished and HasA accumulates in the cytosol (Sapriel et al., 2003). Compared to RTX proteins, where folding in the cytoplasm does not occur due to the lack of calcium ions, HasA rapidly adopts its tertiary structure in the cytosol; a fact, which explains the need for the “anti-folding” activity of SecB (Debarbieux and Wandersman, 2001). HasA is so far the only example where an involvement of SecB has been proven. However, considering the hypothesised chaperone activity of the additional N-terminal domains of the other TISS ABC transporters it seems likely that also in this specific TISS group a chaperone is needed to ensure the unfolded state of the protein prior to secretion. Hence, the involvement of SecB in these TISS without N-terminal appendices cannot be ruled out.

8. Phylogenetic analysis

Sequences of 38 different ABC transporters, which were identified by performing a blast for ABC transporters with or without CLD or C39 domain, were aligned using the program MAFFT (Katoh and Toh, 2008). A phylogenetic tree (Fig. 3) was calculated using the maximum likelihood program PhyML3 (Guindon et al., 2010).

The resulting tree presents three groups of ABC transporters, separated on the basis of their N-terminal domains. This separation agrees clearly with the three distinct groups of TISS ABC transporters described above. Since most of the substrates of the aligned ABC transporters are known, this tree also confirms that CLD ABC transporters export RTX proteins whereas C39 ABC transporters are dedicated to bacteriocins in Gram-positive or microcins in Gram-negative bacteria. The transporters without an N-terminal appendix transport mainly lipases and proteases from Gram-negative bacteria while the C39 ABC transporters contain proteins mainly from Gram-positive bacteria.

9. Conclusions

Due to their similarity in structure and function it seems likely that the CLD has evolved from the C39 domain, even though they differ greatly in their exhibited functions. The phylogenetic analysis also indicates that the segregation of the group of C39 ABC transporters occurred before the segregation of Gram-positive and Gram-negative bacteria, explaining the presence of some C39 transporters in Gram-negative bacteria. The underlying principles of interaction might be

preserved. In the first group, the leader sequence interacts with the C39 domain. In the second group, the RTX domain interacts with the CLD. Interestingly, such interaction is also present in TISS lacking any additional N-terminal domain, here a chaperone like SecB might be generally present. This suggests that the basic principles in all three groups of ABC transporters share many mechanistic similarities.

Acknowledgments

We thank all current and former lab members for contributing to our research on the haemolysin system and apologise to all persons whose work was not properly cited due to space limitations. We are indebted to Barry Holland, University of Paris-Sud for a longstanding and extremely fruitful collaboration. The DFG, EU and Heinrich Heine University Düsseldorf funded research in our lab.

References

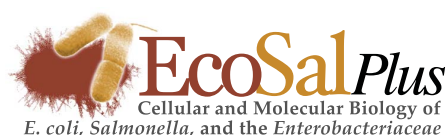
- Akama, H., Matsuura, T., Kashiwagi, S., Yoneyama, H., Narita, S., Tsukihara, T., Nakagawa, A., Nakae, T., 2004. Crystal structure of the membrane fusion protein, MexA, of the multidrug transporter in *Pseudomonas aeruginosa*. *J. Biol. Chem.* 279, 25939–25942.
- Akatsuka, H., Kawai, E., Omori, K., Shibata, T., 1995. The three genes lipB, lipC, and lipD involved in the extracellular secretion of the *Serratia marcescens* lipase which lacks an N-terminal signal peptide. *J. Bacteriol.* 177, 6381–6389.
- Arnoux, P., Haser, R., Izadi, N., Lecroisey, A., Delepierre, M., Wandersman, C., Czjzek, M., 1999. The crystal structure of HasA, a hemophore secreted by *Serratia marcescens*. *Nat. Struct. Biol.* 6, 516–520.
- Awram, P., Smit, J., 1998. The *Caulobacter crescentus* paracrystalline S-layer protein is secreted by an ABC transporter (type I) secretion apparatus. *J. Bacteriol.* 180, 3062–3069.
- Bakkes, P.J., Jenewein, S., Smits, S.H., Holland, I.B., Schmitt, L., 2010. The rate of folding dictates substrate secretion by the *Escherichia coli* hemolysin type I secretion system. *J. Biol. Chem.* 285, 40573–40580.
- Balakrishnan, L., Hughes, C., Koronakis, V., 2001. Substrate-triggered recruitment of the TolC channel-tunnel during type I export of hemolysin by *Escherichia coli*. *J. Mol. Biol.* 313, 501–510.
- Baumann, U., Wu, S., Flaherty, K.M., McKay, D.B., 1993. Three-dimensional structure of the alkaline protease of *Pseudomonas aeruginosa*: a two-domain protein with a calcium binding parallel beta roll motif. *EMBO J.* 12, 3357–3364.
- Benabdelhak, H., Kiontke, S., Horn, C., Ernst, R., Blight, M.A., Holland, I.B., Schmitt, L., 2003. A specific interaction between the NBD of the ABC-transporter HlyB and a C-terminal fragment of its transport substrate hemolysin A. *J. Mol. Biol.* 327, 1169–1179.
- Binet, R., Wandersman, C., 1996. Cloning of the *Serratia marcescens* hasF gene encoding the Has ABC exporter outer membrane component: a TolC analogue. *Mol. Microbiol.* 22, 265–273.
- Bleves, S., Viarre, V., Salacha, R., Michel, G.P., Filloux, A., Voulhoux, R., 2010. Protein secretion systems in *Pseudomonas aeruginosa*: a wealth of pathogenic weapons. *Int. J. Med. Microbiol.* 300, 534–543.
- Chen, J., Lu, G., Lin, J., Davidson, A.L., Quijcho, F.A., 2003. A tweezers-like motion of the ATP-binding cassette dimer in an ABC transport cycle. *Mol. Cell.* 12, 651–661.
- Chervaux, C., Holland, I.B., 1996. Random and directed mutagenesis to elucidate the functional importance of helix II and F-989 in the C-terminal secretion signal of *Escherichia coli* hemolysin. *J. Bacteriol.* 178, 1232–1236.
- Darriba, D., Taboada, G.L., Doallo, R., Posada, D., 2011. ProtTest 3: fast selection of best-fit models of protein evolution. *Bioinformatics* 27, 1164–1165.

- Davidson, A.L., Dassa, E., Orelle, C., Chen, J., 2008. Structure, function, and evolution of bacterial ATP-binding cassette systems. *Microbiol. Mol. Biol. Rev.* 72, 317–364.
- Debarbieux, L., Wandersman, C., 2001. Folded HasA inhibits its own secretion through its ABC exporter. *EMBO J.* 20, 4657–4663.
- Delepelaire, P., 2004. Type I secretion in gram-negative bacteria. *Biochim. Biophys. Acta* 1694, 149–161.
- Delepelaire, P., Wandersman, C., 1998. The SecB chaperone is involved in the secretion of the *Serratia marcescens* HasA protein through an ABC transporter. *EMBO J.* 17, 936–944.
- Dirix, G., Monsieurs, P., Dombrecht, B., Daniels, R., Marchal, K., Vanderleyden, J., Michiels, J., 2004. Peptide signal molecules and bacteriocins in Gram-negative bacteria: a genome-wide in silico screening for peptides containing a double-glycine leader sequence and their cognate transporters. *Peptides* 25, 1425–1440.
- du Plessis, D.J., Nouwen, N., Driessen, A.J., 2011. The Sec translocase. *Biochim. Biophys. Acta* 1808, 851–865.
- Duong, F., Lazdunski, A., Cami, B., Murgier, M., 1992. Sequence of a cluster of genes controlling synthesis and secretion of alkaline protease in *Pseudomonas aeruginosa*: relationships to other secretory pathways. *Gene* 121, 47–54.
- Duquesne, S., Destoumieux-Garzon, D., Peduzzi, J., Rebuffat, S., 2007a. Microcins, gene-encoded antibacterial peptides from enterobacteria. *Nat. Prod. Rep.* 24, 708–734.
- Duquesne, S., Petit, V., Peduzzi, J., Rebuffat, S., 2007b. Structural and functional diversity of microcins, gene-encoded antibacterial peptides from enterobacteria. *J. Mol. Microbiol. Biotechnol.* 13, 200–209.
- Economou, A., Christie, P.J., Fernandez, R.C., Palmer, T., Plano, G.V., Pugsley, A.P., 2006. Secretion by numbers: protein traffic in prokaryotes. *Mol. Microbiol.* 62, 308–319.
- Espinosa-Urgel, M., Salido, A., Ramos, J.L., 2000. Genetic analysis of functions involved in adhesion of *Pseudomonas putida* to seeds. *J. Bacteriol.* 182, 2363–2369.
- Fath, M.J., Zhang, L.H., Rush, J., Kolter, R., 1994. Purification and characterization of colicin V from *Escherichia coli* culture supernatants. *Biochemistry* 33, 6911–6917.
- Gebhard, S., 2012. ABC transporters of antimicrobial peptides in Firmicutes bacteria – phylogeny, function and regulation. *Mol. Microbiol.* 86, 1295–1317.
- Gilson, L., Mahanty, H.K., Kolter, R., 1987. Four plasmid genes are required for colicin V synthesis, export, and immunity. *J. Bacteriol.* 169, 2466–2470.
- Gilson, L., Mahanty, H.K., Kolter, R., 1990. Genetic analysis of an MDR-like export system: the secretion of colicin V. *EMBO J.* 9, 3875–3884.
- Gray, L., Baker, K., Kenny, B., Mackman, N., Haigh, R., Holland, I.B., 1989. A novel C-terminal signal sequence targets *Escherichia coli* haemolysin directly to the medium. *J. Cell. Sci. Suppl.* 11, 45–57.
- Guindon, S., Dufayard, J.F., Lefort, V., Anisimova, M., Hordijk, W., Gascuel, O., 2010. New algorithms and methods to estimate maximum-likelihood phylogenies: assessing the performance of PhyML 3.0. *Syst. Biol.* 59, 307–321.
- Guzzo, J., Duong, F., Wandersman, C., Murgier, M., Lazdunski, A., 1991. The secretion genes of *Pseudomonas aeruginosa* alkaline protease are functionally related to those of *Erwinia chrysanthemi* proteases and *Escherichia coli* alpha-haemolysin. *Mol. Microbiol.* 5, 447–453.
- Havarstein, L.S., Diep, D.B., Nes, I.F., 1995. A family of bacteriocin ABC transporters carry out proteolytic processing of their substrates concomitant with export. *Mol. Microbiol.* 16, 229–240.
- Higgins, M.K., Bokma, E., Koronakis, E., Hughes, C., Koronakis, V., 2004. Structure of the periplasmic component of a bacterial drug efflux pump. *Proc. Natl. Acad. Sci. U.S.A.* 101, 9994–9999.
- Hinsa, S.M., Espinosa-Urgel, M., Ramos, J.L., O'Toole, G.A., 2003. Transition from reversible to irreversible attachment during biofilm formation by *Pseudomonas fluorescens* WCS365 requires an ABC transporter and a large secreted protein. *Mol. Microbiol.* 49, 905–918.
- Holland, I.B., Benabdelhak, H., Young, J., De Lima Pimenta, A., Schmitt, L., Blight, M.A., 2003. Bacterial ABC transporters involved in protein translocation. In: Holland, I.B., Cole, S.P., Kuchler, K., Higgins, C. (Eds.), *ABC Proteins: From Bacteria to Man*. Academic Press, London, pp. 209–241.
- Holland, I.B., Schmitt, L., Young, J., 2005. Type 1 protein secretion in bacteria, the ABC-transporter dependent pathway (review). *Mol. Memb. Biol.* 22, 29–39.
- Hollenstein, K., Dawson, R.J., Locher, K.P., 2007. Structure and mechanism of ABC transporter proteins. *Curr. Opin. Struct. Biol.* 17, 412–418.
- Huber, P., Schmitz, T., Griffin, J., Jacobs, M., Walsh, C., Furie, B., Furie, B.C., 1990. Identification of amino acids in the gamma-carboxylation recognition site on the propeptide of prothrombin. *J. Biol. Chem.* 265, 12467–12473.
- Ishii, S., Yano, T., Ebihara, A., Okamoto, A., Manzoku, M., Hayashi, H., 2010. Crystal structure of the peptidase domain of *Streptococcus* ComA, a bifunctional ATP-binding cassette transporter involved in the quorum-sensing pathway. *J. Biol. Chem.* 285, 10777–10785.
- Jardetzky, O., 1966. Simple allosteric model for membrane pumps. *Nature* 211, 969–970.
- Jones, H.E., Holland, I.B., Baker, H.L., Campbell, A.K., 1999. Slow changes in cytosolic free Ca^{2+} in *Escherichia coli* highlight two putative influx mechanisms in response to changes in extracellular calcium. *Cell Calcium* 25, 265–274.
- Jones, P.M., O'Mara, M.L., George, A.M., 2009. ABC transporters: a riddle wrapped in a mystery inside an enigma. *TIBS* 34, 520–531.
- Katoh, K., Toh, H., 2008. Recent developments in the MAFFT multiple sequence alignment program. *Brief. Bioinform.* 9, 286–298.
- Kenny, B., Chervaux, C., Holland, I.B., 1994. Evidence that residues -15 to -46 of the haemolysin secretion signal are involved in early steps in secretion, leading to recognition of the translocator. *Mol. Microbiol.* 11, 99–109.
- Kenny, B., Taylor, S., Holland, I.B., 1992. Identification of individual amino acids required for secretion within the haemolysin (HlyA) C-terminal targeting region. *Mol. Microbiol.* 6, 1477–1489.
- Koronakis, V., Sharff, A., Koronakis, E., Luisi, B., Hughes, C., 2000. Crystal structure of the bacterial membrane protein TolC central to multidrug efflux and protein export. *Nature* 405, 914–919.
- Lecher, J., Schwarz, C.K., Stoldt, M., Smits, S.H., Willbold, D., Schmitt, L., 2012. An RTX transporter tethers its unfolded substrate during secretion via a unique N-terminal domain. *Structure* 20, 1778–1787.
- Letoffe, S., Delepelaire, P., Wandersman, C., 1990. Protease secretion by *Erwinia chrysanthemi*: the specific secretion functions are analogous to those of *Escherichia coli* alpha-haemolysin. *EMBO J.* 9, 1375–1382.
- Letoffe, S., Delepelaire, P., Wandersman, C., 1996. Protein secretion in gram-negative bacteria: assembly of the three components of ABC protein-mediated exporters is ordered and promoted by substrate binding. *EMBO J.* 15, 5804–5811.
- Létoffé, S., Ghigo, J.M., Wandersman, C., 1994. Secretion of the *Serratia marcescens* HasA protein by an ABC transporter. *J. Bacteriol.* 176, 5372–5377.
- Linhartova, I., Bumba, L., Masin, J., Basler, M., Osicka, R., Kamanova, J., Prochazkova, K., Adkins, I., et al., 2010. RTX proteins: a highly diverse family secreted by a common mechanism. *FEMS Microbiol. Rev.* 34, 1076–1112.
- Lycklama, A.N.J.A., Driessen, A.J., 2012. The bacterial Sec-translocase: structure and mechanism. *Philos. Trans. R. Soc. London* 367, 1016–1028.
- Mackman, N., Nicaud, J.M., Gray, L., Holland, I.B., 1985. Identification of polypeptides required for the export of haemolysin 2001 from *E. coli*. *Mol. Gen. Genet.* 201, 529–536.
- Masi, M., Wandersman, C., 2010. Multiple signals direct the assembly and function of a type 1 secretion system. *J. Bacteriol.* 192, 3861–3869.
- Mikolosko, J., Bobyk, K., Zgurskaya, H.I., Ghosh, P., 2006. Conformational flexibility in the multidrug efflux system protein AcrA. *Structure* 14, 577–587.
- Nakashima, R., Sakurai, K., Yamasaki, S., Nishino, K., Yamaguchi, A., 2011. Structures of the multidrug exporter AcrB reveal a proximal multisite drug-binding pocket. *Nature* 480, 565–569.
- Nicaud, J.M., Mackman, N., Gray, L., Holland, I.B., 1985. Regulation of haemolysin synthesis in *E. coli* determined by HLY genes of human origin. *Mol. Gen. Genet.* 199, 111–116.
- Oswald, C., Holland, I.B., Schmitt, L., 2006. The motor domains of ABC-transporters/what can structures tell us? *Naunyn Schmiedeberg's Arch. Pharmacol.* 372, 385–399.

- Pimenta, A.L., Young, J., Holland, I.B., Blight, M.A., 1999. Antibody analysis of the localisation, expression and stability of HlyD, the MFP component of the *E. coli* haemolysin translocator. *Mol. Gen. Genet.* 261, 122–132.
- Pos, K.M., 2009. Drug transport mechanism of the AcrB efflux pump. *Biochim. Biophys. Acta* 1794, 782–793.
- Sapriel, G., Wandersman, C., Delepelaire, P., 2002. The N terminus of the HasA protein and the SecB chaperone cooperate in the efficient targeting and secretion of HasA via the ATP-binding cassette transporter. *J. Biol. Chem.* 277, 6726–6732.
- Sapriel, G., Wandersman, C., Delepelaire, P., 2003. The SecB chaperone is bifunctional in *Serratia marcescens*: SecB is involved in the Sec pathway and required for HasA secretion by the ABC transporter. *J. Bacteriol.* 185, 80–88.
- Satchell, K.J., 2011. Structure and function of MARTX toxins and other large repetitive RTX proteins. *Annu. Rev. Microbiol.* 65, 71–90.
- Sheps, J.A., Cheung, I., Ling, V., 1995. Hemolysin transport in *Escherichia coli* — point mutants in hlyB compensate for a deletion in the predicted amphiphilic helix region of the hlyA signal. *J. Biol. Chem.* 270, 14829–14834.
- Smit, J., Engelhardt, H., Volker, S., Smith, S.H., Baumeister, W., 1992. The S-layer of *Caulobacter crescentus*: three-dimensional image reconstruction and structure analysis by electron microscopy. *J. Bacteriol.* 174, 6527–6538.
- Smith, P.C., Karpowich, N., Millen, L., Moody, J.E., Rosen, J., Thomas, P.J., Hunt, J.F., 2002. ATP binding to the motor domain from an ABC transporter drives formation of a nucleotide sandwich dimer. *Mol. Cell.* 10, 139–149.
- Sotomayor-Perez, A.C., Ladant, D., Chenal, A., 2011. Calcium-induced folding of intrinsically disordered repeat-in-toxin (RTX) motifs via changes of protein charges and oligomerization states. *J. Biol. Chem.* 286, 16997–17004.
- Su, C.C., Long, F., Zimmermann, M.T., Rajashankar, K.R., Jernigan, R.L., Yu, E.W., 2011. Crystal structure of the CusBA heavy-metal efflux complex of *Escherichia coli*. *Nature* 470, 558–562.
- Su, C.C., Yang, F., Long, F., Reyon, D., Routh, M.D., Kuo, D.W., Mokhtari, A.K., Van Ornam, J.D., et al., 2009. Crystal structure of the membrane fusion protein CusB from *Escherichia coli*. *J. Mol. Biol.* 393, 342–355.
- Thanabalu, T., Koronakis, E., Hughes, C., Koronakis, V., 1998. Substrate-induced assembly of a contiguous channel for protein export from *E. coli*: reversible bridging of an inner-membrane translocase to an outer membrane exit pore. *EMBO J.* 17, 6487–6496.
- Wandersman, C., Delepelaire, P., 1990. TolC, an *Escherichia coli* outer membrane protein required for hemolysin secretion. *Proc. Natl. Acad. Sci. U.S.A.* 87, 4776–4780.
- Welch, R.A., 2001. RTX toxin structure and function: a story of numerous anomalies and few analogies in toxin biology. *Curr. Top. Microbiol. Immunol.* 257, 85–111.
- Welch, R.A., Dellinger, E.P., Minshew, B., Falkow, S., 1981. Haemolysin contributes to virulence of extra-intestinal *E. coli* infections. *Nature* 294, 665–667.
- Wu, K.H., Hsieh, Y.H., Tai, P.C., 2012. Mutational analysis of Cvab, an ABC transporter involved in the secretion of active colicin V. *PloS One* 7, e35382.
- Wu, K.H., Tai, P.C., 2004. Cys32 and His105 are the critical residues for the calcium-dependent cysteine proteolytic activity of CvaB, an ATP-binding cassette transporter. *J. Biol. Chem.* 279, 901–909.
- Xu, Z.J., Moffett, D.B., Peters, T.R., Smith, L.D., Perry, B.P., Whitmer, J., Stokke, S.A., Teintze, M., 1995. The role of the leader sequence coding region in expression and assembly of bacteriorhodopsin. *J. Biol. Chem.* 270, 24858–24863.
- Yin, Y., Zhang, F., Ling, V., Arrowsmith, C.H., 1995. Structural analysis and comparison of the C-terminal transport signal domains of hemolysin A and leukotoxin A. *FEBS Lett.* 366, 1–5.
- Zaitseva, J., Jenewein, S., Jumpertz, T., Holland, I.B., Schmitt, L., 2005. H662 is the linchpin of ATP hydrolysis in the nucleotide-binding domain of the ABC transporter HlyB. *EMBO J.* 24, 1901–1910.

3.2 Chapter II – Mechanistic Variability of Type I Secretion Systems

Title:	Type I Protein Secretion – Deceptively Simple yet with a Wide Range of Mechanistic Variability across the Family
Authors:	Barry Holland, Sandra Peherstorfer, Kerstin Kanonenberg, Michael Lenders, Sven Reimann, Lutz Schmitt
Published in:	<i>EcoSal Plus</i> (2016)
Impact Factor:	3.471
Own Work:	10 % Writing of the manuscript



DOMAIN 4 SYNTHESIS AND PROCESSING OF MACROMOLECULES

Type I Protein Secretion— Deceptively Simple yet with a Wide Range of Mechanistic Variability across the Family

I. BARRY HOLLAND,¹ SANDRA PEHERSTORFER,² KERSTIN KANONENBERG,² MICHAEL LENDERS,² SVEN REIMANN,² AND LUTZ SCHMITT^{2,3}

¹Institute for Integrative Biology (I2BC) and Institute of Genetics and Microbiology, University Paris-Sud, Orsay 91450, France

²Institute of Biochemistry, Heinrich Heine University, 40225 Düsseldorf, Germany

³Center of Excellence on Plant Sciences (CEPLAS), Heinrich Heine University, 40225 Düsseldorf, Germany

Received: 24 November 2015

Accepted: 27 September 2016

Posted: 13 December 2016

Editors: Susan T. Lovett, Brandeis University, Waltham, MA; Harris D. Bernstein, National Institutes of Health, Bethesda, MD

Citation: EcoSal Plus 2013; doi:10.1128/ecosalplus.ESP-0019-2015.

Correspondence: I. Barry Holland, ian-barry.holland@u-psud.fr; Lutz Schmitt, lutz.schmitt@hhu.de

Copyright: © 2016 American Society for Microbiology. All rights reserved. doi:10.1128/ecosalplus.ESP-0019-2015

ABSTRACT A very large type I polypeptide begins to reel out from a ribosome; minutes later, the still unidentifiable polypeptide, largely lacking secondary structure, is now in some cases a thousand or more residues longer. Synthesis of the final hundred C-terminal residues commences. This includes the identity code, the secretion signal within the last 50 amino acids, designed to dock with a waiting ATP binding cassette (ABC) transporter. What happens next is the subject of this review, with the main, but not the only focus on hemolysin HlyA, an RTX protein toxin secreted by the type I system. Transport substrates range from small peptides to giant proteins produced by many pathogens. These molecules, without detectable cellular chaperones, overcome enormous barriers, crossing two membranes before final folding on the cell surface, involving a unique autocatalytic process.

Unfolded HlyA is extruded posttranslationally, C-terminal first. The transenvelope “tunnel” is formed by HlyB (ABC transporter), HlyD (membrane fusion protein) straddling the inner membrane and periplasm and TolC (outer membrane). We present a new evaluation of the C-terminal secretion code, and the structure function of HlyD and HlyB at the heart of this nanomachine. Surprisingly, key details of the secretion mechanism are remarkably variable in the many type I secretion system subtypes. These include alternative folding processes, an apparently distinctive secretion code for each type I subfamily, and alternative forms of the ABC transporter; most remarkably, the ABC protein probably transports peptides or polypeptides by quite different mechanisms. Finally, we suggest a putative structure for the Hly-translocon, HlyB, the multijointed HlyD, and the TolC exit.

INTRODUCTION: THE T1SS FAMILY

The broad family of ATP binding cassette (ABC) transporters found in all kingdoms of life was first detected in *Escherichia coli* as a curiously heterogeneous group of membrane proteins (1). Most of these were importers of

Holland et al.

a variety of small molecules, but surprisingly one was an exporter, HlyB (hemolysin B), that became the prototype of the type I secretion system (T1SS) for translocation of bacterial proteins. This is sometimes also referred to as the ABC-dependent export system. The T1SS can minimally be defined as secreting polypeptides carrying a C-terminal secretion signal and requiring an ABC transporter, with its characteristically highly conserved ATPase domain. As we shall discuss in detail in this review, the T1SS, at least in Gram-negative bacteria, in addition to an ABC transporter, requires a membrane fusion protein (MFP), also embedded in the inner membrane, but reaching across the periplasm to contact a specific outer membrane protein (OMP) to complete the translocon. A more strict definition of the T1SS, but still covering the great majority of known types, includes the requirement that the transport substrate, or allocrite as we shall interchangeably term it, contains multiple calcium ion binding sites. Thus, the most studied and the first group of these secreted proteins to be identified was the repeat in toxins (RTX) family (2–4), containing a varying number of very similar nonapeptide calcium ion binding repeats. These are implicated in the secretion process and located 100 to 200 residues upstream of the secretion signal. The RTX motifs form a unique β -roll structure with aspartate and glycine residues involved in calcium ion binding (5) and, as described in reference 6, over 1,000 RTX proteins are easily detected by a bioinformatic screen of databases.

For other recent general background reviews on different aspects of T1SS, see Linhartova et al. (6), Holland et al. (7), Thomas et al. (8), Lenders et al. (9), the review by Delepelaire, with a survey of a wide range of organisms having the T1SS (10), as well as a comprehensive review by Durand et al. (11) considering the possibilities of this and other protein secretion systems as antibacterial targets. Concerning the regulation of expression of the *hly* determinant and the mode of action of HlyA, there are recent reviews (8, 12), and these topics will not be considered here.

Pathogenicity Factors

RTX proteins include major pathogenicity factors carried by many important pathogens in mammals, insects, and plants. Urinary tract infections are the most common bacterial infections, particularly in females. Although generally easy to treat, severe infection can lead to pyelonephritis. Uropathogenic *E. coli* (UPEC) strains

usually producing the prototype RTX protein, hemolysin A (hemolysin), are the most frequent cause of the disease. New exciting *in vivo* studies, for example, by the Hultgren group, using mouse models and human cell lines, are revealing how expression is regulated during infection by UPEC strains and how HlyA promotes urothelial cell death (13). Some of the other most studied type I proteins secreted by Gram-negative pathogens include, as well as the hemolysins, adenylate cyclase (CyaA [14]) secreted by *Bordetella pertussis* (whooping cough), proteases and lipases secreted by *Pseudomonas* and other Gram-negative species, and other toxins secreted by *E. coli* strains (EHEC [15]). In addition, the newly described T1SS members with giant allocrites (16), the multifunctional-autoprocessing repeats in toxins (MARTX family) are found in chromosomal islands of major human pathogens. This family of extremely large polypeptides (in the range 5,000 to 9,000 kDa) have been described primarily so far from the pathogenicity viewpoint, with very little known about secretion. These include the multitoxin MARTX Vc, encoded by *rtxA_{Vc}* from *Vibrio cholerae* (16–18), and a giant adhesin, LapA, an RTX protein from *Pseudomonas fluorescens*, recently described by Boyd et al. (19). More intriguing, as described later, another giant adhesin, SiiE, containing a completely unrelated set of Ca^{2+} repeats (20), is nevertheless secreted from *Salmonella enterica* via a T1SS. Very recently, a fascinating possibility has also emerged, indicating that the T1SS exists in the obligate parasitic family *Rickettsiaceae*. This T1SS apparently secretes several types of ankyrin proteins that appear to have no Ca^{2+} binding motifs at all (see below).

Peptide Transport

T1SS is also responsible for transport of a huge range of peptides up to approximately 10 kDa, widespread in bacteria (see reviews [21, 22]). However, while transport of these peptides depends on ABC transporters, the secretion signal is located at the N terminus. Secretion of such antibacterial peptides, microcins, bacteriocins, antibiotics, and signaling molecules such as pheromones, has been reported in both Gram-negative and Gram-positive bacteria with frequencies of 33% and 44%, respectively. In Gram-positive strains, a stripped down form of the T1SS, lacking the MFP homologue, is employed. Regrettably, coverage of these fascinating transport systems in this review was not possible and we had also to limit ourselves primarily to T1SS associated with polypeptide transport in Gram-negative bacteria. How-

ever, the recently described crystal structures of ABC transporters for the microcin J25 (MccJ25) from *E. coli* and a peptide from *Clostridium thermocellum* constitute a major advance and, as we shall describe later, an important frame of reference in developing secretion models for the larger polypeptides.

Some General Characteristics of the Type I Proteins

Type I polypeptide-allocries are also almost invariably characterized by having few if any cysteines, being very acidic, with pI values frequently below pH 5. In contrast, these proteins are distributed over an enormous range of sizes, extending from less than 100 to 9,000 amino acids. These latter include some adhesins and others packaging a lethal string of distinct toxins that penetrate host cells before the individual toxins are released by an autoproteolytic process (17, 23). However, all these proteins, at least in the Gram-negative bacteria discussed here, are secreted by an ABC/MFP/OMP translocon, the secretion signal is at the C terminus, and the great majority have RTX repeats of some kind. Some MARTX proteins at least are also characterized by a very large number of other types of repeats (not Ca^{2+} binding), especially toward the N terminus. These repeats are also relatively glycine rich, with an apparently conserved core consensus sequence. Recently, Kim et al. (24) showed that, while not required for secretion by the pathogen *Vibrio vulnificus*, these N-terminal repeats are required for subsequent translocation into the cytosol of the host cell. The MARTX proteins and other novel groups secreted via the T1SS will be discussed in more detail later.

Surprising Variation in the Details of the Secretion Process across the T1SS Family

In our experience, writing a review does not usually mean taking successive short time-outs to revisit some questions, even at the bench, to test new ideas as they arise. Doing this has certainly added stimulation and enjoyment, and we hope that it has produced a better review. Thus, a major theme that developed as we wrote the review is the remarkable way in which we now see the T1SS appearing in many different forms in the bacterial world, for reasons that are not always clear.

Bacterial Protein Secretion Is a Relatively Recent Discovery

In the period up to about 1980, no bacterial protein secretion system had been characterized, and how such

proteins reached the exterior was a mystery. Toxins such as a hemolysin released by Gram-negative bacteria were known, but the mechanism of secretion had not been investigated. Studies of the biogenesis of bacterial membranes were largely restricted to the model laboratory strain *E. coli* K12 that in fact does not secrete any proteins to the medium. Thus, interest in protein translocation was largely confined to unlocking the puzzle of the distinctive partitioning of proteins to the compartments of the cell envelope, inner and outer membranes and periplasm, i.e., the process dependent on the Sec translocon and targeted by an N-terminal “export” or “signal sequence.”

Emergence of a Myriad Secretion Systems

The first clear example of bacterial protein secretion studied in any detail was the secretion of a hemolysin discovered around 1980. This is still the most studied, and it is considered the prototype system. Remarkably, however, by the later 2000s, an amazing variety of protein secretion systems (for a recent review, see reference 25), at least 15 in Gram-negative bacteria had been identified, together with six in Gram-positive bacteria. Four of these systems, designated T1SS, 3, 4, and 6, apparently involve a transenvelope “tunnel,” secreting proteins directly from the cytoplasm to the exterior. The great majority, however, involve an initial step to cross the inner membrane dependent on the Sec system, with the subsequent step to negotiate the outer membrane, surprisingly involving many alternative strategies (for an excellent review series, see reference 26).

The First Authentic Reports of Bacterial Protein Secretion: *E. coli* Hemolysin

These appeared in the early 1950s, notably by Robinson (27) working in the Seamen’s Hospital, Greenwich, United Kingdom, who identified an *E. coli* toxin that was cell associated (nonfilterable), heat labile with calcium ion dependence for activity. However, an apparently truly secreted hemolysin, released from late-exponential phase cells, was only identified in the 1960s (28, 29). Pioneering the modern phase of hemolysin studies, in 1979, the group of Werner Goebel in Würzburg, Germany, cloned a cluster of 3 genes found on a plasmid from a pathogenic *E. coli* strain, and transferred this into an *E. coli* K12 laboratory strain. Thus, Noegel et al. (30) identified two genes required for production of the active hemolysin molecule and at least one gene encoding a transport function. Springer and Goebel (31) studied the process

Holland et al.

of release of active hemolysin from *E. coli* K12. These authors used inhibitors of energy metabolism and protease processing, together with cell fractionation, to distinguish extra- and intracellular hemolysin. They concluded that HlyA was secreted in an energy-dependent process via the periplasm and apparently involving processing of the protoxin to a 55-kDa form able to cross the outer membrane (see also reference 32). However, subsequent studies, benefitting from pulse-chase radiolabeling experiments and more detailed cellular fractionation analysis, quickly demonstrated that HlyA (with a relative mobility equivalent to 107 kDa) was not processed and was secreted directly to the medium (2, 33–35).

T1SS, A NOVEL TRANSENVELOPE SECRETION PROCESS

Introduction

The first sequencing (3) of an *hly* operon by the group of Rod Welch (Fig. 1) from a T1SS genetic determinant located in the chromosome (as are the great majority) of an *E. coli* O4 serotype strain, revealed a putative toxin gene *hlyA*. However, surprisingly, the sequence indicated

the absence of any classical N-terminal signal sequence able to target HlyA (calculated size 110 kDa) to the Sec translocon. Then several studies, including the analysis of another human chromosomal Hly determinant, LE2001 (34, 36, 37) studied by the Holland group, and the plasmid determinant, pHly152, studied first by W. Goebel, demonstrated that HlyA secretion did not involve a periplasmic intermediate (33, 38–40) and did not require SecA (41–43). These results indicated a novel protein translocation pathway and raised the intriguing question, how does this protein negotiate two membranes on its way to the medium?

Identifying the Genes Required for Type I Secretion

The first sequence of the *hly* operon also clearly showed that, in addition to the toxin, this encoded two probable membrane proteins (HlyB and HlyD) and a gene *hlyC*, subsequently shown to be required for activation of the HlyA toxin (44). Transposon mutagenesis and radiolabeling in mini and maxi cells, confirmed independently the identity of the hemolytically active product of the *hlyA* gene, as a nonprocessed polypeptide of 110 kDa. In addition, the products of the genes *hlyB* and *D* were

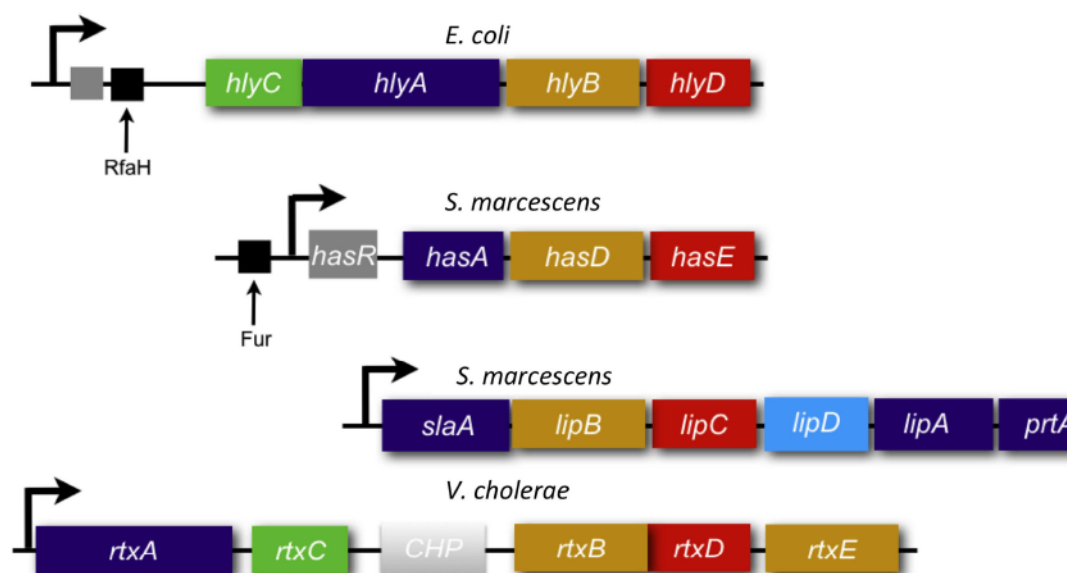


Figure 1 Organization of the *hly*, the *hasA*, and the *slaA/lipA/prtA* operons. The *hly* promoter and the binding site of the transcriptional regulators RfaH (213) or Fur are indicated. In the case of the *has* operon, the surface receptor HasR (gray), and, for the *hly* operon, the acyltransferase HlyC (green), are also encoded within the operon. The *slaA* gene encodes a surface protein, *lipA* a lipase, and *prtA* a metalloprotease. The allocrite or transport substrate genes are indicated in dark blue, the ABC transporters in brown, the MFPs in red, and the OMP, if present in the operon, in light blue. Please note that the outer membrane protein (TolC in the case of HlyA) is frequently not encoded in the corresponding T1SS operon. CHP in the *rtx* operon encodes an additional ABC transporter, but how these two transporters function independently or together is unknown (see the text on page 20).

shown to be located in the inner membrane and essential for translocation to the medium (2, 3, 36, 37, 45, 46). Then in 1990, a major advance by Wandersman and Delepelaire demonstrated that an *E. coli* outer membrane protein, TolC, was also essential for the secretion of HlyA (47). TolC was known to be involved in excretion of a wide range of molecules as well as the import of some bacteriocins, and apparently important in some way for the overall maintenance of the integrity of the outer membrane. The *tolC* gene is not linked to the *hlyA* operon, but the Wandersman group (48) showed that an operon in the phytopathogenic *Erwinia chrysanthemi*, encoding secretion genes for the metalloproteases B and PrtC, also encoded PrtF, a TolC homologue (Fig. 2). This addition of TolC to the putative type I secretion machinery was a crucial finding, providing a potential partner for the inner membrane proteins HlyB, D, and

therefore the means to complete the transport pathway through the outer membrane to the medium.

Importantly, these early studies also showed that HlyC, required to activate HlyA, and later shown by Koronakis and Hughes and colleagues (49, 50) to be a specific acyltransferase (see below), was not required for secretion (44). This is particularly relevant since HlyC with its cofactor, the cellular enzyme ACP (acyl carrier protein-dependent fatty acylation) is an unusual enzyme (51), unexpectedly synthesized in equimolar amounts to HlyA, with which it forms a stoichiometric complex. This led to the appealing hypothesis that HlyC could play a chaperone-like role to maintain HlyA competent for secretion. However, there is no evidence to support this and, in the absence of *hlyC*, there is apparently no effect on secretion of HlyA.

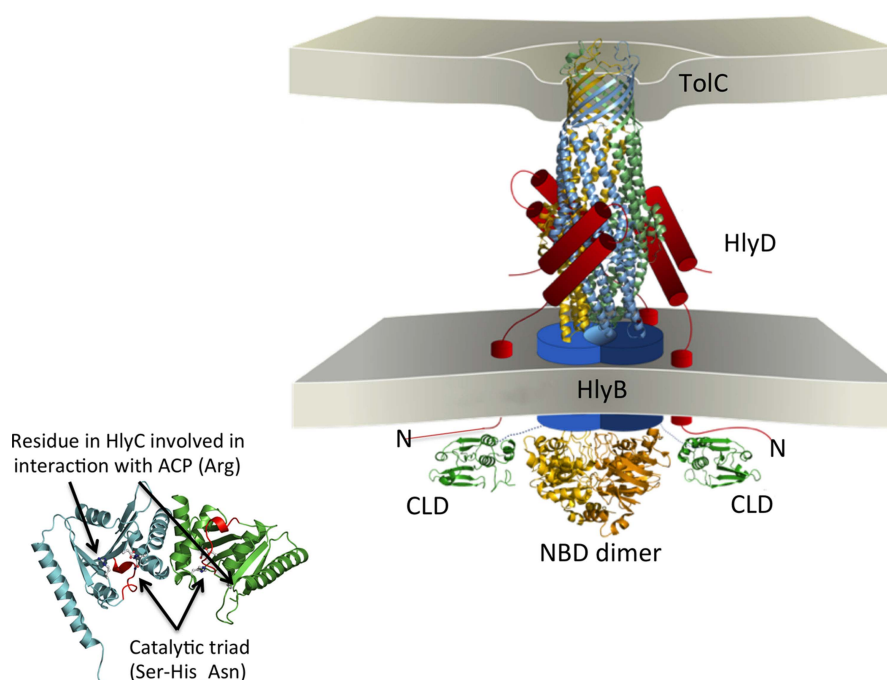


Figure 2 Summary of structural information for the hemolysin A T1SS. (Left) Homology model of dimeric HlyC based on the crystal structure of ApxC (53). The TAAT-specific insertion, which is unique and not present in the GNAT family, is highlighted in red. The Arg residue together with the catalytic triad (composed of a Ser, His, and Asn) that interacts with ACP is shown in ball-and-stick representation. (Right) The NMR structure of the CLD (54) and the crystal structure of the ATP-bound dimer of the NBDs (175) are shown in green and yellow, respectively. The TMD of HlyB and for HlyD are shown schematically as blue and red cylinders, respectively. The trimeric crystal structure of TolC (green/cyan/yellow) (138) is shown in cartoon representation. No structural information for the substrate, HlyA, is available. Please note that the presentation here for the structure, oligomeric state, and the extent of HlyD overlap with TolC is arbitrary. Note, while Koronakis et al. (145) suggested a trimeric arrangement for HlyD, more and more crystal structures and modeling evidence suggest that a closely packed hexameric state, as in other MFP analogues, is essential to maintain a tightly sealed structure. Evidence also suggests a tip-to-tip interaction or a small overlap between the ends of the MFP and TolC as in the AcrAB complex (169). The indicated contact between HlyB and TolC is arbitrary and remains controversial for the analogous tripartite AcrAB-TolC efflux pump (169). See the text for more details.

Holland et al.

The Acyltransferase HlyC: Structure and Function

The *hlyC* gene encodes the acyltransferase HlyC. This enzyme, as indicated above, is not required for secretion of HlyA, but is required for modification of the unfolded HlyA (52) in the cytoplasm prior to transport. In concert with the endogenous *E. coli* acyl-ACP, HlyC transfers acyl groups on to two internal lysine residues (Lys564 and Lys690). The predominant length of the acyl chains is 14, 15, or 17 carbon atoms. Such acyltransferases, including the most studied Gcn5-like *N*-acyltransferase (GNAT) family, are found in all kingdoms of life.

Recently, the Koronakis group (53) reported the crystal structure of an HlyC homologue from *Actinobacillus pleuropneumoniae*, ApxC (Fig. 2). This protein shares 70% amino acid identity with HlyC and can replace *E. coli* HlyC *in vivo* to activate pro-HlyA. The structure of ApxC revealed a dimer, which was supported by analysis of the oligomeric state of ApxC in solution. The monomer is composed of a five-stranded β -sheet flanked by six helices. More intriguing is a deep cleft between the third and fourth strand. This cleft is also present in structures of acyltransferases of the GNAT family and thus appears to present a conserved structural feature of these enzymes. Combined with mutagenesis studies, active site residues important for catalysis were mapped to the deep cleft in the central β -sheet and residues important for ACP interaction were also identified. This structure therefore represents an important advance in our understanding of the mechanism of activation of HlyA-like molecules transported by T1SS and will open up new ways to suppress the activity of these toxins.

Structural Organization of HlyA Including the RTX Motifs

Studies of hemolysin secretion have primarily involved two genetic determinants, both isolated from a human host, the plasmid derivative pHly152, and the chromosomal derivative LE2001 (30, 34). The two determinants show small deviations in amino acid sequence; confusingly, this includes the presence of an additional residue early in the *hlyA* gene in plasmid isolates, thus encoding 1,024 residues, not 1,023 as found with the chromosomal determinants like LE2001. The large N-terminal domain of HlyA contains the hydrophobic regions involved in pore formation, together with lysine residues 563 and 689 (numbering according to the chromosomal borne determinant; 564 and 690, in the plasmid determinant), the sites of acylation by HlyC. Importantly, the sequence

of the *hly* operon (reviewed by Welch [4]) also revealed the presence of many glycine- and aspartate-rich nona-repeats in HlyA, designated as repeats in toxins (RTX) and located toward the C terminus of the protein. The RTX motif usually begins with GG; however, there is no strict consensus, although a sequence considered able to bind a calcium ion is adhered to. Thus, the number of these repeats in *E. coli* hemolysin has variously been reported to be as few as 6 (54) or 11 to 17 (55), depending on the strictness of the consensus applied. The original consensus indicated by the Rod Welch group was, in fact, LXGGXGND, and 13 repeats were identified on this basis. In contrast, Lecher et al. (54), based on the strict consensus sequence, GGXGDXUX (where U is a large or a hydrophobic amino acid), containing the critical G and D residues directly involved in binding Ca^{2+} , identified 6 repeats in two rather closely linked clusters, terminating 173 residues from the C terminus of HlyA. In contrast, for example, the proteases PrtG, PrtB, and PrtC, all from *E. chrysanthemi*, have a single tight cluster of 3 and 4 RTX repeats, respectively, ending approximately 90 amino acids from the C terminus (56, 57).

Structural studies have shown that two nonapeptides bind one Ca^{2+} ion (Fig. 3). The main coordination occurs via the two aspartic acid side chains, but the backbone and side chain interaction of other amino acids within the repeat also contribute to Ca^{2+} coordination. It is important to stress that two consecutive repeats bind the same ion. This arrangement creates a so-called parallel β -roll or parallel β -helix. Within such a motif, a strand is present between the two repeats in the Ca^{2+} -bound state so that the strands back against each other as first described in alkaline protease (5).

A C-TERMINAL SIGNAL FOR TYPE I SECRETION

Evidence for a C-Terminal Secretion Signal and Determining the Minimal Size

In some early studies, it is noteworthy that type I secretion (apparently first so designated in reference 58) was often described in publications as a “signal-independent” secretion system. This was misleading, since it implies no secretion signal is required, while the proponents meant lacking an *N-terminal signal* as is the case for targeting the SecAYEG translocon. Many subsequent studies of the large number of known RTX proteins, where these have been tested, have confirmed the presence of a specific C-terminal secretion signal, i.e., an essential region carrying

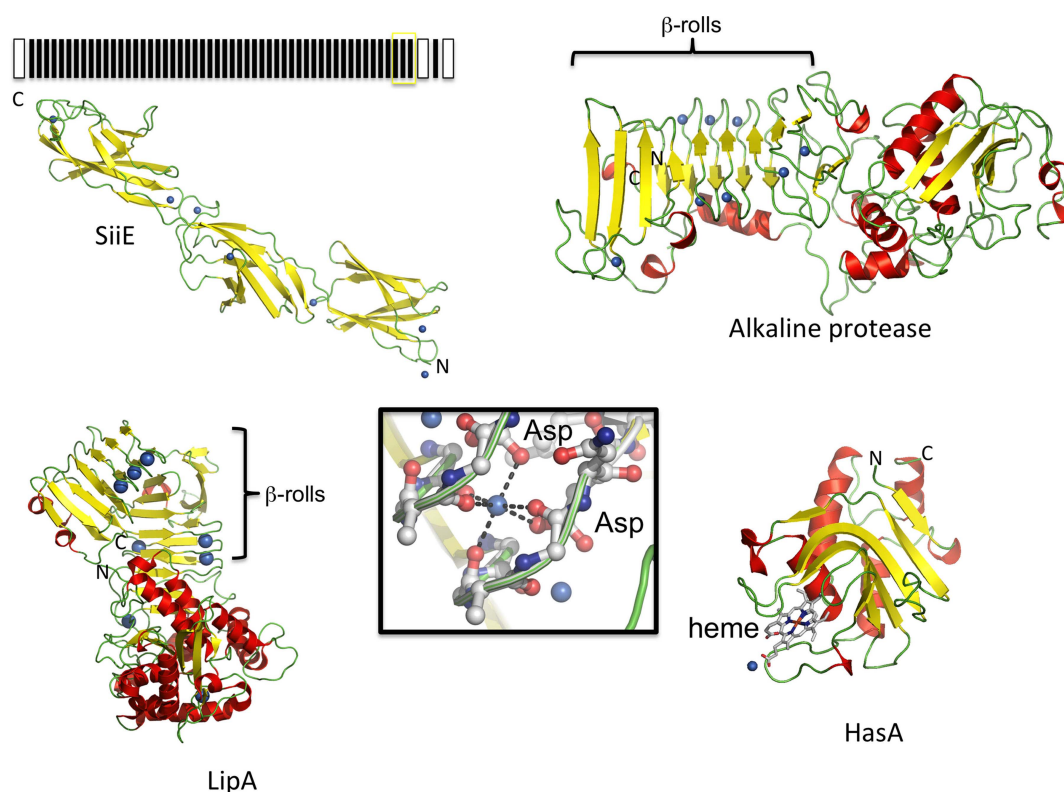


Figure 3 Known structures of substrates of T1SS. Ca^{2+} ions are highlighted as blue spheres and proteins are displayed in cartoon representation. From top to bottom, a fragment of the giant adhesion SiiE that has non-RTX Ca^{2+} binding sites (121), alkaline protease from *P. aeruginosa* (5), T1SS RTX lipase LipA (113), and HasA (110), which lacks a Ca^{2+} binding domain. The β -rolls are highlighted. The N and C termini are indicated. Please note that only a single domain of SiiE is shown. The domain architecture is provided above the structure. SiiE contains 53 so-called Big domains shown as black boxes. The N-terminal coiled coil and the C-terminal insertion are shown as white, rectangular boxes. The three Big domains of SiiE that have been crystallized are highlighted by a yellow box. The molecular architecture of a calcium binding site is summarized in the central black box. One Ca^{2+} ion (blue sphere) is coordinated by two GG repeats through interactions of the Ca^{2+} ion with the carboxylate side chain and two carbonyl oxygens of the peptide bond per GG repeat.

some form of code specific for docking to the T1SS translocon. Although detailed evidence is still surprisingly limited, we presume that the essential role for the secretion signal is recognition by and docking at least with the cognate ABC protein. However, at least for HlyA, as discussed in detail later, the secretion signal likely also specifically binds the MFP component of the translocon.

A potential signal required for type I secretion was first identified in 1985 by Gray et al., who showed that deletion of the C-terminal 27 residues of HlyA completely blocked secretion (40). Confirming the importance of this novel C-terminal signal, fragments constituting the terminal 218 (23 kDa) or 113 residues (12 kDa) of HlyA were shown by the Holland group to be autonomous for secretion, dependent on HlyBD (43, 59). Subsequently,

a HlyA autonomous fragment of only 62 residues was described (60). Finally, using a strategy effectively of upstream internal deletions, Koronakis et al. (33) localized the HlyA secretion signal to the terminal 50 or so residues.

Another autonomous type I secretion targeting region of 50 residues was identified for the alkaline protease from *Pseudomonas aeruginosa* by Duong et al. (61). For the secretion of the protease PrtG from *E. chrysanthemi* (expressed in *E. coli*), Ghigo and Wandersman (56) showed that the C-terminal peptide of 56 residues could be secreted autonomously. Then by constructing internal deletions close to the C terminus, these authors found that retention of only the terminal 29 amino acids was sufficient to promote secretion (albeit at 50% of wild-type [WT] level).

Holland et al.

However, the secretion signal for metalloprotease B, also from *E. chrysanthemi* (62), was located within the terminal 40 residues, and, more recently for a lipase, TliA secreted from *P. fluorescens*, a secretion signal, was located within the C-terminal 105 residues. This region includes three tightly packed RTX, apparently only separated from the likely secretion signal by around 20 residues (63). Similarly, Angkawidjaja et al. (64) described the efficient secretion of alkaline phosphatase fused to the C-terminal 98 residues of the lipase PML (I.3) from *Pseudomonas*. This includes 5 closely packed RTX motifs upstream of the secretion signal. For the 1,706-residue adenylate cyclase toxin (CyaA) the secretion signal has only been mapped by C-terminal deletion, and an approximate location was indicated within the C-terminal 75 residues. However, this deletion analysis by Sebo and Ladant (65) was complicated by the finding that two alternative or secondary secretion signal regions could also be detected further upstream. Finally, the secretion signal for HasA, the small hemophore from *Serratia marcescens*, was reported to be within the 56 C-terminal amino acids (66).

Posttranslational Secretion but Where Are the Chaperones?

The early studies of type I secretion, demonstrating the role for a C-terminal targeting signal, evidently showed that this must be a posttranslational process. This was exciting but raised further questions. For example, how could a very large polypeptide like HlyA, presumably requiring approximately 70 seconds at 37°C to complete its synthesis (assuming a synthesis rate of 15 amino acids per second), be maintained in a secretion competent form, neither aggregating nor being degraded, until the C-terminal docking signal was available? Possible explanations might include extended retention by the ribosome with coupling to transcription-translation of the transport proteins (as recently demonstrated for assembly of the luciferase complex from *Vibrio harveyi* [67]); early tethering to the translocator; segregation to a particular (protected) cellular compartment, capture by chaperone(s); or, less likely, the inherent stability of the unfolded or partially folded state of HlyA and other type I proteins. All these are plausible but most are predicated on the supposition that an additional signal near the *N-terminal region* would be required for early recognition of nascent forms of type I proteins. However, there is no evidence for such signals. This is especially puzzling regarding the many type I proteins now known to be

composed of thousands of residues. Moreover, as discussed below, an enormous variety of heterologous passengers can be secreted when fused upstream of the C-terminal of type I proteins. In the exceptional case of the non-RTX HasA protein, the Sec-system chaperone SecB is essential for secretion (68) and one study has indicated that the general chaperone GroES is required for HlyA secretion (J. Whitehead and J. M. Pratt, University of Liverpool, unpublished results), but this has not been confirmed. Moreover, no chaperones have been implicated in the secretion of any other type I proteins. Therefore, it remains unclear how nascent type I polypeptides remain secretion competent long enough to make a successful docking with the translocon.

A plausible alternative scenario envisaged in a number of previous studies that avoid the need for chaperones is that type I proteins initially fold up rapidly, with the ABC protein involved in coordinating the subsequent unfolding and insertion of the protein into the transport pathway. The recent studies by Bakkes et al. (69) to be discussed below, however, have ruled out such a prefolded state, at least for HlyA.

The C Terminus of HlyA Promotes Secretion of a Wide Variety of Unrelated Proteins

Clear confirmation that a specific C-terminal region signal was necessary and sufficient to promote secretion was obtained by Mackman et al. (43). They fused the C-terminal 218 residues of HlyA (now called HlyA1, containing 3 RTX; Fig. 4) or by fusing the 102 C-terminal amino acids of HlyA (HlyA3, no RTX) to the C terminus of *E. coli* porin OmpF, lacking its normal N-terminal signal. In addition, Gentshev et al. (41) and Hess et al. (70) later reported that alkaline phosphatase, normally an *E. coli* periplasmic protein, was secreted to the medium when its C terminus was fused to an even smaller C-terminal fragment of HlyA containing only 60 terminal residues. However, a recurring caveat here is that, in this and many other reports, the efficiency of secretion per molecule synthesized was not measured, rendering the significance difficult to evaluate.

Subsequently, a very large number of heterologous proteins, mostly fused with the larger (218 residues) C-terminal region of HlyA that contains three RTX motifs, were successfully demonstrated. Moreover, a wide variety of such heterologous passengers formed from cytoplasmic or Sec-dependent, exported proteins were shown to

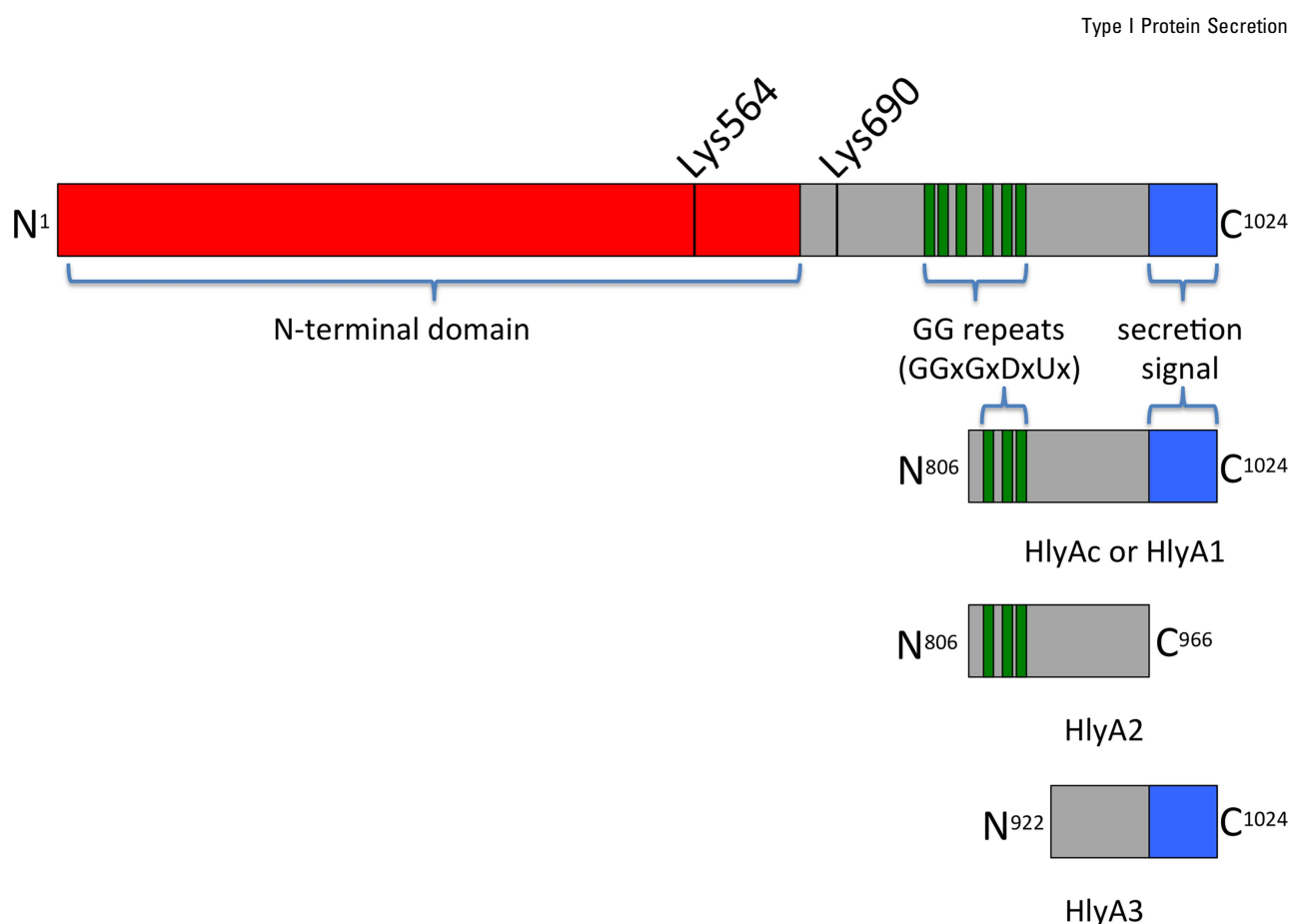


Figure 4 Cartoon representation of the HlyA constructs mentioned in the text. The length of the constructs is scaled to their number of amino acids, which are provided for each construct. The major pore-forming domain of HlyA is shown in red, and the secretion signal is in blue. The individual nona repeats in the RTX domain are shown as vertical green bars. N and C termini are indicated. The fragment of HlyA, A1 contains 208 amino acids, A2 contains 160, and A3 contains 102.

have functional activity, indicating normal folding. The examples include streptokinase (71), beta-lactamase (38), maltose binding protein (69), mammalian intestinal fatty acid binding protein (72), green fluorescent protein (GFP), and alkaline phosphatase (64, 73).

THE RTX MOTIFS: STRUCTURE AND FUNCTION

RTX Are Essential for Secretion of Many but Not All Type I Proteins

The RTX family is now known to be very large and includes, for example, a wide range of enzymes and adhesins in addition to toxins. Nevertheless, the RTX terminology, however defined, still rather tightly describes a large family of prokaryotic proteins whose secretion is dependent on a C-terminal signal and an ABC transporter. Many studies have also shown that RTX motifs

play a role in secretion to the medium of many type I proteins, in particular, very large proteins. One of the best examples is provided by studies of the secretion of a *Pseudomonas* I.3 lipase. Thus, secretion levels were clearly shown to be proportional to the number of RTX motifs retained in different engineered constructs, with barely detectable levels of secreted lipase when 11 or 12 of all the repeats in the WT were removed (74).

In some contrast, it is equally clear that the RTX motifs are dispensable for secretion in some contexts. Thus, type I substrates like the small HasA protein and the bacteriocin colicin V completely lack the RTX motif (Fig. 3). HasA, although having a C-terminal secretion signal, has the special feature that secretion requires the dedicated chaperone SecB, which interacts with the N terminus of HasA. More surprisingly, although secretion is still dependent on an ABC transporter, the 39 residues of ColV,

Holland et al.

constituting the signal sequence, are located at the N terminus of the allocrite. Moreover, unlike HlyA and other large type I polypeptides, the ColV signal sequence is cleaved and the signal removed by a cysteine protease domain found at the N terminus of the cognate ABC transporter (75, 76). As discussed later, a protease domain in the ABC protein is not required for secretion of polypeptides. Instead, fascinatingly, an inactive relic of the protease is essential for secretion of HlyA and some other type I proteins. Such variation in the details of the process among different type I subgroups will recur frequently in this review.

In another specific exception to the rule, the minimal *autonomous* fragment of HlyA, the C-terminal 60 residues, completely lacks RTX but is still apparently secreted quite efficiently. In addition, when certain heterologous “passenger” polypeptides, for example, *E. coli* porin OmpF (43) or alkaline phosphatase (41), were fused to the C-terminal fragment HlyA3 that lacks RTX repeats (Fig. 4), secretion was still obtained. However, these particular passengers have the inherent properties of being normally exported across the inner membrane, and like WT HasA, require the SecB chaperone for normal secretion. They also share another common characteristic, relatively small size. In such cases, the role performed by the RTX, to facilitate calcium ion-dependent folding of substrates emerging from the translocon on to the cell surface, may simply be redundant. Indeed, as suggested by Letoffe and Wandersman (57), many of these results can reasonably be explained, if beyond a maximum size, around 30 kDa, the RTX motifs become essential for secretion (and folding).

Fusion of heterologous passengers to other T1SS secretion signals has also demonstrated successful secretion in the absence of RTX motifs (57, 64, 76). In some cases, the passenger enzyme in the fusion was shown to be active, despite the lack of RTX. However, in the case of a GFP fusion to the signal region of lipase TliA from *P. fluorescens*, the RTX motifs were apparently required for correct folding of GFP (63). Finally, as described below, some naturally occurring type I proteins completely lack RTX, but evolution has thrown up some fascinating alternatives.

Calcium Ion Regulation of Protein Folding: Role of RTX Motifs in Type I Secretion

In vitro experiments with HlyA and fragments thereof, ranging from those with the complete number of RTX

repeats down to truncations having only three repeats, demonstrated that Ca^{2+} is essential for the folding of these proteins (77–79). Folding only occurs in the presence of Ca^{2+} or other divalent ions such as Sr^{2+} or Ba^{2+} but not with Mg^{2+} . Interestingly, folding studies with purified HlyA following its secretion and subsequent unfolding by treatment with EDTA and 8 M urea, indicated that Ca^{2+} -induced folding is not only restricted to the RTX domain but, more importantly, extends to the entire protein (79, 80).

This latter observation is supported by folding studies *in vitro* of maltose binding protein (MBP) or MBP slow folding mutants fused to the C-terminal fragment of HlyA, HlyA1 (Fig. 4 and reference 69), where passengers are folded to give biological activity. As expected, the purified mutant MBP proteins themselves displayed a decreased folding rate, while the velocity of unfolding was not affected. This was also observed with the MBP-HlyA1 fusions. Importantly, in the absence of Ca^{2+} , essentially simulating the *E. coli* cytosol, the slow folding mutants displayed an even slower folding rate when fused to the C-terminal fragment of HlyA. This suggested that long-range interactions were propagated between the MBP and the HlyA moiety. Moreover, the slower the folding of a particular mutant, the greater the influence of Ca^{2+} ions on the folding of the entire fusion protein. This result raised the surprising possibility that the RTX in the absence of Ca^{2+} (as *in vivo*), rather than accelerating folding, can actually slow down the process. Thus, facilitating maintenance of the unfolded state until translocation and surface emergence of passenger domains, their consequent folding and release into the medium is completed. In this sense the RTX exert a negative effect on intracellular folding contrasting with its positive driving of extracellular Ca^{2+} -dependent folding.

The Mechanism of Folding of Adenyl Cyclase Toxin

Detailed studies of calcium ion-dependent folding of the RTX motifs into the characteristic β -roll structures (first identified by reference 5), in an elegant series of experiments concerning the adenylate cyclase toxin (CyaA), have provided fascinating insights into the mechanism. Adenylate cyclase toxin secreted by *B. pertussis* contains around 40 RTX motifs (allowing for some relaxation of the strict consensus) distributed into 5 blocks within the terminal 700 amino acids of the 1,706-residue toxin. This so-called RD (RTX domain) region is required for

binding of the toxin to its integrin receptor on target cells and also contains the approximately 75-residue secretion signal. The last RTX block, finishing around residue 1620 (81), appears to be separated from the secretion signal by a maximum of only 30 amino acids.

Ladant and Chenal and colleagues have shown, using spectroscopic techniques, biochemical and hydrodynamic measurements that the entire RD domain of CyaA, including the secretion signal, in the absence of calcium ions adopts a premolten globule or intrinsically disordered structure. Notably, this contains small amounts of unstable β -sheet (80). Addition of Ca^{2+} (10 mM, mimicking physiological extracellular levels) results in cooperative binding of approximately 1 calcium ion per repeat to form a compact β -roll structure. The folded structure has a reduced net charge, suggested by the authors to reflect neutralization of internal electrostatic repulsions of the aspartates by calcium ions. More detailed subsequent studies, concentrating on *in vitro* folding of RTX block V (9 RTX, approximately residues 1529 to 1620) and its C-terminal flanking region (CTF), demonstrated that this subdomain folded up the entire RD region in the presence of Ca^{2+} (summarized in reference 82). However, remarkably, when separated from the CTF, defined as the residues extending to residue 1680 (reference 81 and Fig. 1), the repeats were unable to bind calcium ions and did not fold. Even with calcium ions present, there was no folding of the RTX without the CTF. This clearly revealed a key role for some downstream amino acids in the initiation or stabilization of the folding process by a mechanism that remains to be elucidated.

Blenner et al. (83) also investigated the mechanism of folding of the block V RTX motifs of CyaA and the role of a similar CTF region. The results also showed that truncation of the CTF resulted in reduced affinity for calcium ions and β -roll formation. Importantly, the authors noted that the CTF itself is rich in aspartic acid residues, and, in fact, replacing this region with a completely unrelated sequence, but nevertheless able to bind calcium ions, restored the ability of the upstream RTX to fold in the presence of calcium ions. It was therefore suggested that the stimulating effect of the CTF was dependent on an entropic stabilization effect.

Largely similar results for calcium ion-dependent cooperative folding of the RTX region of C-terminal fragments of alkaline protease secreted from *P. aeruginosa* were also obtained by Zhang et al. (84). This study

interestingly also demonstrated that the folded RTX domain was directly involved in chaperoning the folding of the *N-terminal* protease domain of this protein.

BIOTECHNOLOGICAL APPLICATIONS OF THE TYPE I SECRETION PROCESS

Introduction

A large number of pro- and eukaryote proteins or fragments of proteins have now been successfully secreted as fusions to C-terminal regions of HlyA and, in several cases, shown to fold correctly (69, 85–88). We recently developed a two-vector system coding for the inner membrane components (HlyB/HlyD) on one plasmid and the fusion protein (gene of interest fused to the N terminus of HlyA1, see Fig. 4) on the other plasmid. Here, successful secretion of slow folding mutants of MBP and an internal fatty acid binding protein was demonstrated (69, 72). Yields were approximately 15 mg/liter of cell culture for the slowest folding mutant of MBP and approximately 1 mg/liter of cell culture for intestinal fatty acid binding protein (IFABP).

Similar results were obtained more recently using C-terminal signals from other type I proteins. In particular, a minimal C-terminal fragment composed of 103 residues, including 4 RTX, from the *P. fluorescens* Tli lipase was used for secretion of epidermal growth factor (EGF) or GFP (63). In addition, the terminal 60 residues of another pseudomonad lipase, PML although lacking RTX, were also able to support secretion in a fusion with alkaline phosphatase as passenger (64). A new vector for use in *P. fluorescens* was described more recently by Ryu et al. (89) that harbors genes for the ABC transporter and the MFP. In this case, genes of interest are fused to the C terminus of the lipase transporter recognition domain (LARD) from the lipase TliA. Successful secretion was shown for GFP and alkaline phosphatase. These examples demonstrate that new approaches are also underway in other laboratories to employ T1SS as a platform for protein production and purification.

Optimizing Secretion of Fusion Proteins: the Rate of Intracellular Folding of HlyA Dictates Secretion Efficiency

It is important to note that, although many different heterologous proteins have been secreted using the C-terminal region of RTX proteins, the great majority of such studies have taken a simple empirical, trial-and-

Holland et al.

error approach: are particular fusions secreted or not? In addition, in most such experiments, protein levels were not measured quantitatively and no attempt was made to determine secretion efficiency, i.e., the number of molecules secreted compared with the number synthesized. Moreover, when measured, yields of secreted fusions were found to be very low, restricted to the high microgram per liter range at best.

Recognizing the limitations of the empirical approach, Bakkes and colleagues recently examined how at least one key factor, fast folding of a passenger domain, might compromise efficient secretion of a given fusion (69). Debarbieux and Wandersman (90) had previously shown that, if HasA (albeit an atypical non-RTX type I protein) was allowed to fold in the cytoplasm before inducing the synthesis of the translocator proteins, it could not be secreted. This result, in fact, appeared to contradict earlier suggestions that type I allocrites might require unwinding (by the ABC protein) prior to secretion. Bakkes et al. (69), taking up this idea, conducted a detailed study of the prototype Hly-T1SS using folding variants of the maltose binding protein (MalE), fused upstream of the C-terminal secretion signal of HlyA via the HlyA1 fusion vector described in the next section. The MalE mutants varied only in their folding properties, with no effect on the unfolding rate. The results showed clearly that the slower the folding rate, the higher the secretion level of the fusion protein. Thus, the folding rate dictates secretion efficiency. Importantly, with the slow-folding mutations that promoted efficient secretion, the activity of MalE in the fusion was not compromised.

These results clearly ruled out the possibility that HlyA folds in the cytoplasm before being secreted, and also demonstrated for the first time experimentally that transport substrates of a T1SS only fold *after* secretion. More importantly, these studies (69) provided a rational platform for the construction of T1SS fusion proteins. If these are secreted poorly, decreasing the folding rate by introducing point mutations is recommended. This strategy was supported by secretion studies on a fusion with intestinal fatty acid binding protein (IFABP). Here, mutations that slowed the folding rate of IFABP increased secretion substantially, again without apparently compromising activity (72). However, mutations that decrease folding of a certain protein cannot be predicted *per se* but have to be determined experimentally. Thus, error-prone PCR or DNA shuffling could be the best

approach, combined with screening for increased secretion levels.

In addition to the importance of the folding rate of the passenger, the expression levels of the inner membrane components of the HlyA T1SS (HlyB and HlyD) are also of prime importance for high yields of secreted protein. Only under conditions in which both membrane proteins were highly expressed was efficient secretion observed (69, 72). However, efficient secretion of heterologous fusion proteins, in general, is likely to be a multifactorial process dependent on several factors, in addition to folding rate and expression levels. Nevertheless, these studies provided an important starting point and, in our hands, the Hly T1SS is a very powerful system for efficient, high-yield secretion.

Generation of Novel Hly Fusion Vectors

A vector encoding the 23-kDa C-terminal of HlyA (HlyA1) was constructed in plasmid pSU. This was designed for easy insertion of coding sequences for different passenger proteins N-terminal to the secretion signal, plus engineered cleavage sites for subsequent enzymatic release of the passenger domain. pSU was combined with plasmid pLG575, encoding both HlyB and D, to promote secretion of different heterologous passengers (72). This HlyA1, 208-residue fragment (see Fig. 4), contains only the distal 3 RTX repeats of WT HlyA plus the approximately 55-residue secretion signal. In addition, this C-terminal fragment of HlyA also contains, upstream of the signal sequence, the binding site for the C39 peptidase-like domain (CLD) of HlyB, as discussed later (Fig. 2). This is the specialized cytoplasmic N-terminal domain that is required for secretion of HlyA, but is also required for secretion of heterologous proteins fused to HlyA1 and smaller fragments from the HlyA C terminus.

ANALYSIS OF THE STRUCTURE-FUNCTION OF THE SIGNAL: AN ENIGMATIC CODE

Type I C-Terminal Secretion Signals, Highly Conserved in Closely Related Transport Substrates, but There Is No Universal Code

The presence of specific C-terminal secretion signals for a wide range of type I proteins is now well established to lie within the terminal 50 to 70 residues. However, identifying the precise function of the signal, in particular, the coding information required for docking with the translocon, has proved difficult.

We previously (91) compared the primary sequence of the C-terminal 60 residues of HlyA and a wide range of functionally quite different type I proteins, including a representative protease, a lipase, degrading enzymes for different surface polymers, S-layer proteins, iron-regulated proteins, different cytotoxins, and a surface

protein required for gliding motility. Remarkably, this analysis revealed no obvious amino acid conservation of these proteins either with HlyA or with each other. In contrast, in our recent survey of the last 60 amino acids of 40 closely related hemolysins, we found a pattern of highly conserved residues (see Fig. 5C). Similarly,

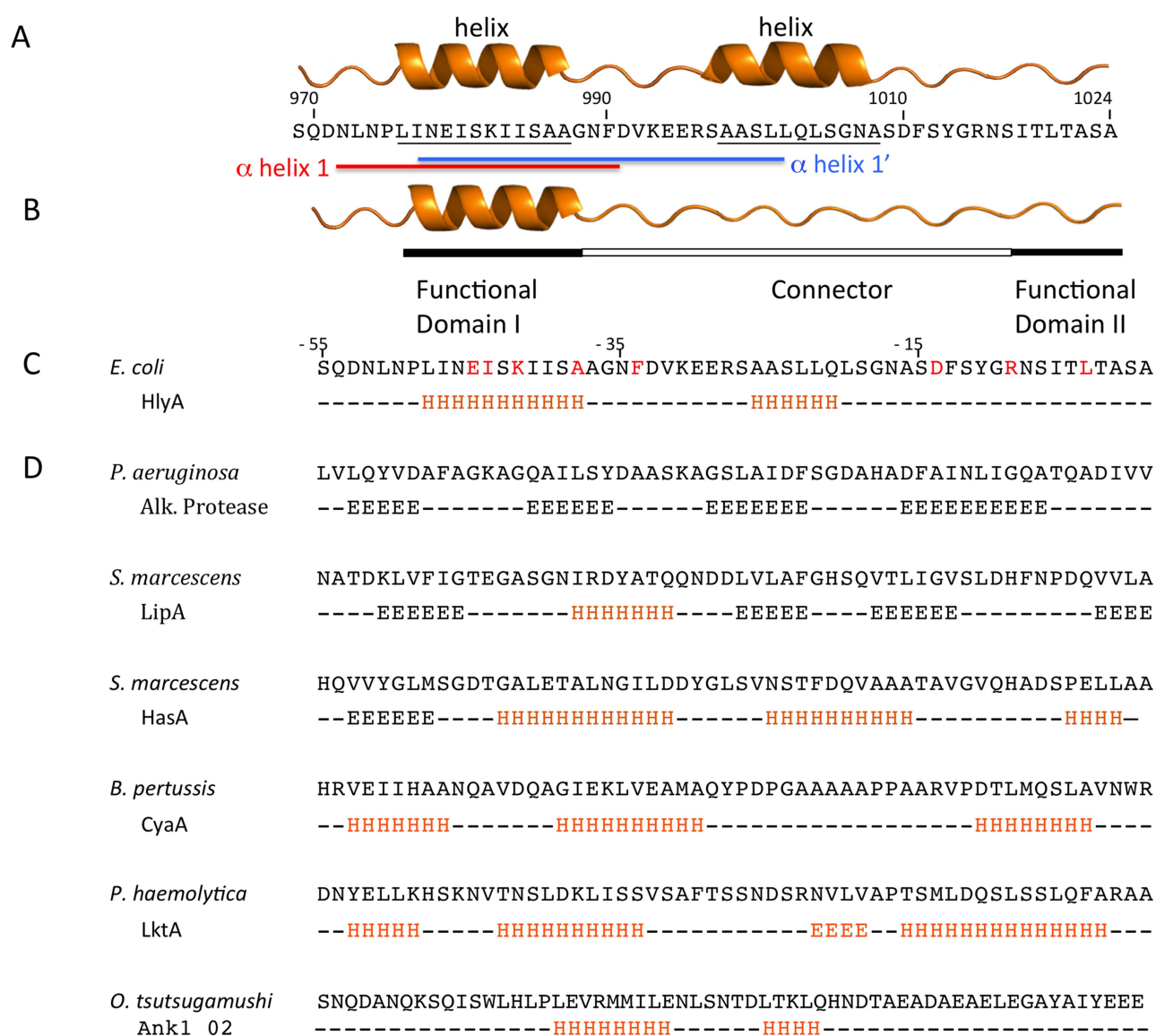


Figure 5 Models for the nature of the secretion signal code. (A) Predicted secondary structure of the C-terminal secretion sequence of HlyA. (B) The Ling model derived from directed combinatorial mutagenesis (104) emphasizes the functional importance of the proximal helix I plus the extreme terminal residues. (C) The linear code model (100, 101) emphasizing individual key residues (highlighted in red) essential for function in the hemolysin subfamily, as derived from single-substitution mutagenesis. (D) Secondary structure predictions for the C-terminal region containing the secretion signal sequence of representatives from other subfamilies of T1SS transport substrates. Note in (D) that β -sheet or α -helical regions are predicted for the C-terminal signal region with little conservation of the primary sequence.

Holland et al.

confirming earlier published reports, we have observed in a smaller sampling the conservation of a different set of C-terminal residues among closely related proteases or lipases. These results, and the more detailed studies discussed below, clearly indicate that there is no single code specific for all type I proteins. Rather, each subgroup appears to retain a largely unique code.

Early studies indeed suggested that at least two subtypes, hemolysin-like and PrtG protease-like groups, can be distinguished at the extreme C terminus, respectively, by a short motif of hydroxylated residues or by three hydrophobic amino acids preceded by an acidic residue, DVLA (56, 92, 93). Nevertheless, the hydroxylated tail is not present in all toxins described as hemolysins, for example, LktA from *Pasteurella haemolytica* (Fig. 5D). Interestingly, a C-terminal “motif” of hydrophobic amino acids preceded by an acidic residue appears conserved not only in proteases, but also in lipases, for example, LipA_{SM} (93). However, other type I substrates, such as adenyl cyclase toxin or the newly studied ankyrins (described below), have C termini lacking either of the hydroxylated or hydrophobic motifs.

Although based on only very limited studies, type I allocrites and components of their translocon also appear to be interchangeable only between systems with very similar transport substrates (see, for example, references 48, 61, 62, 75, 94, and 95). In most cases, this appears to parallel the relative conservation of the inner membrane transporter components, for example, more than 80% conservation *within* the distinct HlyA or the protease-lipase type I systems, but only around 25% between subfamilies (see, for example, reference 96). More puzzlingly, the C-terminal 70 amino acids of the leukotoxin, LktA from *P. haemolytica*, although seemingly with no obvious similarity to the HlyA signal sequence (Fig. 5C and D), is functionally able to replace the C-terminal 58 amino acids of HlyA (97). There have been other claims of the HlyA translocon appearing relatively promiscuous, able to secrete, to some degree, some very unexpected proteins. These include the CyaA toxin (65, 95), protease B from *E. chrysanthemi* (62) and especially the non-RTX protein, bacteriocin ColV (98) with its completely unrelated *N-terminal* signal. However, apparently none of these heterologous systems are able to reciprocate and secrete HlyA. Moreover, with a note of caution these supposed examples of relaxed specificity, often detected only with antibodies and not quantified, might in reality simply reflect very inefficient secretion.

HlyA C-Terminal Signal: Individual Residues Dispersed along the Signal Region Are Important for Function

The great majority of attempts to elucidate the nature of the code carried by type I secretion signals have concerned the prototype HlyA and most of the following sections will be focused primarily on this system. Note that, as indicated above, most studies have involved two *hly* determinants, one located in the chromosome from a pathogenic strain LE2001 (34, 35) and a second encoded on a plasmid, pHly152 (30), with total lengths of 1,023 and 1,024 amino acids, respectively. To avoid confusion in the following discussion involving studies in different laboratories, residues will therefore be identified with respect to their position from the C terminus.

Early random mutagenesis studies from different groups (results summarized in reference 100) immediately suggested that many residues within the signal region were redundant, with many single-residue substitutions having very little or only moderate effects on HlyA protein secretion levels. However, as highlighted in Fig. 5C, 60% to 70% reductions in secretion were obtained in 8 mutants carrying substitutions at positions -46 (Glu), -43 (Lys), -39 (Ala), -35 (Phe), at -45 (Ile), and reductions around 50% at -15 (Asp), -10 (Arg), -5 (Leu). Importantly, construction of different combinations of substitutions at residues E-K (-45) F-L (-35) D-R (-15) gave additive effects, maximally reducing secretion to less than 2% in the triple mutant, as measured by hemolytic activity in liquid cultures and confirmed by SDS-PAGE. Overall, these latter studies also placed the N-terminal boundary of the signal to between position -46 and -53 (100).

A Structural Code or a Linear Code of Individual Residues

Although we are only concerned here with HlyA, it is important to note that, if there is a structural code based on helical secondary structure (therefore able to pass through TolC) it is not conserved in the protease-lipase subfamily, since these proteins appear to have β -sheet rather than helices in the C-terminal region.

As illustrated in Fig. 5, simple inspection of the sequence of the HlyA signal region indicates several characteristics first considered as potential coding information. These are a charged cluster covering residues -29 to -32; a 16-residue “aspartate” box (-30 to -15) flanked by acidic

residues that appeared to be conserved in some other T1SS transport substrates (101), a block of 13 uncharged residues, distal to the charged cluster and overlapping the aspartate box, and, as mentioned above, a cluster of relatively hydrophobic, mostly hydroxylated residues at the extreme terminus (33, 102). However, several mutagenesis experiments to test the possible role of various motifs, in fact, found no functional role for the “aspartate box,” and the charged cluster could also be mutated or even deleted without significant loss of function (97). Similarly, mutagenesis experiments have apparently found no functional role for the 13-residue uncharged region, while mutation or deletion of the extreme C-terminal 6 or 7 residues, as discussed below, affects posttranslational folding rather than secretion *per se*.

There is also confusion in the literature regarding the precise position of two predicted α -helices in the signal region (43, 102, 103, 104), reflecting how the precision of algorithms has markedly improved. For the purpose of this review, we will use the prediction shown in Fig. 5A.

In line with most subsequently published reports, these α -helices will be referred to as the most proximal (–37 to –47), i.e., close to the N terminus of the signal, and a downstream helix (hereafter referred to as helix 2, –21 to –26). However, most studies subsequently concentrated on the possible coding role for *potential amphipathic helices*, overlapping the proximal predicted helix (see Fig. 5A). Thus, Koronakis et al. (33) first postulated a potential 18-residue amphipathic (helix 1) located between amino acids –34 and –51, centered on the sequence EISK (–42 to –45). The identification of an amphipathic helix was based primarily on presentation of the 18 residues on a Schiffer-Edmunson helical wheel and, for simplicity, we will call this helix 1 (or H1) from now on. Then, Stanley et al. (102) provided some mutagenesis data and a helical wheel analysis supporting a functional role for a larger 26-residue amphipathic helix (residues –23 to –48) that we will refer to as helix 1' (H1'). Importantly, this includes the original amphipathic helix 1 but extends to include both the charged cluster as part of helix 2.

In brief, Stanley et al. (102), using internal deletions or random mutagenesis, including the use of degenerate oligonucleotides, identified mutants carrying multiple as well as some single substitutions in the C-terminal signal region, consistent with H1' having a functional role in secretion of HlyA. Notably, other studies (92, 100, 101), using random-site-directed and -saturated mutagenesis of

specific parts of the signal region, found a number of point mutants either consistent or equally clearly not consistent with such an amphipathic helix. Importantly, these latter studies included the demonstration, from experiments where the WT and a poorly secreting mutant were coexpressed in the same cell that secretion of the WT was not affected. That is, the mutations were recessive, indicating that the mutant signals were not engaging the translocon. We wish to emphasize here that, for nonsecreting mutants, without determining the location of HlyA, it is essential to determine the location of HlyA. Is it in the cytoplasm (recessive mutants), stuck in the translocon (dominant mutants), or secreted to the medium, but then degraded or aggregated? Unless this analysis is done, the conclusions that can be drawn regarding the mechanism of secretion, including the role of the signal sequence, are limited. Unfortunately, such further investigation has usually not been pursued.

Ling and colleagues (104–106) used a different approach to the coding problem, a combinatorial analysis inserting large numbers of random peptide sequences into specific regions of the signal region. The results obtained were consistent with a functional role for a proposed 10-residue amphipathic helical structure (–36 to –49) encompassing the “secretion hot spot” EISK (92, 100) that we will return to later. In contrast, a combinatorial library targeted on the terminal 5 amino acids of helix 1' (and a further 6 residues downstream) revealed no functional role, and similarly for the combinatorial analysis of residues –8 to –16 (see Fig. 5 for the residue map). In many of these experiments, hemolytic colony halo size was as a measure of secretion efficiency, with controls to establish the quantitative nature of the procedure. However, in our experience, a large reduction in the amount of secreted protein is required before any obvious change in halo size is evident. Thus, this is a useful but a rough guide to secretion changes. However, for screening signal sequence mutants, the method is limited to analyzing the proximal region of the signal since, as described, later the most distal region is involved in folding of HlyA and therefore activity.

Other studies involving internal deletion analysis specifically examined the role of the charged cluster, DVKEER (–28 to –33) within helix 1', a crucial contributor to amphipathicity. However, these experiments gave contradictory results. Thus, while reference 102 reported that deletion of 11 residues –27 to –37 abolished secretion, the deletion of only the charged cluster still permitted

Holland et al.

71% of the WT secretion level of HlyA (97). These results suggest rather that, in the larger deletion, a residue just outside the charged cluster is important for secretion and an obvious candidate is the phenylalanine at position -35, which is crucial for high-level secretion of HlyA (92, 100).

In summary, from the extensive mutagenesis experiments described above, most possible coding motifs visible in the primary sequence could seemingly be eliminated. Moreover, overall, the mutagenesis results do not support a functional role for the large amphipathic helix 1'. However, the results of the Ling studies remain compatible with a short potential amphipathic helix (residues -38 to -49) having a functional role. On the other hand, mutagenesis experiments have identified 8 individual amino acids critical for function, including four within H1 and a new amphipathic helix defined by the Ling group, the -37 to -44 region. We will return to this important point concerning a linear code rather than a code based on secondary structure.

Physical Techniques in the Search for Secondary Structure in the Secretion Signal

Is there a linear amino acid code, particular secondary structure, a mixture of both, or something entirely different that determines recognition of the signal sequence by the type I translocator? First, it is important to keep in mind that any secondary structural component of the signal code in intracellular HlyA must be able to transit the TolC channel, whose maximum diameter is likely restricted to 20 Å (107). This therefore limits secondary structure during transit to an α -helix.

Nuclear magnetic resonance (NMR) studies of isolated type I signal peptides have been described, but these have not provided definitive evidence for any specific structure. The earliest studies for HasA and PrtG (108, 109) found no secondary structures in aqueous solution. In membrane mimetic environments, with the somewhat ambiguous inclusion of the helix-promoting agent trifluoroethanol, some helical content was detected in the proximal region of the signal, while the rest appeared unstructured. Essentially, similar results were obtained with intact HasA in detergent micelles (110). A circular dichroism (CD) spectrum analysis of the C termini of HlyA (61 residues) and LktA (70 residues) also indicated unstructured peptides in aqueous solution with some helical secondary structure in detergent (111). Similar

results were obtained with an NMR analysis of the HlyA C-terminal secretion signal (61 amino acids) in SDS (106). These results were interpreted, although with a number of caveats, to indicate the presence of two short helices (see Fig. 5A). Importantly, all the experiments involving detergents were apparently predicated on the idea that *in vivo* the signal-ABC protein interaction takes place in a membrane environment, although this has not been substantiated experimentally for any type I protein.

Notably, *in vitro* structural analyses in an aqueous medium of the C termini of the type I proteins, adenylate cyclase toxin (80–82) and the AprA protease from *P. aeruginosa* (84), indicated that, in the absence of calcium ions, the C terminus is largely disordered. The region analyzed in these experiments included the RTX Ca^{2+} -dependent folding domain and the proximal region of the secretion signal, at least up to residue -26 from the terminus (81).

Finally, β -strand structures at the C terminus can be predicted for some proteases and lipases (see Fig. 5C). Moreover, the few available crystal structures for such proteins have antiparallel β -strand sheets in that region (5, 113). However, it is noteworthy that β -strand structures, if formed *in vivo*, are not known to have amphiphilic properties and are too bulky to transit TolC.

In summary, amphiphilic helices are not widely conserved in signal sequences of type I allocrites, and overall the physical evidence for helices in HlyA and HasA is weak, while the CyaA C terminus *in vitro* indeed appears disordered. Therefore, together with inconsistent genetic evidence for a specific functional helix in the HlyA signal, this suggests that the type I secretion signal *in vivo* lacks any functional secondary structure.

The C-Terminal Signal of Type I Allocrites May Have a Dual Role

Type I secretion signal regions appear to have at least two functions, a proximal recognition region (perhaps extending from around -15 to -46 in HlyA), while a few residues at the extreme terminus appear to provide a distinctive function, affecting in some way posttranslocation folding. Thus, end deletion constructs, measuring secretion efficiency based on *hemolytic* activity in liquid cultures (33, 102), reported that removing the C-terminal 7 or 8 amino acids of HlyA reduced secretion by 50% to 70%. Importantly however, later studies

showed that removal of the 6 terminal residues or multiple mutations in this region of HlyA had minimal effects when levels of HlyA *protein* in the medium were analyzed. We concluded that such deletions had a major effect on folding of HlyA to the native, active form, as indicated by hypersensitivity to trypsin and tryptophan fluorescence spectroscopy (92, 103). These results therefore suggested an important functional role near the terminus of the signal, affecting folding in some way, rather than translocon recognition, as required in the model of Stanley et al. (102). Interestingly, mutations within the terminal 4 residues of certain lipases, a motif also relatively well conserved in secreted proteases (115), resulted in reduced stability of the secreted protein. In addition, the deletion of the C-terminal 14 residues of HasA stalled translocation in some unknown way, indicating that this region is not involved in recognition of the translocon (114). Finally, *in vitro* studies with CyaA have indicated that at least the proximal part of the secretion signal may be implicated in RTX-driven, posttranslocational folding. However, alternatively, we might speculate that a few residues at the extreme C termini of type I proteins are required for anchoring the emerging polypeptide to some surface component.

Secretion Signal of HasA

The minimal HasA C-terminal fragment capable of autonomous secretion was found within the last 56 residues (66). Subsequently, Cescau et al. (114) constructed a nonsecreted variant of HasA with the C-terminal 14 amino acids deleted. The truncate was able to fold in the cytoplasm (and therefore bind heme) but was still able to engage the ABC and MFP proteins and to assemble a complete, but stalled translocator that included TolC (shown by affinity purification of the complex). Indeed, with the high level of production of the ABC and MFP proteins employed in these experiments, the majority of cellular TolC was titrated, rendering the cells sensitive to SDS, presumably by depletion of the AcrAB drug and detergent transport pump. As described below, SDS sensitivity can be a useful indicator of stalled translocons.

In addition, Cescau et al. (114) provided preliminary evidence that the truncated signal fragment bound the ABC protein HasD *in vitro*. These results, unfortunately not apparently followed up, suggested that the terminal 14 residues of the HasA secretion signal are not required for docking but might have a role, for example, in stabilization of the secreted protein.

Possible Coding Motifs in Lipase and Protease Secretion Signals

Other more limited studies have been performed to identify possible conserved motifs and essential functions in the secretion signals for lipases and proteases from different Gram-negative species. As also illustrated in Fig. 5 (with representative examples only), the C-terminal sequences and putative secretion signals for proteases and lipases reveal some apparently distinctive features, although these appear quite different from those of both HlyA and HasA.

Ghigo and Wandersman (56) first suggested that the extreme C-terminal sequence DLVL was a secretion 'motif' in both proteases and lipases. Indeed, for the protease PrtG, deletion of this sequence prevented its secretion. However, subsequent studies found that a similar motif, although present, was not required for secretion of lipase LipA from *S. marcescens* (93). In a similar study of the I.3 (PML) lipase by Kuwarhara et al. (115), the hydrophobic residues at the extreme C-terminal motif were also found not to be required for secretion. In addition, these authors showed that the extreme C-terminal motif in the I.3 lipase was required for heat stability of the protein rather than for secretion *per se*.

S. marcescens also secretes the heme binding protein HasA and, intriguingly, the dedicated HasA T1SS is able to secrete, to some extent, PrtA and LipA from this same host. However, reciprocal secretion of HasA_{SM} was not observed. Comparison of the two HasA sequences in fact identified a short motif around residue -17 from the C terminus present only in the *Pseudomonas* HasA. Site-directed mutagenesis confirmed that residues -15 to -19, VTLIG (forming a β -sheet structure in the fully folded proteins) were indeed critical for secretion (93). Based on the testing of hybrid translocators from LipA and HasA translocons, the authors suggested that the motif was specifically involved in targeting the ABC transporter. Moreover, reference 115 confirmed the importance of the conserved VTLIG for secretion of a lipase (PLM) from *Pseudomonas*. It would be important now to test directly the binding of such a motif to the relevant ABC proteins.

Screening Tests for Functional States of the Type I Translocator

The article by Cescau et al. (114), exploiting SDS sensitivity of cells to detect a frozen complex, highlights the use of simple plate tests for easy monitoring of certain states of the translocon. Thus, Blight et al. (116) observed an

Holland et al.

increase in vancomycin sensitivity (but not to another antibiotic, fusidic acid) in *E. coli* K12 expressing *hlyBD* and *hlyA*. However, vancomycin resistance was restored when a highly defective, secretion signal mutant of HlyA was present, indicating that assembly of the whole translocon and active translocation of HlyA increased envelope permeability to vancomycin in some way. Surprisingly, a similar study (117), however, found that the presence of HlyB and D was sufficient to sensitize *E. coli* to the antibiotic, and the reason for these differing results is unclear. In any case, changes in vancomycin sensitivity can be used to screen mutants or the effects of suppressors to test for changes in the function of type I translocons.

Competition experiments, coexpressing WT and mutant forms of type I proteins in the same cell and in the presence of the transport functions, are also useful to distinguish mutants (recessive) blocked in binding to the translocon and mutants (dominant) that engage the translocator, but fail to proceed to the next stage, and therefore titrate available translocons, consequently inhibiting secretion of the WT transport substrate. Combining this with testing for sensitivity to SDS or vancomycin should provide a quick screen for classifying mutants.

THE HlyA SECRETION SIGNAL: PERHAPS NOT SO ENIGMATIC AFTER ALL

Alternative Functional Models

As described above, comparative analysis of C-terminal sequences for T1SS proteins clearly rules out a universal code and the following discussion is restricted to the most studied system, *E. coli* hemolysin secretion. The Hughes-Koronakis group (102) proposed a complicated, but very specific model with particular importance ascribed to the presumed large amphipathic helix (helix 1', Fig. 5). The model proposed that the initial step was insertion of H1' into the membrane as a loop (independently of the transporter proteins, HlyB and HlyD), seemingly with the implication that this permits partitioning of HlyA into the membrane *prior* to docking with the translocator. Then, the C terminus of the signal, covering the last 8 or so residues of HlyA (including the hydroxylated "tail"), was suggested to dock with HlyB. However, the main tenets of the model have not been tested, in particular, the insertion of the signal region into the membrane or whether specific regions of the signal bind directly to the translocon. In fact, now it would generally be supposed that T1SS proteins enter the

translocator via an aqueous chamber exposed to the cytoplasm. The model also appeared to suggest, although did not explicitly state, that the C terminus of HlyA was translocated last. This is clearly at odds with the now generally accepted hypothesis that the C terminus should be the first to reach the surface, and thus facilitate Ca^{2+} -dependent folding of HlyA. Indeed, this has now recently been demonstrated experimentally by the Schmitt group (118). As described below, an eGFP-HlyA-fusion protein forms a stuck intermediate extending across the envelope with the C terminus exposed to the exterior.

Concerning the large helix in the Hughes-Koronakis model, in other studies the terminal 11 residues of the proposed helix 1', including the charged cluster, were found to be dispensable for secretion. Furthermore, based on their combinatorial mutagenesis experiments, the Ling group (104) proposed a second alternative model for a structural code for the signal sequence. As represented in Fig. 5B, the model suggests that domain I, largely encompassing the predicted helical region shown in Fig. 5C (residues -37 to -47, covering the hotspot EISK), is essential for secretion. Domain I in this model (presumably assumed to dock with the translocon), is followed by a long downstream "connector" (residues -9 to -28). This region, as also found by others (100–102, 104), appears to contain little specific coding information. Finally, a relatively hydrophobic region of 9 residues extending to the terminus was identified, termed functional domain II, similar to that described in the Hughes-Koronakis model, also apparently essential for secretion. However, this region, as also discussed above, rather appears to be required for posttranslocational folding and/or stability.

Closing in on a Linear Secretion Code for the HlyA Subfamily

Both the two models above propose that the signal code depends on a helical structure forming *in vivo* prior to partitioning into the membrane or is induced by association with the membrane. In contrast, as described above, based on the identification of individual amino acids essential for secretion of HlyA, and in the absence of strong corroborating evidence that functional helical secondary structures actually exist in the HlyA signal sequence *in vivo*, Kenny et al. (100, 101) proposed a different model, a linear code constituted by up to eight key individual residues, distributed within the region -45 to -15 (see Fig. 5C). These were suggested to act cooperatively for specific docking with the transport proteins

HlyB and HlyD. Notably, these key residues include the EISK motif. Therefore, if we discard the suggested helical nature of domain I, the Ling model would be compatible with this linear model. Indeed, Hui and Ling (104) specifically keep this possibility open, while also considering the possibility that certain key residues might only be functional when presented on helical structure. However, looking at all the evidence available, we clearly favor the simpler linear code for translocon docking, at least for the hemolysins.

Finally, recent studies indeed provide strong support for a conserved specific pattern of several individual amino acids in the hemolysins, with particular prominence of the motif EISK in the proximal region of the signal sequence (L. Schmitt, S. Pebersdorfer, K. Kanonenberg, and I.B. Holland, unpublished data).

T1SS TRANSLOCATION IN *SALMONELLA*, *RICKETTSIA*, AND OTHER BACTERIA: YET MORE VARIETY IN SECRETION SIGNALS AND SECRETION WITHOUT RTX

The MARTX Transporters

Some very recent findings are bringing surprises and new dimensions to T1SS. The group of Karla Satchell has recently pioneered the study of toxins secreted by the type I system in many of the most important pathogenic bacteria. These “giant” multifunctional-autoprocessing repeats in toxins (MARTX), up to 9,000 residues long, frequently contain strings of several distinct toxins. Many studies have concentrated on the structural organization, mode of penetration into host cells, and mechanism of action of these toxins (17). In fact, at least some of these proteins have a slightly variant form of the classical RTX repeat (consensus, GGXGXDXUX) located close to and upstream of the C-terminal secretion signal. However, calcium ion binding and the 3D structure of these MARTX repeats (consensus GGX(N/D)DXHX) has not been described, and, as yet, few details of the actual secretion mechanism have appeared. These ABC transporters, as described later, however, like HlyB, have an additional N-terminal domain, CLD (see Fig. 2). Intriguingly, Boardman and Satchell (119) showed that secretion of RtxA_{VC} and other closely related toxins, requires a 4- rather than a 3-component translocon, with a second gene encoding an additional ABC transporter. The ATPase activity of both ABC proteins is required for secretion, and the authors propose that this may take the form of a heterodimer (see also review in references 24 and 120).

A Novel T1SS in *Salmonella*

Several other more recent studies have now identified a novel T1SS in *Salmonella enterica* with a number of unexpected features. This involves another giant type I transport substrate, (with over 5,000 residues) constituting a nonprocessed, nonfimbrial adhesin, SiiE, that was likely missed in the screen described by Linhartova et al. (6) for RTX proteins. Thus, this type I protein (121) contains 53 closely packed blocks of repeats constituting approximately 90% of the adhesin. However, these are not RTX repeats; nevertheless, each block (shown in Fig. 3) corresponds to about 90 amino acids, with highly conserved sets of dispersed Asp residues that bind Ca²⁺ ions (see also review [20]). Moreover, secretion still apparently depends on an approximately 60-residue secretion signal at the C terminus, with a translocon formed by ABC, MFP, and OMP components, all encoded in the same operon (122). Surprisingly, the *siiE* operon also contains two additional, proximal genes encoding membrane proteins, one with some similarity to the ExbB/TolQ membrane proteins (implicated in harnessing the proton motive force in bacteria for import through the outer membrane), and the other possibly similar to MotB (part of the proton-driven motor controlling flagellum rotation). The authors (123) suggested that these proteins have a novel accessory function possibly to form a proton-conducting channel, linked in some way to secretion or surface fixation of the transported polypeptide. It will be fascinating to discover how indeed these accessory proteins work and whether such partners are required for secretion of other giant type I proteins.

Novel Type I Proteins in *Rickettsia* and *Bacteroidetes*

Rickettsia form a large genus of aerobic, Gram-negative bacteria, living as obligate intracellular parasites in both invertebrate and vertebrate hosts and causing many diseases in humans, including typhus. Organisms such as *Rickettsia typhi*, have reduced genomes of fewer than 900 genes, relying on the host for biosynthesis, for example, of amino acids and nucleosides. The organism is frequently transmitted to humans by fleas, lice, and mites through bites, allowing the bacteria to access the vascular system and to establish residence in endothelial cells of the skin and major organs. So-called scrub typhus is endemic in the Asia-Pacific region with huge numbers of people dying annually of this disease.

Rickettsia and other intracellular bacteria produce several copies of ankyrin proteins as pathogenicity factors. These

Holland et al.

proteins characteristically contain a varying number of tandem repeats (mostly of 33 amino acids) of degenerated sequence but a conserved secondary structure, allowing stacking of the repeats upon each other (124). This presents a platform, maximizing opportunities for protein-protein interactions. Such broad specificity for protein interactions allows the modulation of the action of a wide variety of host proteins and therefore facilitates intracellular survival. One of the first groups to identify potential type I secreted proteins in *Rickettsia* was Wilson et al. (125), using a proteomics approach. In another recent review, Gillespie et al. (126) used a bioinformatics and literature search to identify likely secreted proteins and components of presumed translocation systems in *Rickettsia*. The results revealed at least 19 candidate secreted proteins, including some ankyrins, a near-classical Sec system, and genes encoding at least three secretion pathways, TSS 1, 4, and 5. In parallel, a number of groups, in particular (127), have provided intriguing evidence that many of the 47 ankyrins in the scrub typhus pathogen, *Orientia tsutsugamushi* (member of the *Rickettsiales*), are indeed type I transport substrates.

Indications of 7 putative type I protein translocation systems, as defined by the presence of linked genes encoding an ABC, MFP, and a TolC-like homologue, have been found in the Gram-negative, obligate anaerobe, *Bacteroides fragilis* (125). *B. fragilis* is a member of the phylum *Bacteroidetes*, the largest group of bacteria in the human microbiota, having interesting differences in the lipid composition of membranes and peptidoglycan, compared with the *Proteobacteria*. So far, no potential type I allocrite has been identified, nor sequences encoding RTX motifs in the *B. fragilis* genome, thus pointing to another interesting variation on how to fold up type I proteins following translocation.

FUNCTIONAL ANALYSIS AND ASSEMBLY OF THE TRIPARTITE TRANSLOCON

TolC the Outer Membrane Exit

Multifunctional properties of TolC: a rather nonspecific channel

While the MFP and ABC proteins are specifically and uniquely dedicated to the transport of type I substrates, TolC is an extraordinarily multifunctional and, under some conditions, apparently, an essential protein (128, 129). TolC in *E. coli* can act as an uptake site for colicins but more importantly forms the outer membrane exit of

the tripartite pump with AcrA and AcrB (and other homologues), to efflux a wide range of toxic molecules. These include many cationic dyes, a wide range of antibiotics such as penicillins, detergents such as Triton X-100, SDS, bile acids, and even simple organic solvents (130), fatty acids (131), or cyclic AMP (132). Essentially, TolC appears to act as a rather nonspecific duct, maximizing its range of transported molecules, by associating with a variety of MFPs and membrane transporters. In the absence of TolC, therefore, *E. coli* becomes sensitive to many different molecules.

Although the number of TolC molecules, about 1500, is relatively low (133), interestingly, Krishnamoorthy et al. (134) recently demonstrated that apparently less than 10% of these are sufficient to maintain cells free of toxic levels of an antibiotic like vancomycin. This indicates that TolC is normally present in significant excess, contributing to its overall capacity to participate in the efflux of a wide range of molecules.

For secretion of HlyA, TolC interacts with the ABC transporter, HlyB, and the MFP, HlyD, in the inner membrane. In contrast, when TolC is associated with AcrAB to extrude small molecules, the ABC transporter is replaced by a resistance-nodulation-division (RND) protein (135). This is a secondary active transporter that utilizes the proton gradient across the inner membrane to energize transport. The structures and mechanism of action of such drug transporters is now understood in some detail and, as we will discuss below, this provides an instructive template for the organization of the T1SS translocator.

Thanabalu et al. (136) showed that HlyB and HlyD only formed a detectable complex with TolC upon interaction with the unfolded substrate, HlyA, and only remains associated with TolC during the actual secretion process. However, as we will also argue later, it remains a possibility that T1SS transport substrates simply stabilize normally transient interactions between TolC and its different partners.

Structure of TolC

A structure for TolC was initially obtained by two-dimensional crystallization in 1997 (137) at a resolution of 13 Å. In 2000, a seminal article by the Koronakis laboratory described the crystal structure of TolC at a resolution of 2.1 Å (138) and that the functional unit is a

trimer embedded in the outer membrane of *E. coli*. TolC forms a β -barrel, constituted by a 12-stranded antiparallel β -sheet, by which each monomer contributes four β -strands to the final 12-stranded β -barrel. In contrast to the ligand-specific porins such as maltoporin, this barrel appears to be always open to the extracellular space because the structure lacks a potential plug, corresponding to the loop that forms a plug in the *E. coli* ferrichrome-iron transporter FhuA. Furthermore, and in contrast to classical porins, TolC extends very far (100 Å) into the periplasmic space (Fig. 6). This extended part of TolC adopts an entirely α -helical fold, composed of 12 α -helices, four from each monomer. At the periplasmic end of the structure, the helical bundle has a maximal diameter of only 3.9 Å (139). This indicates that the structure is the closed state, since this is obviously too small to allow transit of even α -helices or small solutes (see Fig. 6).

Noting a series of salt bridges and hydrogen bonds present at the periplasmic entrance of TolC, Koronakis

and colleagues tested the functional implications of this by designing an elegant set of experiments, using site-directed mutagenesis to disrupt these interactions (140, 141). Indeed, this generated a TolC variant with a maximum diameter of 22 Å. This variant, as also shown in Fig. 6, apparently represents the open state compatible with translocation of α -helices of type I proteins or small molecules in the tripartite drug efflux systems. Thus, as proposed by Koronakis et al. (33), the data fit beautifully into a model whereby, during translocation, a molecule like HlyA could induce an “iris-like” opening of the periplasmic “tunnel” of TolC, involving outward sliding of the helices. However, one has to add that this now generally accepted mechanism was challenged by the crystal structure of the TolC homologue VceC in *V. cholerae*. This is required for transport of a range of xenobiotics and small molecules (142). This structure revealed that the key residues apparently responsible for closure of the TolC entrance are not conserved in VceC, raising the interesting possibility that the “iris-like” mechanism proposed for TolC was not necessarily used in all other T1SS or small molecule efflux pumps.

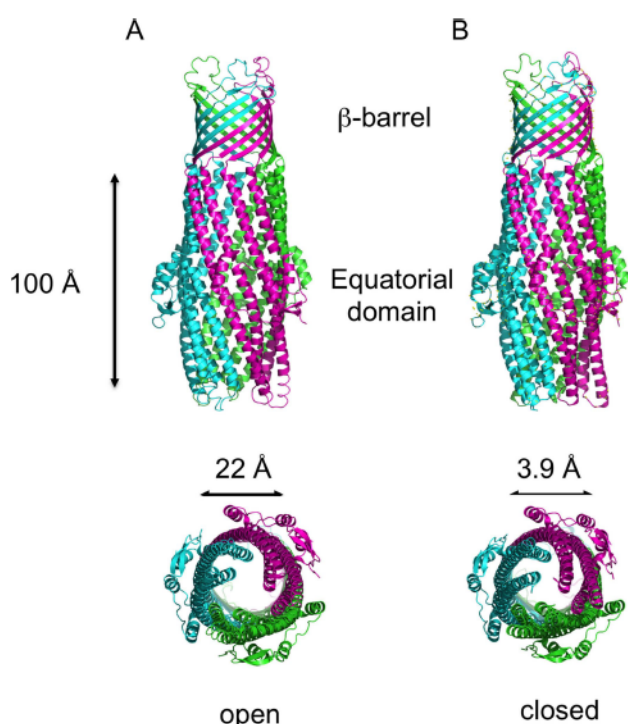


Figure 6 Crystal structures of TolC in (A) the closed (PDB entry 1EKP, [138]) and (B) the open state (PDB entry 2XMN [107]). Each monomer of the TolC trimer is colored differently. The length of the periplasmic helices is highlighted. The maximal opening of the closed and open states of TolC is also indicated below the figure.

The MFP HlyD

Little is known about the structure and functional roles of other type I ABC and MFPs and the following sections will therefore consider only HlyD and HlyB. HlyD from *E. coli* is assigned to the so-called family of bacterial “membrane fusion proteins” or MFPs.

Topology of HlyD

Wang et al. (46), using fusions of beta-lactamase to different sites in HlyD, identified regions rendering cells sensitive or resistant to the antibiotic, depending on the exposure of the inserted enzyme to the cytoplasm or periplasm, respectively. This and cellular fractionation analysis demonstrated that HlyD has a single transmembrane domain (approximately 60 residues) for insertion into the inner membrane. A subsequent detailed analysis using alkaline phosphatase fusions confirmed this topology (143).

Mutational analysis of HlyD, essential for secretion

Genetic analysis of HlyD function has been surprisingly limited; nevertheless, deletion and mutagenesis analysis has indicated several possible functional roles for HlyD, including specific association with HlyB; recognition of HlyA; providing a tightly sealed transenvelope channel;

Holland et al.

ensuring the correct folding state of HlyA; and specific interactions with TolC.

As shown in [Fig. 7](#), the N-terminal extension of HlyD contains several obvious features, a predicted 25-residue amphiphilic helix, a box of five charged amino acids close to the center, and three proline residues toward the terminus. In addition, three positively charged amino acids in the most distal region apparently adjacent to the transmembrane domain (TMD) are likely required for stable association with the membrane bilayer ([144](#)).

Pimenta et al. first showed that deletion of the first 40 amino acids of HlyD blocks secretion completely, while the truncated HlyD remains normally expressed and stably localized to the membrane ([45](#)). Surprisingly, in competition experiments, this HlyD deletion mutant, when coproduced with WT HlyD (and HlyB) does not affect secretion of HlyA, but greatly reduces its hemolytic activity. This suggests the aberrant packing of WT and mutant HlyD molecules in a mixed oligomer, resulting in secretion of misfolded hemolysin (J. Young, A. Pimenta, and I.B. Holland, unpublished results). Mutants with such properties are a recurring finding as indicated in the next section. Indeed, as detailed in the next section, Balakrishnan et al. ([145](#)) confirmed that the cytoplasmic N-terminal extension of HlyD, apparently highly conserved in T1SS hemolysin-like toxins, plays a key role in the recognition of HlyA and then recruitment of TolC into a fully competent translocon.

Schulein et al. ([146](#)) observed some conservation of the C-terminal amino acids of HlyD (especially the last 35 residues) based on the limited range of HlyD-like sequences available at that time. When the 10 C-terminal residues of HlyD were deleted, secretion of HlyA was completely blocked. Similarly, site-directed mutagenesis of the terminal, Leu, Glu, or Arg residues of HlyD demonstrated that these were essential for secretion ([Fig. 8](#)). In competition experiments with expression of both WT HlyD and the truncated HlyD, secretion of HlyA was greatly reduced, indicating that the structure of the mixed oligomer was rendered defective in some way. Curiously, these authors also identified a region of 44 amino acids in HlyD (residues 127 to 170, the proximal part of the helical hairpin; see [Fig. 7](#)), showing a surprising 47% identity with residues 233 to 274 in a β -barrel region of TolC. Deletion of this region also completely blocked HlyA secretion, but unfortunately, analysis of the specific

role of these residues for HlyD function has not subsequently been followed up.

In a different approach ([147](#)), random mutagenesis of *hlyD* in *E. coli* LE2001 was used to obtain several mutants located in the HlyD-periplasmic domain, whose expression, stability, and membrane association were unaffected. The mutants showed a range of novel properties and mapped to different domains of HlyD ([Fig. 8](#)), compatible with defects in different steps in the secretion process. Three mutants, T85I, K404E, and D411N, gave greatly reduced halos on blood plates and secreted little or no HlyA protein. In addition, in T85I, HlyA was not detectable in cell envelopes, suggesting a block early in initiation of secretion. In competition experiments, the D411N and K404E mutations (both mapping to the terminal β -domain) were dominant, apparently also because of formation of a structurally defective mixed HlyD oligomer. Moreover, in this mutant, the secreted HlyA protein had substantially reduced hemolytic activity (Young, Pimenta, and Holland, unpublished). Remarkably, in the same study ([147](#)), the four mutants, T85I (mapping just beyond the TMD), L165Q (proximal coiled-coil region), and V334I and V349I (both in the distal lipoyl region), showed both greatly reduced secretion levels and hemolytic activity of HlyA, but only in the presence of a high calcium ion concentration. Thus, with 10 mM Ca^{2+} , no colony halos formed on blood plates, while, with 1 mM Ca^{2+} , halos formed as seen with WT HlyD. From trypsin treatment of intact cells or isolated envelopes, it appeared that secretion from T85I is blocked by Ca^{2+} at an early step, with evident cytoplasmic accumulation of HlyA. In contrast, with L165Q, HlyA clearly accumulated in the envelope, apparently forming a stuck intermediate, while the two lipoyl mutants, V334I and especially V349I, showed accumulation of HlyA primarily on the cell surface. Moreover, with both lipoyl mutants, HlyA recovered from the medium was shown to be misfolded, since the HlyA protein was hypersensitive to trypsin and the low specific activity was restored to near-WT level after urea denaturation and renaturation. Interestingly, Vakharia et al. ([148](#)) described mutations affecting amino acids in the periplasmic domain of TolC, similarly resulting in reduced activity of the secreted HlyA.

Previous studies have shown that, in *E. coli*, the periplasmic calcium ion concentration increases substantially as the extracellular concentration is increased, bringing periplasmic levels up to at least micromolar, com-

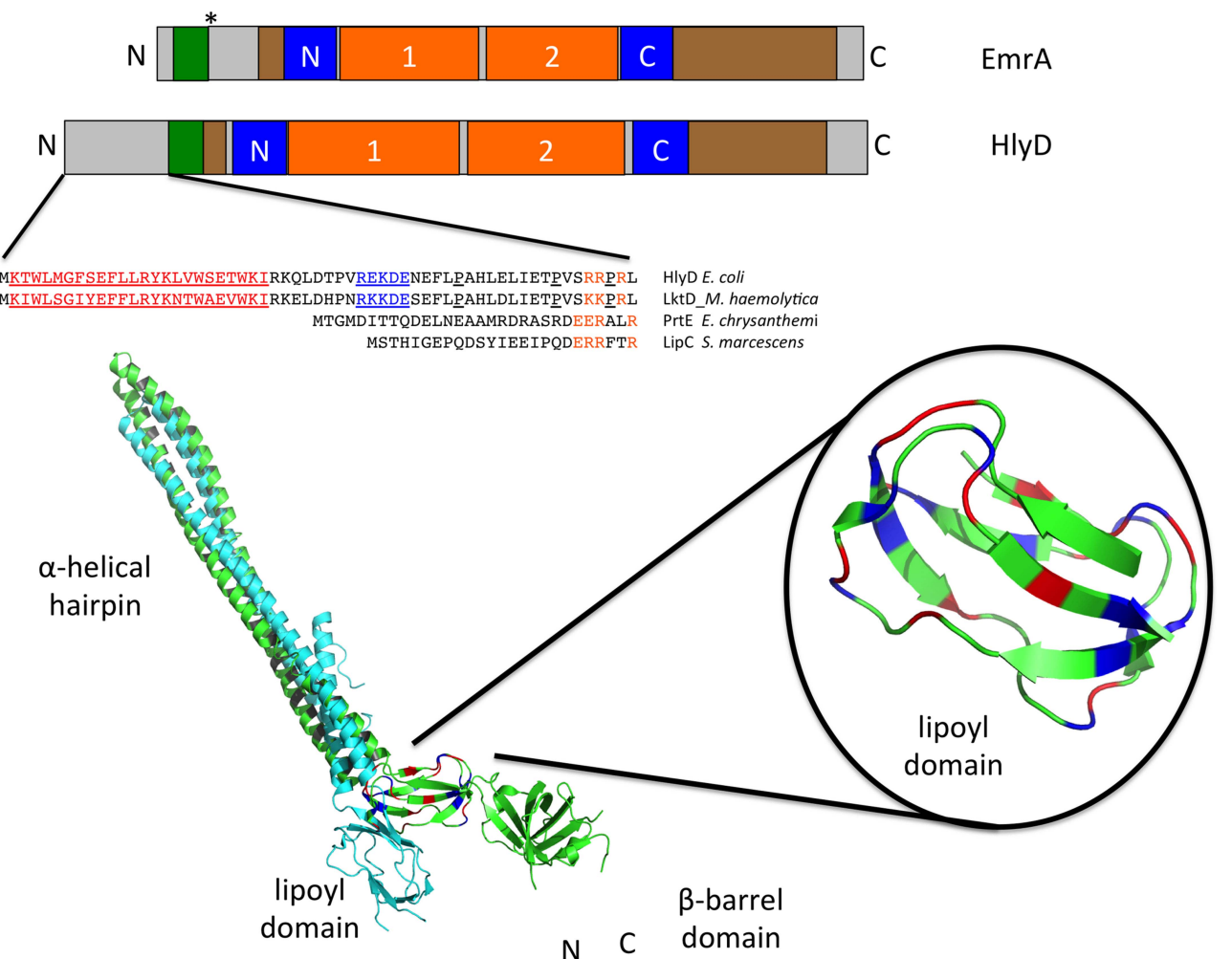


Figure 7 Structural and functional features of EmrA and its homologue HlyD. (Top) The rectangles represent the distinct conserved regions of EmrA from *E. coli* (involved in multidrug transport) and HlyD from *E. coli*, indicating the location of the cytosolic domains, the transmembrane helices, the coiled-coil, the lipoyl and β -barrel domains. Scaling is based on the number of amino acids that contribute to the individual parts. The transmembrane helices are shown in green. The two helical regions of the coiled-coil domain are highlighted by orange boxes and labeled 1 and 2. The two parts of the lipoyl domain are indicated by blue boxes labeled, respectively, N and C for the N- and C-terminal parts of this domain, while the β -barrel domain is represented by brown boxes. The asterisk marks the position of the C terminus of EmrA from *A. aeolicus*, because this protein has no TMD. The zoom-in shows the sequences of the N-terminal cytoplasmic domains of HlyD, and other MFPs involved in type I secretion, PrTE (protease secretion), LipC (lipase), and LktD (another hemolysin). The putative amphipathic helix (letters in red) and the charged cluster (letters in blue) in HlyD, implicated in interaction with HlyA and consequent recruitment of TolC (145), are highlighted. The positions of the domains of EmrA are derived from the crystal structure obtained for EmrA from *A. aeolicus*. The corresponding positions in HlyD are estimated from the predicted secondary structures (including the coiled coil). (Bottom) Cartoon representation of the crystal structure of monomeric EmrA from *A. aeolicus*, which lacks a TMD and an N-terminal cytoplasmic extension (154), with a zoom into the compact form of the associated lipoyl subdomains. The recently determined crystal structure of parts of HlyD (152) is superimposed on the EmrA structure to emphasize the similarity of both proteins (cyan). Black residues in the α -helical hairpin represent the predicted position of the heptad repeats important for coiled-coil formation. In the lipoyl domain, blue residues are identical amino acids in more than 50% of the sequences analyzed in reference 155, while red residues are similar amino acids in more than 50% of the sequences analyzed. Note the closely adjacent N and C termini made possible by the flexible nature of the α -helical hairpin in EmrA. This would also allow movement to facilitate interaction with the cognate outer membrane protein, TolC.

Holland et al.

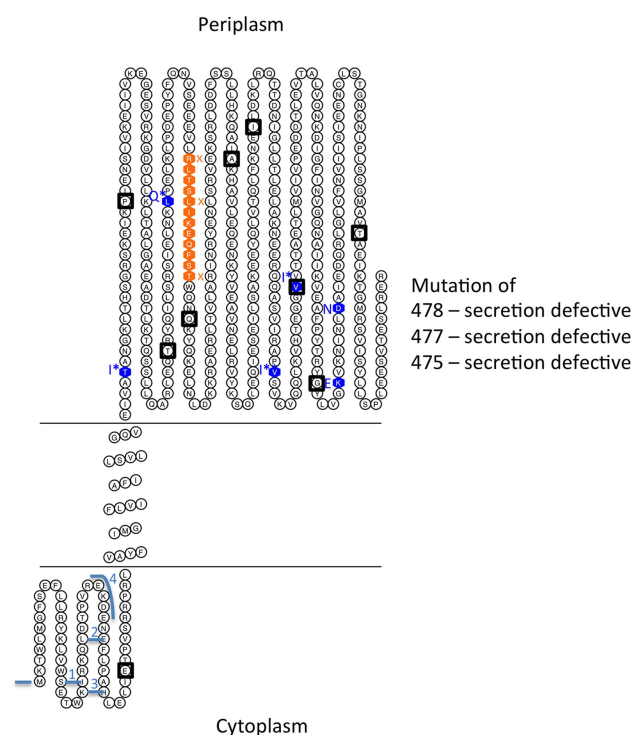


Figure 8 Mapping the position of mutations on a topology map of HlyD. The topology is based on membrane fractionation experiments and beta-lactamase insertions giving antibiotic resistance (46, 147). Each 50th residue is marked by a black box. Residues 150 to 246 and 251 to 327 define the approximate position of the coiled coils, residues 97 to 128 and 328 to 360 for the two half-lipoyl domains, while the major β -barrel occupies the C-terminal domain. The lipoyl domains, in particular, are likely to be involved in tightly packing the HlyD protomers, while the β -barrel by analogy with other MFPs could be involved in interaction with HlyB. Orange residues encompass the position (close to the middle of the helical hairpin) of the reportedly conserved RLT motif proposed to interact with TolC (214). At the N terminus, key regions required for binding HlyA and consequent triggering of TolC recruitment were defined (145) by the N-terminal deletions discussed in the text: deletion 1 removes the first 20 residues (the majority of the putative amphiphilic helix); deletion 2, the first 40 residues; deletion 3, the first 45 residues; and the internal deletion 4 removes the charged cluster, which is especially important for recruitment of TolC. Blue residues indicate secretion-defective mutations from different groups. * marks mutations blocking secretion, conditional on high calcium ion concentrations in the medium (147). These include mutations having possible effects on HlyD packing and map mainly in the lipoyl domain and the β -barrel.

pared with nanomolar in the cytosol (149). We speculate, therefore, that in these Ca^{2+} -sensitive HlyD mutants, to varying degrees, the packing of HlyD protomers or the sealing of interfaces of HlyD with HlyB or TolC are distorted sufficiently to allow penetration of the translocon by calcium ions. We suggest that these bind to the RTX

during transit, triggering some premature structural changes, causing slowing of translocation and ultimately misfolding on the surface or, in the case of the mutant L165Q, actual arrest in the translocator.

The cytoplasmic domain of HlyD is required for HlyA-dependent TolC recruitment

MFPs that participate in ABC-dependent (T1SS) protein translocation invariably, to our knowledge, appear to have a single TMD anchor and a short N-terminal extension into the cytoplasm. However, the length and nature of the extension can vary markedly (Fig. 7). In the case of HlyD, the TMD is preceded by an approximate 59-residue N-terminal extension.

Balakrishnan et al. (145), confirming the importance of the C terminus for secretion described in the previous section by using an N-terminal 45-residue deletion of HlyD to block secretion, demonstrated that the mutant HlyD, in the presence of HlyA,B, was unable to “recruit” TolC into the transenvelope complex. Nevertheless, oligomerization of HlyD and its interaction with HlyB and HlyA, were apparently all retained. Notably, however, in the absence of HlyB, the truncated HlyD failed to bind HlyA, perhaps indicating that HlyB and D bind to overlapping sites in HlyA. Curiously, using a similar cross-linking approach, we found that oligomerization of HlyD, in contrast, was abolished when the N-terminal 40 residues of HlyD were deleted. We have no explanation for this discrepancy (Young, Pimenta, and Holland, unpublished).

As shown in Fig. 7, the first 45 amino acids of HlyD contain a predicted 25-residue amphipathic helix and a downstream cluster of five charged residues. Balakrishnan et al. (145), using other deletion mutants subject to cross-linking *in vivo*, showed that, while both the helical region and the charged cluster were required for secretion, only the charged cluster was necessary for recruiting TolC. However, no clear role was established for the helical region. Nevertheless, the authors were able to propose that the cytoplasmic N terminus of HlyD (apparently with the help of the ABC protein), when sensing the presence of HlyA, mediates transduction of a conformational signal to the periplasmic domain that allows recruitment of TolC. Importantly, however, from more recent comparative genomic analysis, it is clear, although surprising, that this mechanism for recruiting the OMP is not conserved. For secretion of other type I proteins such as the proteases and lipases, the MFP homologue has a very short, quite different N-terminal sequence

compared with that of HlyD. Recruitment of the OMP in these cases must therefore require a different mechanism. For example, in some bacteria, the relevant OMPs and MFPs may inherently be able to form a complex without any special recruitment mechanism. Thus, for the analogous MacAB, TolC-macrolide transporter (153), and similarly for AcrAB, TolC (150), assembly of the entire complex apparently occurs even in the absence of an allocrite.

HlyD shares many structural features with MFP analogues

MFP is a misnomer since these proteins do not promote membrane fusion in the classical sense. Rather, they provide the physical and functional coupling of proteins in transenvelope complexes that straddle the inner and outer membranes; an alternative term also used is “adaptor proteins.” Symmons et al. (151) in an excellent review now introduce a new synonym, periplasmic adaptor proteins (PAPs).

The importance of HlyD in type I transport was, to some extent, initially underestimated, assumed simply to fulfil the role of connecting the inner membrane ABC protein with the outer membrane TolC exit to the medium. Until recently, no HlyD structural data were available, but now a partial structure of HlyD, 277 residues out of 478 and lacking both the cytoplasmic extension and the C terminus, has been published (152). However, many mutational studies and, in particular, crystal structures of functional analogues have brought important insights into what appears to be a quite complex role for HlyD. These homologues include the extensively studied multidrug transporter MFPs, AcrA, EmrA, MacA, and MexA, that form three protein component translocons with AcrB/TolC, EmrB/TolC, MacB/TolC, and MexB/MexX, respectively, in Gram-negative bacteria.

HlyD, as well as MacA, which interestingly is also coupled to an ABC transporter (153), and EmrA (154), linked with a major facilitator superfamily (MFS) secondary transporter to provide energy, all dock with TolC in the outer membrane. These proteins, like HlyD, have a single TMD peptide anchor close to the N terminus, embedded in the inner membrane. In the case of HlyD, this TMD is preceded by the cytoplasmic extension of about 60 amino acids, required for recruiting TolC, as discussed in the previous section. AcrA, in contrast, is anchored in the membrane from the periplasmic side by a lipid modification of the N terminus. This AcrA architecture pre-

sumably facilitates capture of drug molecules from the bilayer or periplasm, while the TMD and the N-terminal extension in HlyD permits direct contact with the HlyB TMD and with HlyA in the cytoplasm.

Although HlyD, as well as AcrA, MexA, and other family members share less than 25% identity, Johnson and Church (155) identified a number of well-conserved structural motifs in the large periplasmic domains of all these proteins (see also reference 151). As shown in Fig. 7, there is an extensive helical hairpin, strongly predicted to form coiled coils, toward the N terminus, for example, in EmrA. HlyD is also predicted to have a long helical region with two blocks of likely coiled coil and, as confirmed by the partial structure of HlyD, remarkably similar to that of EmrA (Fig. 7). Importantly, the hairpin domain in HlyD and EmrA is flanked at each end by a short half-“lipoyl” domain. This widely conserved lipoyl module is known to activate a number of enzymes, involving a switch in architecture from two well-separated halves to a fused globule of two lipoyl domains. However, in the functional form of MFP proteins, the lipoyl domains are always apparently associated in a compact structure. Other predicted structures conserved to varying degrees in MFP proteins are some β -sheet, N-terminal to the helical hairpin, an extended β -barrel domain toward the C terminus, followed by a disordered C-terminal domain (151, 155).

Importantly, MFPs appear to be very flexible molecules, with, in particular, flexible “joints” at the borders of the distinct domains. This presumably facilitates the acrobatics required to achieve stable contacts with proteins across two membranes and its oligomerization to form a tightly sealed palisade around its inner and outer membrane partners (156, 157). Moreover, the folding of the helical hairpin, formed by the coiled-coil region of AcrA, EmrA, and therefore very probably HlyD (Fig. 7), brings both the N- and C-terminal regions together, close to the inner membrane, available for interaction with the associated inner membrane energy transducer. Interestingly, exciting new structural models of a number of drug efflux pumps can provide important pointers to the positioning of HlyD in the translocon.

HlyB the ABC Transporter

Topology of HlyB

The topology of HlyB, an ABC half-size transporter, was deduced experimentally in 1991 (46) from the con-

Holland et al.

struction of beta-lactamase fusions throughout the length of the protein. The results, where an externally exposed beta-lactamase confers penicillin resistance on strains carrying a fusion, indicated six transmembrane domains (TMDs) in reasonable agreement with those predicted by algorithms. The fusion data also appeared to indicate two additional domains near the N terminus, but these were poorly predicted. In fact, sequence data indicated strong homology in this region with a cysteine protease, although with defective catalytic site (91) likely to prevent activity. Interestingly, Gentshev and Goebel (158) subsequently reported a topology analysis of HlyB, using beta-galactosidase and alkaline phosphatase fusions, showing differences in the precise position of the transmembrane helices (TMHs), but also identifying eight possible TMHs, including two in the N-terminal region. However, as described later, the N-terminal CLD domain (Fig. 2) was recently shown by Lecher et al. (54) to constitute an ancient but inactive C39 cysteine protease, nevertheless essential for secretion of HlyA. The topology of HlyB shown in Fig. 9, is a composite cartoon combining all the fusion data from Wang et al. (46) and Gentshev and Goebel (158). In addition, an arbitrarily fixed TMD length of 25 residues was adopted, with the exception of TM2 where the fusion data were otherwise more difficult to accommodate in the model. Importantly, in view of the recent demonstration that the CLD binds to the C terminus of HlyA, this region is now reassigned to the cytoplasm. The model, in particular, indicates a single large periplasmic loop P1 (a possible interaction site for HlyD), and two very small loops, P2 and P3, with two relatively large cytoplasmic loops, C1 and C2. In addition, the model predicts two regions of approximately 25 and 36 amino acids, with perhaps important functional roles, separating the TMDs from the CLD and nucleotide binding (NBD) domains.

Mutational analysis of HlyB

Surprisingly, few mutagenesis studies targeting the membrane spanning half of HlyB have been reported. Unfortunately, therefore, this very important approach has been seriously neglected. However, several mutants obtained for the NBD domain in a variety of ABC transporters, including HlyB, have considerably enlightened the analysis of the catalytic action of the NBDs by confirming the important role of many of the highly conserved residues. However, since these mutations have already been studied in great detail in many different ABC proteins (159), they will not be considered further here.

As summarized in Fig. 9, a few HlyB mutations linked to the membrane domain give intriguing phenotypes but, so far, have been much less instructive in linking structure to function than comparable HlyD studies. Several mutants were isolated by random mutagenesis by Blight et al. (116); two of these (G10R, and P624L) showed novel temperature-sensitive secretion defects. Residue G10 was located close to the N terminus, indicating that this region that we now call the CLD might have a specific role in the secretion process. The mutation P624L is located in the P-loop of the NBD. This is a highly conserved residue, and its implication in HlyA secretion is intriguing since this amino acid is highly conserved in both pro- and eukaryote ABC transporters, forming part of the Pro-loop linking the two domains of the NBD (160), and just downstream of the “signature” motif (LSGG). Another temperature-sensitive secretion mutant, G408D, was located in the deduced periplasmic loop P3 between TMDs 5 and 6. The corresponding region, in some cases covering up to 12 to 15 residues, we found was quite well conserved in a wide range of bacterial ABC transporters, but also in the eukaryotic ABC proteins, Pgp, Pfmdr, and CFTR. Saturation mutagenesis of the region, residues 399 to 412 (see Fig. 9), yielded mutations, I401T and D404G, giving no hemolytic colonies and approximately 20% of WT levels of HlyA hemolytic activity when measured in liquid cultures. In addition, a double mutant S402P, D404K completely lacking secretion of HlyA was obtained by site-directed mutagenesis. Therefore, in this region of 8 residues, at least four amino acids are essential for HlyB function.

Figure 9 also illustrates the location of the suppressor mutations in HlyB (161, and next section) that restored, at least to low levels, the secretion of HlyA deleted for the proximal or the distal halves of the 50- to 60-residue HlyA secretion signal. These suppressor mutations are widely dispersed throughout HlyB, with the authors suggesting that they might define the binding site for HlyA. However, these mutations are not site specific, and thus it appears more likely that they represent possibly unrelated structural changes, somehow bypassing the need for the full signal.

Two additional secretion mutants (Fig. 9), E256K and S279L, were found in cross-linking experiments to be defective in oligomer formation of HlyD *in vivo* (Pimenta, Young, and Holland, unpublished). This suggests that these are possible regions involved in formation of the HlyB, D complex.

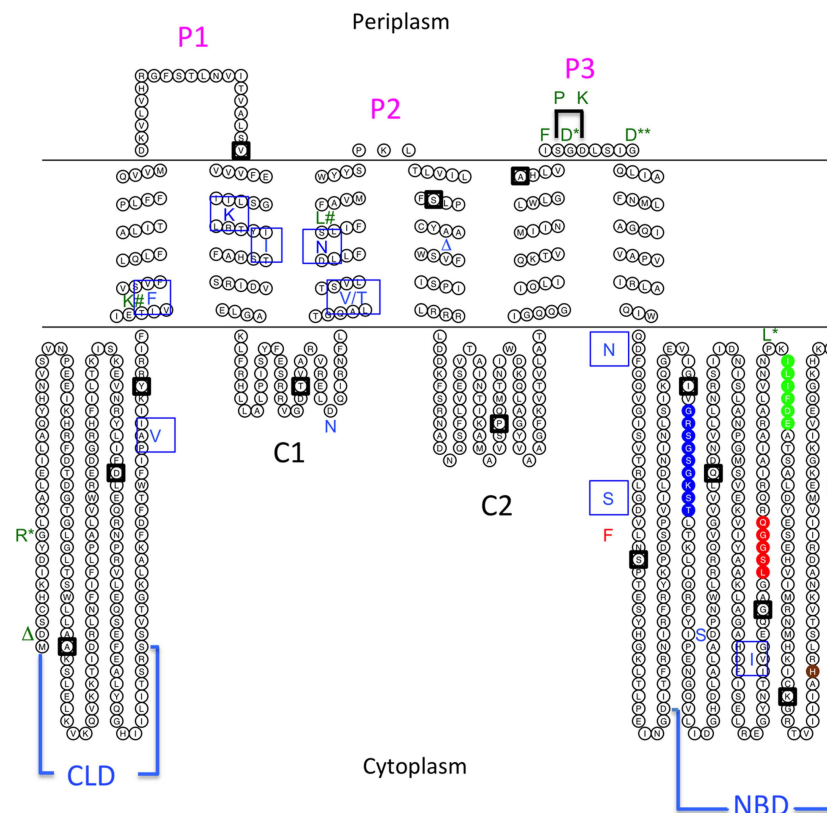


Figure 9 Mutations localized to the HlyB topology model. This is a composite based on beta-lactamase, beta-galactosidase, and alkaline phosphatase insertions, as described in the text. Each 50th residue in the sequence is marked by the black box. The crystal structures of the CLD and NBD were derived from purified fragments, residue 1 to 130 and residue 467 to the terminus, respectively. The conserved motifs Walker A, C-loop, Walker B, and the histidine of the H-loop, all in the NBD, are highlighted in blue, red, green, and brown, respectively. Letters indicate mutations identified in different genetic screens. Green letters highlight those mutations that affected the level of secretion, including three temperature sensitive mutations marked *, one of which (marked **) also grew poorly at 42°C. Letters in blue boxes are mutations in HlyB suppressing one or other of two deletion mutations in the HlyA secretion signal. Residues additionally marked by a # affected the oligomerization of HlyD, while triangles are secretion-defective insertions. Note the “hotspot” for mutations in the relatively well-conserved region, predicted to be periplasmic domain P3. In the case of ambiguities, for the periplasm the residue substituted is to the right. See text for other details.

HlyB interacts with the HlyA secretion signal

Current evidence indicates that the C-terminal region of HlyA interacts with HlyB, not only via the N-terminal CLD, but also with the NBDs. It is not yet clear if these binding sites in HlyA do or do not overlap and whether they are close to the HlyA binding site of the HlyD N-terminal extension discussed above.

Different laboratories, using various chimeric translocons formed from combinations of cognate and noncognate ABC, MFP, and OMP proteins, have shown that selectivity controlling secretion of type I protein HasA and a lipase resides in the cognate ABC protein (162). As far as we are aware, however, a similar analysis has not been done for the Hly system.

However, the Ling group (summarized in Zhang et al. [161]) isolated HlyB mutations suppressing the effect of either of two HlyA secretion signal mutants. One mutation (del 1) deleted the proximal half of the presumed 58-residue signal (including helix I and the charged cluster) leaving residual secretion at about 5% of WT. The other mutation deleted essentially the distal half of the signal sequence, residual secretion being reduced to less than 1%. However, again as noted above, effects of the distal deletion would include misfolding of secreted molecules and therefore an apparent secretion defect.

Putative suppressors, obtained following random mutagenesis of *hlyB*, were screened for increases in hemolytic

Holland et al.

colony halo sizes. The secretion levels of the finally purified suppressors were quantified by hemolytic assay in liquid cultures. In view of the reservations above regarding hemolytic colonies, not surprisingly perhaps, levels of secretion by the suppressors of the HlyA terminal deletion were poor, with most increasing only 2% to 5%. However, levels 10% to 20% of WT were obtained with suppressors of the proximal deleted signal. In total, 21 suppressors were obtained, with one mutant, A629V selected independently by both deletions.

The majority of the suppressors map around the membrane domains and flanking cytosolic part of HlyB, as predicted by the topology analysis presented in [Fig. 9](#). The authors concluded that the suppressors, in general, defined specific residues directly forming the binding site for the HlyA C-terminal secretion signal. However, while it cannot be ruled out that some of these HlyB mutations, particularly those selected against the N-terminal deletion, might affect an HlyA binding site, deletions cannot be suppressed allele specifically. Alternatively, we suggest that the results may reflect more indirect mechanisms of suppression that, nevertheless, if exploited further, might provide useful insights into the mechanism of action of HlyB. Finally, Zhang et al. ([161](#)) remarkably also showed that the mutants restored some level of secretion to HlyA deleted for the entire terminal 58 amino acids. This is a puzzling if not a worrying result, being very difficult to explain.

Surface plasmon resonance studies of the isolated NBD of HlyB have also demonstrated directly an interaction with a C-terminal fragment of HlyA ([163](#)). This interaction (with an affinity of 4 μ M) was strictly dependent on the presence of the HlyA secretion sequence, since its deletion completely abolished the interaction. Interestingly, the dissociation rate of the interaction was accelerated in the presence of nucleotides, ATP or ADP, suggesting that the interaction is fine-tuned in the biological context. Interestingly, since the C terminus of HlyA is now known to be clearly translocated first, binding of the signal region to HlyB must be readily and rapidly reversible.

With a different T1SS, Delepelaire ([164](#)) also demonstrated that the ABC-ATPase activity of a partially purified PrtD from *E. chrysanthemi* was regulated *in vitro* by the cognate signal sequence. Thus, the natural C-terminal secretion sequence inhibited ATPase activity almost completely, although with perhaps a surprisingly low K_i of approximately 0.2 μ M, indicating tight binding. These

results for both HlyB and PrtD point to a common interaction between the secretion sequence of the substrate and the ABC transporter. This, plus the additional evidence for binding of the CLD upstream of the signal, within the distal RTX region, contributes to an emerging molecular picture of the sequence of events leading to initiation of HlyA secretion.

Coassociation of HlyB and HlyD

A number of studies looking at the ability of chimeric translocons to secrete different allocrites have indicated that specific interactions between the MFP and ABC proteins, and between MFP and OMPs, are required for specificity, i.e., secretion of a particular polypeptide. However, there is as no evidence yet of interactions between the OMP and the ABC protein. In the analogous tripartite drug transporters, it is still not completely clear when, if, and precisely how the analogous inner and outer membrane components interact (see reference [156](#)).

HlyB and D form a constitutive complex: stability of HlyD depends on HlyB and TolC

A number of genetic studies have indicated that the ABC and MFP proteins of the Hly, Prt (protease), and Cva (colicin V) translocons interact. More directly, evidence for interactions has been obtained by using copurification with an affinity tag or in cross-linking experiments ([136](#), [165](#), [166](#)). Other support for an interaction between the ABC and MFP proteins comes from measuring their stabilities in cells. For the Hly T1SS, both HlyD ([45](#)) and HlyB (Young, Pimenta, and Holland, unpublished) are synthesized constitutively throughout the growth phase with both the laboratory strain and the pathogenic strain, LE2001. Notably, this expression is not coupled to the synthesis of HlyA, whose production (at least in laboratory cultures) is usually restricted to a relatively brief window during late-exponential phase ([35](#), [45](#), [103](#)). Moreover, in the presence of TolC, but in the absence of HlyB, HlyD becomes less stable, with a half-life of approximately 100 min at 37°C, compared with 5 h when both HlyB and TolC are present. However, in the absence of TolC, the presence of HlyB actually renders D highly unstable, with a half-life of 36 min ([45](#)). All these results are consistent with conformational changes perhaps required in all three proteins to achieve assembly of a functional complex. However, this has not been demonstrated directly, although there is strong evidence for this in the analogous bacterial drug transport complexes (see reference [156](#)).

Preformed transporter complexes in other T1SS

Interestingly, the CvaB (ABC) and the CvaA (MFP) proteins of the colicin V translocator were also found to depend on each other for stability, while both are very unstable in the absence of TolC (165). In addition, interaction of TolC with CvaA appeared to induce structural changes in the latter, enhancing its sensitivity to intracellular proteases when TolC was absent. Notably in these studies, although the ABC and MFP were present, the transport substrate was absent, thus suggesting that *all three* proteins of the translocon can form a complex, independently of the allocrite. Surprisingly, a major gap in our knowledge is the absence of any reports, as far as we are aware, on the structure of these ABC MFP complexes, the stoichiometry, or the detailed nature of the protein-protein interfaces. However, useful information is forthcoming from different approaches to identify regions of the analogous MFPs, AcrA, MacA, EmrA, and CusB involved in drug efflux with the cognate transporter. These have indicated that the C-terminal membrane proximal domain, β -barrel, and lipoyl domains can in some cases be involved in interactions with the cognate energy transducer (see the recent review [156]). Of particular relevance, perhaps, are studies with the Mac-efflux pump in *E. coli*, where MacA (MFP) forms a complex with its partner MacB, an ABC transporter, also involving possible interactions between the respective TMDs (167). Moreover, with this Mac-macrolide efflux system, the periplasmic domain of MacA (the MFP) not only stabilizes the ATP-bound form of the associated MacB, ABC, but also stimulates its ATPase activity (153, 167). This suggests a greater degree of coordinated activity between the MFP and the energizing component than encountered so far.

Isolation of an assembled translocon for HasA

Letoffe et al. (166) first showed that, in cells producing the transport substrate, an entire translocon containing the ABC, MFP, and OMP could be isolated from cells as a single complex present in the detergent-solubilized membrane protein fraction. This was obtained by copurification through specific affinity binding to the tagged allocrite, but without cross-linking to stabilize protein interactions. Instead, a strategy was used to maintain protein interactions that involved frozen transport complexes in which the allocrite is “engaged” but secretion is blocked. Two systems were studied for the secretion of protease C from *Erwinia* and HasA from *S. marcescens*, but we shall only consider HasA. For such studies the

hemophore HasA is a good choice, since, when folded, this can easily be detected by its specific affinity for heme. HasA as the tagged allocrite, was coexpressed with the heterologous Prt-transport proteins from *E. chrysanthemi*. This T1SS secretes several proteases but does not secrete HasA. However, HasA nevertheless blocked the translocon in some way. Consequently, all three Prt-transport proteins, ABC, MFP, and OMP, could be specifically purified together with the heme-affinity-purified HasA. In addition, all three transport proteins were still copurified when a translocon was used that does allow secretion of HasA, i.e., a chimera with the cognate ABC protein (HasD) coexpressed with the MFP and OMP from the Prt system. This indicates that the active transport complex somewhat surprisingly appeared very stable, even during detergent extraction.

Interestingly, but also surprisingly, when *fully folded* HasA (purified from culture supernatants) was added *in vitro* to proteins solubilized from cells expressing the Prt transport proteins, HasA still successfully interacted and copurified with the ABC protein. However, there was no interaction with the MFP and TolC proteins. When purified HasA was added to solubilized membrane proteins from cells previously primed to assemble the Prt translocon *in vivo*, by the presence of a cognate transport substrate (protease B), all three transport proteins were again affinity purified with HasA. This, albeit indirect evidence showed that functional assembly of the complete Prt complex required the *in vivo* presence of the cognate allocrite to form a sufficiently tight association to survive the extraction procedure. Hwang et al. (165) concluded that the MFP, OMP complex in these experiments, unlike HlyB with HlyD, did not form a strong association in the absence of transport substrate.

When only a single transport protein (ABC, MFP, or OMP) was expressed in cells together with the allocrite, Letoffe et al. (166) also confirmed that the ABC protein (that is PrtD) could be detected in association with HasA. The authors concluded that, for this particular T1SS translocon, assembly is initiated by the ABC-allocrite association (with no detectable direct docking of allocrite and the MFP). This is followed by an ABC and MFP interaction that triggers recruitment of the OMP to complete assembly of the complex. A subsequent study from the same group (114) in fact showed that a specific region of the signal sequence of HasA, via an interaction with the ABC transporter, promoted recruitment of TolC.

Holland et al.

These studies were an important advance, and the results overall provided coherent conclusions. Nevertheless, the experimental setup had some limitations, particularly the assumption that all the possible protein interactions would resist detergent solubilization. The study also showed that *folded* HasA was able to bind the ABC protein *in vitro* with HlyA, while the CLD interacts with an unfolded HlyA, independent of the secretion sequence, the isolated NBD interacted with folded HlyA1. This was strictly dependent on the secretion signal but it is not excluded that this region was unfolded.

Isolation of the Hly translocon

In a subsequent and somewhat simpler system, Thanabalu et al. (136) analyzed possible interactions involving HlyB or HlyD using these proteins carrying an N-terminal histidine affinity tag. Importantly, putative complexes in this case were “frozen” by cross-linking *in vivo* with a reversible cross-linker. An HlyB, HlyD complex was detected even in the absence of HlyA and TolC. However, all three transporter proteins could be copurified in a complex when coexpressed with HlyA, clearly showing that the transport substrate was required to recruit the outer membrane component TolC. Importantly, tagged HlyD and, in particular, HlyB, when produced separately, could still be copurified together with HlyA, indicating that this interaction can occur before the complete translocon is established. Moreover, the authors did not apparently rule out the idea that both HlyB and HlyD might bind HlyA in a coordinated manner. However, the results indicated that HlyD but not HlyB could be cross-linked to TolC confirming that HlyD formed the “bridge” to the OMP. Using an HlyB mutant defective in ATPase activity to block secretion, these authors also found that ATP hydrolysis was not required for assembly of the whole complex, oligomerization of HlyD (detected as cross-linked trimers), the interaction of HlyB and HlyD, or their binding to HlyA. This therefore is also a “frozen complex.” It is frustrating, however, as in virtually all other similar experiments in the literature, that no attempts were made to determine at which stage secretion was blocked in the frozen complex, is the allocrite simply bound to the translocon or is it able subsequently to enter the “channel” to form a stalled intermediate.

Notably, in these studies in contrast to the analysis of HasA secretion discussed above, Thanabalu et al. identified preformed HlyBD complexes and, in particular, an important early role for the MFP in recognition of HlyA (136). This appeared to represent a fundamental differ-

ence with assembly of the Prt complex. Consequently, it is important to consider whether interaction of the allocrite with PrtE (MFP) was missed by Letoffe et al. (166) because of insufficient stability in the absence of cross-linking. On the contrary, it now seems more likely that the role of the MFP in the two systems is indeed fundamentally different, since an allocrite binding site in PrtE, analogous to that in HlyD, simply does not exist (Fig. 7). However, the Thanabalu et al. experiments gave no indication of which regions of HlyD (or B) and HlyA interact, and this still remains unknown. However, as described above, a subsequent analysis by Balakrishnan et al. (145) identified the HlyD binding site for HlyA and how this plays a key role by coupling binding of HlyA to assembly of the translocon. Finally, Thanabalu et al. sketched out a speculative model of the secretion process (136). This suggested that HlyA binds to HlyB and D, sequentially or simultaneously, to the same or different sites in HlyA. This triggers conformational changes in HlyD and recruitment of TolC, concomitant with opening of the transport channel, composed of HlyD and TolC multimers, but not the ABC protein itself. A ratcheted transit of HlyA through the envelope was then envisaged, involving the proton motive force.

Envisaging a possible structure for the Hly translocon

High-resolution structures for the N termini and C termini of HlyB, the CLD, and NBD, respectively, have been obtained, but no structure yet for the crucially important membrane domain, likely to form the initial pore leading to the HlyD channel. In addition, a partial structure for HlyD has recently been described (152), while only the RTX β -roll structure is known for the hemolysin itself. In contrast, several recent structural studies, combined with model building suggest how the known crystal structures of, for example, AcrA, AcrB, and TolC are organized in the complete pump. These studies have involved much debate, not yet concluded, concerning the precise contribution of each subunit to the putative transenvelope transport pathway. This includes whether the inner membrane protein (AcrB or MexB) contacts the OMP, and, especially contentious, how does the long (approximately 140 Å) strikingly funnel-shaped MFP at its narrowest point make contact with the outer membrane protein. For the construction of pseudo-atomic structural models of such drug pumps, the crystal structures of three partners were superimposed on low-resolution cryo-electron microscopy structures. These have confirmed the formation of a contiguous structure

from cytoplasm to the exterior with AcrA and probably AcrB forming the walls of the periplasmic channel (see figure 6 of Du et al. [168] for this beautiful structure). Notably, the model of Du et al. (169) seems to confirm that AcrB and TolC do not interact. The Du et al. model also indicates that the termini of the long TolC helices protrude into the upper reaches of the AcrA funnel sufficient to give quite a small wraparound of TolC by AcrA. A similar study by Kim et al. (170) described essentially the same overall organization with the difference that the respective tips of AcrA and TolC intermesh with no real overlapping.

Borrowing from these models gives a rather good idea of the overall organization of the distal half or more of the HlyA translocon. Thus, we suggest that the TolC trimer and an HlyD hexamer interact to form a tightly sealed upper chamber with its central transport channel. Similarly, the drug pump models can be used to predict some of the interfaces that might form the lower chamber. In particular, in line with the structural similarities with EmrA, HlyD should form tightly sealed HlyD protomers, involving lipoyl:lipoyl interactions. Interactions between HlyD and HlyB, by analogy with the drug transporters, would probably involve periplasmic domains of the ABC protein, with the C-terminal β -barrel domain of HlyD protomers enwrapping the HlyB TMDs to form the lower part of the translocon channel. Finally, TolC itself is probably a relatively nonspecific passageway, not only for small molecules, but evidently also for polypeptides since many heterologous passenger proteins fused to the HlyA secretion signal have been successfully transported through TolC. However, beyond that, the drug pump models are not helpful. AcrB, for example, in contrast to HlyB, has an extremely large periplasmic domain, functions in a completely different way as a proton antiporter, and allows drug molecules access to the translocon from the membrane or periplasm rather than from the cytoplasm. Clearly, only the structure of an entire HlyB interacting with HlyD can solve this problem. Finally, while small drug molecules accumulating in the MFP-OMP chambers could be expected ultimately to diffuse outward to the exterior, this cannot explain the extrusion of huge polypeptides that presumably require propulsive force of some kind, a problem that remains for the future.

STRUCTURE FUNCTION OF ABC TRANSPORTERS

A major goal of research in this TISS field is to understand the function of a unique member of this very large

and ubiquitous ABC transporter family that is involved in polypeptide transport. These ancient transporters are quite remarkable in terms of the enormous range in size and complexity of the transport substrates, while relying on the same basic energy-transducing unit. This implies an inherent plasticity to facilitate coupling of the transport and energizing domains as these have evolved to encompass more and more allocrites. Transporting gigantic protein polymers would seem to be the ultimate in this evolutionary process. To understand this fully, not only detailed knowledge of the translocation pathway at the atomic level, but also the accompanying mechanism of catalysis of ATP and its coupling to allocrite movement will be required. Before coming to the specific properties of the HlyB transporter, it is appropriate, therefore, to review here the available information concerning the structure-function of the wider ABC family of transporters.

The Structure of the ABC ATPase

The first crystal structure of a purified ABC NBD domain was reported in 1998 by Hung et al. (171). This structure of HisP, the ATPase component of the histidine importer complex from *Salmonella enterica* serovar Typhimurium, revealed a monomer with ATP bound between the conserved Walker A and B motifs. In addition to the conserved RecA or F1 ATPase fold, two ABC protein-specific subdomains were identified. These are, respectively, a β -sheet domain that harbors an aromatic residue interacting with the adenine moiety of bound nucleotides, and an entirely helical subdomain that contains the conserved C-loop motif, the hallmark of ABC transporters. No other interactions between the adenine ring and the NBD were detected in the HisP structure and all subsequently determined structures. This explains why ABC transporters do not possess true nucleotide specificity, and ATPase activity can also be energized by different nucleotides such as GTP, CTP, or UTP.

Several biochemical analyses of HisP, other isolated NBDs, or full-length transporters have revealed cooperativity in ATP hydrolysis. This by definition indicates the presence of more than one ATP binding site during a single catalytic cycle. Therefore, the initial HisP monomeric structure was unable to explain the ATPase activity and to solve the puzzle, various dimeric arrangements of the NBDs were subsequently suggested. The correct architecture of the NBD dimer was finally proposed by Jones and George (172), based on simula-

Holland et al.

tions. The elegantly simplistic solution they arrived at was subsequently verified by the crystal structure of MJ0796, an isolated NBD from *Methanocaldococcus janaschii* (173). As shown in Fig. 10B, in the HlyB dimer, an ATP molecule is sandwiched between the Walker A of one monomer and the C-loop (the hallmark of ABC transporters, consensus sequence LSGGQ/R) of the opposing monomer, the so-called head-to-tail arrangement of NBDs. Thus, ATP acts as molecular glue, and the dimer is stable in the presence of ATP, but not ADP, since the C-loop of the opposing NBD interacts only with the γ -phosphate moiety of ATP. This fundamental arrangement has now been observed in all structures of isolated NBDs in the presence of ATP, with more than 40 structures deposited in the protein data bank. These include the NBD of HlyB (174, 175), but also, more recently, the structures of several full-length ABC transporters determined at resolutions ranging from 2.5 to 4.5 Å (see reviews [176, 177]).

The Mechanism of ATP Hydrolysis by ABC Proteins Is Still Controversial

Results of experiments designed to uncover the mechanism of ATP hydrolysis, including those for HlyB, interestingly point to subtle differences in the mode of action of individual ABC transporters. Mutational studies have identified two amino acid residues crucial for ATP hydrolysis: one is the glutamate adjacent to the classic Walker B motif present in all P-loop NTPases

(178), and the other is the histidine of the H-loop, another universally conserved sequence motif of ABC transporters (179). Replacement of this glutamate by glutamine abolished ATPase activity *in vitro* in, for example, MalK, the NBD of the maltose importer (180); BmrA, a bacterial drug transporter (181); or MJ0796, the NBD of an ABC transporter with an unknown transport substrate (182). This mutation was actually employed to crystallize the ATP-bound, dimer state of the MJ0796 NBD (173). However, in the isolated NBD of HlyB, the same substitution E to Q, resulted in a residual ATPase activity of approximately 10% (183), while the isolated, similarly mutated NBD of the yeast mitochondrial ABC transporter Mdl1 displayed a very low but measurable level of ATPase activity (184). However, an approximately 20% residual activity was identified for the E to Q mutant form of GlcV, an NBD from a thermophilic ABC transporter (185). In contrast, mutation of the conserved histidine of HlyB resulted in a complete loss of ATPase activity. Similar results were obtained for the maltose and histidine importers (186, 187), while, in the case of the yeast ABC transporter Pdr5, ATPase activity was completely unaffected when the histidine was substituted. Intriguingly, however, this mutated transporter displayed a changed spectrum of transported substrates (188), surprisingly emphasizing the importance of the histidine residue in determining allocrite specificity. Together these results might suggest different mechanisms of ATP hydrolysis in certain ABC transporters, and extrapolations from one system to the other should be done with caution.

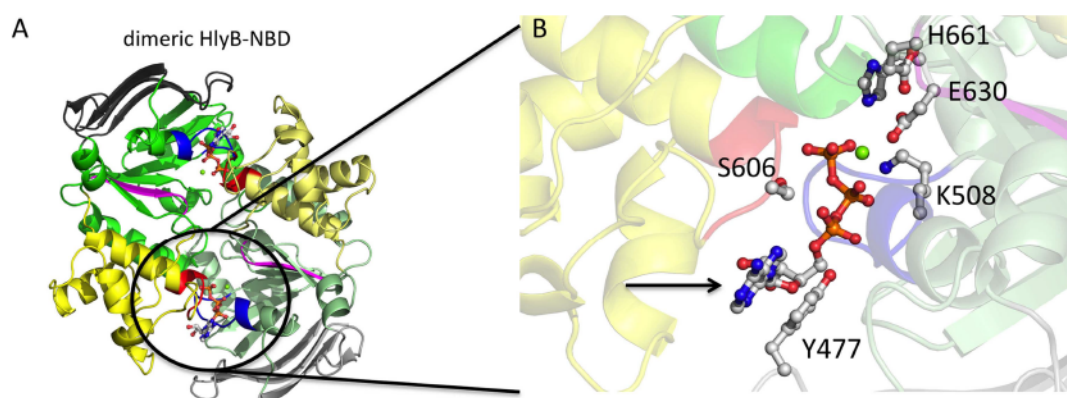


Figure 10 (A) ATP/Mg²⁺ bound H662A structure for the head-to-tail dimer of the HlyB-NBD (174). The RecA core of the NBD is shown in green and pale green, respectively, while the α -helical subdomain in yellow/pale yellow and the β -subdomain in gray. The conserved motifs Walker A, Walker B, and C-loop are highlighted in blue, magenta, and red, respectively. Conserved residues interacting with the nucleotide (arrowed) sandwiched between the two monomers are highlighted in ball-and-stick representation and labeled. The bound cofactor Mg²⁺ is shown as a green sphere. (B) Zoom into the ATP binding site. Please note that S606 (from the conserved C-loop) resides in the opposite monomer.

As discussed above, two particularly important amino acids for catalytic activity have been identified in different NBDs, the glutamate of the Walker B motif, involved in binding the magnesium ion, and the histidine of the conserved H-loop. In MJ0796, as indicated above, mutation of the glutamate to glutamine abolished ATPase activity completely and the term general “catalytic base” was coined (182). However, as also indicated above, substitution of the histidine in HlyB by alanine abolished ATPase activity completely, while residual activity was observed in the case of the E/Q mutant (174, 183). Moreover, in a detailed biochemical analysis of ATP hydrolysis *in vitro*, several lines of evidence obtained were more consistent with a mechanism of *substrate-assisted catalysis*, emphasizing the role of the histidine, rather than *general base catalysis* giving the key role to glutamate. Therefore, the term “linchpin” (174) was also coined, and a critical role for a catalytic dyad composed of the histidine and the glutamate was postulated, in which the side chain of the glutamate interacts with the imidazole side chain of the histidine that, in turn, stabilizes the attacking water.

Subsequently, Oldham et al. (189) described structures of the maltose importer in the ground and transition states. For the latter, transition state analogues, i.e., vanadate and metallofluorides, were used. In these structures, the attacking water molecule, which has to be in line with the bond to be broken, was unambiguously identified as the glutamate, while the histidine was not in direct contact with the attacking water. However, the conclusion of Senior (190) that ABC transporters therefore operate by using general base catalysis does not take into account the limitations of crystal structures. The term “general base catalysis” refers to the kinetics of a reaction and operates if, and only if, proton abstraction is the *rate-limiting step* of the reaction. This certainly cannot be deduced from a static crystal structure. Rather, for example, isotope experiments should be used to demonstrate general base catalysis, where the reaction is performed in D₂O instead of H₂O or in a mixture of both. Since the mass of D₂O is larger than that of H₂O, more energy is required to abstract a deuterium compared with a proton. If proton abstraction is the rate-limiting step, the overall reaction velocity will be slower in D₂O. Such experiments have been performed so far only for the isolated NBD of HlyB (174) and the isolated NBD of Mdl1 (191). In both cases, no evidence for “general base catalysis” was observed. Thus, the precise catalytic mechanism for ATP hydrolysis is still not finally resolved and will require further

investigation. Moreover, the possibility that different ABC-ATPases employ different mechanisms to fuel allocrite translocation through the hydrolysis of ATP is not excluded.

Mechanism of Translocation of Small Molecules by ABC Transporters: Current Model

The first crystal structure of a full-length ABC transporter in 2002 (192) was for the vitamin B₁₂ importer from *E. coli* (BtuCD). Now, there are more than 15 structures of ABC import and export systems deposited in the protein data bank at various stages of their transport and catalytic cycles. However, the most complete system, in terms of structural information for the entire transport cycle, is that for maltose import in *E. coli* (180, 189, 193). Moreover, this is also supplemented by a wealth of functional data. From all these studies (recently reviewed by Jones and George [176]), an atomic resolution picture is emerging of how, at least for small molecules, the chemical energy stored in ATP is coupled to the movement of a transport substrate across a biological membrane. Without going into great detail, the “two-side-access” model proposed in 1966 by Oleg Jardetszky (194) to explain the mode of action of membrane pumps appears to be valid for many ABC transporters. In the resting state of the transporter, the allocrite binding site is accessible from the exterior (importers) or from the cytosol (exporters). Binding of ATP leads to dimerization of the NBDs, and the effect of the resulting conformational changes is transmitted to the TMDs, via the so-called coupling helices. These are present at the terminus of particular long helices extending directly from the TMDs into the cytoplasm. Thus, each TMD of an ABC exporter is in constant contact with both NBDs, while one TMD contacts only one NBD in ABC import systems. The coupling helices first defined in structures of a putative bacterial drug transporter, Sav1866 (195), have been confirmed by structures of other ABC transporters (196–202). The coupling helices are roughly oriented parallel to the membrane plane and form crucial contact points between TMDs and NBDs, communicating the status of the membrane domain and the energy source to drive transport.

In current models, largely constructed to explain the translocation of small molecules such as anticancer drugs or nutrients, the consequence of NBD dimerization switches the accessibility of a binding site for a given molecule, from the exterior to the cytosol (importers)

Holland et al.

or from the cytosol to the exterior (exporters), resulting finally in release of the molecule. Subsequent ATP hydrolysis resets the system, and the resting state is restored. One has to keep in mind that, in addition to the two important alternating conformational states (inward-facing and outward-facing), an intervening occluded state must be adopted during the transport cycle, in which both sides of the transporter must be sealed. Otherwise, the transporter would adopt a conformation during its transport cycle, where both sides are accessible, a scenario producing an immediate, lethal dissipation of the proton motive force across the membrane.

Small Peptides Are Secreted by an “Alternating Access” Pathway but Large Polypeptides Require a Different Mechanism

Recently, Choudhury et al. (197) reported the crystal structure of an *E. coli* ABC peptide transporter, McjD, in the presence of a nonhydrolyzable ATP analogue. The structure revealed a novel outward-occluded state. The structure includes a large cavity (approximately 5900 \AA^3 , $40 \times 21 \times 10 \text{ \AA}$), facing the cytoplasm, apparently able to bind the microcin, MccJ25, a 21-amino-acid, uniquely lasso-shaped, antimicrobial peptide. The outward-occluded conformation and other highly conserved structural features strongly suggest that McjD uses the alternating access mechanism to couple ATP utilization to microcin transport across the inner membrane of *E. coli*. Final release of this microcin to the medium is apparently dependent on TolC (203), another example of this amazing general purpose duct. However, there appears to be no information available concerning the presumed requirement for an HlyD homologue in microcin release.

More recently, highly important and exciting new structural information was also obtained from the crystals of an ABC transporter (PCAT) apparently secreting a peptide from the Gram-positive *C. thermocellum*. Although the natural transport substrate for this transporter has not been characterized, one gene of the operon encodes a 90-amino-acid protein that likely represents a bacteriocin. The structure of PCAT was obtained both for the nucleotide-free and a nonhydrolyzable ATP-bound form at 3.6 \AA and 5.5 \AA resolution, respectively (204). Based on the two conformations, open to the cytosol in the nucleotide-free state and closed on both sides of the membrane in the ATP-bound state, a large cavity facing the cytoplasm was visible in the absence of ATP.

This cavity is sufficient to accommodate an entire small folded protein, such as a bacteriocin, after removal of the leader sequence. The PCAT transporter contains a C39 peptidase domain very similar in structure to the HlyB CLD described below (see also Fig. 2). This cleaves after the double-glycine motif of the N-terminal leader prior to translocation across the cell membrane. Interestingly, the C39 domain was only visible in the electron density of the nucleotide-free state of the transporter, while invisible in the ATP-bound state. This indicated a large degree of flexibility for the C39 domain in the latter conformation and the authors suggested that the two C39 subunits effectively move in a coordinated way from the periphery of the homodimer to deliver the peptide directly to the translocation site in the large cavity. The authors proposed, therefore, that the classical alternating access model was able to explain translocation of this peptide in a single step across the membrane, and, in this Gram-positive organism with no outer membrane, an additional adaptor protein is not required.

However, in marked contrast to microcins and bacteriocins other T1SS transport substrates range from 20 kDa to huge, close to 900-kDa polypeptides, and the available evidence suggests that all of them are transported in the unfolded state (69). Thus, as also concluded by Lin et al. (204), one has to question whether the “simple” alternating access mechanism applies to most T1SS ABC transporters, since the size of the unfolded substrate is evidently too large to be transported in one step. Moreover, if type I secretion involves ratchet-like translocation through a narrow pore as seen with the classical Sec system, it is difficult, if not impossible, to envision an occluded state. If not alternating access, HlyB could perhaps adopt a structure more related to the Sec translocon and simply deliver HlyA across the inner membrane into the HlyD channel. Alternatively, similar to the action of the ABC protein SUR that regulates the opening of the Kir_{ATP} potassium channel, HlyB might control the opening of an HlyD, TolC channel for extrusion of HlyA to the exterior, without directly contributing to the channel for HlyA. Finally, the most recent structural analysis of an ABC transporter, PglK (205), revealed that the lipid-linked oligosaccharide from *Campylobacter jejuni*, in order to inverse its orientation in the bilayer, is “flipped” along a novel pathway formed by PglK. The process requires an outward-facing conformation of PglK, but in this case there is no inward-facing conformation involved. This further emphasizes the plasticity

of the ABC protein, and we can anticipate a fascinating solution to the puzzle of polypeptide transport by the T1SS from future structural data.

STRUCTURE FUNCTION OF THE PROTOTYPE TYPE I ABC TRANSPORTER HLYB

Structural Insights into the Catalytic Cycle of the HlyB NBD

The isolated NBD of HlyB has been investigated in great detail in terms of biochemistry and structure ([160](#), [163](#), [174](#), [175](#), [206](#)). Crystal structures of all states of the catalytic cycle have been determined for the wild-type or mutant NBDs. These structures, combined with determination of biochemical parameters, revealed much about the mechanism of ATP hydrolysis (see below). In addition, structural analysis was essential to identify residues of the NBD responsible for cooperativity in ATP hydrolysis and, for example, to define a role for the D-loop, a highly conserved motif of ABC transporters but without apparent function hitherto ([175](#)).

As in many other ABC-ATPases, the isolated NBDs of HlyB display cooperativity with a Hill coefficient of approximately 1.4 ([183](#)). In other words, the two ATP binding sites are not equal; that is, one of the many events leading to hydrolysis of bound ATP, binding, dimerization of the NBDs, ADP and/or phosphate release and dimer dissociation, is differently timed in the two sites. Otherwise, classic Michaelis-Menten kinetics would be observed. In fact, cooperativity requires asymmetry between the two ATP binding sites, and the structures of the ATP-bound states of ABC dimers did not at first reveal any obvious asymmetry. However, after analysis of the HlyB crystal structure and a subsequent sequence analysis of more than 10,000 NBD sequences, two residues apparently of particular significance with respect to asymmetry were identified for site-directed mutagenesis ([175](#)). These residues (R611 and D551 in the HlyB-NBD) are located one residue downstream of the C-loop and Q-loop, respectively. In the ATP/Mg²⁺-bound form, captured in the crystal structure of the HlyB NBD dimer shown in [Fig. 10](#), these two residues are able to form a salt bridge but only within one monomer. This is because, in the other monomer, the distance between the two residues is too great. Importantly, in the absence of the bridge, a tunnel opens, reaching from the position of the γ -phosphate to the exterior, while the tunnel is closed in the other monomer by the salt bridge. These important

findings represent a first glimpse of asymmetry in an ABC-NBD dimer.

Zaitseva et al. excitingly also showed that the change of only one of these bridge residues to alanine (R/D to R/A or A/D) drastically reduced ATPase activity, but, more importantly, abolished cooperativity. Changing the R-D interaction to K-E resulted in reduced ATPase activity, but restored cooperativity ([175](#)). These results indicate that the R-D interaction is at the heart of cooperativity because it regulates phosphate release from one of the two ATP binding sites. In the case of the alanine mutations, the tunnel would be open at both sites and the two phosphates released simultaneously, rather than sequentially. The importance of the R611-D551 interaction was subsequently confirmed for the antigen (peptide) transporter (TAP) ([207](#)).

The role of the D-loop, a highly conserved motif very useful for the identification of ABC proteins, has been elusive. In the crystal structure of the NBD of HlyB, the aspartate of the D-loop interacts with a serine residue of the Walker A motif of the opposing NBD ([Fig. 10B](#)). This is another example of an interdomain interaction between the two NBDs involving highly conserved motifs. In this case indicating an important role for the D-loop in sensing the presence of ATP in the opposing ATP binding site. Recent elegant studies by the Tampé laboratory have also emphasized the importance of the D-loop in the transport of immunopeptides by the TAP transporter ([208](#)). Similar conclusions were obtained from the analysis of other ABC transporters such as the vitamin B₁₂ importer ([209](#)).

The Extinct Peptidase Domain CLD in HlyB Interacts with the HlyA C Terminus: NMR Structural Analysis

Early studies noted that HlyB, compared with many other bacterial ABC transporters, has an extended N-terminal domain, but its role has been a mystery. Curiously, this N-terminal domain, covering approximately 130 amino acid residues, was identified from its sequence as a member of the cysteine-dependent C39 peptidase family. These particular peptidases are only found so far in active form in bacterial ABC transporters involved in the secretion of small peptides, including bacteriocins. In these molecules, the corresponding protease cleavage sites are found in the *N-terminal secretion signal*, C-terminal to a double-glycine motif. Obviously, HlyA does not contain an N-terminal targeting signal and does not undergo any

Holland et al.

proteolytic processing. In fact, the catalytically essential cysteine of the C39 peptidase domain in HlyB is replaced by a tyrosine, resulting in loss of protease activity. Thus, the N-terminal domain of HlyB was termed a “C39-like peptidase domain” (CLD).

In a major advance in 2012, Lecher et al. (54) revealed an important function for the CLD, since its deletion completely abolished secretion of HlyA. In further detailed studies, the purified CLD was shown to interact with the *unfolded* but not with folded HlyA or the truncate HlyA1. However, the 160-residue HlyA2, C-terminal fragment that lacks the C-terminal 58 residues encompassing the secretion signal (see Fig. 4), still binds to the CLD. This clearly showed that the binding site was located upstream of the secretion signal close to 3 RTX repeats (characterized, *coincidentally or otherwise* by double-GG motifs), somewhere between residues 805 and 965.

To explore the structural details of the CLD and possible residues involved in binding to HlyA, the solution structure shown in Fig. 2 was determined by NMR. First, this revealed no obvious structural differences between the CLD and an authentic C39 peptidase domain (ComA-PEP [210]). However, subtle but important differences in the respective active sites were detected. While the aspartate residue of the catalytic triad of the C39 peptidase domains was found in an identical conformation in the CLD, the histidine residue was flipped by nearly 180° out of its canonical conformation. This novel position was stabilized by π - π interactions with a tryptophan residue. Interestingly, pairwise sequence comparison of many CLD domains in other ABC transporters revealed that in CLDs associated with T1SS, the combination of the absence of cysteine and the flipped histidine positioning was always present, while, in the authentic peptidase domains, the expected histidine and cysteine residues were also found and located at the same position, compatible with catalytic activity. This analysis might allow a robust and easy identification of new RTX-transporting systems in the future, based on the sequence of the CLD.

Finally, exciting results were obtained when an NMR analysis was used to determine the localization of residues in the CLD specifically engaged in binding to the HlyA C terminus. First, it is important to note that the published binding site for the normal C39 peptidase substrate, the GG cleavage motif, does not coincide with the site of HlyA binding in the CLD. However, intriguingly, the CLD residues binding to HlyA were found to be

on the *opposite* side of the molecule to that shown to bind the classical GG motif. However, the significance of this finding may have to await determination of the molecular details of the CLD binding site within the RTX domain of HlyA. Notwithstanding this, the current data strongly suggest that the CLD participates in a very early step of the secretion process. Thus, Lecher et al. (54) proposed that the role of the CLD is to act as a receptor to position the unfolded HlyA in the close vicinity of the T1SS. Such a role could provide an additional initial tethering of HlyA (together with HlyD and the NBDs of HlyB) in coordinating its entry into the transport channel. Indeed, significant support for this idea comes from the recent structural analysis of a bacteriocin transporter PCAT discussed above.

An eGFP-HlyA-Fusion Protein Forms a Stuck Intermediate Extending across the Envelope with the C Terminus Exposed to the Exterior

Clear proof that HlyA is indeed extruded progressively through the envelope from the cytoplasm to the exterior was demonstrated very recently by Lenders et al. (118), who engineered the C-terminal HlyA1 fragment of HlyA (termed HlyAc in that publication), or full-length HlyA in a fusion to the C terminus of the fast-folding eGFP protein. The latter passenger rapidly folds in the cytoplasm and stalls further translocation. Employment of antibodies to HlyA1 or HlyA and measurement of fluorescence from eGFP showed conclusively that the N and the C termini of the fusion were in the cytoplasm and external medium, respectively. Importantly, the results in this paper also settled any doubts that the C terminus is secreted first, and, consequently, that the RTX region is immediately available for calcium ion-dependent folding of HlyA as the unfolded molecule emerges on the cell surface.

A DEVELOPING MODEL FOR HLYA TRANSLOCATION

We have tried to develop a model that portrays in a simple way what in reality is an intricate series of sequential intermolecular interactions between the C terminus of HlyA and the ABC and MFP proteins, and the consequent interaction with the OMP TolC. These interactions are likely to involve reciprocal short- and long-range conformational changes in the transport proteins that result in their assembly as a contiguous transenvelope structure. Equally, apparently multiple interactions between the HlyA C terminus and HlyB then prepare

for the coordinated insertion of the HlyA C terminus into the transport channel. Progressive extrusion of the largely unstructured HlyA then proceeds across the periplasm, through the peptidoglycan mesh, through TolC, and finally autocatalytic folding of the emerging protein on the cell surface. We divide this complex process into hypothetical steps simply for convenience.

HlyB dimers and probably HlyD hexamers form a stable complex, independently of HlyA. We propose that the TMDs of HlyD encircle the membrane domains of the HlyB dimer, and, in this ground state, we assume that ATP is already bound to HlyB, but the NBDs are not tightly closed. In step 1, when the synthesis of HlyA is complete or nearly complete, the secretion signal, and one or more GG residues in the preceding RTX, bind to the NBDs and CLD of HlyB, respectively. Sequentially or simultaneously, the cytoplasmic extension of HlyD also has to bind to HlyA (location unknown). Multiple events are then somehow coordinated the tethering of both HlyD and HlyB to HlyA, the promotion of long-range “reorganization” of the periplasmic domains of the HlyD hexamer to recruit TolC into the fully assembled translocon. At this stage, the TolC exit may be open to the exterior, as has been suggested for the assembled pseudotomac AcrAB/TolC complex, but other parts in the pathway may remain closed.

We suggest, in step 2, the C-terminal region of HlyA is delivered by the CLDs to a specific cytoplasmic part of the HlyB domain; binding of the HlyA signal to HlyD, CLD, and NBDs is reversed. These coordinated events, we speculate, constitute the trigger that creates the “translocation” site, a narrow pore, in the membrane domain of HlyB. We further speculate that this allows HlyA direct access to the contiguous channel formed first by HlyD and then TolC. In the purely hypothetical step 3, with the energetics still completely unclear, we could envisage that translocation occurs with sequential insertion of successive segments of HlyA into the transenvelope channel, thus resembling the threading of polypeptides through the Sec translocon. Notably, among the many transport processors dependent on ABC proteins, T1SS is seemingly unique in requiring continued consumption of energy during a protracted segmental transit of the polypeptide. In step 4, folding of HlyA in the calcium ion-rich exterior should commence as soon as the C-terminal RTX domain emerges from TolC. Whether, or to what extent, extracellular folding *per se* contributes energetically to the threading mechanism remains

unclear. Similarly, still unknown is the timing of additional key steps such as induced dimerization of the ATP-loaded NBDs; hydrolysis of ATP and the disassembly of the translocon remain to be elucidated.

CONCLUSIONS AND PERSPECTIVES, FOCUSING PRIMARILY ON THE HLY SYSTEM

Novel Features

HlyA secretion depends upon a novel C-terminal secretion signal recognized by both MFP and ABC components of the translocon. At the heart of the translocon, the ABC transporter itself has novel characteristics, distinguishing it from the majority of this super family. HlyA secretion also has other features not shared by some other type I secretion systems. Moreover, from very recent findings, including our own revisiting of databases for unpublished material, it became clear that several aspects of the mechanism of type I secretion manifests itself in many forms, possibly related to allocrite type or the nature of the producing species.

Much Still to Learn about the Utilization of ATP

Despite the availability of several crystal structures for NBDs and entire ABC transporters, the specific step promoted by binding of the allocrite, binding of ATP, or precisely how and why, and at what stage, ATP hydrolysis is finally triggered, still remain relatively unclear for most ABC transporters, including HlyB. Moreover, a major fundamental step, central to our understanding of the action of ABC transporters, often sidestepped (even in recent reviews), is whether binding of ATP is spontaneous or triggered by the binding of the transport substrate. The literature is confusing, with some models presented with ATP already bound, while others show binding of the transport substrate triggering ATP binding. Encouragingly, recent studies of the effect of allocrites on the ATPase cycle with purified proteins, for example, the maltose transporter or the peptide transporter by TAP (involved in adaptive immunity) incorporated into proteoliposomes or nanodiscs, are specifically addressing these important issues (208, 211). In both cases, binding of ATP and the allocrites were clearly shown to be quite independent events. In addition, a recent beautiful structural analysis of different forms of a lipid flippase, the ABC transporter PglK, Perez et al. (205) proposed that the ground state of the transporter is the ATP-bound form. In fact, with the cellular ATP concentration at 3.5 mM, severalfold higher than the ATP affinity constant

Holland et al.

of ABC transporters, ABC proteins should always be present with ATP bound. Thus, normally, we expect that the ATP-loaded NBDs are somehow constrained and do not dimerize; rather, they are poised to close on the appearance of the transport substrate.

HlyB Function, Fascinating So Far but Surely Much More to Come

HlyB, interestingly, binds to two sites in HlyA. The NBDs bind to the secretion signal, while the N-terminal CLD (inactive C39 protease domain) binds (or tethers) HlyA close to the GG-rich RTX, just upstream of the signal sequence. Notably, however, the corresponding binding site in CLD, as determined by NMR, intriguingly is distinct from the binding site for GG repeats in the ancestral protease. The precise role of the CLD in HlyA secretion remains unclear, while a CLD is not required for secretion of small to “middle sized” proteins such as the proteases and lipases. Interestingly, the recent PCAT structure of a peptide transporter discussed above prompts the idea that a CLD picks up the C-terminal end of a type I protein, which is then guided to the translocation site. However, the HlyA secretion signal binds to the NBDs of HlyB, suggesting that the ABC protein may be implicated in coordinating an early initiation event with regulation of ATPase activity.

High-resolution structures of HlyB and studies of the precise stage, allocrite recognition, translocon assembly, or something else that blocks secretion when the CLD is absent, should illuminate the specific role of the HlyB CLD.

Different Type I Protein Families Appear to Have a “Personalized” Secretion Code

The hypothesis, based on available evidence, is that for HlyA (and related hemolysins), the secretion code is composed of a dispersed pattern of specific individual residues centered on the apparently conserved cluster EISK ([100](#), [101](#)) rather than on structural motifs. Such a signal code could provide a “lock and key” mechanism for docking with either or both HlyB and HlyD. However, a limited alignment analysis of the C termini of other type I proteins suggests that different subgroups have a distinctive code. The signal sequence also appears to have an additional role, with the extreme few residues, again apparently different sets for different subgroups, somehow affecting posttranslocational folding or stability. However, the nature of this phenomenon remains a mystery.

Translocon Specificity

Translocon selectivity in T1SS, i.e., translocon specificity for a given polypeptide, appears to reside (in the different subfamilies) in the secretion code and its docking target, the ABC protein. However, in distinction from the CLD and NBDs, if there is a specific binding site for HlyA in the membrane domain of HlyB, it is not yet identified. Curiously, for HlyA, specificity may also be determined by binding to HlyD, but it is not clear how many other type I proteins share this property.

Type I Proteins: Calcium Ion-Dependent Autonomous Folding on the Cell Surface

Many type I proteins, including HlyA, are secreted into potentially hostile environments where chaperones are absent. For HlyA, evolution has neatly solved the chaperone problem by providing RTX repeats (or their analogues, in some cases) to promote autonomous folding in the environment replete with the catalyst Ca^{2+} . Moreover, several authors have presented the persuasive idea that calcium ion/RTX-dependent folding could also provide some or most of the required energy to “pull” large type I RTX proteins through the translocon. Until recently, this proposition had not been tested experimentally. Now, Bumba et al. ([212](#)) with the adenylate cyclase have shown that Ca^{2+} -dependent folding is not essential, but rather appears to accelerate CyaA translocation. It remains to be seen if this role in augmenting energy requirement for translocation is conserved. In addition, these findings will reawaken the debate on what are the fundamental energy requirements for transport.

ABC Transporters Secreting Large Polypeptides Utilize a Novel Mechanism

The exciting first structures of T1SS ABC transporters secreting small peptides have revealed an overall structure consistent with the generally agreed mechanism for the export of small molecules by a very wide range of ABC transporters, that is, the alternating access model ([194](#)). In contrast, it is clear that HlyB and other T1SS homologues cannot transport a *large unfolded polypeptide* to shift the whole molecule to the exterior in a single step, as required for the alternating access mechanism, and therefore must function in a fundamentally different way. Notably, the recent structure of the bacterial lipid-oligosaccharide flippase ([205](#)) suggests a novel mechanism for an ABC exporter different from alternating access. This involves the formation of a transport pathway or “pore” within the membrane domain of the ABC

protein. This system offers a simpler alternative concept for HlyA translocation that requires HlyA-induced reorganization of the membrane domain in HlyB to create the transport pore that connects directly to the HlyD-TolC channel.

Envisioning the Structure of the Translocon and the Role of HlyD

Homologues of HlyD involved in drug transport, such as AcrA, appear to form a sealed channel crossing the periplasm, and it seems very probable that HlyD plays the same role in formation of the Hly translocon. Notably, also among the related drug transporters, MacA forms a complex with an ABC transporter and AcrA, MacA (*E. coli*), and EmrA (from *Aquifex aeolicus*) all dock with TolC. In addition, like HlyD, MacA and EmrA also have a single N-terminal TMD embedded in the inner membrane. These shared properties of HlyD mutants lead to the prediction that 6 HlyD protomers, together with HlyB and TolC, form a contiguous transenvelope channel.

The flexible nature of the periplasmic domain of such MFPs presumably is also a key factor in sealing and then stabilizing the fragile translocation “tunnel” across the gel-like, volume-variable periplasm. Reflecting this, HlyD, in some way not yet clear, appears important for the smooth transit of HlyA to the surface and its subsequent folding. Finally, in view of the recent exciting pseudoatomic models of the tripartite *E. coli* multidrug drug efflux pumps (169), which include both TolC and structural homologues of HlyD, we are now able to build a picture of the possible structure of the Hly translocon.

Although crucial details are still lacking, the N terminus of HlyD clearly plays a crucial role in the early engagement of HlyA and the consequent recruitment of TolC into the translocon “on demand.” However, surprisingly, this function is not conserved in many other T1SS, for both large and small allocrites. Consequently, how such a regulated assembly of the translocon is managed in other type I systems remains unclear. Conceivably, transient associations of these translocon components may simply be stabilized by interaction with the transport substrate.

T1SS Subtypes Display a Remarkable Variety of Mechanistic Detail

A striking realization during the preparation of this review was the surprisingly large number of variations between different subgroups of type I proteins regarding

important details of the secretion mechanism. One of the most dramatic but puzzling variations is the likelihood that different subgroups have their own secretion signal code, presumably requiring corresponding sequence or structural variations of the cytosolic part of the cognate ABC transporter. Another major puzzle is that, while the N-terminal cytoplasmic domain of HlyD has a fundamental role in the secretion process, this is not conserved in many other T1SS. Type I proteins include giants up to close to 9,000 amino acids, and growing evidence indicates a range of variations to accommodate secretion of some of these proteins: the accessory CLD domain, a variety of novel auxiliary translocon components and a possible contribution of extracellular folding to the energetics of transport for some proteins. Similarly, the emerging evidence that, while small peptides can be secreted via an alternating access mechanism facilitated by the ABC transporter, larger proteins are presumably extruded through some kind of “pore.” This would mean yet-to-be-discovered sequence and structural variation in the corresponding transport domain for the T1SS ABC transporters. Moreover, for the giant type I proteins, likely with conceivably extremely long transit times, modifications to meet the greater energy needs are inevitable.

There are also variations in the T1SS, although less clear-cut, in posttranslocational folding mechanisms. The extreme C-terminal motifs that may be involved do not appear to be conserved and, although in many cases this folding depends upon RTX motifs and extracellular Ca^{2+} ions, a recently discovered exception in *S. enterica* indicates a likely independent evolutionary event that has created an alternative calcium ion binding site.

While the recruitment of CLDs to the ABC protein appears to be an expedient linked to allocrite size, justification for the sophisticated structure-function of the HlyD N terminus is more difficult to comprehend. Interestingly, however, as first pointed out by Rod Welch (3), several characteristics of the sequence of the *hly* determinant, including the low GC content, indicated that this was a recent acquisition by *E. coli* from an unrelated species. This unfamiliar neighborhood might have selected for the secondary recruitment of a novel system for linking the MFP into a stable complex with TolC. In fact, frequent lateral transmission of pathogenicity factors followed by subsequent adaptation to local physiology could explain other forms of T1SS variations and, indeed, similar phenomena might reasonably be expected in other bacterial secretion systems. The prevalence of such

Holland et al.

a variety of forms of T1SS emphasizes that a mechanistic paradigm with one type I protein is no guarantee that this will be conserved widely.

ACKNOWLEDGMENTS

L.S. thanks all current and former lab members for their continuous and successful work on the Hly system. The DFG, EU, the NRW Research School Biostruct, the Manchot Graduate School “Molecules of Infection”, the CLIB Graduate Cluster, and HHU supported our research. I.B.H. wishes to thank wholeheartedly the many colleagues in both Leicester and Orsay whose unstinting contributions made these Hly studies so exciting, successful, and certainly great fun. The list is long, but Nigel Mackman, Brendan Kenny, and Mark Blight stand out for their enthusiasm and creative insights. The Wellcome Trust, the MRC, the EU Framework programs and many others generously funded the work and I am especially grateful to the Universities of Leicester and Paris-Sud and the CNRS for their longstanding support. I am also extremely grateful to Simone S  r for her patient and critical editing of the text. Finally, I.B.H. acknowledges very helpful discussions with in particular, Harris Bernstein, Roman Gerlach, Michael Hensel, Daniel Ladant, Ben Luisi, Dijun Du, Karla Satchell, and Helen Zgurskaya.

Conflict of interest: The authors declare no conflicts.

ADDENDUM IN PROOF

While this manuscript was in review, Lenders et al. reported the quantitative analysis of the HlyA T1SS. They were able to determine the secretion rate of 16 amino acids per transporter and sec and demonstrated that Ca ions had no influence on the actual secretion rate (M.H. Lenders, T. Beer, S.H. Smits, and L. Schmitt, *Sci Rep* 6:33275, 2016, doi:10.1038/srep33275).

REFERENCES

- Higgins CF, Hiles ID, Salmond GP, Gill DR, Downie JA, Evans IJ, Holland IB, Gray L, Buckel SD, Bell AW, et al. 1986. A family of related ATP-binding subunits coupled to many distinct biological processes in bacteria. *Nature* 323:448–450.
- Felmlee T, Pellett S, Lee EY, Welch RA. 1985. *Escherichia coli* hemolysin is released extracellularly without cleavage of a signal peptide. *J Bacteriol* 163:88–93.
- Felmlee T, Pellett S, Welch RA. 1985. Nucleotide sequence of an *Escherichia coli* chromosomal hemolysin. *J Bacteriol* 163:94–105.
- Welch RA. 1991. Pore-forming cytolysins of gram-negative bacteria. *Mol Microbiol* 5:521–528.
- Baumann U, Wu S, Flaherty KM, McKay DB. 1993. Three-dimensional structure of the alkaline protease of *Pseudomonas aeruginosa*: a two-domain protein with a calcium binding parallel beta roll motif. *EMBO J* 12:3357–3364.
- Linhartova I, Bumba L, Masin J, Basler M, Osicka R, Kamanova J, Prochazkova K, Adkins I, Hejnova-Holubova J, Sadilkova L, Morova J, Sebo P. 2010. RTX proteins: a highly diverse family secreted by a common mechanism. *FEMS Microbiol Rev* 34:1076–1112.
- Holland IB, Schmitt L, Young J. 2005. Type 1 protein secretion in bacteria, the ABC-transporter dependent pathway. *Mol Memb Biol* 22:29–39.
- Thomas S, Holland IB, Schmitt L. 2014. The type 1 secretion pathway – the hemolysin system and beyond. *Biochim Biophys Acta* 1843:1629–1641.
- Lenders MH, Reimann S, Smits SH, Schmitt L. 2013. Molecular insights into type I secretion systems. *Biol Chem* 394:1371–1384.
- Deleplaire P. 2004. Type I secretion in gram-negative bacteria. *Biochim Biophys Acta* 1694:149–161.
- Durand E, Verger D, Rego AT, Chandran V, Meng G, Fronzes R, Waksman G. 2009. Structural biology of bacterial secretion systems in gram-negative pathogens–potential for new drug targets. *Infect Disord Drug Targets* 9:518–547.
- Wiles TJ, Mulvey MA. 2013. The RTX pore-forming toxin alpha-hemolysin of uropathogenic *Escherichia coli*: progress and perspectives. *Future Microbiol* 8:73–84.
- Nagamatsu K, Hannan TJ, Guest RL, Kostakioti M, Hadjifrangiskou M, Binkley J, Dodson K, Raivio TL, Hultgren SJ. 2015. Dysregulation of *Escherichia coli* alpha-hemolysin expression alters the course of acute and persistent urinary tract infection. *Proc Natl Acad Sci USA* 112:E871–E880.
- Ladant D, Ullmann A. 1999. *Bordetella pertussis* adenylate cyclase: a toxin with multiple talents. *Trends Microbiol* 7:172–176.
- Bielaszewska M, Aldick T, Bauwens A, Karch H. 2014. Hemolysin of enterohemorrhagic *Escherichia coli*: structure, transport, biological activity and putative role in virulence. *Int J Med Microbiol* 304:521–529.
- Dolores J, Satchell KJ. 2013. Analysis of *Vibrio cholerae* genome sequences reveals unique rtxA variants in environmental strains and an rtxA-null mutation in recent altered El Tor isolates. *MBio* 4:e00624. doi:10.1128/mBio.00624-12.
- Satchell KJ. 2011. Structure and function of MARTX toxins and other large repetitive RTX proteins. *Annu Rev Microbiol* 65:71–90.
- Satchell KJ. 2015. Multifunctional-autoprocessing repeats-in-toxin (MARTX) toxins of vibrios. *Microbiol Spectr* 3. doi:10.1128/microbiolspec.VE-0002-2014.
- Boyd CD, Smith TJ, El-Kirat-Chatel S, Newell PD, Dufrene YF, O’Toole GA. 2014. Structural features of the *Pseudomonas fluorescens* biofilm adhesin LapA required for LapG-dependent cleavage, biofilm formation, and cell surface localization. *J Bacteriol* 196:2775–2788.
- Barlag B, Hensel M. 2015. The giant adhesin SiiE of *Salmonella enterica*. *Molecules* 20:1134–1150.
- Dirix G, Monsieus P, Dombrecht B, Daniels R, Marchal K, Vanderleyden J, Michiels J. 2004. Peptide signal molecules and bacteriocins in Gram-negative bacteria: a genome-wide in silico screening for peptides containing a double-glycine leader sequence and their cognate transporters. *Peptides* 25:1425–1440.
- Duquesne S, Petit V, Peduzzi J, Rebuffat S. 2007. Structural and functional diversity of microcins, gene-encoded antibacterial peptides from enterobacteria. *J Mol Microbiol Biotechnol* 13:200–209.
- Prochazkova K, Shuvalova LA, Minasov G, Voburka Z, Anderson WF, Satchell KJ. 2009. Structural and molecular mechanism for autoprocessing of MARTX toxin of *Vibrio cholerae* at multiple sites. *J Biol Chem* 284:26557–26568.
- Kim BS, Gavin HE, Satchell KJ. 2015. Distinct roles of the repeat-containing regions and effector domains of the *Vibrio vulnificus* multifunctional-autoprocessing repeats-in-toxin (MARTX) toxin. *MBio* 6. doi:10.1128/mBio.00324-15.
- Costa TR, Felisberto-Rodrigues C, Meir A, Prevost MS, Redzej A, Trokter M, Waksman G. 2015. Secretion systems in Gram-negative bacteria: structural and mechanistic insights. *Nat Rev Microbiol* 13:343–359.
- Economou A, Dalbey RE. 2014. Protein trafficking and secretion in bacteria. *Biochim Biophys Acta* 1843:1427. doi:10.1016/j.bbamcr.2014.04.007.

27. Robinson GL. 1951. The haemolysin of *Bacterium coli*. *J Gen Microbiol* 5:788–792.
28. Lovell R, Rees TA. 1960. A filterable haemolysin from *Escherichia coli*. *Nature* 188:755–756.
29. Snyder IS, Koch NA. 1966. Production and characteristics of hemolysins of *Escherichia coli*. *J Bacteriol* 91:763–767.
30. Noegel A, Rdest U, Springer W, Goebel W. 1979. Plasmid cistrons controlling synthesis and excretion of the exotoxin alpha-haemolysin of *Escherichia coli*. *Mol Gen Genet* 175:343–350.
31. Springer W, Goebel W. 1980. Synthesis and secretion of hemolysin by *Escherichia coli*. *J Bacteriol* 144:53–59.
32. Hartlein M, Schiessl S, Wagner W, Rdest U, Kreft J, Goebel W. 1983. Transport of hemolysin by *Escherichia coli*. *J Cell Biochem* 22:87–97.
33. Koronakis V, Koronakis E, Hughes C. 1989. Isolation and analysis of the C-terminal signal directing export of *Escherichia coli* hemolysin protein across both bacterial membranes. *EMBO J* 8:595–605.
34. Mackman N, Holland IB. 1984. Functional characterization of a cloned haemolysin determinant from *E. coli* of human origin, encoding information for the secretion of a 107K polypeptide. *Mol Gen Genet* 196:129–134.
35. Mackman N, Holland IB. 1984. Secretion of a 107 K dalton polypeptide into the medium from a haemolytic *E. coli* K12 strain. *Mol Gen Genet* 193:312–315.
36. Mackman N, Nicaud JM, Gray L, Holland IB. 1985. Genetical and functional organisation of the *Escherichia coli* haemolysin determinant 2001. *Mol Gen Genet* 201:282–288.
37. Mackman N, Nicaud JM, Gray L, Holland IB. 1985. Identification of polypeptides required for the export of haemolysin 2001 from *E. coli*. *Mol Gen Genet* 201:529–536.
38. Chervaux C, Sauvonnnet N, Le Clainche A, Kenny B, Hung AL, Broome-Smith JK, Holland IB. 1995. Secretion of active beta-lactamase to the medium mediated by the *Escherichia coli* haemolysin transport pathway. *Mol Gen Genet* 249:237–245.
39. Felmler T, Welch RA. 1988. Alterations of amino acid repeats in the *Escherichia coli* hemolysin affect cytolytic activity and secretion. *Proc Natl Acad Sci USA* 85:5269–5273.
40. Gray L, Mackman N, Nicaud JM, Holland IB. 1986. The carboxy-terminal region of haemolysin 2001 is required for secretion of the toxin from *Escherichia coli*. *Mol Gen Genet* 205:127–133.
41. Gentschev I, Hess J, Goebel W. 1990. Change in the cellular localization of alkaline phosphatase by alteration of its carboxy-terminal sequence. *Mol Gen Genet* 222:211–216.
42. Gray L, Baker K, Kenny B, Mackman N, Haigh R, Holland IB. 1989. A novel C-terminal signal sequence targets *Escherichia coli* haemolysin directly to the medium. *J Cell Sci Suppl* 11:45–57.
43. Mackman N, Baker K, Gray L, Haigh R, Nicaud JM, Holland IB. 1987. Release of a chimeric protein into the medium from *Escherichia coli* using the C-terminal secretion signal of haemolysin. *EMBO J* 6:2835–2841.
44. Nicaud JM, Mackman N, Gray L, Holland IB. 1985. Characterisation of HlyC and mechanism of activation and secretion of haemolysin from *E. coli* 2001. *FEBS Lett* 187:339–344.
45. Pimenta AL, Young J, Holland IB, Blight MA. 1999. Antibody analysis of the localisation, expression and stability of HlyD, the MFP component of the *E. coli* haemolysin translocator. *Mol Gen Genet* 261:122–132.
46. Wang RC, Seror SJ, Blight M, Pratt JM, Broome-Smith JK, Holland IB. 1991. Analysis of the membrane organization of an *Escherichia coli* protein translocator, HlyB, a member of a large family of prokaryote and eukaryote surface transport proteins. *J Mol Biol* 217:441–454.
47. Wandersman C, Delepelaire P. 1990. TolC, an *Escherichia coli* outer membrane protein required for hemolysin secretion. *Proc Natl Acad Sci USA* 87:4776–4780.
48. Letoffe S, Delepelaire P, Wandersman C. 1990. Protease secretion by *Erwinia chrysanthemi*: the specific secretion functions are analogous to those of *Escherichia coli* alpha-haemolysin. *EMBO J* 9:1375–1382.
49. Stanley P, Hyland C, Koronakis V, Hughes C. 1999. An ordered reaction mechanism for bacterial toxin acylation by the specialized acyltransferase HlyC: formation of a ternary complex with acylACP and protoxin substrates. *Mol Microbiol* 34:887–901.
50. Stanley P, Packman LC, Koronakis V, Hughes C. 1994. Fatty acylation of two internal lysine residues required for the toxic activity of *Escherichia coli* hemolysin. *Science* 266:1992–1996.
51. Issartel JP, Koronakis V, Hughes C. 1991. Activation of *Escherichia coli* prohaemolysin to the mature toxin by acyl carrier protein-dependent fatty acylation. *Nature* 351:759–761.
52. Thomas S, Smits SH, Schmitt L. 2014. A simple in vitro acylation assay based on optimized HlyA and HlyC purification. *Anal Biochem* 464:17–23.
53. Greene NP, Crow A, Hughes C, Koronakis V. 2015. Structure of a bacterial toxin-activating acyltransferase. *Proc Natl Acad Sci USA* 112:E3058–E3066.
54. Lecher J, Schwarz CK, Stoldt M, Smits SH, Willbold D, Schmitt L. 2012. An RTX transporter tethers its unfolded substrate during secretion via a unique N-terminal domain. *Structure* 20:1778–1787.
55. Sanchez-Magraner L, Viguera AR, Garcia-Pacios M, Garcillan MP, Arrondo JL, de la Cruz F, Goni FM, Ostolaza H. 2007. The calcium-binding C-terminal domain of *Escherichia coli* alpha-hemolysin is a major determinant in the surface-active properties of the protein. *J Biol Chem* 282:11827–11835.
56. Ghigo JM, Wandersman C. 1994. A carboxyl-terminal four-amino acid motif is required for secretion of the metalloprotease PrtG through the *Erwinia chrysanthemi* protease secretion pathway. *J Biol Chem* 269:8979–8985.
57. Letoffe S, Wandersman C. 1992. Secretion of CyaA-PrtB and HlyA-PrtB fusion proteins in *Escherichia coli*: involvement of the glycine-rich repeat domain of *Erwinia chrysanthemi* protease B. *J Bacteriol* 174:4920–4927.
58. Salmond GP, Reeves PJ. 1993. Membrane traffic wardens and protein secretion in gram-negative bacteria. *Trends Biochem Sci* 18:7–12.
59. Nicaud JM, Mackman N, Gray L, Holland IB. 1986. The C-terminal, 23 kDa peptide of *E. coli* haemolysin 2001 contains all the information necessary for its secretion by the haemolysin (Hly) export machinery. *FEBS Lett* 204:331–335.
60. Jarchau T, Chakraborty T, Garcia F, Goebel W. 1994. Selection for transport competence of C-terminal polypeptides derived from *Escherichia coli* hemolysin: the shortest peptide capable of autonomous HlyB/HlyD-dependent secretion comprises the C-terminal 62 amino acids of HlyA. *Mol Gen Genet* 245:53–60.
61. Duong F, Lazdunski A, Murgier M. 1996. Protein secretion by heterologous bacterial ABC-transporters: the C-terminus secretion signal of the secreted protein confers high recognition specificity. *Mol Microbiol* 21:459–470.
62. Delepelaire P, Wandersman C. 1990. Protein secretion in gram-negative bacteria. The extracellular metalloprotease B from *Erwinia chrysanthemi* contains a C-terminal secretion signal analogous to that of *Escherichia coli* alpha-hemolysin. *J Biol Chem* 265:17118–17125.

Holland et al.

63. Park Y, Moon Y, Ryoo J, Kim N, Cho H, Ahn JH. 2012. Identification of the minimal region in lipase ABC transporter recognition domain of *Pseudomonas fluorescens* for secretion and fluorescence of green fluorescent protein. *Microb Cell Fact* **11**:60. doi:10.1186/1475-2859-11-60.
64. Angkawidjaja C, Kuwahara K, Omori K, Koga Y, Takano K, Kanaya S. 2006. Extracellular secretion of *Escherichia coli* alkaline phosphatase with a C-terminal tag by type I secretion system: purification and biochemical characterization. *Protein Eng Des Sel* **19**:337–343.
65. Sebo P, Ladant D. 1993. Repeat sequences in the *Bordetella pertussis* adenylate cyclase toxin can be recognized as alternative carboxy-proximal secretion signals by the *Escherichia coli* alpha-haemolysin translocator. *Mol Microbiol* **9**:999–1009.
66. Letoffe S, Ghigo JM, Wandersman C. 1994. Secretion of the *Serratia marcescens* HasA protein by an ABC transporter. *J Bacteriol* **176**:5372–5377.
67. Shieh YW, Minguez P, Bork P, Auburger JJ, Guilbride DL, Kramer G, Bukau B. 2015. Operon structure and cotranslational subunit association direct protein assembly in bacteria. *Science* **350**:678–680.
68. Sapriel G, Wandersman C, Delepelaire P. 2002. The N terminus of the HasA protein and the SecB chaperone cooperate in the efficient targeting and secretion of HasA via the ATP-binding cassette transporter. *J Biol Chem* **277**:6726–6732.
69. Bakkes PJ, Jenewein S, Smits SH, Holland IB, Schmitt L. 2010. The rate of folding dictates substrate secretion by the *Escherichia coli* hemolysin type 1 secretion system. *J Biol Chem* **285**:40573–40580.
70. Hess J, Gentschev I, Goebel W, Jarchau T. 1990. Analysis of the haemolysin secretion system by PhoA-HlyA fusion proteins. *Mol Gen Genet* **224**:201–208.
71. Kern I, Ceglowski P. 1995. Secretion of streptokinase fusion proteins from *Escherichia coli* cells through the hemolysin transporter. *Gene* **163**:53–57.
72. Schwarz CK, Landsberg CD, Lenders MH, Smits SH, Schmitt L. 2012. Using an *E. coli* Type 1 secretion system to secrete the mammalian, intracellular protein IFABP in its active form. *J Biotechnol* **159**:155–161.
73. Erb K, Vogel M, Wagner W, Goebel W. 1987. Alkaline phosphatase which lacks its own signal sequence becomes enzymatically active when fused to N-terminal sequences of *Escherichia coli* haemolysin (HlyA). *Mol Gen Genet* **208**:88–93.
74. Kwon HJ, Haruki M, Morikawa M, Omori K, Kanaya S. 2002. Role of repetitive nine-residue sequence motifs in secretion, enzymatic activity, and protein conformation of a family I.3 lipase. *J Biosci Bioeng* **93**:157–164.
75. Fath MJ, Skvirsky RC, Kolter R. 1991. Functional complementation between bacterial MDR-like export systems: colicin V, alpha-hemolysin, and *Erwinia* protease. *J Bacteriol* **173**:7549–7556.
76. Gilson L, Mahanty HK, Kolter R. 1990. Genetic analysis of an MDR-like export system: the secretion of colicin V. *EMBO J* **9**:3875–3884.
77. Ostolaza H, Soloaga A, Goni FM. 1995. The binding of divalent cations to *Escherichia coli* alpha-haemolysin. *Eur J Biochem* **228**:39–44.
78. Soloaga A, Ramirez JM, Goni FM. 1998. Reversible denaturation, self-aggregation, and membrane activity of *Escherichia coli* alpha-hemolysin, a protein stable in 6 M urea. *Biochemistry* **37**:6387–6393.
79. Thomas S, Bakkes PJ, Smits SH, Schmitt L. 2014. Equilibrium folding of pro-HlyA from *Escherichia coli* reveals a stable calcium ion dependent folding intermediate. *Biochim Biophys Acta* **1844**:1500–1510.
80. Chenal A, Guijarro JI, Raynal B, Delepierre M, Ladant D. 2009. RTX calcium binding motifs are intrinsically disordered in the absence of calcium: implication for protein secretion. *J Biol Chem* **284**:1781–1789.
81. Sotomayor Perez AC, Karst JC, Davi M, Guijarro JI, Ladant D, Chenal A. 2010. Characterization of the regions involved in the calcium-induced folding of the intrinsically disordered RTX motifs from the *bordetella pertussis* adenylate cyclase toxin. *J Mol Biol* **397**:534–549.
82. Sotomayor Perez AC, Karst JC, Davi M, Guijarro JI, Ladant D, Chenal A. 2015. Characterization of the regions involved in the calcium-induced folding of the intrinsically disordered RTX motifs from the *bordetella pertussis* adenylate cyclase toxin. *J Mol Biol* **397**:534–549.
83. Blenner MA, Shur O, Szilvay GR, Cropek DM, Banta S. 2010. Calcium-induced folding of a beta roll motif requires C-terminal entropic stabilization. *J Mol Biol* **400**:244–256.
84. Zhang L, Conway JF, Thibodeau PH. 2012. Calcium-induced folding and stabilization of the *Pseudomonas aeruginosa* alkaline protease. *J Biol Chem* **287**:4311–4322.
85. Blight MA, Chervaux C, Holland IB. 1994. Protein secretion pathway in *Escherichia coli*. *Curr Opin Biotechnol* **5**:468–474.
86. Gentschev I, Mollenkopf H, Sokolovic Z, Hess J, Kaufmann SH, Goebel W. 1996. Development of antigen-delivery systems, based on the *Escherichia coli* hemolysin secretion pathway. *Gene* **179**:133–140.
87. Spreng S, Dietrich G, Goebel W, Gentschev I. 1999. The *Escherichia coli* haemolysin secretion apparatus: a potential universal antigen delivery system in gram-negative bacterial vaccine carriers. *Mol Microbiol* **31**:1596–1598.
88. Tzschaschel BD, Guzman CA, Timmis KN, de Lorenzo V. 1996. An *Escherichia coli* hemolysin transport system-based vector for the export of polypeptides: export of Shiga-like toxin IIeB subunit by *Salmonella typhimurium* aroA. *Nat Biotechnol* **14**:765–769.
89. Ryu J, Lee U, Park J, Yoo DH, Ahn JH. 2015. A vector system for ABC transporter-mediated secretion and purification of recombinant proteins in *Pseudomonas* species. *Appl Environ Microbiol* **81**:1744–1753.
90. Debarbieux L, Wandersman C. 2001. Folded HasA inhibits its own secretion through its ABC exporter. *EMBO J* **20**:4657–4663.
91. Holland IB, Benabdelhak H, Young J, De Lima Pimenta A, Schmitt L, Blight MA. 2003. Bacterial ABC transporters involved in protein translocation, p 209–241. In Holland IB, Cole SPC, Kuchler K, Higgins CF (ed), *ABC Proteins: From Bacteria to Man*. Academic Press, San Diego, CA.
92. Chervaux C, Holland IB. 1996. Random and directed mutagenesis to elucidate the functional importance of helix II and F-989 in the C-terminal secretion signal of *Escherichia coli* hemolysin. *J Bacteriol* **178**:1232–1236.
93. Omori K, Idei A, Akatsuka H. 2001. *Serratia* ATP-binding cassette protein exporter, Lip, recognizes a protein region upstream of the C terminus for specific secretion. *J Biol Chem* **276**:27111–27119.
94. Guzzo J, Duong F, Wandersman C, Murgier M, Lazdunski A. 1991. The secretion genes of *Pseudomonas aeruginosa* alkaline protease are functionally related to those of *Erwinia chrysanthemi* proteases and *Escherichia coli* alpha-haemolysin. *Mol Microbiol* **5**:447–453.
95. Masure HR, Au DC, Gross MK, Donovan MG, Storm DR. 1990. Secretion of the *Bordetella pertussis* adenylate cyclase from *Escherichia coli* containing the hemolysin operon. *Biochemistry* **29**:140–145.

96. Akatsuka H, Kawai E, Omori K, Shibatani T. 1995. The three genes lipB, lipC, and lipD involved in the extracellular secretion of the *Serratia marcescens* lipase which lacks an N-terminal signal peptide. *J Bacteriol* 177:6381–6389.
97. Zhang F, Greig DI, Ling V. 1993. Functional replacement of the hemolysin A transport signal by a different primary sequence. *Proc Natl Acad Sci USA* 90:4211–4215.
98. van Belkum MJ, Worobo RW, Stiles ME. 1997. Double-glycine-type leader peptides direct secretion of bacteriocins by ABC transporters: colicin V secretion in *Lactococcus lactis*. *Mol Microbiol* 23:1293–1301.
99. Hess JL, Pyper JM, Clements JE. 1986. Nucleotide sequence and transcriptional activity of the caprine arthritis-encephalitis virus long terminal repeat. *J Virol* 60:385–393.
100. Kenny B, Chervaux C, Holland IB. 1994. Evidence that residues -15 to -46 of the haemolysin secretion signal are involved in early steps in secretion, leading to recognition of the translocator. *Mol Microbiol* 11:99–109.
101. Kenny B, Taylor S, Holland IB. 1992. Identification of individual amino acids required for secretion within the haemolysin (HlyA) C-terminal targeting region. *Mol Microbiol* 6:1477–1489.
102. Stanley P, Koronakis V, Hughes C. 1991. Mutational analysis supports a role for multiple structural features in the C-terminal secretion signal of *Escherichia coli* haemolysin. *Mol Microbiol* 5:2391–2403.
103. Jumpertz T, Chervaux C, Racher K, Zouhair M, Blight MA, Holland IB, Schmitt L. 2010. Mutations affecting the extreme C terminus of *Escherichia coli* haemolysin A reduce haemolytic activity by altering the folding of the toxin. *Microbiology* 156:2495–2505.
104. Hui D, Ling V. 2002. A combinatorial approach toward analyzing functional elements of the *Escherichia coli* hemolysin signal sequence. *Biochemistry* 41:5333–5339.
105. Hui D, Morden C, Zhang F, Ling V. 2000. Combinatorial analysis of the structural requirements of the *Escherichia coli* hemolysin signal sequence. *J Biol Chem* 275:2713–2720.
106. Yin Y, Zhang F, Ling V, Arrowsmith CH. 1995. Structural analysis and comparison of the C-terminal transport signal domains of hemolysin A and leukotoxin A. *FEBS Lett* 366:1–5.
107. Pei XY, Hinchliffe P, Symmons MF, Koronakis E, Benz R, Hughes C, Koronakis V. 2011. Structures of sequential open states in a symmetrical opening transition of the TolC exit duct. *Proc Natl Acad Sci USA* 108:2112–2117.
108. Wolff N, Delepelaire P, Ghigo JM, Delepierre M. 1997. Spectroscopic studies of the C-terminal secretion signal of the *Serratia marcescens* haem acquisition protein (HasA) in various membrane-mimetic environments. *Eur J Biochem* 243:400–407.
109. Wolff N, Ghigo JM, Delepelaire P, Wandersman C, Delepierre M. 1994. C-terminal secretion signal of an *Erwinia chrysanthemi* protease secreted by a signal peptide-independent pathway: proton NMR and CD conformational studies in membrane-mimetic environments. *Biochemistry* 33:6792–6801.
110. Izadi-Pruneyre N, Wolff N, Redeker V, Wandersman C, Delepierre M, Lecroisey A. 1999. NMR studies of the C-terminal secretion signal of the haem-binding protein, HasA. *Eur J Biochem* 261:562–568.
111. Zhang F, Yin Y, Arrowsmith CH, Ling V. 1995. Secretion and circular dichroism analysis of the C-terminal signal peptides of HlyA and LktA. *Biochemistry* 34:4193–4201.
112. Arnoux P, Haser R, Izadi N, Lecroisey A, Delepierre M, Wandersman C, Czjzek M. 1999. The crystal structure of HasA, a hemophore secreted by *Serratia marcescens*. *Nat Struct Biol* 6:516–520.
113. Meier R, Drepper T, Svensson V, Jaeger KE, Baumann U. 2007. A calcium-gated lid and a large beta-roll sandwich are revealed by the crystal structure of extracellular lipase from *Serratia marcescens*. *J Biol Chem* 282:31477–31483.
114. Cescau S, Debarbieux L, Wandersman C. 2007. Probing the in vivo dynamics of type I protein secretion complex association through sensitivity to detergents. *J Bacteriol* 189:1496–1504.
115. Kuwahara K, Angkawidjaja C, Koga Y, Takano K, Kanaya S. 2011. Importance of an extreme C-terminal motif of a family I.3 lipase for stability. *Protein Eng Des Sel* 24:411–418.
116. Blight MA, Pimenta AL, Lazzaroni JC, Dando C, Kotelevets L, Seror SJ, Holland IB. 1994. Identification and preliminary characterization of temperature-sensitive mutations affecting HlyB, the translocator required for the secretion of haemolysin (HlyA) from *Escherichia coli*. *Mol Gen Genet* 245:431–440.
117. Wandersman C, Letoffe S. 1993. Involvement of lipopolysaccharide in the secretion of *Escherichia coli* alpha-haemolysin and *Erwinia chrysanthemi* proteases. *Mol Microbiol* 7:141–150.
118. Lenders MHH, Weidtkamp-Peters S, Kleinschrodt D, Jaeger K-E, Smits SHJ, Schmitt L. 2015. Directionality of substrate translocation of the hemolysin A Type I secretion system. *Sci Rep* 5:12470. doi:10.1038/srep12470.
119. Boardman BK, Satchell KJ. 2004. *Vibrio cholerae* strains with mutations in an atypical type I secretion system accumulate RTX toxin intracellularly. *J Bacteriol* 186:8137–8143.
120. Satchell KJ. 2007. MARTX, multifunctional autoprocessing repeats-in-toxin toxins. *Infect Immun* 75:5079–5084.
121. Griessl MH, Schmid B, Kassler K, Braunsman C, Ritter R, Barlag B, Stierhof YD, Sturm KU, Danzer C, Wagner C, Schaffer TE, Sticht H, Hensel M, Muller YA. 2013. Structural insight into the giant Ca(2)(+)-binding adhesin SiiE: implications for the adhesion of *Salmonella enterica* to polarized epithelial cells. *Structure* 21:741–752.
122. Gerlach RG, Jackel D, Stecher B, Wagner C, Lupas A, Hardt WD, Hensel M. 2007. *Salmonella* Pathogenicity Island 4 encodes a giant non-fimbrial adhesin and the cognate type 1 secretion system. *Cell Microbiol* 9:1834–1850.
123. Wille T, Wagner C, Mittelstadt W, Blank K, Sommer E, Malengo G, Dohler D, Lange A, Sourjik V, Hensel M, Gerlach RG. 2014. SiiA and SiiB are novel type I secretion system subunits controlling SPI4-mediated adhesion of *Salmonella enterica*. *Cell Microbiol* 16:161–178.
124. Jernigan KK, Bordenstein SR. 2014. Ankyrin domains across the Tree of Life. *PeerJ* 2:e264. doi:10.7717/peerj.264.
125. Wilson MM, Anderson DE, Bernstein HD. 2015. Analysis of the outer membrane proteome and secretome of *Bacteroides fragilis* reveals a multiplicity of secretion mechanisms. *PLoS One* 10:e0117732. doi:10.1371/journal.pone.0117732.
126. Gillespie JJ, Kaur SJ, Rahman MS, Rennoll-Bankert K, Sears KT, Beier-Sexton M, Azad AF. 2015. Secretome of obligate intracellular Rickettsia. *FEMS Microbiol Rev* 39:47–80.
127. VieBrock L, Evans SM, Beyer AR, Larson CL, Beare PA, Ge H, Singh S, Rodino KG, Heinzen RA, Richards AL, Carlyon JA. 2014. *Orientia tsutsugamushi* ankyrin repeat-containing protein family members are Type 1 secretion system substrates that traffic to the host cell endoplasmic reticulum. *Front Cell Infect Microbiol* 4:186. doi:10.3389/fcimb.2014.00186.
128. Dhamdhare G, Zgurskaya HI. 2010. Metabolic shutdown in *Escherichia coli* cells lacking the outer membrane channel TolC. *Mol Microbiol* 77:743–754.
129. Ruiz C, Levy SB. 2014. Regulation of acrAB expression by cellular metabolites in *Escherichia coli*. *J Antimicrob Chemother* 69:390–399.

Holland et al.

130. Nikaido H. 1996. Multidrug efflux pumps of gram-negative bacteria. *J Bacteriol* **178**:5853–5859.
131. Lennen RM, Politz MG, Kruziki MA, Pfleger BF. 2013. Identification of transport proteins involved in free fatty acid efflux in *Escherichia coli*. *J Bacteriol* **195**:135–144.
132. Hantke K, Winkler K, Schultz JE. 2011. *Escherichia coli* exports cyclic AMP via TolC. *J Bacteriol* **193**:1086–1089.
133. Tikhonova EB, Zgurskaya HI. 2004. AcrA, AcrB, and TolC of *Escherichia coli* form a stable intermembrane multidrug efflux complex. *J Biol Chem* **279**:32116–32124.
134. Krishnamoorthy G, Tikhonova EB, Dhamdhare G, Zgurskaya HI. 2013. On the role of TolC in multidrug efflux: the function and assembly of AcrAB-TolC tolerate significant depletion of intracellular TolC protein. *Mol Microbiol* **87**:982–997.
135. Pos KM. 2009. Drug transport mechanism of the AcrB efflux pump. *Biochim Biophys Acta* **1794**:782–793.
136. Thanabalu T, Koronakis E, Hughes C, Koronakis V. 1998. Substrate-induced assembly of a contiguous channel for protein export from *E. coli*: reversible bridging of an inner-membrane translocase to an outer membrane exit pore. *EMBO J* **17**:6487–6496.
137. Koronakis V, Li J, Koronakis E, Stauffer K. 1997. Structure of TolC, the outer membrane component of the bacterial type I efflux system, derived from two-dimensional crystals. *Mol Microbiol* **23**:617–626.
138. Koronakis V, Sharff A, Koronakis E, Luisi B, Hughes C. 2000. Crystal structure of the bacterial membrane protein TolC central to multidrug efflux and protein export. *Nature* **405**:914–919.
139. Koronakis V, Eswaran J, Hughes C. 2004. Structure and function of TolC: the bacterial exit duct for proteins and drugs. *Annu Rev Biochem* **73**:467–489.
140. Andersen C, Koronakis E, Bokma E, Eswaran J, Humphreys D, Hughes C, Koronakis V. 2002. Transition to the open state of the TolC periplasmic tunnel entrance. *Proc Natl Acad Sci USA* **99**:11103–11108.
141. Andersen C, Koronakis E, Hughes C, Koronakis V. 2002. An aspartate ring at the TolC tunnel entrance determines ion selectivity and presents a target for blocking by large cations. *Mol Microbiol* **44**:1131–1139.
142. Federici L, Du D, Walas F, Matsumura H, Fernandez-Recio J, McKeegan KS, Borges-Walmsley MI, Luisi BF, Walmsley AR. 2005. The crystal structure of the outer membrane protein VceC from the bacterial pathogen *Vibrio cholerae* at 1.8 Å resolution. *J Biol Chem* **280**:15307–15314.
143. Schulein R, Gentschev I, Mollenkopf HJ, Goebel W. 1992. A topological model for the haemolysin translocator protein HlyD. *Mol Gen Genet* **234**:155–163.
144. Gavel Y, von Heijne G. 1992. The distribution of charged amino acids in mitochondrial inner-membrane proteins suggests different modes of membrane integration for nuclearly and mitochondrially encoded proteins. *Eur J Biochem* **205**:1207–1215.
145. Balakrishnan L, Hughes C, Koronakis V. 2001. Substrate-triggered recruitment of the TolC channel-tunnel during type I export of hemolysin by *Escherichia coli*. *J Mol Biol* **313**:501–510.
146. Schulein R, Gentschev I, Schlor S, Gross R, Goebel W. 1994. Identification and characterization of two functional domains of the hemolysin translocator protein HlyD. *Mol Gen Genet* **245**:203–211.
147. Pimenta AL, Racher K, Jamieson L, Blight MA, Holland IB. 2005. Mutations in HlyD, part of the type I translocator for hemolysin secretion, affect the folding of the secreted toxin. *J Bacteriol* **187**:7471–7480.
148. Vakharia H, German GJ, Misra R. 2001. Isolation and characterization of *Escherichia coli* tolC mutants defective in secreting enzymatically active alpha-hemolysin. *J Bacteriol* **183**:6908–6916.
149. Jones HE, Holland IB, Baker HL, Campbell AK. 1999. Slow changes in cytosolic free Ca²⁺ in *Escherichia coli* highlight two putative influx mechanisms in response to changes in extracellular calcium. *Cell Calcium* **25**:265–274.
150. Tikhonova EB, Yamada Y, Zgurskaya HI. 2011. Sequential mechanism of assembly of multidrug efflux pump AcrAB-TolC. *Chem Biol* **18**:454–463.
151. Symmons MF, Marshall RL, Bavro VN. 2015. Architecture and roles of periplasmic adaptor proteins in tripartite efflux assemblies. *Front Microbiol* **6**:513. doi:10.3389/fmicb.2015.00513.
152. Kim JS, Song S, Lee M, Lee S, Lee K, Ha NC. 2016. Crystal structure of a soluble fragment of the membrane fusion protein HlyD in a type I secretion system of gram-negative bacteria. *Structure* **24**:477–485.
153. Modali SD, Zgurskaya HI. 2011. The periplasmic membrane proximal domain of MacA acts as a switch in stimulation of ATP hydrolysis by MacB transporter. *Mol Microbiol* **81**:937–951.
154. Hinchliffe P, Greene NP, Paterson NG, Crow A, Hughes C, Koronakis V. 2014. Structure of the periplasmic adaptor protein from a major facilitator superfamily (MFS) multidrug efflux pump. *FEBS Lett* **588**:3147–3153.
155. Johnson JM, Church GM. 1999. Alignment and structure prediction of divergent protein families: periplasmic and outer membrane proteins of bacterial efflux pumps. *J Mol Biol* **287**:695–715.
156. Zgurskaya HI, Weeks JW, Ntrel AT, Nickels LM, Wolloscheck D. 2015. Mechanism of coupling drug transport reactions located in two different membranes. *Front Microbiol* **6**:100. doi:10.3389/fmicb.2015.00100.
157. Du D, van Veen HW, Luisi BF. 2015. Assembly and operation of bacterial tripartite multidrug efflux pumps. *Trends Microbiol* **23**:311–319.
158. Gentschev I, Goebel W. 1992. Topological and functional studies on HlyB of *Escherichia coli*. *Mol Gen Genet* **232**:40–48.
159. Davidson AL, Dassa E, Orelle C, Chen J. 2008. Structure, function, and evolution of bacterial ATP-binding cassette systems. *Microbiol Mol Biol Rev* **72**:317–364.
160. Schmitt L, Benabdelhak H, Blight MA, Holland IB, Stubbs MT. 2003. Crystal structure of the ABC-domain of the ABC-transporter HlyB: Identification of a variable region within the hecal domain of ABC-domains. *J Mol Biol* **330**:333–342.
161. Zhang F, Sheps JA, Ling V. 1998. Structure-function analysis of hemolysin B. *Methods Enzymol* **292**:51–66.
162. Binet R, Wandersman C. 1995. Protein secretion by hybrid bacterial ABC-transporters: specific functions of the membrane ATPase and the membrane fusion protein. *EMBO J* **14**:2298–2306.
163. Benabdelhak H, Kiontke S, Horn C, Ernst R, Blight MA, Holland IB, Schmitt L. 2003. A specific interaction between the NBD of the ABC-transporter HlyB and a C-terminal fragment of its transport substrate haemolysin A. *J Mol Biol* **327**:1169–1179.
164. Delepelaire P. 1994. PrtD, the integral membrane ATP-binding cassette component of the *Erwinia chrysanthemi* metalloprotease secretion system, exhibits a secretion signal-regulated ATPase activity. *J Biol Chem* **269**:27952–27957.
165. Hwang J, Zhong X, Tai PC. 1997. Interactions of dedicated export membrane proteins of the colicin V secretion system: CvaA, a member of the membrane fusion protein family, interacts with CvaB and TolC. *J Bacteriol* **179**:6264–6270.

166. Letoffe S, Delepelaire P, Wandersman C. 1996. Protein secretion in gram-negative bacteria: assembly of the three components of ABC protein-mediated exporters is ordered and promoted by substrate binding. *EMBO J* 15:5804–5811.
167. Tikhonova EB, Devroy VK, Lau SY, Zgurskaya HI. 2007. Reconstitution of the *Escherichia coli* macrolide transporter: the periplasmic membrane fusion protein MacA stimulates the ATPase activity of MacB. *Mol Microbiol* 63:895–910.
168. Du D, van Veen HW, Murakami S, Pos KM, Luisi BF. 2015. Structure, mechanism and cooperation of bacterial multidrug transporters. *Curr Opin Struct Biol* 33:76–91.
169. Du D, Wang Z, James NR, Voss JE, Klimont E, Ohene-Agyei T, Venter H, Chiu W, Luisi BF. 2014. Structure of the AcrAB-TolC multidrug efflux pump. *Nature* 509:512–515.
170. Kim JS, Jeong H, Song S, Kim HY, Lee K, Hyun J, Ha NC. 2015. Structure of the tripartite multidrug efflux pump AcrAB-TolC suggests an alternative assembly mode. *Mol Cells* 38:180–186.
171. Hung LW, Wang IX, Nikaido K, Liu PQ, Ames GF, Kim SH. 1998. Crystal structure of the ATP-binding subunit of an ABC transporter. *Nature* 396:703–707.
172. Jones PM, George AM. 2002. Mechanism of ABC transporters: a molecular dynamics simulation of a well characterized nucleotide-binding subunit. *Proc Natl Acad Sci USA* 99:12639–12644.
173. Smith PC, Karpowich N, Millen L, Moody JF, Rosen J, Thomas PF, Hunt JF. 2002. ATP binding to the motor domain from an ABC transporter drives formation of a nucleotide sandwich dimer. *Mol Cell* 10:139–149.
174. Zaitseva J, Jenewein S, Jumpertz T, Holland IB, Schmitt L. 2005. H662 is the linchpin of ATP hydrolysis in the nucleotide-binding domain of the ABC transporter HlyB. *EMBO J* 24:1901–1910.
175. Zaitseva J, Oswald C, Jumpertz T, Jenewein S, Wiedenmann A, Holland IB, Schmitt L. 2006. A structural analysis of asymmetry required for catalytic activity of an ABC-ATPase domain dimer. *EMBO J* 25:3432–3443.
176. Jones PM, George AM. 2014. A reciprocating twin-channel model for ABC transporters. *Q Rev Biophys* 47:189–220.
177. Jumpertz T, Holland IB, Schmitt L. 2009. ABC transporters - a smart example of a molecular machinerie, p 1–34. In Ponte-Sucre A (ed), *ABC Transporters in Microorganisms: Research, Innovation and Value as Targets against Drug Resistance*. Caister Academic Press, Poole, United Kingdom.
178. Vetter IR, Wittinghofer A. 1999. Nucleoside triphosphate-binding proteins: different scaffolds to achieve phosphoryl transfer. *Q Rev Biophys* 32:1–56.
179. Schmitt L, Tampe R. 2002. Structure and mechanism of ABC transporters. *Curr Opin Struct Biol* 12:754–760.
180. Oldham ML, Khare D, Quiocho FA, Davidson AL, Chen J. 2007. Crystal structure of a catalytic intermediate of the maltose transporter. *Nature* 450:515–521.
181. Orelle C, Dalmás O, Gros P, Di Pietro A, Jault JM. 2003. The conserved glutamate residue adjacent to the Walker-B motif is the catalytic base for ATP hydrolysis in the ATP-binding cassette transporter BmrA. *J Biol Chem* 278:47002–47008.
182. Moody JE, Millen L, Binns D, Hunt JF, Thomas PJ. 2002. Cooperative, ATP-dependent association of the nucleotide binding cassettes during the catalytic cycle of ATP-binding cassette transporters. *J Biol Chem* 277:21111–21114.
183. Zaitseva J, Jenewein S, Wiedenmann A, Benabdelhak H, Holland IB, Schmitt L. 2005. Functional characterization and ATP-induced dimerization of the isolated ABC-domain of the haemolysin B transporter. *Biochemistry* 44:9680–9690.
184. Janas E, Hofacker M, Chen M, Gompf S, van der Does C, Tampe R. 2003. The ATP hydrolysis cycle of the nucleotide-binding domain of the mitochondrial ATP-binding cassette transporter Mdl1p. *J Biol Chem* 278:26862–26869.
185. Verdon G, Albers SV, van Oosterwijk N, Dijkstra BW, Driessen AJ, Thunnissen AM. 2003. Formation of the productive ATP-Mg²⁺-bound dimer of GlcV, an ABC-ATPase from *Sulfolobus solfataricus*. *J Mol Biol* 334:255–267.
186. Davidson AL, Sharma S. 1997. Mutation of a single MalK subunit severely impairs maltose transport activity in *Escherichia coli*. *J Bacteriol* 179:5458–5464.
187. Shyamala V, Baichwal V, Beall E, Ames GF. 1991. Structure-function analysis of the histidine permease and comparison with cystic fibrosis mutations. *J Biol Chem* 266:18714–18719.
188. Ernst R, Kueppers P, Klein CM, Schwarzmueller T, Kuchler K, Schmitt L. 2008. A mutation of the H-loop selectively affects rhodamine transport by the yeast multidrug ABC transporter Pdr5. *Proc Natl Acad Sci USA* 105:5069–5074.
189. Oldham ML, Chen J. 2011. Snapshots of the maltose transporter during ATP hydrolysis. *Proc Natl Acad Sci USA* 108:15152–15156.
190. Senior AE. 2011. Reaction chemistry ABC-style. *Proc Natl Acad Sci USA* 108:15015–15016.
191. van der Does C, Presenti C, Schulze K, Dinkelaker S, Tampe R. 2005. Kinetics of the ATP hydrolysis cycle of the nucleotide-binding domain of MDL1 studied by a novel site-specific labeling technique. *J Biol Chem* 281:5694–5701.
192. Locher KP, Lee AT, Rees DC. 2002. The *E. coli* BtuCD structure: a framework for ABC transporter architecture and mechanism. *Science* 296:1091–1098.
193. Khare D, Oldham ML, Orelle C, Davidson AL, Chen J. 2009. Alternating access in maltose transporter mediated by rigid-body rotations. *Mol Cell* 33:528–536.
194. Jardetzky O. 1966. Simple allosteric model for membrane pumps. *Nature* 211:969–970.
195. Dawson RJ, Locher KP. 2006. Structure of a bacterial multidrug ABC transporter. *Nature* 443:180–185.
196. Aller SG, Yu J, Ward A, Weng Y, Chittaboina S, Zhuo R, Harrell PM, Trinh YT, Zhang Q, Urbatsch IL, Chang G. 2009. Structure of P-glycoprotein reveals a molecular basis for poly-specific drug binding. *Science* 323:1718–1722.
197. Choudhury HG, Tong Z, Mathavan I, Li Y, Iwata S, Zirah S, Rebuffat S, van Veen HW, Beis K. 2014. Structure of an antibacterial peptide ATP-binding cassette transporter in a novel outward occluded state. *Proc Natl Acad Sci USA* 111:9145–9150.
198. Jin MS, Oldham ML, Zhang Q, Chen J. 2012. Crystal structure of the multidrug transporter P-glycoprotein from *Caenorhabditis elegans*. *Nature* 490:566–569.
199. Kodan A, Yamaguchi T, Nakatsu T, Sakiyama K, Hipolito CJ, Fujioka A, Hirokane R, Ikeguchi K, Watanabe B, Hiratake J, Kimura Y, Suga H, Ueda K, Kato H. 2014. Structural basis for gating mechanisms of a eukaryotic P-glycoprotein homolog. *Proc Natl Acad Sci USA* 111:4049–4054.
200. Lee JY, Yang JG, Zhitnitsky D, Lewinson O, Rees DC. 2014. Structural basis for heavy metal detoxification by an Atm1-type ABC exporter. *Science* 343:1133–1136.
201. Shintre CA, Pike AC, Li Q, Kim JI, Barr AJ, Goubin S, Shrestha L, Yang J, Berridge G, Ross J, Stansfeld PJ, Sansom MS, Edwards AM, Bountra C, Marsden BD, von Delft F, Bullock AN, Gileadi O, Burgess-Brown NA, Carpenter EP. 2013. Structures of ABCB10, a human ATP-binding cassette transporter in apo- and nucleotide-bound states. *Proc Natl Acad Sci USA* 110:9710–9715.

Holland et al.

202. Srinivasan V, Pierik AJ, Lill R. 2014. Crystal structures of nucleotide-free and glutathione-bound mitochondrial ABC transporter Atm1. *Science* **343**:1137–1140.
203. Delgado MA, Solbiati JO, Chiuchiolo MJ, Farias RN, Salomon RA. 1999. *Escherichia coli* outer membrane protein TolC is involved in production of the peptide antibiotic microcin J25. *J Bacteriol* **181**: 1968–1970.
204. Lin DY, Huang S, Chen J. 2015. Crystal structures of a polypeptide processing and secretion transporter. *Nature* **523**:425–430.
205. Perez C, Gerber S, Boilevin J, Bucher M, Darbre T, Aebi M, Reymond JL, Locher KP. 2015. Structure and mechanism of an active lipid-linked oligosaccharide flippase. *Nature* **524**:433–438.
206. Benabdelhak H, Schmitt L, Horn C, Jumel K, Blight MA, Holland IB. 2005. Positive cooperative activity and dimerization of the isolated ABC-ATPase domain of HlyB from E.coli. *Biochem J* **368**:1–7.
207. Procko E, Gaudet R. 2008. Functionally important interactions between the nucleotide-binding domains of an antigenic peptide transporter. *Biochemistry* **47**:5699–5708.
208. Grossmann N, Vakkasoglu AS, Hulpke S, Abele R, Gaudet R, Tampe R. 2014. Mechanistic determinants of the directionality and energetics of active export by a heterodimeric ABC transporter. *Nat Commun* **5**:5419. [doi:10.1038/ncomms6419](https://doi.org/10.1038/ncomms6419).
209. Korkhov VM, Mireku SA, Locher KP. 2012. Structure of AMP-PNP-bound vitamin B12 transporter BtuCD-F. *Nature* **490**:367–372.
210. Ishii S, Yano T, Ebihara A, Okamoto A, Manzoku M, Hayashi H. 2010. Crystal structure of the peptidase domain of Streptococcus ComA, a bifunctional ATP-binding cassette transporter involved in the quorum-sensing pathway. *J Biol Chem* **285**:10777–10785.
211. Bao H, Dalal K, Cytrynbaum E, Duong F. 2015. Sequential action of MalE and maltose allows coupling ATP hydrolysis to translocation in the MalFGK2 transporter. *J Biol Chem* **290**:25452–25460.
212. Bumba L, Masin J, Macek P, Wald T, Motlova L, Bibova I, Klimova N, Bednarova L, Veverka V, Kachala M, Svergun DI, Barinka C, Sebo P. 2016. Calcium-driven folding of RTX domain beta-rolls ratchets translocation of RTX proteins through type I secretion ducts. *Mol Cell* **62**:47–62.
213. Artsimovitch I, Landick R. 2002. The transcriptional regulator RfaH stimulates RNA chain synthesis after recruitment to elongation complexes by the exposed nontemplate DNA strand. *Cell* **109**:193–203.
214. Lee M, Jun SY, Yoon BY, Song S, Lee K, Ha NC. 2012. Membrane fusion proteins of type I secretion system and tripartite efflux pumps share a binding motif for TolC in gram-negative bacteria. *PLoS One* **7**:e40460. [doi:10.1371/journal.pone.0040460](https://doi.org/10.1371/journal.pone.0040460).

3.3 Chapter III – Type I Secretion Systems – Recent Findings

Title:	Type I secretion system – it takes three and a substrate
Authors:	Kerstin Kanonenberg, Olivia Spitz, Isabelle N. Erenburg, Tobias Beer, Lutz Schmitt
Published in:	<i>FEMS Microbiology Letters</i> (2018)
Impact Factor:	1.735
Own Work:	30 % Writing of the manuscript



FEMS Microbiology Letters, 365, 2018, fny094

doi: [10.1093/femsle/fny094](https://doi.org/10.1093/femsle/fny094)

Advance Access Publication Date: 10 April 2018

Minireview

MINIREVIEW – Physiology & Biochemistry

Type I secretion system—it takes three and a substrate

Kerstin Kanonenberg, Olivia Spitz, Isabelle N. Erenburg, Tobias Beer and Lutz Schmitt*

Institute of Biochemistry, Heinrich Heine University, 40225 Düsseldorf, Germany

*Corresponding author: Institute of Biochemistry, Heinrich Heine University, Düsseldorf, Universitätsstr. 1, 40225 Düsseldorf, Germany.

Tel: +49-211-81-10773; Fax: +49-211-81-15310; E-mail: lutz.schmitt@hhu.de

One sentence summary: An overview of type I secretion systems of Gram-negative bacteria and a summary of the recent developments is provided.

Editor: Lily Karamanou

ABSTRACT

Type I secretion systems are widespread in Gram-negative bacteria and mediate the one-step translocation of a large variety of proteins serving for diverse purposes, including nutrient acquisition or bacterial virulence. Common to most substrates of type I secretion systems is the presence of a C-terminal secretion sequence that is not cleaved during or after translocation. Furthermore, these protein secretion nanomachineries are always composed of an ABC transporter, a membrane fusion protein, both located in the inner bacterial membrane, and a protein of the outer membrane. These three membrane proteins transiently form a ‘tunnel channel’ across the periplasmic space in the presence of the substrate. Here we summarize the recent findings with respect to structure, function and application of type I secretion systems.

Keywords: protein secretion; ABC transporter; secretion sequence; RTX toxin

INTRODUCTION

Bacteria have a need for secreting a variety of proteins and other molecules to the extracellular space, for nutrient acquisition (e.g. iron-scavenger proteins), biofilm formation (adhesins) or host invasion (virulence factors, e.g. exotoxins).

Secretory pathways have been of major research interest over the past decades and depending on the definition applied, a minimum of 15 different secretion systems has been identified so far in Gram-negative bacteria (reviewed in Costa et al. 2015). Here, the outer membrane imposes an additional problem as secreted macromolecules have to cross a second, the outer membrane. These secretion systems are capable of exporting a diverse range of small molecules, DNA and proteins to the extracellular space or even directly into the cytosol of a target cell. They vary greatly in composition and molecular mechanism, but can be easily divided into two major subgroups based on the presence or absence of a periplasmic transport intermediate during the secretion process.

Type I, III and IV secretion systems are double-membrane-spanning export machineries where the substrate is secreted in

one step from the cytosol to the extracellular space (type I). The latter two are even capable of delivering their substrate directly into the cytosol of the target cell, thus traversing three membranes (Fig. 1). Obviously, all these secretion systems require a ‘tunnel channel’-like architecture, composed of a minimum of 3 but up to more than 10 membrane-localized proteins (Fig. 1). For further information, the reader is referred to Economou and Dalbey (2014) and Costa et al. (2015) for a review series covering the details of most bacterial secretion systems.

This review highlights the recent advances in research concerning specifically type I secretion systems (T1SS), setting the focus mainly on new structural insights that have been obtained over the last years. T1SS are often referred to as the most ‘simple’ representative considering that they are composed of only three membrane proteins (also see Delepelaire 2004; Kanonenberg, Schwarz and Schmitt 2013; Thomas, Holland and Schmitt 2014; Holland et al. 2016 for various aspects of T1SS).

Many Gram-negative pathogens make use of T1SS to secrete a great variety of virulence factors. The discovery of the first T1SS substrate dates back to as far as 1979 when the Goebel

Received: 6 February 2018; Accepted: 9 April 2018

© FEMS 2018. All rights reserved. For permissions, please e-mail: journals.permissions@oup.com

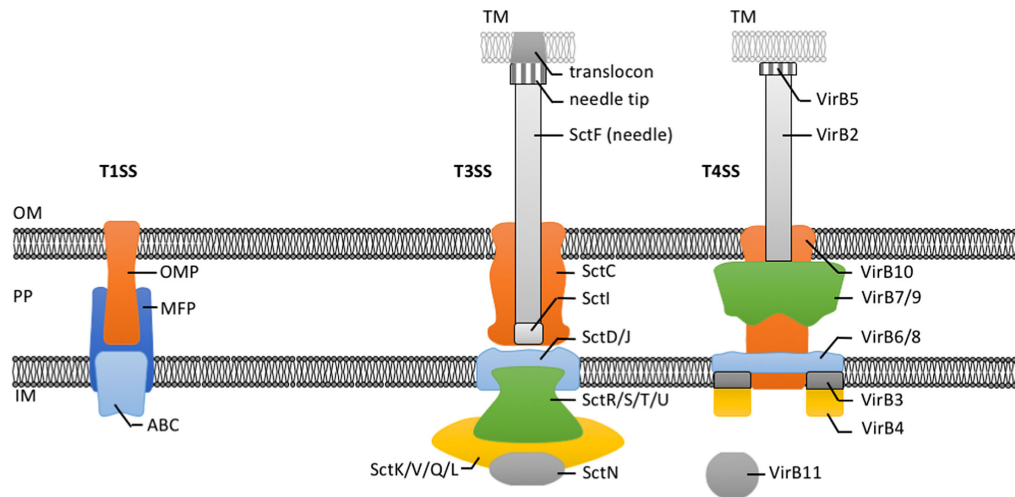


Figure 1. Cartoon of secretion systems from Gram-negative bacteria that translocate their substrates in one step across two (T1SS) or three membranes (T3SS and T4SS). OM: outer membrane, PP: periplasm, IM: inner membrane, OMP: outer membrane protein, MFP: membrane fusion protein, ABC: ABC transporter. Proteins forming the T3SS and T4SS and their putative location are indicated.

laboratory identified hemolysin A (HlyA), named after its ability to lyse erythrocytes from uropathogenic *Escherichia coli* strains (Noegel et al. 1979). Subsequently, the nucleotide sequence of HlyA was determined (Felmlee, Pellett and Welch 1985). Additional studies from the laboratories of Koronakis, Holland and Goebel (Mackman and Holland 1984; Mackman et al. 1985a,b, 1987; Gray et al. 1986, 1989; Felmlee and Welch 1988; Koronakis, Koronakis and Hughes 1989; Gentschev, Hess and Goebel 1990; Chervaux et al. 1995) demonstrated that secretion of HlyA occurred without any periplasmic intermediate and was Sec independent. Moreover, HlyA carried a C-terminal secretion signal indicating an unknown secretion mechanism.

The analysis of the sequence of the *hly* operon (Felmlee, Pellett and Welch 1985) revealed the presence of two additional membrane proteins and a third component in addition to the substrate HlyA. The third component, HlyC, turned out to be essential for the activation of HlyA, but not for secretion per se (Nicaud et al. 1985). HlyC was shown to act as a cytosolic acyltransferase acylating two internal lysine residues of the unfolded HlyA prior to secretion. This required equimolar amounts of the acyl carrier protein (Issartel, Koronakis and Hughes 1991; Stanley, Koronakis and Hughes 1991; Stanley et al. 1994, 1999; Thomas, Smits and Schmitt 2014). Only recently, the crystal structure of an HlyC homolog was reported (Greene et al. 2015) that will open up new approaches to understand the function of this unusual acyltransferase at the molecular level.

HlyD, one of the membrane proteins encoded by the *hly* operon, belongs to the family of bacterial membrane fusion proteins (MFPs) (Symmons, Marshall and Bavro 2015) that is unique to Gram-negative bacteria. The second membrane protein, HlyB, is a member of the ABC transporter family (Davidson et al. 2008), which is found in all kingdoms of life. Since HlyB and HlyD were localized to the inner membrane (Mackman et al. 1985a,b; Wang et al. 1991; Pimenta et al. 1999), the lack of periplasmic intermediates raised an obvious question—How does HlyA reach the extracellular space? This issue was addressed by the Wandersman group, who identified TolC, a ubiquitous and polyvalent outer membrane protein, as the missing, third component of the HlyA-T1SS (Wandersman and Delepelaire 1990). A complex of the two inner membrane proteins and TolC form the 'tunnel

channel' that allows the one-step secretion of HlyA. Apart from T1SS, TolC is involved in the extrusion of toxic components (Koronakis, Eswaran and Hughes 2004), for example by being part of tripartite drug efflux systems such as the AcrA-AcrB/TolC complex (Du et al. 2014).

In other T1SS, more than one transport substrate (Letoffe, Delepelaire and Wandersman 1990) or the TolC homolog (Letoffe, Ghigo and Wandersman 1994) can be encoded in the operon. Thus, there are no strict requirements on the genetic level for the operon organization of T1SS, but several lines of evidence suggest that a minimal unit composed of the gene coding for the transport substrate, the ABC transporter and the MFP is present in all operons. In addition, some degree of promiscuity with respect to the transported substrate exists, since the Hly system of *E. coli* was successfully used to secrete, for example, CyaA from *Bordetella pertussis* (Masure et al. 1990; Sebo and Ladant 1993), FrpA from *Neisseria meningitidis* (Thompson and Sparling 1993) or PaxA from *Pasteurella aerogenes* (Kuhnert et al. 2000).

T1SS SUBSTRATES

For the vast majority of T1SS substrates, all the information necessary and sufficient for secretion is encoded in the extreme C-terminus, which is not cleaved during or after translocation. This was recognized early on (Gray et al. 1986) and was one of the first indications that HlyA was secreted independently of the Sec system. However, a small group of substrates (class II microcins) contain an N-terminal propeptide, which is cleaved by a C39 peptidase domain on the ABC transporter prior to secretion (Hwang, Zhong and Tai 1997).

The actual secretion signal of the Hly system was shown to be confined to the last 50 to 60 most extreme C-terminal amino acids (Koronakis, Koronakis and Hughes 1989) but its size and nature varies from system to system. The reader is referred to a review (Holland et al. 2016), which summarizes our current knowledge on T1SS secretion signals, still leaving many unanswered questions that need to be addressed in future research.

Upstream to the secretion sequence of HlyA, aspartate and glycine-rich nonapeptide repeats were identified (Welch 1991).

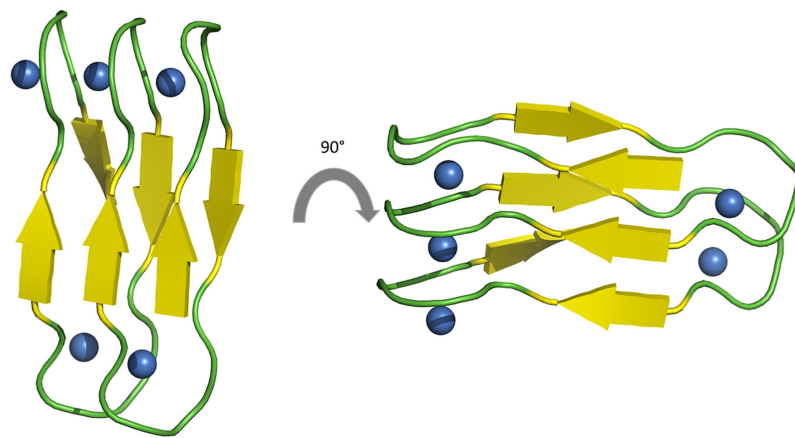


Figure 2. A zoom into the β -roll motif of an alkaline protease (Baumann et al. 1993). Ca^{2+} ions and the Ca^{2+} binding region are shown as blue spheres and in cartoon representation, respectively.

These have the consensus sequence GGXGXDXUX (where X can be any amino acid and U is a large hydrophobic amino acid) and the term ‘GG repeats’ or ‘repeats-in-toxins’ (RTX) was coined by Rod Welch. These repeats form the hallmark of an entire family of proteins including lipases, proteases, adhesins, S-layer proteins or toxins (reviewed by Linhartova et al. 2010).

Structural studies on the T1SS-secreted alkaline protease from *Pseudomonas aeruginosa* (Baumann et al. 1993) and other substrates (Baumann et al. 1993; Izadi-Pruneyre et al. 1999; Meier et al. 2007; Griessl et al. 2013) revealed that the coordination of one Ca^{2+} by two RTX motifs via the side chains of the aspartate residues and the backbone of the first two glycine residues creates a so-called β -roll or β -helix motif (Fig. 2).

RTX substrates of T1SS bind Ca^{2+} ions in the high micromolar range, for example $\sim 500 \mu\text{M}$ for CyaA from *Bordetella pertussis* (Chenal et al. 2009; Sotomayor Perez et al. 2015) or $\sim 150 \mu\text{M}$ for HlyA from *E. coli* (Ostolaza, Soloaga and Goni 1995; Sanchez-Magraner et al. 2007; Thomas et al. 2014). This binding induces folding of the entire RTX protein. As the concentration of free Ca^{2+} ions in the bacterial cytosol is in the high nanomolar range (Jones et al. 1999), RTX proteins remain unfolded until they reach the extracellular space, where Ca^{2+} concentrations of up to 10 mM result in immediate binding and protein folding.

The N-terminal moiety of T1SS substrates encodes for functionality, i.e. lipolytic, hemolytic, proteolytic, adhesive or any other activity. A recent data mining approach of 840 bacterial genome sequences (Linhartova et al. 2010) identified ~ 1000 RTX proteins, being extremely variable in size (up to 900 kDa, Hinsä et al. 2003) and function, but conforming to the general arrangement of T1SS substrates, functional domain/RTX domain/secretion sequence. The number of RTX domains in an individual RTX-protein scales to some extent with the molecular weight (Linhartova et al. 2010), but the presence of these characteristic motifs is ubiquitous and highlights their functional importance.

The iron siderophore HasA from *Serratia marcescens* represents an exception (Letoffe, Ghigo and Wandersman 1994). With a size of 19 kDa it is the smallest substrate of a T1SS identified so far and interestingly lacks the entire RTX domain, but contains a C-terminal secretion sequence (Izadi-Pruneyre et al. 1999). Interestingly, it is the only T1SS substrate known which requires a chaperone, SecB, for secretion (Sapriel, Wandersman and Delepleire 2002; Bakkes et al. 2010).

FUNCTIONAL INSIGHTS

Early on, Koronakis and coworkers (Thanabalu et al. 1998; Balakrishnan, Hughes and Koronakis 2001) demonstrated for the HlyA T1SS that upon interaction of the substrate with the inner membrane proteins (HlyB and HlyD), TolC is recruited and a ‘channel tunnel’ is formed through which HlyA is secreted at the cost of ATP hydrolysis. After substrate translocation is completed, TolC disassembles from the complex, leaving HlyB and HlyD as a stable complex in the inner membrane, ready to start another round of substrate secretion.

Deletion studies proved that the cytosolic domain of HlyD (residues 1–60) forms the hub from which assembly of the secretion complex is initiated (Balakrishnan, Hughes and Koronakis 2001). Complementary data were provided by *in vitro* surface plasmon resonance experiments demonstrating that the isolated nucleotide-binding domain (NBD) of the ABC transporter also interacts with the substrate (Benabdelhak et al. 2003). Interestingly, this interaction was strictly limited to the C-terminal secretion signal.

Indirect (Kenny, Haigh and Holland 1991; Debarbieux and Wandersman 2001) and direct evidence (Bakkes et al. 2010) demonstrated that substrates of T1SS are translocated in an unfolded state. In an elegant set of experiments, Wandersman and colleagues observed that the presence of folded HasA actually inhibited the secretion of newly synthesized HasA (Debarbieux and Wandersman 2001). Subsequently, they addressed the underlying principles of this *cis* inhibition (Cescau, Debarbieux and Wandersman 2007) and surprisingly, the results of this study demonstrated that the interaction of unfolded HasA with the inner membrane complex also occurs outside the region encoding the secretion sequence, identifying a second, non-overlapping binding site. This interaction resulted in stable recruitment of the outer membrane protein TolC, which could be reversed by adding *in cis* the isolated secretion sequence. This pointed toward an intermolecular activity that triggered complex dissociation (Cescau, Debarbieux and Wandersman 2007).

All structural and functional data obtained for ABC transporters so far indicate that the transport mechanism used by these primary active transporters to shuttle their substrates from one side of the membrane to the other follows the ‘alternating two site access model’ for membrane transporters (Jardetzky 1966). However, the unfolded state and the mere

physical length (up to 9000 amino acids) of substrates of T1SS make it impossible to apply this generally accepted mechanism also for ABC transporters involved in T1SS. Although some research has been carried out on this issue, there is still very little understanding of the mechanism of secretion through the transenvelope channel.

In contrast to the canonical organization of ABC transporters, HlyB harbors an additional N-terminal domain, a cytosolic appendix (Kanonenberg, Schwarz and Schmitt 2013). Based on the primary structure of HlyB, the first ~130 amino acids belong to the family of C39 peptidases, a subfamily of the papain superfamily of cysteine proteases (Havarstein, Diep and Nes 1995; Wu and Tai 2004). These peptidases are unique to ABC transporters and are only found in bacteriocin exporters (Havarstein, Diep and Nes 1995). In principle, the protein family of bacteriocins is limited to Gram-positive bacteria, but a few members can also be found in Gram-negative strains, e.g. Colicin V in *E. coli*. Using a type I secretion apparatus but retaining the typical N-terminally cleaved propeptide, these peptides form a small yet unique group amongst type I substrates (Hwang, Zhong and Tai 1997).

However, in many T1SS ABC transporters such as HlyB the catalytically active cysteine residue is replaced by a tyrosine, resulting in a corrupted catalytic triad. Lecher et al. (2012) therefore established the term 'C39 peptidase-like domain' (CLD). NMR studies revealed an identical tertiary structure compared to C39 peptidase domains (Ishii et al. 2010). A conserved interaction of the histidine residue in the corrupted active center with a tryptophan residue was discovered, which is now commonly used to distinguish C39 peptidase domains from CLDs (Lecher et al. 2012; Kanonenberg, Schwarz and Schmitt 2013). In a set of *in vitro* functional and structural studies, Lecher et al. (2012) confirmed binding of unfolded substrate to the isolated CLD that was independent of the secretion signal. The substrate-binding site was mapped by chemical perturbation experiments and results were subsequently confirmed by mutational studies. These results suggest that the CLD acts as a receptor that grabs unfolded HlyA and positions it for subsequent translocation. It remains speculative whether the CLD also plays a role in preventing folding and degradation of the substrate in the cytosol and further studies are needed to establish its precise function and mechanism of action.

Within the field of study, the question of directionality of type I secretion has long been under debate. The concept of stalling the HlyA T1SS by using substrate N-terminally fused to fast folding enhanced green fluorescent protein (eGFP) (Evdokimov et al. 2006) finally answered this question (Lenders et al. 2015). Folded eGFP in the cytosol served as a 'plug' while the C-terminal moiety inserted into the channel tunnel and protruded partially into the extracellular space, where it prevented backsliding by adopting its tertiary structure. A combination of fluorescence and super-resolution microscopy exploiting the autofluorescence of eGFP in the cytosol and immunofluorescence-based methods to detect the secreted C-terminus of the substrate demonstrated that the secretion sequence appears first on the external surface of the cell envelope.

QUANTITATIVE ANALYSIS

The concept of stalling a T1SS (as described in section 'Functional insights') not only offered the possibility to address the directionality of transport but was also exploited to determine the secretion rate of the HlyA T1SS (Lenders et al. 2016). Importantly,

the fluorescence of Cy3-labeled antibody was first employed to quantify the total number of active HlyA T1SS translocons per cell. Interestingly, the derived number was in good agreement with the absolute number of HlyB dimers present in the membrane, as determined by quantitative western blot analysis, using a standard of purified HlyB (Reimann et al. 2016) of known concentrations. By experimentally quantifying the amount of secreted substrate, the secretion rate of the HlyA T1SS was determined to be 16 amino acids per transporter per second. Thus, it requires 90 s to secrete one complete HlyA molecule. This rate is roughly 10-fold lower than the rate of SecA-dependent protein translocation across the inner membrane, which operates at a calculated rate of ~152–228 amino acids per second per transporter (Schiebel et al. 1991; Uchida, Mori and Mizushima 1995). Intriguingly, the rate of HlyA secretion is very similar to the rate of bacterial protein synthesis at the ribosome, which was calculated to be 10–20 amino acids per second (Young and Bremer 1976). Whether this similarity is of any relevance and results from some sort of connection still has to be addressed experimentally.

In earlier studies, the proton motive force (pmf) was identified as being essential for substrate secretion (Koronakis, Hughes and Koronakis 1991). In our hands, however, an influence of the pmf on the secretion rate was not observed (unpublished data), supporting recent results on CyaA, an exotoxin from *B. pertussis* (Bumba et al. 2016), whose secretion is also independent from the pmf. This seminal study also demonstrated a clear influence of the extracellular Ca^{2+} concentration on the secretion efficiency. Thus, the presence of Ca^{2+} accelerated CyaA secretion by generating intramolecular Brownian ratchets. In other words, this process is passive but involves ratcheted translocation events. Nevertheless, these data do not support the hypothesis that the binding of Ca^{2+} ions to the RTX domains represents a driving force of prime importance for secretion (Chenal et al. 2009; Thomas et al. 2014). This is in striking contrast to the secretion of HlyA (Lenders et al. 2016), where changes in the Ca^{2+} concentration in the medium or even the complete absence of Ca^{2+} did not influence the secretion rate, which remained at 16 amino acids per transporter per second. However, one has to stress that Ca^{2+} is crucial for the functionality of HlyA and that in the absence of Ca^{2+} the pore-forming activity was abolished (Lenders et al. 2016). These findings suggest a certain variety in the molecular mechanism of secretion amongst different T1SS, which may be influenced by the size of the substrate or the arrangement of the RTX domains. Thus, it is suggested that a Brownian ratchet mechanism combined with a pulling force is operational in CyaA (Bumba et al. 2016), but absent in HlyA (Lenders et al. 2016) and further experiments especially involving other T1SS are required to settle this issue.

STRUCTURAL INSIGHTS

Structural elucidation, together with functional characterization, is a powerful tool to investigate the transport mechanisms of membrane proteins. The very first structural information of a T1SS component was derived from two-dimensional crystals of the outer membrane protein TolC from *E. coli*. Even at a resolution of 12 Å, apart from the trimeric β -barrel nature, the presence of a novel periplasmic domain became evident (Koronakis et al. 1997). Only a few years later, solving the crystal structure of TolC at 2.1 Å revealed the novel fold of this funnel-like domain (Koronakis et al. 2000). This is composed out of 12 α -helices that protrude 100 Å into the periplasmic space. Including the

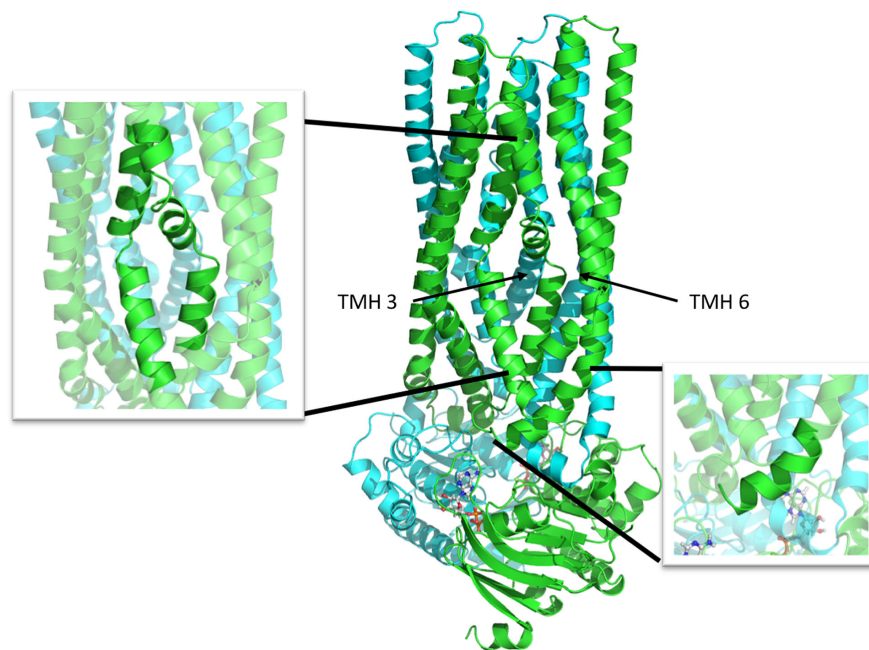


Figure 3. Cartoon representation of AaPrtd (Morgan, Acheson and Zimmer 2017). Monomers are shown in green and cyan. The bound nucleotides are shown in stick representation. The kinked helices 3 and 6 (TMH3 and TMH6) are highlighted for one monomer (left zoom-in). The right zoom-in highlights the coupling helix 1.

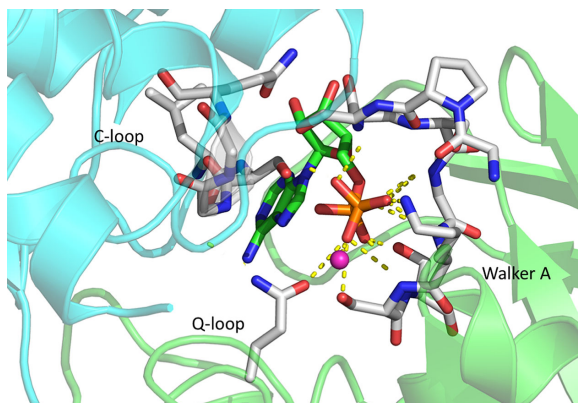


Figure 4. Zoom into the nucleotide-binding site of AaPrtd (Morgan, Acheson and Zimmer 2017) formed by both NBDs colored in green and cyan. ADP is shown in stick representation, the co-factor Mg^{2+} as magenta sphere. The conserved motifs interacting with the bound ADP molecule are labeled and highlighted in stick representation. Interactions are visualized by dashed, yellow lines.

12-stranded β -barrel (3 per monomer) the total length of the protein adds up to 140 Å. The structure was interpreted to represent a closed state as the inner diameter of the water-filled β -barrel of 20 Å narrows to only 3.9 Å at the periplasmic gate of TolC.

Based on this structural information, alanine mutations were placed within the region of the periplasmic gate in order to disrupt the closed state of TolC. Conductivity measurements in black lipid membranes led to a model, in which an ‘iris-like’ opening of the inner helices opens the periplasmic gate and therefore allows substrate translocation (Andersen et al. 2002a,b). Later on, this model was confirmed by structural information (Bavro et al. 2008; Pei et al. 2011).

Starting in 2003, a series of crystal structures paired with functional analysis on the NBD of the ABC transporter HlyB was

published (Benabdelhak et al. 2003, 2005; Schmitt et al. 2003; Zaitseva et al. 2005a, 2006). These studies offered valuable insights into the motor domain of a T1SS and its detailed molecular mechanism of ATP hydrolysis (Zaitseva et al. 2005b,c; Hanekop et al. 2006; Oswald, Holland and Schmitt 2006).

Additional insights into the structure of T1SS were obtained only recently, when the crystal structure of the ABC transporter of a putative T1SS from the hyperthermophilic Gram-negative bacterium *Aquifex aeolicus* (AaPrtd) was published. It shares a sequence identity of 40% with Prtd from *Dickeya dadantii*, but neither the substrate nor the MFP homolog of AaPrtd was identified (Morgan, Acheson and Zimmer 2017). The structure of the homodimer was determined at a resolution of 3.15 Å and reflected the ADP/ Mg^{2+} -bound state (Fig. 3). The presence of six transmembrane helices (TMH) per monomer and the canonical fold of the NBDs is typical for ABC transporters. Interestingly, the arrangement of the NBDs in the ADP-bound state seems to represent the occluded state (Morgan, Acheson and Zimmer 2017), which contradicts the accepted view that ATP binding induces dimerization of the two NBDs (Locher 2004, 2016; Oswald, Holland and Schmitt 2006).

The ADP molecule is coordinated by residues of the Walker A motif and the glutamine residue of the Q-loop, and also by the serine residue of the C-loop of the opposing NBD resulting in dimerization (Fig. 4). However, a similar architecture has been observed in the crystal structure of Sav1866 from *Staphylococcus aureus* (Dawson and Locher 2006) raising the question of how this architecture fits into the well-established view that only ATP induces formation of the NBD dimer.

The architecture of the TMHs of AaPrtd is distinct from that of other ABC export systems. Generally, ABC transporters contain two coupling helices (CH1 and CH2), which interact with the NBDs. In AaPrtd, the interaction conferred by CH1 is taken over by TMH2, which extends into a loop region that continues without any secondary structure into TMH3.

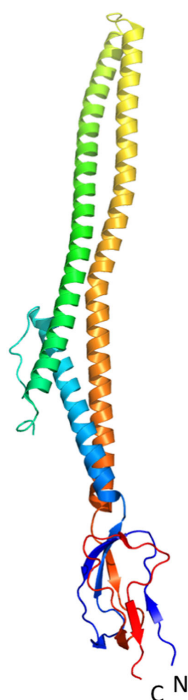


Figure 5. Crystal structure of a soluble fragment of HlyD from *E. coli* (Kim et al. 2016) that highlights the coiled-coil interaction of the helices. The lipoyl domain is colored in red and blue. N- and C-termini are indicated.

Furthermore, TMH3 and TMH6 are kinked at the approximate position of the lipid head groups, splitting TMH6 into two and TMH3 into three separate helices—a novel architecture—not been observed before (Morgan, Acheson and Zimmer 2017), neither in the bacteriocin transporter McjD (Choudhury et al. 2014) nor in the peptide transporter TAP 1/2 (Oldham, Grigorieff and Chen 2016). The kinks create a restriction within the putative substrate channel. The fact that residues lining this restriction are stabilized by interactions with conserved amino acids emphasizes their functional importance. Although the functionality of AaPrtD has not been demonstrated yet and the identity of the MFP and the transport substrate remain elusive, the structure provided the first glimpse of a T1SS ABC transporter and presents a platform to design new and exciting experiments.

Proteins from the family of MFPs are not only an indispensable part of T1SS but have also been intensively studied in the context of bacterial tripartite drug efflux pumps, such as the AcrB-AcrA-TolC system (Du et al. 2014) or the MacA-MacB-TolC system (Fitzpatrick et al. 2017). Until 2016, structural information was limited to MFPs involved in drug efflux (for a recent review, see Symmons, Marshall and Bavro 2015), while for T1SS MFPs only recently has some limited structural information become available (Kim et al. 2016). In 2016, the crystal structure of a soluble fragment of HlyD, comprising the α -helical domain and lipoyl domain, was published (Kim et al. 2016). However, the construct used for structure determination lacked not only the first 95 N-terminal amino acids, including the cytoplasmic domain (residues 1–59) and the single TMH of HlyD (residues 60–80), but also the last 106 C-terminal residues (residues 373–478), corresponding to the entire membrane proximal domain (Fig. 5).

In contrast to the majority of structurally described MFPs that contain two α -helices, the unusually long (115 Å) α -helical domain of HlyD is built out of three helices, of which helix 3 in-

teracts in an anti-parallel coiled-coil fashion with helix 1 and 2. Based on structural comparison with AcrA (Kim et al. 2010) and sequence conservation analysis, a model was proposed, where the α -helical tip located between helix 2 and 3 forms the interaction site with TolC (Kim et al. 2016). Only recently, in 2017, the crystal structure of the α -helical domain and the lipoyl domain of LipC, the MFP of the lipase secretion system from *Serratia marcescens*, was reported (Murata et al. 2017). Interestingly, the α -helical domain also contained three helices, which might be a common feature of T1SS MFPs.

The AcrA-AcrB-TolC (Du et al. 2014) and the MacA-MacB-TolC (Fitzpatrick et al. 2017) structures revealed a hexameric arrangement of the corresponding MFPs. Contradictory findings provided by cross-linking studies in *E. coli* suggest a trimeric state of HlyD as the functional unit (Thanabalu et al. 1998). Even though in principle a hexameric state seems more likely and is also supported by a model (Kim et al. 2016) based on the available crystal structure of MacA (Yum et al. 2009), the oligomeric state of T1SS MFPs is still under debate and the subject is still in need of further investigation.

BIOTECHNOLOGICAL APPLICATIONS

By achieving the secretion of fusion proteins in high amounts into the extracellular medium, large-scale purification can be significantly simplified, which reflects an attractive approach for biotechnological applications.

The relatively simple nature of T1SS and the C-terminal secretion signal raised interest in their use in biotechnological applications. Two main areas became the focus of intensive research: heterologous protein secretion, in general (Blight and Holland 1994) and antigen production for vaccination (Sebo et al. 1999; Spreng et al. 1999).

Here, we will only focus on the applicability of T1SS for the secretion of heterologous proteins. Based on the T1SS of TliA, a thermostable lipase from *P. fluorescens* (Park et al. 2012), a versatile secretion system was engineered (Ryu et al. 2015). The C-terminal secretion signal of TliA was fused either to GFP or alkaline phosphatase, and both proteins were secreted into the medium. The hydrophobic nature of the secretion signal even allowed subsequent purification via hydrophobic interaction chromatography. Secretion of fusion proteins was further enhanced by engineering a negative net charge by introducing aspartate clusters in the fusion proteins of interest (Byun et al. 2017). These constructs go hand in hand with the direction of the membrane potential, which is positive on the surface of bacteria. This favors the translocation of negatively charged proteins since the directionality of the potential acts electrophoretically (Cao, Kuhn and Dalbey 1995).

The other T1SS that has been extensively studied for the purpose of heterologous protein secretion is the HlyA T1SS from *E. coli*. With the identification of HlyA1 (Nicaud et al. 1986), a 23 kDa, C-terminal fragment of HlyA encouraging the secretion sequence and three of six RTX domains, research efforts were intensified to exploit the system for the secretion of heterologous proteins. The studies of Debarbieux and Wandersman (2001) and Bakkes et al. (2010) stressed the importance of folding rates in the successful secretion of fusion proteins. Remarkably, the natural folding rate of a protein fused to HlyA1 decreased dramatically, which increased the range of possible fusion partners and increased the yields of the proteins of interest (Bakkes et al. 2010).

Only recently, a new expression vector was established that impressively improved secretion efficiencies of various

fusion proteins (Khosa et al. 2018). Here, a 5'-untranslated region (UTR) was identified that increased the amount of secreted HlyA1 several-fold and that, most surprisingly, does contain nucleotides belonging to the coding sequence of HlyC. The region was mapped to an area enriched in adenosine- and uracil nucleotides, located ~36 base pairs upstream from the start codon of HlyA1. Nevertheless, the most striking result to emerge from this data in terms of biotechnological application is that besides boosting the secretion efficiency of HlyA1, the vector enabled the secretion of fast-folding fusion proteins that could not be secreted until then (Khosa et al. 2018). This is likely due to the fact that this 5'-UTR is recognized by ribosomal protein S1 and targeted to the ribosome for faster and more efficient translation. Certainly, these findings could open up new avenues for the exploitation of T1SS and highlights their potential biotechnological and pharmaceutical value. Furthermore, they emphasize the necessity not to limit biotechnological engineering to the mere coding sequence of a protein.

OUTLOOK

Since its discovery nearly 40 years ago, T1SS have been the subject of numerous fruitful studies and the basic outline of the secretion process is by now well established. However, much uncertainty still exists about the detailed mechanism of transport. Ongoing, exciting research should address, for example, additional structural information, the stoichiometry of the T1SS complexes, the nature of the secretion signal and biochemical insights into recognition and processing of the substrate.

ACKNOWLEDGEMENTS

We apologize to all our colleagues whose research could not be appropriately referenced due to space limitation. We thank all current and former members of the Institute of Biochemistry for support and valuable discussion. LS wishes to gratefully acknowledge his long term and highly fruitful collaboration with Prof. I. Barry Holland and his laboratory at the University of Orsay, France.

FUNDING

Research on the hemolysin T1SS is funded by the DFG through CRC 1208 (project A01 to LS) and the Manchot Graduate School Molecules of Infections III (to LS).

Conflict of interest. None declared.

REFERENCES

- Andersen C, Koronakis E, Bokma E et al. Transition to the open state of the TolC periplasmic tunnel entrance. *P Natl Acad Sci USA* 2002a;99:11103–8.
- Andersen C, Koronakis E, Hughes C et al. An aspartate ring at the TolC tunnel entrance determines ion selectivity and presents a target for blocking by large cations. *Mol Microbiol* 2002b;44:1131–9.
- Bakkes PJ, Jenewein S, Smits SH et al. The rate of folding dictates substrate secretion by the *Escherichia coli* hemolysin Type 1 secretion system. *J Biol Chem* 2010;285:40573–80.
- Balakrishnan L, Hughes C, Koronakis V. Substrate-triggered recruitment of the TolC channel-tunnel during type I export of hemolysin by *Escherichia coli*. *J Mol Biol* 2001;313:501–10.
- Baumann U, Wu S, Flaherty KM et al. Three-dimensional structure of the alkaline protease of *Pseudomonas aeruginosa*: a two-domain protein with a calcium binding parallel beta roll motif. *EMBO J* 1993;12:3357–64.
- Bavro VN, Pietras Z, Furnham N et al. Assembly and channel opening in a bacterial drug efflux machine. *Mol Cell* 2008;30:114–21.
- Benabdelhak H, Kiontke S, Horn C et al. A specific interaction between the NBD of the ABC-transporter HlyB and a C-terminal fragment of its transport substrate haemolysin A. *J Mol Biol* 2003;327:1169–79.
- Benabdelhak H, Schmitt L, Horn C et al. Positive cooperative activity and dimerization of the isolated ABC-ATPase domain of HlyB from *E. coli*. *Biochem J* 2005;368:1–7.
- Blight MA, Holland IB. Heterologous protein secretion and the versatile *Escherichia coli* haemolysin translocator. *Trends Biotechnol* 1994;12:450–5.
- Bumba L, Masin J, Macek P et al. Calcium-driven folding of RTX domain beta-Rolls ratchets translocation of RTX proteins through type I secretion ducts. *Mol Cell* 2016;62:47–62.
- Byun H, Park J, Kim SC et al. A lower isoelectric point increases signal sequence-mediated secretion of recombinant proteins through a bacterial ABC transporter. *J Biol Chem* 2017;292:19782–91.
- Cao G, Kuhn A, Dalbey RE. The translocation of negatively charged residues across the membrane is driven by the electrochemical potential: evidence for an electrophoresis-like membrane transfer mechanism. *EMBO J* 1995;14:866–75.
- Cescau S, Debarbieux L, Wandersman C. Probing the in vivo dynamics of type I protein secretion complex association through sensitivity to detergents. *J Bacteriol* 2007;189:1496–504.
- Chenal A, Guijarro JI, Raynal B et al. RTX calcium binding motifs are intrinsically disordered in the absence of calcium. *J Biol Chem* 2009;284:1781–9.
- Chervaux C, Sauvonnnet N, Le Clainche A et al. Secretion of active beta-lactamase to the medium mediated by the *Escherichia coli* haemolysin transport pathway. *Mol Gen Genet* 1995;249:237–45.
- Choudhury HG, Tong Z, Mathavan I et al. Structure of an antibacterial peptide ATP-binding cassette transporter in a novel outward occluded state. *P Natl Acad Sci USA* 2014;111:9145–50.
- Costa TR, Felisberto-Rodrigues C, Meir A et al. Secretion systems in Gram-negative bacteria: structural and mechanistic insights. *Nat Rev Microbiol* 2015;13:343–59.
- Davidson AL, Dassa E, Orelle C et al. Structure, function, and evolution of bacterial ATP-binding cassette systems. *Microbiol Mol Biol R* 2008;72:317–64, table of contents.
- Dawson RJ, Locher KP. Structure of a bacterial multidrug ABC transporter. *Nature* 2006;443:180–5.
- Debarbieux L, Wandersman C. Folded HasA inhibits its own secretion through its ABC exporter. *EMBO J* 2001;20:4657–63.
- Delepelaire P. Type I secretion in gram-negative bacteria. *BBA-Mol Cell Res* 2004;1694:149–61.
- Du D, Wang Z, James NR et al. Structure of the AcrAB-TolC multidrug efflux pump. *Nature* 2014;509:512–5.
- Economou A, Dalbey RE. Preface to special issue on protein trafficking and secretion in bacteria. *Biochim Biophys Acta* 2014;1843:1427.
- Evdokimov AG, Pokross ME, Egorov NS et al. Structural basis for the fast maturation of Arthropoda green fluorescent protein. *EMBO Rep* 2006;7:1006–12.

- Felmlee T, Pellett S, Welch RA. Nucleotide sequence of an *Escherichia coli* chromosomal hemolysin. *J Bacteriol* 1985;163:94–105.
- Felmlee T, Welch RA. Alterations of amino acid repeats in the *Escherichia coli* hemolysin affect cytolytic activity and secretion. *P Natl Acad Sci USA* 1988;85:5269–73.
- Fitzpatrick AWP, Llabres S, Neuberger A et al. Structure of the MacAB-TolC ABC-type tripartite multidrug efflux pump. *Nat Microbiol* 2017;2:17070.
- Gentschev I, Hess J, Goebel W. Change in the cellular localization of alkaline phosphatase by alteration of its carboxy-terminal sequence. *Mol Gen Genet* 1990;222:211–6.
- Gray L, Baker K, Kenny B et al. A novel C-terminal signal sequence targets *Escherichia coli* haemolysin directly to the medium. *J Cell Sci* 1989;11:45–57.
- Gray L, Mackman N, Nicaud JM et al. The carboxy-terminal region of haemolysin 2001 is required for secretion of the toxin from *Escherichia coli*. *Mol Gen Genet* 1986;205:127–33.
- Greene NP, Crow A, Hughes C et al. Structure of a bacterial toxin-activating acyltransferase. *P Natl Acad Sci USA* 2015;112:E3058–66.
- Griessl MH, Schmid B, Kassler K et al. Structural insight into the giant Ca^{2+} -binding adhesin SiiE: implications for the adhesion of salmonella enterica to polarized epithelial cells. *Structure* 2013;21:741–52.
- Hanekop N, Zaitseva J, Jenewein S et al. Molecular insights into the mechanism of ATP-hydrolysis by the NBD of the ABC-transporter HlyB. *FEBS Lett* 2006;580:1036–41.
- Havarstein LS, Diep DB, Nes IF. A family of bacteriocin ABC transporters carry out proteolytic processing of their substrates concomitant with export. *Mol Microbiol* 1995;16:229–40.
- Hinsa SM, Espinosa-Urgel M, Ramos JL et al. Transition from reversible to irreversible attachment during biofilm formation by *Pseudomonas fluorescens* WCS365 requires an ABC transporter and a large secreted protein. *Mol Microbiol* 2003;49:905–18.
- Holland IB, Peherstorfer S, Kanonenberg K et al. Type I protein secretion-deceptively simple yet with a wide range of mechanistic variability across the family. *EcoSal Plus* 2016;7:1–46.
- Hwang J, Zhong X, Tai PC. Interactions of dedicated export membrane proteins of the colicin V secretion system: CvaA, a member of the membrane fusion protein family, interacts with CvaB and TolC. *J Bacteriol* 1997;179:6264–70.
- Ishii S, Yano T, Ebihara A et al. Crystal structure of the peptidase domain of *Streptococcus* ComA, a Bifunctional ATP-binding cassette transporter involved in the quorum-sensing pathway. *J Biol Chem* 2010;285:10777–85.
- Issartel JP, Koronakis V, Hughes C. Activation of *Escherichia coli* prohaemolysin to the mature toxin by acyl carrier protein-dependent fatty acylation. *Nature* 1991;351:759–61.
- Izadi-Pruneyre N, Wolff N, Redeker V et al. NMR studies of the C-Terminal secretion signal of the haem-binding protein, HasA. *Eur J Biochem* 1999;261:562–8.
- Jardetzky O. Simple allosteric model for membrane pumps. *Nature* 1966;211:969–70.
- Jones HE, Holland IB, Baker HL et al. Slow changes in cytosolic free Ca^{2+} in *Escherichia coli* highlight two putative influx mechanisms in response to changes in extracellular calcium. *Cell Calcium* 1999;25:265–74.
- Kanonenberg K, Schwarz CK, Schmitt L. Type I secretion systems - a story of appendices. *Res Microbiol* 2013;164:596–604.
- Kenny B, Haigh R, Holland IB. Analysis of the haemolysin transport process through the secretion from *Escherichia coli* of PCM, CAT or beta-galactosidase fused to the Hly C-terminal signal domain. *Mol Microbiol* 1991;5:2557–68.
- Khosa S, Scholz R, Schwarz C et al. An A/U-Rich enhancer region is required for high-level protein secretion through the HlyA Type I secretion system. *Appl Environ Microb* 2018;84:e01163–17.
- Kim HM, Xu Y, Lee M et al. Functional relationships between the AcrA hairpin tip region and the TolC aperture tip region for the formation of the bacterial tripartite efflux pump AcrAB-TolC. *J Bacteriol* 2010;192:4498–503.
- Kim JS, Song S, Lee M et al. Crystal structure of a soluble fragment of the membrane fusion protein HlyD in a Type I secretion system of gram-negative bacteria. *Structure* 2016;24:477–85.
- Koronakis V, Eswaran J, Hughes C. Structure and function of TolC: the bacterial exit duct for proteins and drugs. *Annu Rev Biochem* 2004;73:467–89.
- Koronakis V, Hughes C, Koronakis E. Energetically distinct early and late stages of HlyB/HlyD-dependent secretion across both *Escherichia coli* membranes. *EMBO J* 1991;10:3263–72.
- Koronakis V, Koronakis E, Hughes C. Isolation and analysis of the C-terminal signal directing export of *Escherichia coli* hemolysin protein across both bacterial membranes. *EMBO J* 1989;8:595–605.
- Koronakis V, Li J, Koronakis E et al. Structure of TolC, the outer membrane component of the bacterial type I efflux system, derived from two-dimensional crystals. *Mol Microbiol* 1997;23:617–26.
- Koronakis V, Sharff A, Koronakis E et al. Crystal structure of the bacterial membrane protein TolC central to multidrug efflux and protein export. *Nature* 2000;405:914–9.
- Kuhnert P, Heyberger-Meyer B, Nicolet J et al. Characterization of PaxA and its operon: a cohemolytic RTX toxin determinant from pathogenic *Pasteurella aerogenes*. *Infect Immun* 2000;68:6–12.
- Lecher J, Schwarz CK, Stoldt M et al. An RTX transporter tethers its unfolded substrate during secretion via a unique N-terminal domain. *Structure* 2012;20:1778–87.
- Lenders MH, Beer T, Smits SH et al. In vivo quantification of the secretion rates of the hemolysin A Type I secretion system. *Sci Rep* 2016;6:33275.
- Lenders MH, Weidtkamp-Peters S, Kleinschrodt D et al. Directionality of substrate translocation of the hemolysin A Type I secretion system. *Sci Rep* 2015;5:12470.
- Letoffe S, Delepelaire P, Wandersman C. Protease secretion by *Erwinia chrysanthemi*: the specific secretion functions are analogous to those of *Escherichia coli* alpha-haemolysin. *EMBO J* 1990;9:1375–82.
- Letoffe S, Ghigo JM, Wandersman C. Secretion of the *Serratia marcescens* HasA protein by an ABC transporter. *J Bacteriol* 1994;176:5372–7.
- Linhartova I, Bumba L, Masin J et al. RTX proteins: a highly diverse family secreted by a common mechanism. *FEMS Microbiol Rev* 2010;34:1076–112.
- Locher KP. Structure and mechanism of ABC transporters. *Curr Opin Struct Biol* 2004;14:426–31.
- Locher KP. Mechanistic diversity in ATP-binding cassette (ABC) transporters. *Nat Struct Mol Biol* 2016;23:487–93.
- Mackman N, Baker K, Gray L et al. Release of a chimeric protein into the medium from *Escherichia coli* using the C-terminal secretion signal of haemolysin. *EMBO J* 1987;6:2835–41.
- Mackman N, Holland IB. Functional characterization of a cloned haemolysin determinant from *E. coli* of human origin, encoding information for the secretion of a 107K polypeptide. *Mol Gen Genet* 1984;196:129–34.

- Mackman N, Nicaud JM, Gray L et al. Genetical and functional organisation of the *Escherichia coli* haemolysin determinant 2001. *Mol Gen Genet* 1985a;201:282–8.
- Mackman N, Nicaud JM, Gray L et al. Identification of polypeptides required for the export of haemolysin 2001 from *E. coli*. *Mol Gen Genet* 1985b;201:529–36.
- Masure HR, Au DC, Gross MK et al. Secretion of the *Bordetella pertussis* adenylate cyclase from *Escherichia coli* containing the hemolysin operon. *Biochemistry* 1990;29:140–5.
- Meier R, Drepper T, Svensson V et al. A Calcium-gated lid and a large beta-Roll sandwich are revealed by the crystal structure of extracellular lipase from *Serratia marcescens*. *J Biol Chem* 2007;282:31477–83.
- Morgan JL, Acheson JF, Zimmer J. Structure of a Type-1 secretion system ABC transporter. *Structure* 2017;25:522–9.
- Murata D, Okano H, Angkawidjaja C et al. Structural basis for the *Serratia marcescens* lipase secretion system: Crystal structures of the membrane fusion protein and Nucleotide-Binding domain. *Biochemistry* 2017;56:6281–91.
- Nicaud JM, Mackman N, Gray L et al. Regulation of haemolysin synthesis in *E. coli* determined by HLY genes of human origin. *Mol Gen Genet* 1985;199:111–6.
- Nicaud JM, Mackman N, Gray L et al. The C-terminal, 23 kDa peptide of *E. coli* haemolysin 2001 contains all the information necessary for its secretion by the haemolysin (Hly) export machinery. *FEBS Lett* 1986;204:331–5.
- Noegel A, Rdest U, Springer W et al. Plasmid cistrons controlling synthesis and excretion of the exotoxin alpha-haemolysin of *Escherichia coli*. *Mol Gen Genet* 1979;175:343–50.
- Oldham ML, Grigorieff N, Chen J. Structure of the transporter associated with antigen processing trapped by herpes simplex virus. *Elife* 2016;5:e21289.
- Ostolaza H, Soloaga A, Goni FM. The binding of divalent cations to *Escherichia coli* alpha-haemolysin. *Eur J Biochem* 1995;228:39–44.
- Oswald C, Holland IB, Schmitt L. The motor domains of ABC-transporters. *N-S Arch Pharmacol* 2006;372:385–99.
- Park Y, Moon Y, Ryoo J et al. Identification of the minimal region in lipase ABC transporter recognition domain of *Pseudomonas fluorescens* for secretion and fluorescence of green fluorescent protein. *Microb Cell Fact* 2012;11:60.
- Pei XY, Hinchliffe P, Symmons MF et al. Structures of sequential open states in a symmetrical opening transition of the TolC exit duct. *P Natl Acad Sci USA* 2011;108:2112–7.
- Pimenta AL, Young J, Holland IB et al. Antibody analysis of the localisation, expression and stability of HlyD, the MFP component of the *E. coli* haemolysin translocator. *Mol Gen Genet* 1999;261:122–32.
- Reimann S, Poschmann G, Kanonenberg K et al. Interdomain regulation of the ATPase activity of the ABC transporter haemolysin B from *Escherichia coli*. *Biochem J* 2016;473:2471–83.
- Ryu J, Lee U, Park J et al. A vector system for ABC transporter-mediated secretion and purification of recombinant proteins in *pseudomonas* species. *Appl Environ Microb* 2015;81:1744–53.
- Sanchez-Magraner L, Viguera AR, Garcia-Pacios M et al. The Calcium-binding C-terminal domain of *Escherichia coli* alpha-hemolysin is a major determinant in the surface-active properties of the protein. *J Biol Chem* 2007;282:11827–35.
- Sapriel G, Wandersman C, Delepelaire P. The N terminus of the HasA protein and the SecB chaperone cooperate in the efficient targeting and secretion of HasA via the ATP-binding cassette transporter. *J Biol Chem* 2002;277:6726–32.
- Schiebel E, Driessen AJ, Hartl FU et al. Delta mu H⁺ and ATP function at different steps of the catalytic cycle of preprotein translocase. *Cell* 1991;64:927–39.
- Schmitt L, Benabdelhak H, Blight MA et al. Crystal structure of the nucleotide-binding domain of the ABC-transporter haemolysin B: identification of a variable region within ABC helical domains. *J Mol Biol* 2003;330:333–42.
- Sebo P, Ladant D. Repeat sequences in the *Bordetella pertussis* adenylate cyclase toxin can be recognized as alternative carboxy-proximal secretion signals by the *Escherichia coli* alpha-haemolysin translocator. *Mol Microbiol* 1993;9:999–1009.
- Sebo P, Moukrim Z, Kalhous M et al. In vivo induction of CTL responses by recombinant adenylate cyclase of *Bordetella Pertussis* carrying multiple copies of a viral CD8(+) T-cell epitope. *FEMS Immunol Med Mic* 1999;26:167–73.
- Sotomayor Perez AC, Karst JC, Davi M et al. Characterization of the regions involved in the calcium-induced folding of the intrinsically disordered RTX motifs from the *Bordetella pertussis* adenylate cyclase toxin. *J Mol Biol* 2015;397:534–49.
- Spreng S, Dietrich G, Goebel W et al. The *Escherichia coli* haemolysin secretion apparatus: a potential universal antigen delivery system in gram-negative bacterial vaccine carriers. *Mol Microbiol* 1999;31:1596–8.
- Stanley P, Hyland C, Koronakis V et al. An ordered reaction mechanism for bacterial toxin acylation by the specialized acyl-transferase HlyC: formation of a ternary complex with acyl-ACP and protoxin substrates. *Mol Microbiol* 1999;34:887–901.
- Stanley P, Koronakis V, Hughes C. Mutational analysis supports a role for multiple structural features in the C-terminal secretion signal of *Escherichia coli* haemolysin. *Mol Microbiol* 1991;5:2391–403.
- Stanley P, Packman LC, Koronakis V et al. Fatty acylation of two internal lysine residues required for the toxic activity of *Escherichia coli* hemolysin. *Science* 1994;266:1992–6.
- Symmons MF, Marshall RL, Bavro VN. Architecture and roles of periplasmic adaptor proteins in tripartite efflux assemblies. *Front Microbiol* 2015;6:513.
- Thanabalu T, Koronakis E, Hughes C et al. Substrate-induced assembly of a contiguous channel for protein export from *E. coli*: reversible bridging of an inner-membrane translocase to an outer membrane exit pore. *EMBO J* 1998;17:6487–96.
- Thomas S, Bakkes PJ, Smits SH et al. Equilibrium folding of pro-HlyA from *Escherichia coli* reveals a stable calcium ion dependent folding intermediate. *BBA-Proteins Proteom* 2014;1844:1500–10.
- Thomas S, Holland IB, Schmitt L. The Type 1 secretion pathway - The hemolysin system and beyond. *Biochim Biophys Acta* 2014;1843:1621–41.
- Thomas S, Smits SH, Schmitt L. A simple in vitro acylation assay based on optimized HlyA and HlyC purification. *Anal Biochem* 2014;464:17–23.
- Thompson SA, Sparling PF. The RTX cytotoxin-related FrpA protein of *Neisseria meningitidis* is secreted extracellularly by meningococci and by HlyBD⁺ *Escherichia coli*. *Infect Immun* 1993;61:2906–11.
- Uchida K, Mori H, Mizushima S. Stepwise movement of preproteins in the process of translocation across the cytoplasmic membrane of *Escherichia coli*. *J Biol Chem* 1995;270:30862–8.
- Wandersman C, Delepelaire P. TolC, an *Escherichia coli* outer membrane protein required for hemolysin secretion. *P Natl Acad Sci USA* 1990;87:4776–80.
- Wang RC, Seror SJ, Blight M et al. Analysis of the membrane organization of an *Escherichia coli* protein translocator, HlyB, a

- member of a large family of prokaryote and eukaryote surface transport proteins. *J Mol Biol* 1991;**217**:441–54.
- Welch RA. Pore-forming cytolysins of gram-negative bacteria. *Mol Microbiol* 1991;**5**:521–8.
- Wu KH, Tai PC. Cys 32 and His 105 are the critical residues for the calcium-dependent cysteine proteolytic activity of CvaB, an ATP-binding cassette transporter. *J Biol Chem* 2004;**279**:901–9.
- Young R, Bremer H. Polypeptide-chain-elongation rate in *Escherichia coli* B/r as a function of growth rate. *Biochem J* 1976;**160**:185–94.
- Yum S, Xu Y, Piao S et al. Crystal structure of the periplasmic component of a tripartite macrolide-specific efflux pump. *J Mol Biol* 2009;**387**:1286–97.
- Zaitseva J, Jenewein S, Jumpertz T et al. H662 is the linchpin of ATP hydrolysis in the nucleotide-binding domain of the ABC transporter HlyB. *EMBO J* 2005a;**24**:1901–10.
- Zaitseva J, Jenewein S, Oswald C et al. A molecular understanding of the catalytic cycle of the nucleotide-binding domain of the ABC transporter HlyB. *Biochem Soc Trans* 2005b:990–5.
- Zaitseva J, Jenewein S, Wiedenmann A et al. Functional characterization and ATP-induced dimerization of the isolated ABC-domain of the haemolysin B transporter. *Biochemistry* 2005c;**44**:9680–90.
- Zaitseva J, Oswald C, Jumpertz T et al. A structural analysis of asymmetry required for catalytic activity of an ABC-ATPase domain dimer. *EMBO J* 2006;**25**:3432–43.

3.4 Chapter IV – Functional Characterisation of Reconstituted HlyB

Title: **Functional Reconstitution of HlyB, a Type I Secretion ABC Transporter, in Saposin-A Lipoprotein Nanoparticles**

Authors: Kerstin Kanonenberg, Sander H. J. Smits, Lutz Schmitt

Published in: *submitted*

Impact Factor:

Own Work: 60 %
Overexpression and purification of HlyB and HlyA
Functional reconstitution of HlyB
Functional analyses, ATPase assays
Data analysis
Writing of the manuscript

Functional Reconstitution of HlyB, a Type I Secretion ABC Transporter, in Saposin-A Nanoparticles

Kerstin Kanonenberg, Sander HJ Smits, Lutz Schmitt*

Institute of Biochemistry, Heinrich Heine University, Duesseldorf, Germany

*Corresponding author: Institute of Biochemistry, Heinrich-Heine-University, Düsseldorf, Universitätsstr 1, 40225 Düsseldorf, Germany. Tel: +49-211-81-10773; Fax: +49-211-81-15310; E-mail: lutz.schmitt@hhu.de

Abstract

Type I secretion systems (T1SS) are ubiquitous transport machineries in Gram-negative bacteria. They comprise a relatively simple assembly of three membrane-localised proteins: an inner-membrane complex composed of an ABC transporter and a membrane fusion protein and a TolC-like outer membrane component. T1SS transport a wide variety of substrates with broad functional diversity.

The ABC transporter haemolysin B (HlyB), for example, is part of the haemolysin A-T1SS in *Escherichia coli*. In contrast to canonical ABC transporters, an accessory domain, a C39 peptidase-like domain (CLD), is located at the N-terminus of HlyB and is essential for secretion.

In this study, we have established an optimised purification protocol for HlyB and the subsequent reconstitution employing the saposin-A nanoparticle system. We point out the negative influence of free detergent on the basal ATPase activity of HlyB, studied the influence of a lysolipid or lipid matrix on the activity and present functional studies with the full-length substrate proHlyA in its folded and unfolded states, which both have modulating effects on the ATPase activity.

Introduction

Secretion systems are essential means for prokaryotic organisms to deliver a large set of nascent proteins, including virulence factors, from the cytoplasm to the extracellular environment. In Gram-negative bacteria, secretion of molecules needs to be achieved across both membranes. Thus, many secretory pathways have evolved that export their substrate, in some cases with a periplasmic intermediate while some mediate the export in one step, across both membranes. The prototype type 1 secretion system (T1SS), however, has no such intermediate (1).

One of the most prominent members of the T1SS is the haemolysin A (HlyA) secretion system from *Escherichia coli* (*E. coli*) (2). The substrate, the haemolytically active exotoxin HlyA, is secreted unfolded and in one step, without periplasmic intermediate, across both membranes (3-5). T1SS generally comprise a relatively simple assembly of an ABC transporter and a membrane fusion protein (MFP) in the inner membrane, and a TolC-like outer membrane protein. In case of the HlyA-T1SS, these are haemolysin B (HlyB), haemolysin D (HlyD) and TolC, respectively (6,7). While HlyB and HlyD form a complex in the inner membrane, TolC, which is also involved in many other export processes, is only recruited upon substrate recognition in the cytosol (8).

The substrate HlyA contains a secretion signal that has been located to the last 50-60 C-terminal amino acids (4,9,10). Additionally, HlyA belongs to the family of RTX-proteins (“repeats in toxin”), whose characteristics is the presence of a variable number of nonapeptide repeats (RTX-domains) that bind calcium ions and trigger folding of the protein in the extracellular space (5,11,12). Two lysine-acylations activate the toxin prior to secretion (43). Secretion takes place C-terminus first (5) leaving open for debate how substrates of several 100 kDa in size are kept unfolded in the cytosol until secretion is initiated. The secretion rate was determined to be 16 amino acids per second per transporter (13).

The ABC transporter HlyB fuels the secretion process by ATP-hydrolysis. Interaction between the nucleotide binding domain (NBD) of HlyB and the substrate HlyA has been demonstrated, suggesting an additional function in addition to providing energy for export

(14). The detailed mechanism of ATP-hydrolysis of the isolated HlyB-NBD has been investigated in great detail (15-18). More importantly, HlyB contains an additional cytosolic domain at its N-terminus that is essential for secretion (19,20). A similar N-terminal domain is known for bacteriocin exporters, which contain a C39-peptidase domain that cleaves the signal peptide of the substrate prior to export (21). Despite its identical tertiary structure compared to C39 peptidase domains, the additional domain of HlyB does not catalyse a proteolytic reaction. This is due to a corrupted and inactivated (mutated/degenerated) catalytic triad (20,22). Subsequently, the term C39-peptidase-like domain (CLD) was coined (20). The unfolded substrate interacts with the CLD, independently of its C-terminal secretion signal (20). Thus, receptor or chaperone-like activity has been proposed for the CLD, but its precise function and mechanism are not yet understood.

The bottleneck in studying membrane proteins *in vitro* is often related to the requirement to purify membrane proteins to high purity and homogeneity. When using detergents for their extraction from membranes, membrane proteins are pulled out of their natural environment. Furthermore, the presence of monomeric detergent can result in binding to non-native locations on the membrane protein, for example between helices or in hydrophilic areas (23-25). This may have a negative effect on the activity of a membrane protein in detergent solution (26). To overcome this alter issue, membrane proteins can be reconstituted into artificial lipid bilayer systems, such as liposomes or nanodiscs. Reconstitution into liposomes results in a two-compartment system that is a great advantage in studying transport processes (27). A 13-fold higher ATPase activity of proteoliposome-reconstituted ABC transporter BmrA has been reported in comparison to detergent-solubilised preparations (28-30). Liposomes can be prepared with defined lipid compositions, which also makes them a suitable tool for studying the influence of lipids on a membrane protein. However, due to their large size, liposomes are not suitable for downstream purification processes such as size exclusion chromatography (SEC).

The nanodisc system offers the advantage that the membrane protein is incorporated into a small yet water-soluble particle, where the lipid composition may be tailored (31-33). Nanodiscs of well-defined dimensions have facilitated the handling of reconstituted protein and have been shown to be a suitable tool for diverse applications in biophysics or structural biology (33). A very recent, additional development is a saposin-A derived lipoprotein

nanoparticle system (Figure 1) (34). *In vivo*, proteins belonging to the saposin-family modulate the lipid composition of lysosome membranes (35,36). Their lipid binding properties, paired with their composition out of amphipathic helices containing six disulphide bridges, result in the formation of very stable and uniform nanoparticles (34). Surprisingly, even in the presence of detergent saposin-A forms dimeric structures incorporating a small bilayer of detergent molecules (37). Purified saposin-A can be used as carriers of small lipid bilayers with embedded membrane proteins (34). An advantage is the easy purification of saposin-A, the rapid process of reconstitution, and the very practicable separation of “full” and “empty” nanoparticles (34,38-40). The focus of studies applying the saposin-A system so far has been on structural biology, showing its suitability for cryo EM (38), solution NMR (39), or SAXS (40), while functional studies on saposin-A reconstituted proteins are lacking.

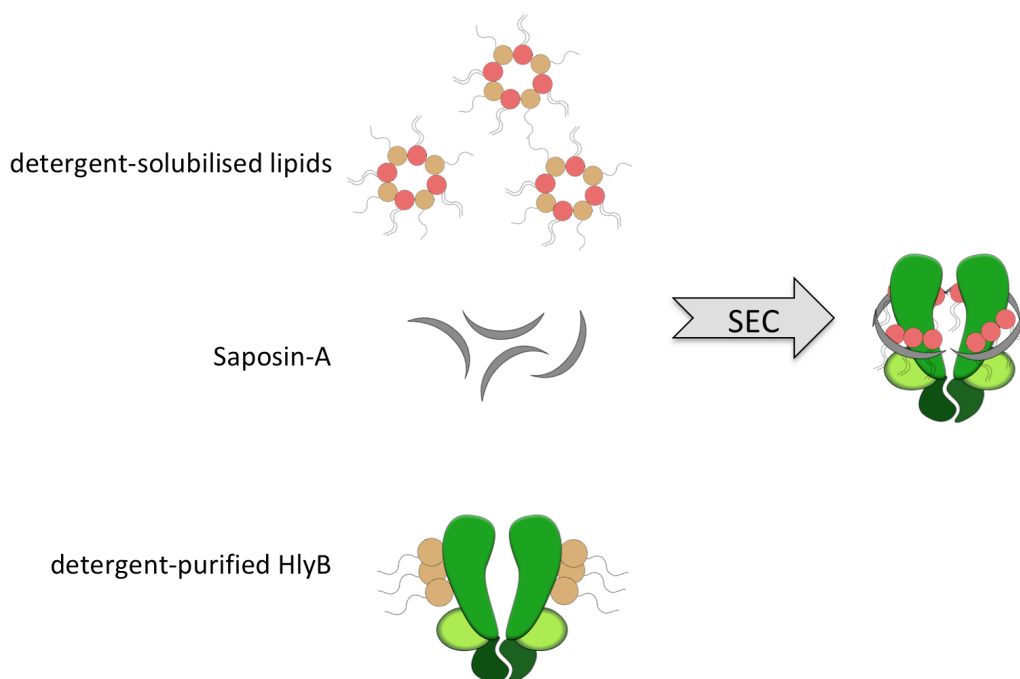


Figure 1: Visualisation of membrane protein reconstitution applying the saposin-A lipoprotein nanoparticle system (34).

Here, we report the functional reconstitution of the *E. coli* ABC transporter HlyB from the HlyA-T1SS into saposin-based nanoparticles. We show that the system is suitable for the functional characterisation of the ABC transporter. Equally important, reconstitution in nanoparticles was achieved not only in the presence of lipids, but for the first time also in the presence of detergent-like lysolipids. The functional data of reconstituted HlyB revealed important differences from those obtained for detergent-solubilised HlyB, especially in

comparison to a truncated mutant lacking the CLD (41). By characterising the T1SS-ABC transporter *in vitro*, we are aiming at understanding the function of the different domains during the secretion process.

Experimental Procedures

Cloning of the plasmid pBADHisHlyB-D551A

The plasmid pBADHisHlyBD551A was created by introducing a point mutation into pBADHisHlyB (41). For this, the plasmid was amplified with Pfu-polymerase (NEB) using the primers GGTGTGTTGCAGGCAAATGTGCTGCTTAATCG (forward) and CGATTAAGCAGCACATTTGCCTGCAACACAACC (reverse). Methylated bacterial DNA was digested using DpnI (NEB) and the PCR product was used to transform *E. coli* XL-1 blue cells. The introduction of the point mutation was confirmed by sequencing.

Construction of the expression strain for HlyB by genomic modification

To delete *acrAB* from *E. coli* C41(DE3) $\Delta ompF$ strain, the lambda-red recombinase system was employed, following published protocols (42). Briefly, the plasmid pKD4 carrying a kanamycin-resistance cassette was amplified using the overhang primers ACTTTTGACCATTGACCAATTTGAAATCGGACACTCGAGGTTTACATATGAGTAG GCTGGAGCTGCTTC (forward) and TTACGCGGCCTTAGTGATTACACGTTGTATCAATGATGATCGACAGTATGATGGG AATTAGCCATGGTCC (reverse). The insertion of the kanamycin-resistance cassette using the plasmid pKD46 and its deletion with plasmid pCP20 were confirmed by PCR and subsequent sequencing using the primers CACATCGAGGATGTGTTG (forward) and GCCCTCTCGTTTGTAG (reverse).

Overexpression and purification of HlyB

E. coli C41(DE3) $\Delta ompF\Delta acrAB$ cells were transformed with pBADHisHlyB, pBADHisHlyB Δ CLD, pBADHisHlyB-H622A (41) or pBADHisHlyB-D551A plasmids and selected on LB-agar plates containing 100 μ g/mL ampicillin. All HlyB variants were overexpressed, purified and reconstituted using the same protocols, described below. An overnight culture with 2YT medium and 100 μ g/mL ampicillin was inoculated with a single colony and incubated at 200 rpm, 37 °C for 15 h. The main culture was grown in 5L-baffled flasks, containing 1 L of 2YT medium with 100 μ g/mL ampicillin. Expression cultures were inoculated to OD₆₀₀ of 0.1 and grown at 37 °C, 200 rpm to OD₆₀₀ of 2.5. Protein expression was induced by adding arabinose to a final concentration of 10 mM. Incubation was continued for 3 h and cells were harvested by centrifugation.

Membranes were isolated by a two-step centrifugation procedure. First, cells were resuspended in buffer P (50 mM NaH₂PO₄ pH 8, 300 mM NaCl) and lysed by passing three times through a cell disruptor (Microfluidizer M-110L, Microfluidics) at 1.5 kbar. Undisrupted cells and cell debris were removed by low-spin centrifugation at 18,000 xg for 30 min at 4 °C. Membranes were collected from the supernatant by ultra-centrifugation at 150,000 xg for 90 min at 4 °C. Membrane pellets were homogenised in buffer P supplemented with 10 % (v/v) glycerol and stored at -80 °C.

For the purification of HlyB, membranes of 0.5 L cell culture were diluted with buffer P to a protein concentration of 10 mg/mL and solubilised with 0.5 % (w/v) fos-choline 14 for 1 h at 8 °C. Solubilised membranes were filtered (0.45 µm), diluted two-fold using buffer P supplemented with 2 mM imidazole and loaded on Zn²⁺-charged immobilised metal-ion affinity chromatography (IMAC) column (5 mL HiTrap Chelating HP, GE Healthcare). The column was washed with 8 mL of buffer P including 0.015 % (w/v) DDM and 2 mM imidazole. Non-specifically bound proteins were removed by washing with 18 mL buffer P supplemented with 0.015 % (w/v) DDM and 40 mM imidazole. HlyB was eluted with buffer P containing 0.015 % (w/v) DDM and 25 mM EDTA.

Expression and purification of proHlyA from inclusion bodies

E. coli BL21(DE3) cells were transformed with pSU-HlyA (43) and exposed on selective LB-agar plates containing 100 µg/mL ampicillin. An overnight culture with 2YT medium and 100 µg/mL ampicillin was inoculated with a single colony and incubated for 15 h at 200 rpm, 37 °C. The main cultures were grown in 5 L-baffled flasks, containing 1 L of selective 2YT medium with 100 µg/mL ampicillin. Main cultures were inoculated from the overnight culture to OD₆₀₀ of 0.1 and grown at 37 °C, 200 rpm to OD₆₀₀ of 0.6. ProHlyA expression was induced by adding IPTG to a final concentration of 1 mM. Incubation was continued for 4 h and cells were harvested by centrifugation.

For proHlyA purification, the cells were resuspended in buffer A (50 mM HEPES pH 7.4, 150 mM NaCl, 10 % (w/v) glycerol, 0.05 % (w/v) NaN₃) and lysed by passing three times through the cell disruptor at 1.5 kbar. Inclusion bodies were collected by centrifugation at 18,000 xg for 30 min. The pellets were washed and centrifuged successively in (1) buffer W1 (50 mM HEPES, pH 7.4, 50 mM EDTA, 1 % (w/v) Triton X-100, 0.05 % (w/v) NaN₃) and (2) buffer W2 (50 mM HEPES, pH 7.4, 1 mM EDTA, 1 M NaCl, 0.05 % (w/v) NaN₃). The pellet was solubilised overnight in buffer S (20 mM HEPES pH 7.4, 20 mM NaCl, 6 M urea).

Insoluble material was removed by ultra-centrifugation (150,000 xg, 30 min, 4°C) and the urea-solubilised inclusion bodies were stored at -80°C.

Expression and purification of saposin-A

Overexpression and purification of saposin-A was performed following the described protocol (34) with minor modifications. Briefly, *E. coli* Rosetta-gami-2 (DE3) cells (Novagen) were transformed with pSapA plasmid (34) and grown on selective LB-agar plates containing 25 µg/mL chloramphenicol and 30 µg/mL kanamycin. An overnight culture of 2YT medium supplemented with 25 µg/mL chloramphenicol and 30 µg/mL kanamycin was inoculated with a single colony and shaken at 200 rpm, 37 °C for 20 h. Main cultures of 1 L 2YT medium in 5 L-baffled flasks, supplemented with 30 µg/mL kanamycin, were inoculated to OD₆₀₀ of 0.1 using the overnight culture. Cells were grown to OD₆₀₀ of 1 (approximately 7 h) at 200 rpm, 37 °C. Protein expression was induced by adding IPTG to a final concentration of 0.7 mM and continued for 3 h at 200 rpm, 37 °C.

For the purification of saposin-A, cells were resuspended in buffer A (20 mM HEPES, pH 7.5, 150 mM NaCl, 20 mM imidazole) and lysed by passing three times through the cell disruptor at 1.5 kbar. Lysed cells were centrifuged at 26,000 xg for 30 min and the supernatant was heated to 85 °C for 10 min, followed by a second centrifugation step at 26,000 xg for 30 min. The supernatant was applied to a Ni²⁺-charged IMAC column (5 mL HiTrap Chelating HP, GE Healthcare). The column was washed with 15 column volumes (CV) using buffer A, followed by 10 CV buffer A supplemented with 40 mM imidazole. Elution was performed with buffer A containing 400 mM imidazole. The eluted protein was concentrated to a final volume of 5 mL (Amicon Ultra-15, MWCO = 10,000 Da, Merck/Millipore), centrifuged at 100,000 xg for 10 min and subjected to SEC on HiLoad 16/600 Superdex 200 pg column (GE Healthcare) in buffer B (20 mM HEPES pH 7.5, 150 mM NaCl). The purified saposin-A was stored at a concentration of 1.2 mg/mL at -20 °C.

Reconstitution of HlyB into saposin-A nanoparticles

Reconstitution procedures were adapted from (34). Either 60 µL of 5 mg/mL DOPC in 100 mM HEPES, pH 8, 250 mM NaCl, 1 % (w/v) DDM or 40 µL of 5 mg/mL LPC in 100 mM HEPES, pH 8, 250 mM NaCl, 1 % (w/v) DDM were heated to 30 °C for 5 min. 60 µL IMAC-purified HlyB (1.4 – 1.6 mg/mL) was added (protein : lipid ratio = 1 : 390) and incubated at

30 °C for 5 min. 60 µL saposin-A (1.2 mg/mL) were added, followed by another incubation at 30 °C for 5 min. After adding 500 µL buffer H (100 mM HEPES, pH 8, 250 mM NaCl), samples were incubated at room/ambient temperature for 5 min. 5 aliquots were pooled and concentrated to a final volume of 1 mL (Amicon Ultra-15, MWCO = 100,000 Da, Merck/Millipore). Protein was subjected to SEC in buffer H on a Superose 6 Increase 10/300GL column (GE Healthcare).

ATPase assays

Determination of the amount of free phosphate was carried out to quantify the hydrolytic activity of HlyB (44). For basal ATPase activity, 15 µL of HlyB in buffer H were supplemented with 5 µL of 50 mM MgCl₂. Control reactions did not contain MgCl₂. Reactions were started by adding ATP to final concentrations ranging from 0 to 8 mM (total reaction volume 25 µL), and incubated for 40 min at 25°C.

To measure the modulation of the ATPase activity by substrate, folded and unfolded proHlyA was added to the assay in final concentrations ranging from 0 – 10 µM. Folded proHlyA was prepared in buffer H supplemented with 10 mM CaCl₂, unfolded proHlyA in buffer H supplemented with 4 M urea and 10 mM EDTA. Buffers were exchanged to buffer H supplemented with 2 mM CaCl₂ or 4 M urea, respectively.

10 µL of HlyB were supplemented with 5 µL of 50 mM MgCl₂ and 5 µL of proHlyA. Reactions were started by adding 5 µL of 20 mM ATP and incubated for 30 min (stimulatory effects) or 60 min (inhibitory effects) at 25 °C.

The effects of free LPC on HlyB ATPase activity were determined by adding 5 µL of LPC to the assay in final concentrations ranging from 0.1 µM to 1 mM. Assays were conducted as described for proHlyA.

Reactions were stopped by transferring the reaction volume (25 µL) into 175 µL 10 mM H₂SO₄. The free phosphate concentration was determined by adding 50 µL of staining solution (0.096 % (w/v) malachite green, 1.48 % (w/v) ammonium molybdate, 0.173 % (w/v) Tween-20 in 2.36 M H₂SO₄) and incubated for 8 min at room/ambient temperature. Quantification was performed by measuring the absorbance at 595 nm (iMark Microplate Reader, Bio Rad). Data points were fitted using GraphPad Prism7 Software (GraphPad).

Determination of kinetic parameters of the ATPase activity

The experimental data sets were fitted to one of the following equations:

Equation 1, the Hill equation, is:

$$v = \frac{v_{max}[S]^h}{K_{0.5}^h + [S]^h}$$

In equation 1, v corresponds to the enzyme velocity as a function of the substrate concentration $[S]$, v_{max} is the maximum enzyme velocity, h is the Hill coefficient, $K_{0.5}$ is the substrate concentration at half-maximum enzyme velocity.

Equation 2, the Michaelis-Menten equation, with substrate inhibition is:

$$v = \frac{v_{max}[S]}{K_m + [S](1 + \frac{[S]}{K_i})}$$

Here, K_m is the Michaelis-Menten constant and K_i the dissociation constant for substrate binding to the enzyme. It is assumed that two substrate molecules can bind to the enzyme, which results in a stimulatory or inhibitory effect, respectively.

Equation 3, which assumes two independent binding sites, is:

$$v = \frac{K_1 K_2 v_0 + K_2 v_{max} + v_{min} [S]^2}{K_1 K_2 + K_2 [S] + [S]^2}$$

Here, v_{min} is the minimum enzyme velocity, K_1 the substrate concentration at half-maximum stimulation, K_2 the substrate concentration at half-maximum inhibition. Equation 3 was adapted from (41).

Results

Expression and purification of the ABC transporter HlyB using a new expression strain, *E. coli* C41(DE3) $\Delta ompF\Delta acrAB$

The deletion of *ompF* and *acrAB* from the genome of *E. coli* C41(DE3) was found to substantially increase the yield and the purity of isolated recombinant HlyB (Figure 2).

The use of fos-choline 14 (FC-14) as a suitable detergent for the solubilisation of HlyB was adopted from a previous study (41). The detergent was exchanged to 0.015 % (w/v) DDM or 0.003 % (w/v) LMNG while HlyB was immobilised on the IMAC column. Both DDM and LMNG yielded approximately 6 mg of pure and homogeneous HlyB per litre of bacterial cell culture (Figure 2). The homogeneity after purification was assessed by SEC. The elution profiles were comparable for DDM and LMNG-purified protein (Figure 2B). Equivalent amounts of protein were obtained for HlyB, HlyB Δ CLD, HlyB-H622A and HlyB-D551A.

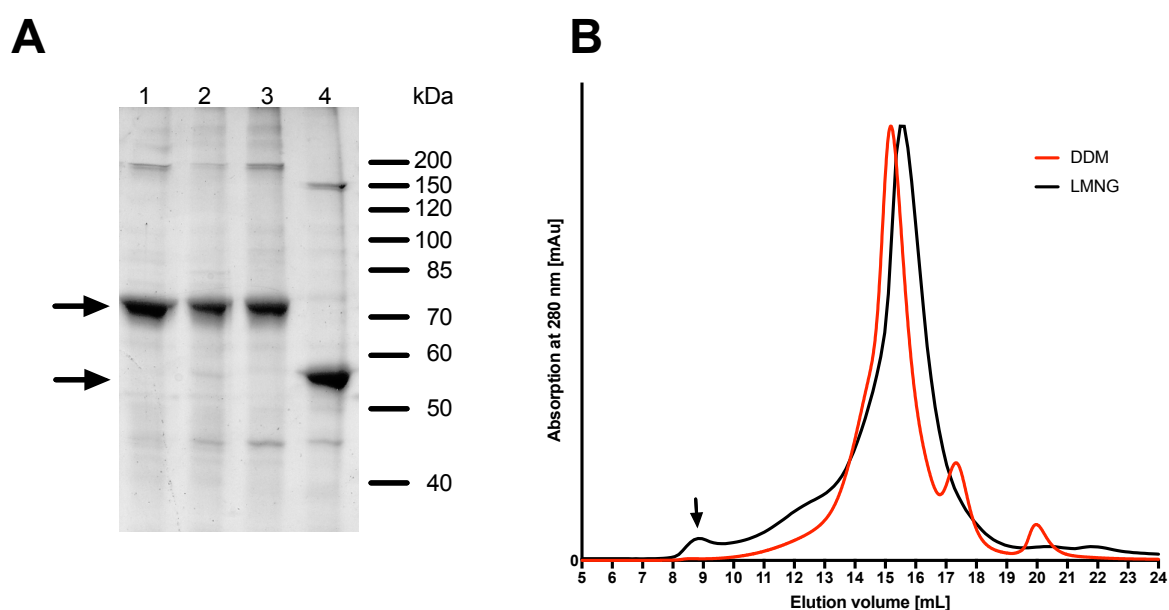


Figure 2: Purification of HlyB. (A) SDS-PAGE of purified HlyB (1), HlyB-H622A (2), HlyB-D551A (3) and HlyB Δ CLD (4), stained with CBB. The arrows indicate the monomers of HlyB, HlyB H622A and HlyB D551A (molecular weight 82 kDa, runs at ~ 70 kDa) and HlyB Δ CLD (65 kDa, runs at 55 kDa) (45). (B) SEC of purified HlyB (Superose 6 10/300GL Increase column) in LMNG (black line) and DDM (red line). The arrow indicates the void volume of the column.

Reconstitution of HlyB into saposin-A lipoprotein-nanoparticles

In the crystal structure of saposin-A dimer a bilayer-like assembly of detergent molecules trapped between the protein protomers was observed (37). To assess the influence of the

density of the lipid bilayer around HlyB on its functional properties we prepared saposin-A nanoparticles using DOPC (two fatty acid tails, high-density lipid bilayer with low curvature) or LPC (one fatty acid tail, low-density lipid bilayer with high positive curvature) (46,47).

While general guidelines for saposin-A nanoparticle reconstitution have been previously described (34), we set out to optimise the ratio HlyB : saposin-A : (lyso)lipid for achieving high yields of reconstituted HlyB.

To optimise the reconstitution using DOPC, the amount of HlyB was kept constant and the amounts of lipids and saposin-A were varied, and the reconstituted products were analysed by SEC (Figure 3A). The optimum HlyB : saposin-A : DOPC ratio was found to be 1 : 8 : 390. Increasing amounts of DOPC resulted in the formation of larger species of particles.

The reconstitution of HlyB into saposin-A nanoparticles using LPC was also optimised (Figure 3B). Strikingly, the optimum HlyB : saposin-A : LPC molar ratio was also 1 : 8 : 390 (Figure 3B), suggesting that the lipid packing within the nanoparticles was largely determined by head groups, and so was comparable for DOPC and LPC. Too much saposin-A resulted in non-separated peaks on SEC, while too low amounts provoked heterogeneity of reconstituted HlyB. Furthermore, for successful reconstitution the choice of detergent during the purification of HlyB also needed to be optimised.

While the optimum ratio resulted in a homogeneous preparation of DDM-purified HlyB with two distinctively separated peaks of reconstituted HlyB and “empty” saposin-A particles (Figure 3B and 3C), the use of LMNG-purified HlyB resulted in less homogeneous preparations of HlyB-containing particles (Figure 3B), even though the purified protein was equally homogeneous in both detergents (Figure 2B).

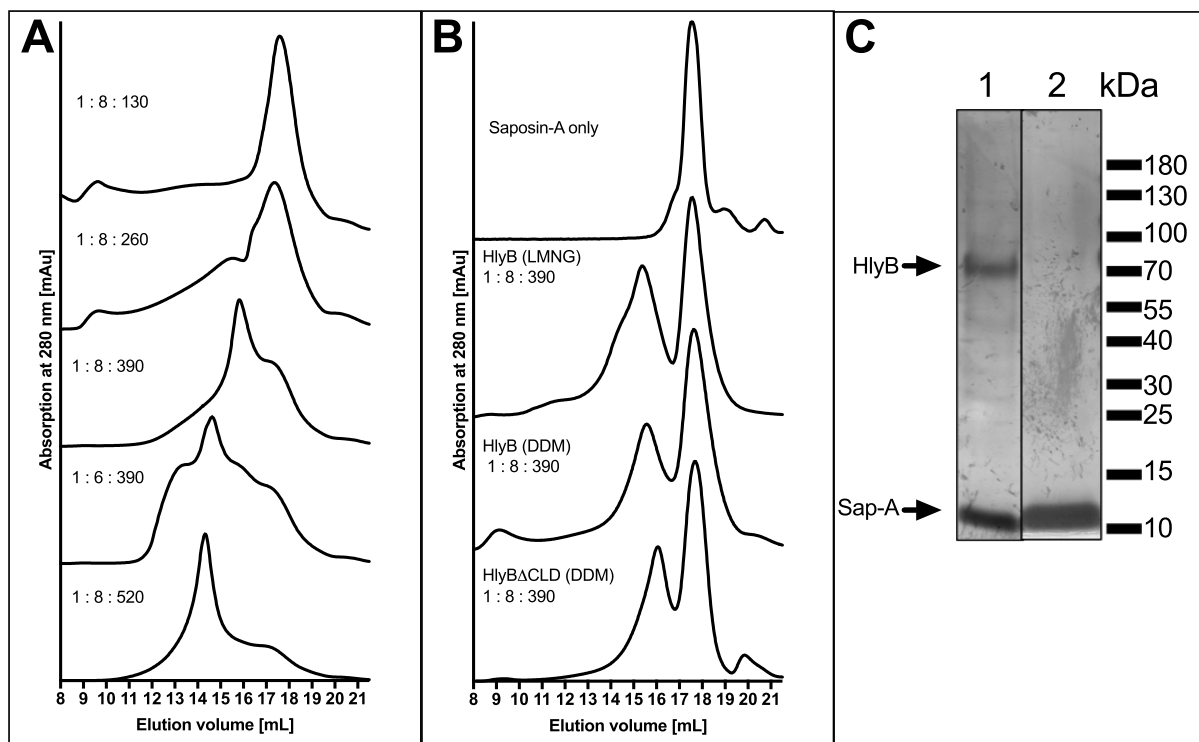


Figure 3: Reconstitution of HlyB and HlyB Δ CLD into saposin lipoprotein nanoparticles. The optimum molar ratio was identified to be 1 : 8 : 390 (HlyB : saposin-A : lipids) for DOPC as well as for LPC, which results in homogeneous peaks. (A) Optimisation of the reconstitution into DOPC-saposin-A nanoparticles. Ratios were molar ratios of HlyB : saposin-A : DOPC. (B) Optimisation of the reconstitution of HlyB into LPC-saposin-A nanoparticles. The use of LMNG-purified HlyB resulted in preparations of lower homogeneity. (C) SDS-PAGE of reconstituted HlyB (DDM) into LPC-particles after SEC on a 3-20% gradient silver-stained gel. Bands were visible for HlyB at 70 kDa and saposin-A at 10 kDa (both indicated by arrows). (1) Sample taken from peak at elution volume 15.5 mL (reconstituted HlyB), (2) sample taken from peak at elution volume 17.8 mL (“empty” saposin-A particles).

The reconstitutions of HlyB Δ CLD, HlyB-D551A and HlyB-H622A produced comparable results.

Basal ATPase activity of reconstituted HlyB

The basal ATPase activity of reconstituted HlyB was measured by quantifying the release of inorganic phosphate from the hydrolysis of ATP (44). The ATP concentration was varied from 0 to 8 mM, while the concentrations of HlyB and MgCl₂ were kept constant. The ATPase activities of HlyB, HlyB Δ CLD, HlyB-D551A and HlyB-H622A were assessed in LPC-saposin-A nanoparticles. The results are summarised in Figure 4A (solid lines).

HlyB-H622A, a HlyB mutant defective in ATP hydrolysis (17,41), showed no ATP hydrolysis under the experimental conditions and served as a negative control.

The data for HlyB and HlyB Δ CLD displayed a non-linear behaviour and were fitted using the Hill-equation. The data showed a clear sigmoidal fit and, within the standard errors, the ATPase kinetic parameters of both proteins, HlyB and HlyB Δ CLD, were equal, with Hill coefficients of 2.1 ± 0.6 and 2.5 ± 0.8 , respectively. The v_{\max} and $K_{0.5}$ values for HlyB and HlyB Δ CLD were $70 \pm 7 \text{ nmol mg}^{-1} \text{ min}^{-1}$, $1.6 \pm 0.3 \text{ mM}$ (HlyB), and $79 \pm 8 \text{ nmol mg}^{-1} \text{ min}^{-1}$, $1.8 \pm 0.3 \text{ mM}$ (HlyB Δ CLD), respectively. The kinetic parameters of the basal ATPase activity are summarised in table 1.

The aspartate residue 551 was previously suggested to play an important role in the communication between the two ATP-binding domains and the asymmetric phosphate release. This resulted in a reduced ATPase activity and loss of cooperativity, as evident from studies of the isolated NBD (48). We analysed this mutation in the context of the full-length ABC transporter and observed that HlyB-D551A showed no hydrolytic activity under the experimental conditions (Figure 4A).

Next, we measured the basal ATPase activity of HlyB and HlyB Δ CLD in DOPC-saposin-A particles (Figure 4A, dashed lines). The kinetic parameters were equal within the standard errors to those in LPC-saposin-A particles and are summarised in table 1.

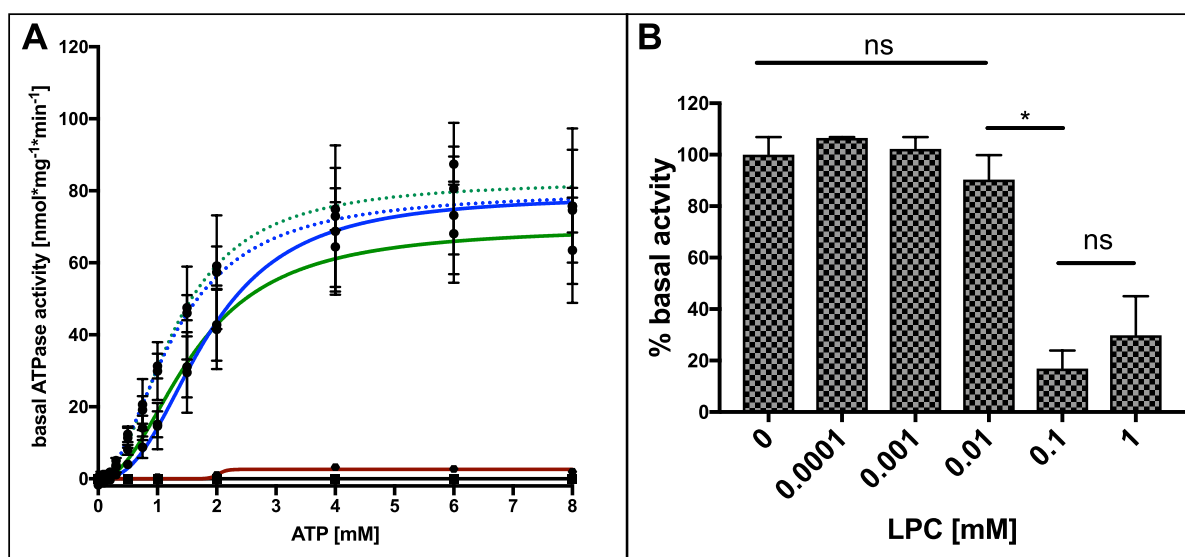


Figure 4: (A) Kinetic measurements of the basal ATPase activity of HlyB in LPC (green line) and DOPC (green dashed line), HlyB Δ CLD in LPC (blue solid line) and DOPC (blue dashed line), HlyB D551A in LPC (red solid line) and HlyB H622A in LPC (black line). Error bars represent SEM of a minimum of two replicates. (B) Influence of free LPC on the basal ATPase activity of DOPC-reconstituted HlyB. Error bars represent SEM of minimum three replicates. (ns: not significant, *: $p < 0.05$)

Table 1: Summary of the kinetic parameters of HlyB and HlyB Δ CLD \pm SEM of minimum two replicates.

	$K_{0.5}$ [mM]	v_{\max} [nmol min ⁻¹ mg ⁻¹]	h	k_{cat} [min ⁻¹]
HlyB (LPC)	1.6 \pm 0.3	70.0 \pm 6.6	2.1 \pm 0.6	5.8 \pm 0.5
HlyB (DOPC)	1.3 \pm 0.1	82.9 \pm 1.9	2.1 \pm 0.2	6.8 \pm 0.2
HlyB Δ CLD (LPC)	1.8 \pm 0.3	78.7 \pm 7.6	2.5 \pm 0.8	5.3 \pm 0.5
HlyB Δ CLD (DOPC)	1.3 \pm 0.1	79.9 \pm 4.3	1.9 \pm 0.3	5.4 \pm 0.3

We assessed the impact of free detergent on the activity of HlyB by adding increasing concentrations of LPC to the assay using DOPC-reconstituted protein. LPC concentrations exceeding 0.01 mM significantly reduced the basal ATPase activity of HlyB to approximately 10 % of the original ATPase activity (Figure 4B). Thus, we conclude that the ATPase activity of HlyB is strongly affected by the presence of free detergent and its incorporation into micelles. This effect can be prevented by reconstitution into saposin-A particles, independent of the nature of the lipid bilayer (DOPC or LPC).

Folded and unfolded substrates modulate the ATPase activity of HlyB in different ways

Differences between DOPC- and LPC-reconstituted HlyB became apparent in functional assays with the full-length substrate proHlyA in its unfolded and folded states.

In contrast to other studies conducted with detergent-purified HlyB, where a shortened version of the natural substrate was used in the ATPase assays (41), we aimed to employ the full-length, yet haemolytically inactive precursor form of HlyA, proHlyA. Haemolytic activity of HlyA requires two acylations at K563 and K689 and these are absent in proHlyA. Importantly, these acylations are irrelevant for the secretion process and the secretion rate (43).

A particular challenge of working with the full-length substrate is its size (110 kDa) and its tendency to aggregate already at low concentrations when kept unfolded in the Ca²⁺-unbound state. In order to mimic the *in vivo* situation, where unfolded substrate interacts with the ABC transporter, proHlyA was prepared in stock-solutions containing 4 M urea, which resulted in a final urea concentration of 0.8 M in the ATPase assay, which did not influence the basal ATPase activity of HlyB (not shown). Folded proHlyA was prepared by adding Ca²⁺ to and removing urea from the buffer.

Measurements with both types of proHlyA, folded and unfolded, were conducted at substrate concentrations ranging from 0 to 10 μM , respectively. ATPase activity was measured at uniform ATP, MgCl_2 and HlyB concentrations. The chosen concentration of ATP of 4 mM was approximately three-fold above the $K_{0.5}$ to ensure quantitative ATP saturation of HlyB. The observed effects thus resulted from interactions of the substrate with the ABC transporter, since no ATPase activity of folded or unfolded proHlyA alone was observed.

No interaction of the unfolded substrate and HlyB was observed in DOPC-particles, reflected by a constant basal-level ATPase activity even at high substrate concentration (Figure 5).

However, unfolded and folded proHlyA was found to interact differently with HlyB reconstituted in LPC-particles, resulting in opposing modulating effects. Adding the unfolded substrate resulted in an inhibition of the basal ATPase activity by approximately 30%, while the folded substrate resulted in a stimulation of ATP hydrolysis by 60 % (Figure 6).

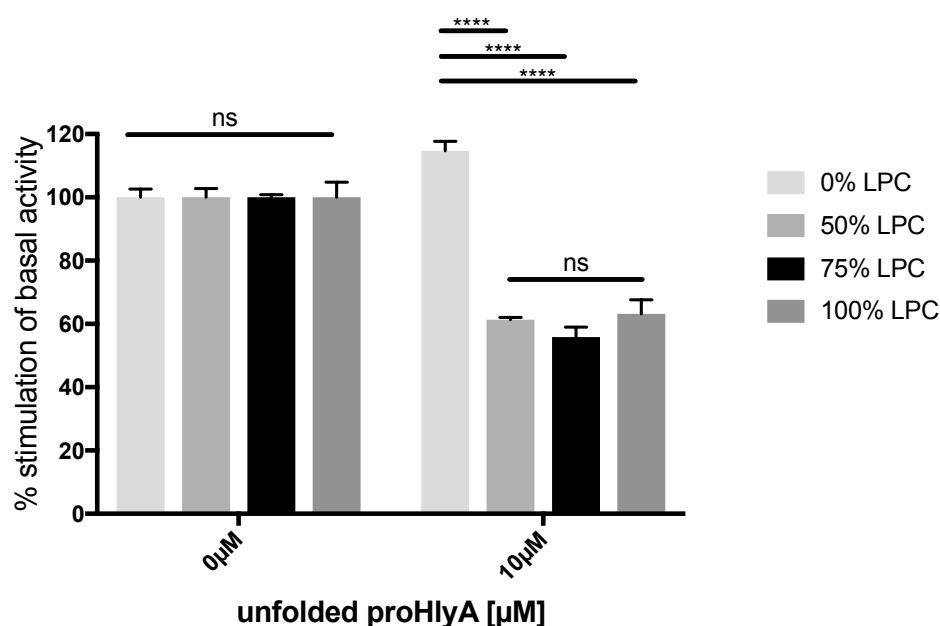


Figure 5: Stimulation of the basal ATPase activity of HlyB by 10 μM of proHlyA substrate reconstituted with different DOPC/ LPC mixtures. No stimulation can be observed when no LPC is added to the mixture. Error bars represent SEM of minimum two replicates. (ns: not significant, ****: $p < 0.0001$)

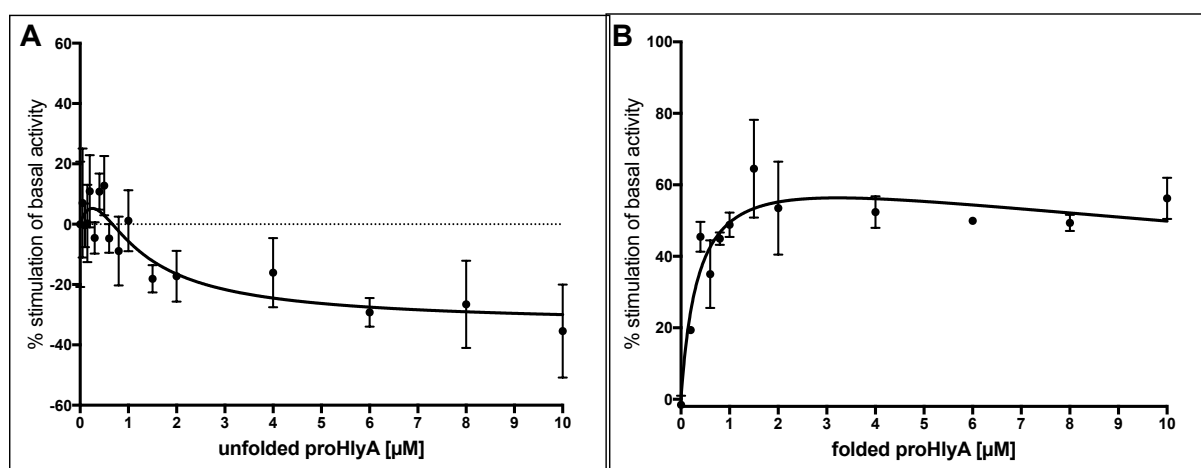


Figure 6: Kinetic measurements of HlyB in LPC-particles in the presence of (A) unfolded proHlyA and (B) folded proHlyA. The dashed line in (A) reflects the basal ATPase activity in the absence of substrate. Error bars represent SEM of a minimum of three biological replicates.

To further characterise the impact of DOPC on the stimulating behaviour of proHlyA on HlyB, we prepared mixed DOPC-LPC-particles by using mixtures containing 0 – 100 % (molar ratio) LPC. We observed the inhibitory effect of proHlyA already with 50 % (w/v) LPC (Figure 5).

The N-terminal CLD of HlyB is required for a specific interaction with unfolded substrate

As the cytoplasm-exposed CLD of HlyB has been speculated to interact with the substrate prior to translocation, we employed the truncated mutant HlyB Δ CLD to investigate the effect of the domain on the ATPase activity in the native-like environment of saposin-A nanoparticles. HlyB Δ CLD was reconstituted in LPC particles and its ATPase activity was measured in the presence and absence of unfolded or folded substrate.

Based on the observed non-linear profile in the presence of folded substrate, the data was fitted using the Michaelis-Menten model including substrate inhibition, suggesting a nearly two-fold stimulation of the basal ATPase activity. Adding unfolded substrate resulted in a four-fold stimulation of the basal ATPase activity with a strong substrate inhibition at higher concentrations.

It is important to highlight that the observed differences to HlyB are only due to the absence of the N-terminal CLD, as the assays were performed under identical conditions.

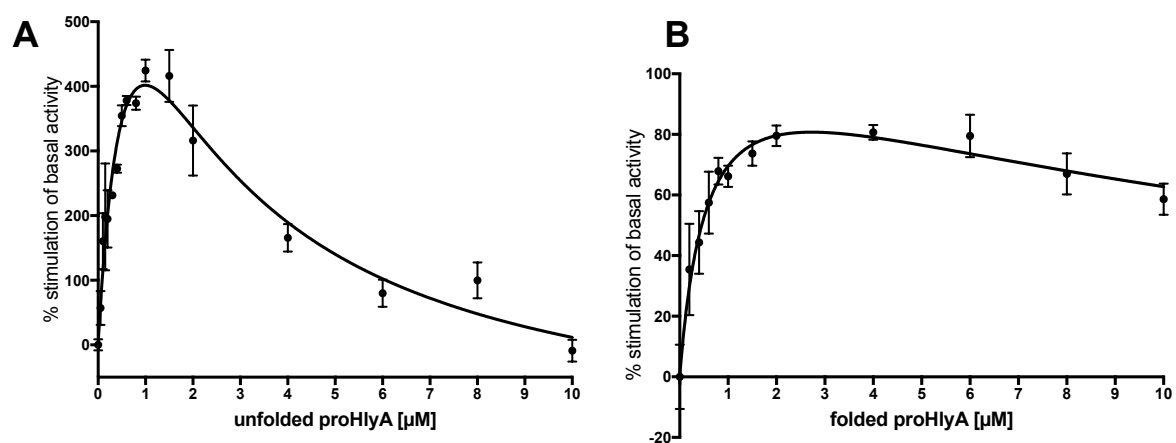


Figure 7: Kinetic measurements of HlyB Δ CLD in the presence of (A) unfolded proHlyA and (B) folded proHlyA. Error bars represent SEM of minimum two biological replicates.

Discussion

Type I secretion systems are ubiquitous amongst Gram-negative bacteria. Despite their high abundance and relatively simple build, the secretion mechanism is not yet fully understood. HlyB is the ABC transporter that is part of the HlyA-type I secretion system in *E. coli*. Its purification and initial biochemical data in detergent solution have been reported (41). Some ABC transporters contain additional accessory domains, which can be involved in substrate recognition and/or processing prior to transport. HlyB contains a CLD at its N-terminus, whose presence was shown to be essential for secretion *in vivo*. To study its influence on the interaction with the substrate, an HlyB derivative lacking this domain was created and termed HlyB Δ CLD (41).

By the use of the new expression strain *E. coli* C41(DE3) $\Delta ompF \Delta acrAB$, where the membrane proteins OmpF, AcrA and AcrB were genomically deleted, we were able to greatly increase the yield of purified HlyB and avoid OmpF and AcrAB as common impurities, especially present after solubilising membranes with fos-choline (49). In this study, we provide first data for a functionally reconstituted ABC transporter in saposin-lipoprotein nanoparticles (34).

OmpF is often upregulated during over-expression of membrane proteins, including HlyB, and its high abundance and stability, combined with a certain affinity for IMAC columns make it an often-observed impurity in purified membrane protein samples (49). This is also reflected by the number of available crystal structures (50,51).

AcrB contains histidine-rich domains, which confer substantial affinity for IMAC columns and thus render it also a widespread impurity in membrane protein preparations (52). Tendency of AcrB to crystallise easily and from small concentrations has also led to numerous structures of this protein in the pdb database (53,54).

The use of an OmpF and AcrAB deficient C41(DE3)-strain resolved the problem of persistent impurities (41). Furthermore, the protein was found to be stable and homogeneous in the non-ionic detergent DDM, whereas only LMNG has been previously observed to prevent the protein's aggregation and precipitation (Figure 2).

Even though purification was possible in DDM as well as in LMNG, reconstitution into saposin-lipoprotein nanoparticles was more efficient when employing DDM. A possible explanation might be a tight interaction of LMNG with the solubilised protein, which,

combined with the detergent's low cmc, might prevent the formation of homogeneous particles. This was indeed observed upon SEC, as the same reconstitution conditions in DDM and LMNG solutions produced homogeneous (DDM) and heterogeneous (LMNG) particles, respectively (Figure 3). Thus, our new expression strain also enhanced the availability of HlyB for reconstitution procedures.

The reconstitution of saposin-A particles was performed with a range of different phospholipids and natural extracts (38). Interestingly, reconstitution does not work using *E. coli* total lipid extracts or pure phosphatidylethanolamine, which makes up the largest portion of *E. coli* membranes (55). Thus, to achieve the reconstitution of *E. coli* membrane proteins, such as HlyB, the compromise of a non-native lipid environment had to be accepted.

DOPC is a commonly employed phospholipid for reconstitution experiments and it has been used before in combination with the saposin-A system (38). In this case, a phosphatidylcholine head group carries two mono-unsaturated esterified fatty acid tails, which results in a slightly negative membrane curvature of DOPC bilayers (56), which adopt a lamellar structure in aqueous solution (57,58).

LPCs are present in natural membranes in low amounts where they have functions in regulation of cell responses or signalling (46,59,60). They share the same head group with DOPC but contain only one fatty acid tail. The bulky head group and the presence of only one fatty acid tail results in an "inverted cone-shape" of LPC (61,62), thus the spontaneous curvature is positive. In solution, LPC forms micelles (46,63).

Saposin-A has been shown to form bilayer-like structures with detergents in an otherwise detergent-free environment (37). The crystal structure of saposin-A has been determined in the presence and absence of detergent molecules (37). In this structure, saposin-A forms a small bilayer-like structure with detergents, which somewhat resembles a phospholipid bilayer. Two monomers of saposin-A surround approximately 40 molecules of LDAO, a zwitterionic detergent (37).

By using LPC as well as DOPC for the reconstitution of HlyB, we aimed at producing very different lipid environments around the membrane protein. The saposin-A derived reconstitution system was developed by Frauenfeld et al. (34) in order to provide a more convenient solution to examine membrane proteins embedded in a lipid bilayer by cryo

electron microscopy. Since its publication in 2016, the system has been successfully employed in a number of biophysical applications (34,38) yet there are little to no data available for the functional properties of a membrane protein within saposin-lipoprotein nanoparticles.

In this study, we have embedded the ABC transporter HlyB in detergent-derived saposin-A particles, which enabled us to conduct functional studies with its dedicated substrate. Furthermore, the results highlight the importance of using systems that allow for studies in detergent-free buffers, since free detergent molecules may have a large impact on membrane proteins activity and/ or functionality (26); an effect that we also observed for HlyB (Figure 4B).

Some minor adjustments in the amount of saposin-A used resulted in very pure and homogeneous protein preparations with highly reproducible ATPase activity. The separation of “full” and “empty” lipoprotein particles was achieved by SEC, as it resulted in well-separated peaks. We conclude that the saposin-A system is a seminal approach not only for structural, but also for the functional characterisation of membrane proteins.

In some buffer conditions, HlyB was inactive in detergent solution (not shown). However, reconstitution restored the basal ATPase activity of HlyB and HlyB Δ CLD when using LPC or DOPC for reconstitution. Detergent micelles can only mimic the phospholipid bilayer to a certain extent, and binding to regions of the protein outside the TMDs or in-between helices can lead to structural distortions and to functional inactivation of the protein. As these effects are often reversible upon detergent removal, the reconstitution into artificial lipid bilayer systems can restore the protein’s activity.

Our results reveal the negative impact of free detergent on the activity of HlyB. Adding free LPC to DOPC-reconstituted HlyB significantly reduced its activity to approximately 10% (Figure 4B). We assume that the solubilisation of the saposin-lipoprotein particles and the subsequent incorporation of HlyB into micelles, combined with high concentrations of free detergent are responsible for this effect. These results are in good agreement with studies performed with detergent-solubilised HlyB, where the determined v_{\max} of HlyB corresponds to approximately 10% of the v_{\max} determined in saposin-particles (Figure 8) (41).

In a previous study, it was observed that detergent-purified HlyB exhibits a maximum basal ATPase activity that is 10-fold lower than that of HlyB Δ CLD, while the other kinetic parameters were not affected (41). However, our results using reconstituted HlyB reveal

different functional properties in native-like environment (figure 4A). The kinetic parameters of the basal ATPase activity, including the turnover number, were equal between HlyB and HlyB Δ CLD within standards errors (table 1). Notably, the k_{cat} values obtained for both reconstituted proteins are within the range of the k_{cat} of HlyB Δ CLD measured in detergent solution (41). This suggests that the observed difference of HlyB and HlyB Δ CLD in detergent is due to distinct influences of detergent on both proteins. We speculate that this might be due to a lower stability of full-length protein, which was also reflected in our experiments by lower yields after reconstitution and higher susceptibility to aggregation upon concentrating the protein. This made it slightly more difficult to handle HlyB and made it necessary to proceed rapidly with downstream applications after purification. As expected, both proteins show a strong cooperativity for ATP binding or hydrolysis, as was described before for wildtype HlyB and isolated NBDs (17,41). The different behaviour in detergent solution and upon reconstitution has been described for other ABC transporters such as the maltose importer, P-gp (ABCB1) or MsbA (64-66) and highlights the importance of the lipid environment for the ABC transporter.

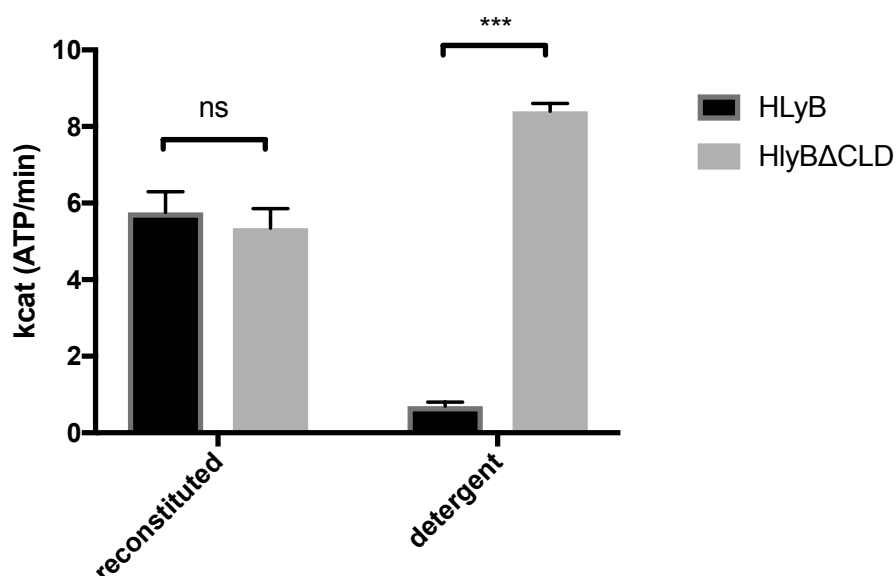


Figure 8: Comparison of the turnover numbers of HlyB and HlyB Δ CLD in detergent solution and reconstituted into saposin-lipoprotein nanoparticles. Error bars represent SEM of minimum two biological replicates. Ns: not significant, ***: $p < 0.001$.

As expected, the reconstituted H622A mutant did not show any hydrolytic activity (Figure 4), a result described before for the isolated NBDs as well as detergent-purified HlyB (17,41). Exchanging D551 to alanine in the isolated NBD of HlyB resulted in a loss of cooperativity

and a ten-fold decrease in maximum enzyme velocity (48). In the full-length protein, however, the mutation resulted in inactivation of the protein (Figure 4), emphasising the possible different behaviour of isolated domains compared to fully assembled proteins.

While the nature of the detergent within the saposin-lipoprotein particle did not influence the basal ATPase activity of HlyB, we observed modulating effects of the substrate proHlyA when using LPC-reconstituted protein but not with DOPC (Figure 4, Figure 5).

RTX proteins are secreted in an unfolded manner through type I secretion translocators (13,67). Thus, it was assumed that the ABC transporter does not necessarily recognise folded HlyA. However, previous measurements performed in detergent solution indicated an interaction of a folded C-terminal fragment including the postulated secretion signal with the ABC transporter. Our measurements in saposin-particles with folded full-length proHlyA confirmed the stimulatory effect, which was found to be independent of the presence of the CLD (Figure 6, Figure 7). Earlier studies localised an interaction site within the TMDs, which led to a stimulation of the ATPase activity (41). However, this does not necessarily reflect a physiologically relevant interaction, since the substrate is only present in an unfolded state in the cytosol. At higher substrate concentrations we observe an inhibition of the ATPase activities of HlyB and HlyB Δ CLD (Figure 6, Figure 7), which is a widespread phenomenon in enzyme kinetics (68).

When adding unfolded proHlyA to the activity assay a very weak stimulation was observed, while at higher concentration a substantial inhibition of the ATPase activity of HlyB, dropping below the basal ATPase activity, was observed (Figure 6). We assume that the unfolded substrate is inserted into the transport channel of HlyB, but due to the lack of the other components of the secretion system the stalled HlyA locks the transporter resulting in inhibition of ATPase activity. The stimulatory interaction at low concentrations might be important for the proper orientation and/ or insertion of the substrate.

In contrast, notably, we observed a dramatic four-fold stimulation of the basal ATPase activity of HlyB Δ CLD with unfolded proHlyA (Figure 7). Thus, we suggest that the CLD is involved in placing HlyA into the translocation channel, sufficient to block the ATPase. In HlyB Δ CLD, an inhibition of the ATPase can also be observed, but at higher substrate concentrations. This suggests the possible entry of the substrate to the translocation channel independently from the CLD, but whether these concentrations are physiologically relevant

remains questionable. Furthermore, a possible role of the CLD in preventing the substrate from aggregating needs to be considered.

Summary

In our study, we show the strong interplay between reconstitution of an ABC transporter and its functionality. Furthermore, we demonstrated that the properties of a lipid bilayer can influence stimulation of an ABC transporter by its substrate, and that this is not necessarily reflected by a change in the basal ATPase activity. We established a protocol to embed an ABC transporter in detergent-derived lipoprotein particles and point out that rather the presence of free detergent micelles than detergents *per se* affect the functionality of a membrane protein. Furthermore, we report functional assays of HlyB for the first time with the 100 kDa full-length substrate.

Acknowledgements

We thank Philippe Delepelaire and Bruno Miroux (Laboratoire de Biologie Physico-Chimique des Protéines Membranaires, CNRS, University Paris Diderot, Sorbonne Paris Cité, Institut de Biologie Physico-Chimique, Paris, France) for generously providing us with the *E. coli* C41(DE3) $\Delta ompF$ strain. Special thanks to Jens Frauenfeld for providing us with the expression plasmid for Saposin-A and detailed protocols. We would like to thank Klaas Martinus Pos, Goethe University Frankfurt, for the kind provision of an AcrAB-deficient *E. coli* strain. Furthermore, we would like to thank Tobias Beer for cloning the HlyB-D551A mutant and the Institute of Biochemistry, especially Alexej Kedrov, for stimulating discussions. This work was funded by CRC1208 (project A01 to L.S.).

References

1. Costa, T. R., Felisberto-Rodrigues, C., Meir, A., Prevost, M. S., Redzej, A., Trokter, M., and Waksman, G. (2015) Secretion systems in Gram-negative bacteria: structural and mechanistic insights. *Nat Rev Microbiol* **13**, 343-359
2. Holland, I. B., Peherstorfer, S., Kanonenberg, K., Lenders, M., Reimann, S., and Schmitt, L. (2016) Type I Protein Secretion-Deceptively Simple yet with a Wide Range of Mechanistic Variability across the Family. *EcoSal Plus* **7**
3. Noegel, A., Rdest, U., Springer, W., and Goebel, W. (1979) Plasmid cistrons controlling synthesis and excretion of the exotoxin alpha-haemolysin of *Escherichia coli*. *Mol Gen Genet* **175**, 343-350
4. Koronakis, V., Koronakis, E., and Hughes, C. (1989) Isolation and analysis of the C-terminal signal directing export of *Escherichia coli* hemolysin protein across both bacterial membranes. *EMBO J* **8**, 595-605
5. Lenders, M. H., Weidtkamp-Peters, S., Kleinschrodt, D., Jaeger, K. E., Smits, S. H., and Schmitt, L. (2015) Directionality of substrate translocation of the hemolysin A Type I secretion system. *Sci Rep* **5**, 12470
6. Felmler, T., Pellett, S., and Welch, R. A. (1985) Nucleotide sequence of an *Escherichia coli* chromosomal hemolysin. *J Bacteriol* **163**, 94-105
7. Wandersman, C., and Delepelaire, P. (1990) TolC, an *Escherichia coli* outer membrane protein required for hemolysin secretion. *Proc Natl Acad Sci U S A* **87**, 4776-4780
8. Balakrishnan, L., Hughes, C., and Koronakis, V. (2001) Substrate-triggered recruitment of the TolC channel-tunnel during type I export of hemolysin by *Escherichia coli*. *J Mol Biol* **313**, 501-510
9. Gray, L., Mackman, N., Nicaud, J. M., and Holland, I. B. (1986) The carboxy-terminal region of haemolysin 2001 is required for secretion of the toxin from *Escherichia coli*. *Mol Gen Genet* **205**, 127-133
10. Gray, L., Baker, K., Kenny, B., Mackman, N., Haigh, R., and Holland, I. B. (1989) A novel C-terminal signal sequence targets *Escherichia coli* haemolysin directly to the medium. *J Cell Sci Suppl* **11**, 45-57
11. Welch, R. A. (1991) Pore-forming cytolysins of gram-negative bacteria. *Mol Microbiol* **5**, 521-528
12. Linhartova, I., Bumba, L., Masin, J., Basler, M., Osicka, R., Kamanova, J., Prochazkova, K., Adkins, I., Hejnova-Holubova, J., Sadilkova, L., Morova, J., and Sebo, P. (2010) RTX proteins: a highly diverse family secreted by a common mechanism. *FEMS Microbiol Rev* **34**, 1076-1112
13. Lenders, M. H., Beer, T., Smits, S. H., and Schmitt, L. (2016) In vivo quantification of the secretion rates of the hemolysin A Type I secretion system. *Sci Rep* **6**, 33275
14. Benabdelhak, H., Kiontke, S., Horn, C., Ernst, R., Blight, M. A., Holland, I. B., and Schmitt, L. (2003) A specific interaction between the NBD of the ABC-transporter HlyB and a C-terminal fragment of its transport substrate haemolysin A. *J Mol Biol* **327**, 1169-1179
15. Hanekop, N., Zaitseva, J., Jenewein, S., Holland, I. B., and Schmitt, L. (2006) Molecular insights into the mechanism of ATP-hydrolysis by the NBD of the ABC-transporter HlyB. *FEBS Lett* **580**, 1036-1041
16. Zaitseva, J., Jenewein, S., Oswald, C., Jumpertz, T., Holland, I. B., and Schmitt, L. (2005) A molecular understanding of the catalytic cycle of the nucleotide-binding domain of the ABC transporter HlyB. *Biochem Soc Trans* **33**, 990-995
17. Zaitseva, J., Jenewein, S., Jumpertz, T., Holland, I. B., and Schmitt, L. (2005) H662 is the linchpin of ATP hydrolysis in the nucleotide-binding domain of the ABC transporter HlyB. *EMBO J* **24**, 1901-1910

18. Zaitseva, J., Jenewein, S., Wiedenmann, A., Benabdelhak, H., Holland, I. B., and Schmitt, L. (2005) Functional characterization and ATP-induced dimerization of the isolated ABC-domain of the haemolysin B transporter. *Biochemistry* **44**, 9680-9690
19. Kanonenberg, K., Schwarz, C. K., and Schmitt, L. (2013) Type I secretion systems - a story of appendices. *Res Microbiol* **164**, 596-604
20. Lecher, J., Schwarz, C. K., Stoldt, M., Smits, S. H., Willbold, D., and Schmitt, L. (2012) An RTX transporter tethers its unfolded substrate during secretion via a unique N-terminal domain. *Structure* **20**, 1778-1787
21. Havarstein, L. S., Diep, D. B., and Nes, I. F. (1995) A family of bacteriocin ABC transporters carry out proteolytic processing of their substrates concomitant with export. *Mol Microbiol* **16**, 229-240
22. Ishii, S., Yano, T., Ebihara, A., Okamoto, A., Manzoku, M., and Hayashi, H. (2010) Crystal structure of the peptidase domain of Streptococcus ComA, a bifunctional ATP-binding cassette transporter involved in the quorum-sensing pathway. *J Biol Chem* **285**, 10777-10785
23. Zhou, H. X., and Cross, T. A. (2013) Influences of membrane mimetic environments on membrane protein structures. *Annu Rev Biophys* **42**, 361-392
24. Cross, T. A., Murray, D. T., and Watts, A. (2013) Helical membrane protein conformations and their environment. *Eur Biophys J* **42**, 731-755
25. Zoonens, M., Comer, J., Masscheleyn, S., Pebay-Peyroula, E., Chipot, C., Miroux, B., and Dehez, F. (2013) Dangerous liaisons between detergents and membrane proteins. The case of mitochondrial uncoupling protein 2. *J Am Chem Soc* **135**, 15174-15182
26. White, J. F., and Grishammer, R. (2010) Stability of the neurotensin receptor NTS1 free in detergent solution and immobilized to affinity resin. *PLoS One* **5**, e12579
27. Johnson, Z. L., and Lee, S. Y. (2015) Liposome reconstitution and transport assay for recombinant transporters. *Methods Enzymol* **556**, 373-383
28. Orelle, C., Dalmas, O., Gros, P., Di Pietro, A., and Jault, J. M. (2003) The conserved glutamate residue adjacent to the Walker-B motif is the catalytic base for ATP hydrolysis in the ATP-binding cassette transporter BmrA. *J Biol Chem* **278**, 47002-47008
29. Steinfels, E., Orelle, C., Fantino, J. R., Dalmas, O., Rigaud, J. L., Denizot, F., Di Pietro, A., and Jault, J. M. (2004) Characterization of YvcC (BmrA), a multidrug ABC transporter constitutively expressed in Bacillus subtilis. *Biochemistry* **43**, 7491-7502
30. Ravaut, S., Do Cao, M. A., Jidenko, M., Ebel, C., Le Maire, M., Jault, J. M., Di Pietro, A., Haser, R., and Aghajari, N. (2006) The ABC transporter BmrA from Bacillus subtilis is a functional dimer when in a detergent-solubilized state. *Biochem J* **395**, 345-353
31. Denisov, I. G., Grinkova, Y. V., Lazarides, A. A., and Sligar, S. G. (2004) Directed self-assembly of monodisperse phospholipid bilayer Nanodiscs with controlled size. *J Am Chem Soc* **126**, 3477-3487
32. Ritchie, T. K., Grinkova, Y. V., Bayburt, T. H., Denisov, I. G., Zolnerciks, J. K., Atkins, W. M., and Sligar, S. G. (2009) Chapter 11 - Reconstitution of membrane proteins in phospholipid bilayer nanodiscs. *Methods Enzymol* **464**, 211-231
33. Denisov, I. G., and Sligar, S. G. (2016) Nanodiscs for structural and functional studies of membrane proteins. *Nat Struct Mol Biol* **23**, 481-486
34. Frauenfeld, J., Loving, R., Armache, J. P., Sonnen, A. F., Guettou, F., Moberg, P., Zhu, L., Jegerschold, C., Flayhan, A., Briggs, J. A., Garoff, H., Low, C., Cheng, Y., and Nordlund, P. (2016) A saposin-lipoprotein nanoparticle system for membrane proteins. *Nat Methods* **13**, 345-351
35. Bruhn, H. (2005) A short guided tour through functional and structural features of saposin-like proteins. *Biochem J* **389**, 249-257
36. Olmeda, B., Garcia-Alvarez, B., and Perez-Gil, J. (2013) Structure-function correlations of pulmonary surfactant protein SP-B and the saposin-like family of proteins. *Eur Biophys J* **42**, 209-222

37. Popovic, K., Holyoake, J., Pomes, R., and Prive, G. G. (2012) Structure of saposin A lipoprotein discs. *Proc Natl Acad Sci U S A* **109**, 2908-2912
38. Lyons, J. A., Boggild, A., Nissen, P., and Frauenfeld, J. (2017) Saposin-Lipoprotein Scaffolds for Structure Determination of Membrane Transporters. *Methods Enzymol* **594**, 85-99
39. Chien, C. H., Helfinger, L. R., Bostock, M. J., Solt, A., Tan, Y. L., and Nietlispach, D. (2017) An Adaptable Phospholipid Membrane Mimetic System for Solution NMR Studies of Membrane Proteins. *J Am Chem Soc* **139**, 14829-14832
40. Flayhan, A., Mertens, H. D. T., Ural-Blimke, Y., Martinez Molledo, M., Svergun, D. I., and Low, C. (2018) Saposin Lipid Nanoparticles: A Highly Versatile and Modular Tool for Membrane Protein Research. *Structure* **26**, 345-355 e345
41. Reimann, S., Poschmann, G., Kanonenberg, K., Stuhler, K., Smits, S. H., and Schmitt, L. (2016) Interdomain regulation of the ATPase activity of the ABC transporter haemolysin B from *Escherichia coli*. *Biochem J* **473**, 2471-2483
42. Datsenko, K. A., and Wanner, B. L. (2000) One-step inactivation of chromosomal genes in *Escherichia coli* K-12 using PCR products. *Proc Natl Acad Sci U S A* **97**, 6640-6645
43. Thomas, S., Smits, S. H., and Schmitt, L. (2014) A simple in vitro acylation assay based on optimized HlyA and HlyC purification. *Anal Biochem* **464**, 17-23
44. Baykov, A. A., Evtushenko, O. A., and Avaeva, S. M. (1988) A malachite green procedure for orthophosphate determination and its use in alkaline phosphatase-based enzyme immunoassay. *Anal Biochem* **171**, 266-270
45. Rath, A., Glibowicka, M., Nadeau, V. G., Chen, G., and Deber, C. M. (2009) Detergent binding explains anomalous SDS-PAGE migration of membrane proteins. *Proc Natl Acad Sci U S A* **106**, 1760-1765
46. Fuller, N., and Rand, R. P. (2001) The influence of lysolipids on the spontaneous curvature and bending elasticity of phospholipid membranes. *Biophys J* **81**, 243-254
47. Yoo, J., and Cui, Q. (2009) Curvature generation and pressure profile modulation in membrane by lysolipids: insights from coarse-grained simulations. *Biophys J* **97**, 2267-2276
48. Zaitseva, J., Oswald, C., Jumpertz, T., Jenewein, S., Wiedenmann, A., Holland, I. B., and Schmitt, L. (2006) A structural analysis of asymmetry required for catalytic activity of an ABC-ATPase domain dimer. *EMBO J* **25**, 3432-3443
49. Wiseman, B., Kilburg, A., Chaptal, V., Reyes-Mejia, G. C., Sarwan, J., Falson, P., and Jault, J. M. (2014) Stubborn contaminants: influence of detergents on the purity of the multidrug ABC transporter BmrA. *PLoS One* **9**, e114864
50. Kefala, G., Ahn, C., Krupa, M., Esquivies, L., Maslennikov, I., Kwiatkowski, W., and Choe, S. (2010) Structures of the OmpF porin crystallized in the presence of foscholine-12. *Protein Sci* **19**, 1117-1125
51. Chaptal, V., Kilburg, A., Flot, D., Wiseman, B., Aghajari, N., Jault, J. M., and Falson, P. (2016) Two different centered monoclinic crystals of the *E. coli* outer-membrane protein OmpF originate from the same building block. *Biochim Biophys Acta* **1858**, 326-332
52. Veessler, D., Blangy, S., Cambillau, C., and Sciara, G. (2008) There is a baby in the bath water: AcrB contamination is a major problem in membrane-protein crystallization. *Acta Crystallogr Sect F Struct Biol Cryst Commun* **64**, 880-885
53. Camara-Artigas, A., Hirasawa, M., Knaff, D. B., Wang, M., and Allen, J. P. (2006) Crystallization and structural analysis of GADPH from *Spinacia oleracea* in a new form. *Acta Crystallogr Sect F Struct Biol Cryst Commun* **62**, 1087-1092
54. Lohkamp, B., and Dobritsch, D. (2008) A mixture of fortunes: the curious determination of the structure of *Escherichia coli* BL21 Gab protein. *Acta Crystallogr D Biol Crystallogr* **64**, 407-415
55. Morein, S., Andersson, A., Rilfors, L., and Lindblom, G. (1996) Wild-type *Escherichia coli* cells regulate the membrane lipid composition in a "window" between gel and non-lamellar structures. *J Biol Chem* **271**, 6801-6809

-
56. Kollmitzer, B., Heftberger, P., Rappolt, M., and Pabst, G. (2013) Monolayer spontaneous curvature of raft-forming membrane lipids. *Soft Matter* **9**, 10877-10884
 57. Luzzati, V., and Husson, F. (1962) The structure of the liquid-crystalline phasis of lipid-water systems. *J Cell Biol* **12**, 207-219
 58. Rand, R. P., Fuller, N. L., Gruner, S. M., and Parsegian, V. A. (1990) Membrane curvature, lipid segregation, and structural transitions for phospholipids under dual-solvent stress. *Biochemistry* **29**, 76-87
 59. Pliotas, C., Dahl, A. C., Rasmussen, T., Mahendran, K. R., Smith, T. K., Marius, P., Gault, J., Banda, T., Rasmussen, A., Miller, S., Robinson, C. V., Bayley, H., Sansom, M. S., Booth, I. R., and Naismith, J. H. (2015) The role of lipids in mechanosensation. *Nat Struct Mol Biol* **22**, 991-998
 60. Dan, N., and Safran, S. A. (1998) Effect of lipid characteristics on the structure of transmembrane proteins. *Biophys J* **75**, 1410-1414
 61. Stiasny, K., and Heinz, F. X. (2004) Effect of membrane curvature-modifying lipids on membrane fusion by tick-borne encephalitis virus. *J Virol* **78**, 8536-8542
 62. Chernomordik, L. V., Vogel, S. S., Sokoloff, A., Onaran, H. O., Leikina, E. A., and Zimmerberg, J. (1993) Lysolipids reversibly inhibit Ca(2+)-, GTP- and pH-dependent fusion of biological membranes. *FEBS Lett* **318**, 71-76
 63. Henriksen, J. R., Andresen, T. L., Feldborg, L. N., Duelund, L., and Ipsen, J. H. (2010) Understanding detergent effects on lipid membranes: a model study of lysolipids. *Biophys J* **98**, 2199-2205
 64. Callaghan, R., Berridge, G., Ferry, D. R., and Higgins, C. F. (1997) The functional purification of P-glycoprotein is dependent on maintenance of a lipid-protein interface. *Biochim Biophys Acta* **1328**, 109-124
 65. Bao, H., and Duong, F. (2012) Discovery of an auto-regulation mechanism for the maltose ABC transporter MalFGK2. *PLoS One* **7**, e34836
 66. Eckford, P. D., and Sharom, F. J. (2010) The reconstituted Escherichia coli MsbA protein displays lipid flippase activity. *Biochem J* **429**, 195-203
 67. Bakkes, P. J., Jenewein, S., Smits, S. H., Holland, I. B., and Schmitt, L. (2010) The rate of folding dictates substrate secretion by the Escherichia coli hemolysin type 1 secretion system. *J Biol Chem* **285**, 40573-40580
 68. Reed, M. C., Lieb, A., and Nijhout, H. F. (2010) The biological significance of substrate inhibition: a mechanism with diverse functions. *Bioessays* **32**, 422-429

3.5 Chapter V – A New Expression Strain for Membrane Proteins

Title: Improving the Overexpression and Purification of Membrane Proteins by Altering the Membrane Lipid Composition of C41(DE3)

Authors: Kerstin Kanonenberg, Jorge Royes, Alexej Kedrov, Gereon Poschmann, Philippe Delepelaire Olivia Spitz, Tobias Beer, Kai Stühler, Bruno Miroux, Lutz Schmitt

Published in: *to be submitted*

Impact Factor:

Own Work: 40 %
Genomic deletion of *acrAB*
Overexpression of membrane proteins
Purification of HlyB
Solubilisation assays
Data analysis
Writing of the manuscript

Improving the Overexpression and Purification of Membrane Proteins by Altering the Membrane Lipid Composition of C41(DE3)

Kerstin Kanonenberg¹, Jorge Royes², Alexej Kedrov¹, Gereon Poschmann³, Philippe Delepelaire⁴, Olivia Spitz¹, Diana Kleinschrodt¹, Kai Stühler³, Bruno Miroux^{2*}, Lutz Schmitt^{1*}

¹ – Institute of Biochemistry, Heinrich-Heine-University Duesseldorf, Germany

² – Laboratoire de Biologie Physico-Chimique des Protéines Membranaires, CNRS, IBPC, University Paris Diderot, Sorbonne Paris Cité, Paris, France

³ – Molecular Proteomics Laboratory, Biomedizinisches Forschungszentrum (BMFZ), Heinrich-Heine-University Duesseldorf, Germany

⁴ – PASTEUR, CNRS, Département de chimie, École normale supérieure, PSL University, Sorbonne Université, 75005 Paris, France

*: To whom correspondence should be addressed:

Bruno Miroux, Laboratoire de Biologie Physico-Chimique des Protéines Membranaires, CNRS, University Paris Diderot, Sorbonne Paris Cité, Institut de Biologie Physico-Chimique, 13 rue Pierre et Marie Curie, 75005 Paris, France, Email: bruno.miroux@ibpc.fr

Lutz Schmitt, Institute of Biochemistry, Heinrich-Heine-University Duesseldorf, Universitaetsstr. 1, 40225 Duesseldorf, Germany

Phone: +49211-81-10773, Fax: 49211-81-15310, Email: lutz.schmitt@hhu.de

Abstract

The overexpression and purification of membrane proteins to high purity and homogeneity is a challenging task. Over time, several strains have been developed that decrease the toxic side-effects and thus result in higher bio mass and protein yield. However, two major contaminants have been identified in membrane protein preparations from *E. coli*: the outer membrane porin OmpF and AcrB, which is part of a tripartite efflux pump. Both proteins crystallise from low concentrations and diverse conditions, which make them a major problem especially in membrane protein crystallography. In this study, we present a C41(DE3)-derived expression strain that is depleted of these two proteins. Interestingly, we not only found an increase in protein purity but an overall improved membrane protein overexpression. We have applied the strain in a number of homo- and heterologous overexpression experiments and provide further analysis of the strain in terms of lipid and protein composition. From our results, we suggest a linkage between the observed phenotype and an altered membrane biogenesis. Our study therefore provides a completely new approach for strain-improvement for membrane protein production by altering the membrane environment.

Introduction

The genomes of prokaryotes, eukaryotes and archaea contain about 20 – 30 % of genes coding for membrane proteins (1). However, they are still underrepresented in biochemical and structural studies, despite their undeniable physiological and medical importance – about 70 % of all drug targets are membrane proteins (2).

The bottleneck of studying membrane proteins *in vitro* is on one hand their overexpression, and on the other hand the requirement for highly pure and homogeneous protein.

Due to the limited availability of overexpression hosts, *Escherichia coli* remains first choice for obtaining large amounts of homo- or heterologously overexpressed (membrane) proteins. Regularly, the T7 promoter system is employed for this purpose. However, its five-times elevated speed in comparison to the endogenous *E. coli* RNA polymerase often results in toxic side-effects for the expression host (3,4). The overexpression of membrane proteins often leads to saturation of the Sec translocon, consequently resulting in protein aggregation in the cytosol and an inefficient ATP synthase, which further intensifies the toxic side-effects (5).

Thus, overcoming these toxic effects is a primary goal when developing new expression strains as this consequently leads to an increase in biomass, which is normally associated with a greater yield of target protein.

Early on, it was attempted to select for, or engineer, *E. coli* strains that show an improved expression of membrane proteins. Mainly the promoter regions were targeted in these studies. The first strains to be developed were the so-called “Walker strains”, namely *E. coli* C41(DE3) and *E. coli* C43(DE3) (6). Ever since, these strains have been widely used for the successful overexpression of membrane proteins. The genomic analysis of both strains revealed mutations in the lacUV promoter (5), which resulted in a decrease in the rate of translation, subsequently preventing the saturation of the membrane protein biogenesis machinery (5,7). A deletion of a few kilobase pairs in C43(DE3) and an additional mutation in *lacI* further improved the expression of some proteins (8). A considerable effect is for example the altered membrane biogenesis resulting in the formation of internal membranes in *E. coli* C43(DE3) (9).

On the basis of the mutated lacUV promoter in *E. coli* C41(DE3) and C43(DE3), the Lemostrains were developed by targeted genomic modification of *E. coli* (5). By introducing a

rhamnose-inducible promoter into the genome, which allows for adjusted activity of the T7 repressor T7 lysozyme, the overexpression of a range of membrane protein was optimised (5).

A recent advance in strain development are *E. coli* C44(DE3) and *E. coli* C45(DE3) (10). These strains comprise a novel regulation system for the T7 RNA polymerase, which reduces the availability of the T7 RNA polymerase, leading to substantial enhancement of the overexpression of a range of bacterial and eukaryotic membrane proteins (10).

For the purification of membrane proteins the choice of detergent is crucial. However, it is often laborious and time-consuming to find the optimum detergent or detergent combination for a specific membrane protein, which can strongly affect yield and functionality of a membrane protein *in vitro* (11,12).

Two common impurities in membrane protein preparations from *Escherichia coli* are OmpF and AcrB. AcrB is part of the tripartite efflux pump AcrAB-TolC (13), while OmpF functions as a trimeric outer membrane porin (14). Both proteins crystallise easily even from very low concentrations, which is reflected also by the large number of available structures for both proteins in the protein databank (15-17).

The AcrAB-TolC efflux pump facilitates the extrusion of a variety of substances across both membranes and is mainly known for its function in drug resistance (18). It also mediates the transport of long chain and short chain fatty acids across the lipid bilayer (19). Histidine-rich domains confer substantial affinity for IMAC columns, making it an obstinate impurity (15). OmpF is a protein of high abundance and stability with a certain affinity for IMAC columns. It is often upregulated during overexpression of membrane proteins, which renders it a widespread impurity in membrane protein purification (14,20).

In this study, we created a new expression strain derived from *E. coli* C41(DE3) that lacks the genes encoding AcrAB and OmpF. The initial goal was to significantly improve the purity of overexpressed membrane proteins and thus facilitate their crystallisation and/ or functional studies. Surprisingly, the deletion of these two proteins resulted in a strain with heavily altered membrane characteristics, which did not only increase the amount of overexpressed membrane proteins, but also largely enhanced their availability due to increased solubilisation efficiency. Thus, we present a completely new approach to modify and

improve *E. coli* strains for membrane protein overproduction, which was mainly achieved by a change in the protein and lipid composition of the membrane.

Materials and Methods

Construction of the expression strains *E. coli* C41(DE3) $\Delta ompF$ and *E. coli* C41(DE3) $\Delta ompF\Delta acrAB$

OmpF-deleted mutants were prepared from JW0192 $\Delta ompF$ knockout (*E. coli* K12 BW25113) described in Keio collection (21) by P1 transduction of *E. coli* C41(DE3) (22). *OmpF* knockouts were selected using kanamycin resistance. Finally, kanamycin resistance was removed from *OmpF* knockouts by FLP-FRT recombination (23).

To additionally delete *acrAB* from *E. coli* C41(DE3) $\Delta ompF$, the lambda-red recombinase system was employed, following published protocols (24). The plasmid pKD4 carrying a kanamycin resistance cassette was amplified using the forward and reverse overhang primers ACTTTTGACCATTGACCAATTTGAAATCGGACACTCGAGGTTTACATATGAGTAG GCTGGAGCTGCTTC and TTACGCGGCCTTAGTGATTACACGTTGTATCAATGATGATCGACAGTATGATGGG AATTAGCCATGGTCC, respectively. The genomic insertion of the kanamycin resistance gene using the pKD46-encoded lambda-red recombinase and its subsequent deletion with the pCP20-encoded Flp-recombinase were confirmed by PCR- and sequencing analysis using the primers CACATCGAGGATGTGTTG (forward) and GCCCTCTCGTTTGTAG (reverse).

Overexpression of HlyB and other ABC transporters

All plasmids used for the overexpression of ABC transporters are derived from the arabinose-inducible pBAD vector system and carry an ampicillin resistance gene.

E. coli strains C41(DE3), C41(DE3) $\Delta ompF$ or C41(DE3) $\Delta ompF\Delta acrAB$ were transformed with pBAD-ABC transporter (25) and selected on agar plates containing 100 μ g/mL ampicillin. Overnight cultures with 2YT-medium supplemented with 100 μ g/mL ampicillin were inoculated with single colonies and incubated at 200 rpm, 37 °C for 15 hours. Main cultures were grown in 5 L baffled flasks, containing 1 L of 2YT-medium with 100 μ g/mL ampicillin. Expression cultures were inoculated to an OD₆₀₀ of 0.1 and grown at 200 rpm, 37 °C until OD₆₀₀ had reached 2.5. The expression of the ABC transporters was induced by adding arabinose to a final concentration of 10 mM and incubation was continued for 3 h and cells were harvested by centrifugation.

Overexpression of SecY and YidC

E. coli C41(DE3), C41(DE3) $\Delta ompF$ and C41(DE3) $\Delta ompF\Delta acrAB$ were transformed with the plasmids pEK20 (SecYEG) (26) or pEM183 (YidC) (27). Positive clones were selected on agar plates containing 100 μ g/mL ampicillin. Overnight cultures with 2YT-medium and 100 μ g/mL ampicillin were inoculated with single colonies and incubated at 200 rpm, 37 °C for 15 h. Main cultures were grown at 200 rpm, 37 °C in 5 L baffled flasks containing 1 L of 2YT-medium supplemented with 100 μ g/mL ampicillin. Protein expression of SecY and YidC was induced by adding arabinose to a final concentration of 10 mM and IPTG to a final concentration of 1 mM, respectively. Cells were further incubated for 3 h and subsequently harvested by centrifugation.

Purification of membranes from *E. coli* cells

For all strains and overexpressed proteins the same protocol for the extraction of the membrane-fraction was employed. Cells were resuspended in buffer P containing 50 mM NaH₂PO₄, pH 8, 300 mM NaCl and lysed by passing three times through a cell-disruptor (Microfluidics) at 1.5 kbar. Undisrupted cells and cell debris was removed by centrifugation at 18,000 xg for 30 min at 4 °C. Membranes were collected from the supernatant by a subsequent high-spin centrifugation step at 150,000 xg for 90 min at 4 °C. Membrane pellets were homogenised in buffer P, supplemented with 10 % glycerol, and stored at -80 °C.

Purification of HlyB from *E. coli* C41(DE3) $\Delta ompF\Delta acrAB$ membranes

Membranes of 500 mL of cell culture were diluted to a final concentration of 10 mg/mL using buffer P. Membranes were solubilised with either 0.5 % (w/v) fos-choline 14, 1 % (w/v) DDM, 1 % (w/v) Triton X-100 or 1 % (w/v) LMNG for 1 hour at 8 °C. Non-solubilised material was removed by filtration (pore size: 0.45 μ m) without the need of an additional centrifugation step. Solubilised membranes were diluted 1:4 with buffer P, supplemented with 2 mM imidazole and loaded on an IMAC (immobilised metal ion affinity chromatography) column (5 mL HiTrap Chelating HP, GE Healthcare, loaded with Zn²⁺). The column was washed with 8 mL of buffer P supplemented with 0.015 % (w/v) DDM or 0.003 % (w/v) LMNG and 2 mM imidazole. Non-specifically bound proteins were removed by washing with 18 mL of buffer P, supplemented with detergent and 40 mM imidazole. HlyB was eluted with buffer P containing the corresponding detergent and 25 mM EDTA.

Purification of SecY and YidC from *E. coli* membranes

Overexpressed recombinant SecYEG and YidC proteins containing poly-histidine tags were purified via one-step Ni²⁺-NTA-based chromatography, as previously described (27,28). Briefly, isolated membranes were solubilised with 1 % DDM in 50 mM HEPES pH 7.4, 300 mM KCl, 100 μ M TCEP and complete protease inhibitor cocktail, and incubated with Ni²⁺-NTA agarose (Qiagen) in presence of 5 mM imidazole. After extensive wash with 50 mM HEPES pH 7.4, 150 mM KCl, 0.1 % DDM, and 20 mM imidazole, the imidazole concentration was increased to 300 mM to elute proteins of interest. Protein concentrations were determined using NanoDrop UV-Vis spectrophotometer based on calculated extinction coefficients, 71,000 M⁻¹ cm⁻¹ for the SecYEG complex, and 96,000 M⁻¹ cm⁻¹ for YidC.

Membrane-fractionation by analytical ultracentrifugation

Continuous sucrose gradients (20-70% sucrose, 50 mM HEPES pH 7.4, 150 mM KCl, 5 mM MgCl₂, and cOmplete protease inhibitor cocktail) were prepared in centrifuge tubes using the Gradient Station (BioComp Instruments). Membranes from studied strains containing over-expressed YidC were loaded on top of the gradients and subjected to ultracentrifugation for 16 h at 30,000 rpm in SW40 rotor (Beckman Coulter). Gradients were fractionated from top to bottom using the Gradient Station (fraction volume 1 mL). Prior SDS-PAGE analysis of the fractions, proteins were precipitated by adding trichloroacetic acid to the final concentration 10 %, pellets were washed with acetone and resuspended in SDS-PAGE loading buffer (5 min at 95 °C).

Growth curves of *E. coli* strains

Growth curves were measured in 96-well plates on a microplate reader by monitoring the absorbance at 600 nm (Tecan Platereader). Cultures were inoculated to an OD₆₀₀ of 0.15 and growth was monitored in triplicates over 10 hours.

Genome sequencing

Chromosomal DNA preparation and genome sequencing and analysis of *E. coli* C41(DE3) $\Delta ompF\Delta acrAB$ was performed as described elsewhere (10).

Analysis of the proteomes of *E. coli* strains by quantitative mass spectrometric analysis

E. coli samples for mass spectrometry (four individual replicate cultures per group) were prepared as described (29). Briefly, proteins from bacterial cells were extracted with lysis buffer (30 mM tris(hydroxymethyl)aminomethane, 2 M thiourea, 7 M urea, and 4 % (w/v) 3-[(3-cholamidopropyl)dimethylammonio]-1-propanesulfonate, pH 8.5) and 5 µg shortly separated in a polyacrylamide gel (about 5 mm running distance). Bands from silver-stained gels were cut out, de-stained, washed, reduced, alkylated with iodoacetamide and proteins were digested with trypsin. Peptides were extracted from the gel and ~500 ng per sample analysed by liquid chromatography coupled mass spectrometry (analogous to (29)). An Ultimate 3000 rapid separation liquid chromatography system (RSLC, Thermo Scientific) was used for sample separation on a 20 cm length C18 chromatography column by a 2 h gradient. Peptides were directly injected into the QExactive plus (Thermo Scientific) triple quadrupole Orbitrap hybrid mass spectrometer via an electrospray nano source interface. The mass spectrometer was operated in data dependent positive mode. After recording of survey spectra at a resolution of 70,000, up to 10 precursors were isolated by the quadrupole, fragmented by higher-energy collisional dissociation and fragment spectra recorded at a resolution of 17,500 in the Orbitrap analyzer.

Database searches and quantification of precursor ion intensities was done within the MaxQuant environment (version 1.6.1.0, MPI for Biochemistry, Planegg, Germany) with standard parameters if not stated otherwise. The UniProt KB proteome dataset for *E. coli* BL21 (UP000002032, downloaded on 27th of June 2018), supplemented with an entry for HlyB was used for spectra identification. The match between runs option was enabled as well as label-free quantification. Proteins and peptides were accepted at a false discovery rate of 1 %. For quantitative analysis only proteins were considered showing at least 2 different identified peptides and four valid values in at least one sample group. Statistical analysis (ANOVA) was performed within Perseus 1.6.2.2 (MPI for Biochemistry, Planegg, Germany) and the R environment (version 3.4.1, the R Foundation for Statistical Computing, post-hoc test) on log2 normalised intensities; missing values were filled in before with a downshifted (1.8 standard deviations) normal distribution (width 0.3 standard deviations). A one-dimensional annotation enrichment was calculated within Perseus 1.6.2.2 on the basis of annotations provided by UniProt KB (downloaded on 8th October, 2018). Coverage of the *E. coli* proteomes was approximately 40 %.

Lipid extraction

Lipids from HlyB overexpressing *E.coli* C41(DE3), C41(DE3) $\Delta ompF$ or C41(DE3) $\Delta ompF\Delta acrAB$ (3 independent replicas of each sample) were extracted using a procedure adapted from Bligh and Dyer (31). Chloroform (1.25 mL) and methanol (2.50 mL) were sequentially added to a membrane suspension (1.00 mL) in phosphate buffer (50 mM, pH = 8.0) containing 1 M NaCl. Samples were vortexed for 10 min at RT and chloroform (1.25 mL) and water (1.25 mL) were added. The organic phase (lower phase) was collected and the extraction procedure was repeated on the remaining aqueous phase. Combined organic layers were evaporated to dryness under an argon stream and stocked at -20 °C under inert atmosphere.

Analysis of the lipidomes of *E. coli* strains by mass spectrometric analysis

Phospholipid separation and quantification

Phospholipids for standard solution preparation, cardiolipin (CL) sodium salt from bovine heart (≥ 98 % purity), L- α -phosphatidylethanolamine (PE) (≥ 97 % purity) and L- α -phosphatidylglycerol sodium (PG) ($\geq 99\%$ purity) both from egg yolk, were purchased from Sigma-Aldrich. Stock standard solutions of each phospholipid were prepared in chloroform at 0.5, 0.4, 0.3, 0.2, 0.1, 0.05 and 0.025 mg/mL.

Organic HPLC grade solvents, *n*-heptane, chloroform and LC/MS grade methanol and absolute ethanol were purchased from VWR International. ULC-MS grade 2-propanol and water were purchased from Biosolve Chemicals. LC-MS grade acetic acid and triethylamine (99.5 % purity) were purchased from Sigma-Aldrich.

Phospholipid separation by polar headgroup was performed on a Thermofisher Dionex U-3000 RSLC system. The separation of lipids was performed on a PVA-Sil column (150 x 2.1 mm I.D., 120 Å) from YMC Europe GmbH thermostated at 35 °C. Chromatographic method was adapted from Ramos *et al.* (32). Flow rate was set at 0.400 mL/min and 5 μ L of sample (diluted 1200x for PE quantification and 600x for PG and CL quantification) was injected. Mobile phase composition and chromatographic program is given (table 1). Isopropanol rinsing phase followed by a column equilibration phase were added at the end of the chromatographic program and performed before injecting a new sample.

Table 1: Mobile phase composition and chromatographic program.

Time (min)	A ^a	B ^b	C ^c	D ^d
0	98	2	0	0
2	98	2	0	0
8	12	88	0	0
22	0	60	40	0
26	0	60	40	0
27	0	0	0	100
29	0	0	0	100
30	98	2	0	0
44	98	2	0	0

^a *n*-heptane/2-propanol (98:2 v/v)^b chloroform/2-propanol (65:35 v/v)^c methanol/water (95:5 v/v)^d 2-propanol

All mobile phases contained 0.08% v/v triethylamine and 1.00% v/v acetic acid.

Detection

Separated phospholipids were analysed with a dual detection system consisting of a Corona-CAD Ultra detector and LTQ-Orbitrap Velos Pro MS detector equipped with an H-ESI II probe from ThermoFisher Scientific. After separation, HPLC effluent was split using a mixing tee, thus 250 µL/min entered to the Corona-CAD and 150 µL/min entered the mass spectrometer. To increase the flow entering the corona-CAD and maintain good aerosol stability, absolute ethanol was added with a second mixing tee with a flow of 200 µL/min.

The corona-CAD nebuliser was set to 30 °C and 5 bar of nitrogen pressure. The LTQ-Orbitrap Velos Pro MS detector spray voltage was set to 3.3 kV. Probe temperature was set to 200 °C. Sheath, auxiliary and sweep gas flow rates were set to 20, 8 and 0 (a.u.), respectively. Capillary temperature was set to 325 °C and S-lens RF level to 60 %. Analysis was performed in negative mode to obtain structural information on phospholipid fatty chains. The MS detector, equipped with two combined analysers (a double linear ion trap (LTQ) and an orbital trap), provided fast fragmentation at low resolution and complete high-resolution

spectra at the same time. Detection was carried out either in full MS Scan (100,000 resolution) and data dependant MS² and MS³ with collision induced dissociation in the CID fragmentation (collision energy set to 35).

Phospholipid identification

The used chromatographic method used separates the phospholipids by means of their polar headgroup. Retention time was calibrated using commercial PG, PE and CL standards. Subsequently, the fatty acid species were assigned for each family of phospholipids. Phospholipid identification was performed as previously described (33), combining high-resolution mass detection in full scan mode and MS²/MS³ fragmentation in data dependant mode. In minor *m/z* peaks, MSⁿ fragmentation was not always available. In these cases, only the number of carbons and unsaturations of the species were indicated. Sn1 and sn2 acyl chain position were not determined. Oxidised CL identification was performed as previously described (33,34).

Solubilisation assays

HlyB was overexpressed in *E. coli* C41(DE3), C41(DE3) $\Delta ompF$ and C41(DE3) $\Delta ompF\Delta acrAB$ and membranes were isolated as described above. Solubilisation assays were performed in 96 well plates. The solubilisation efficiency was assessed by measuring the turbidity of the membrane solution by determining its absorbance at 595 nm. For all membranes, the data was normalised to 100 % solubilisation, which was determined by adding 5 % (w/v) SDS.

Detergents were added to final concentrations ranging from 0 to 2 % (w/v). Plates were then incubated for 10 min and subsequently measured at 595 nm. Data was evaluated using GraphPad Prism 7 software (Graph Pad).

Results

Construction of the expression strain *E. coli* C41(DE3) Δ *ompF* Δ *acrAB* by genomic modification

Subsequent to the deletion of *ompF*, *acrAB* was deleted by employing the lambda-red recombinase system. Both genomic deletions were confirmed by PCR and subsequent sequencing of the full genome of *E. coli* C41(DE3) Δ *ompF* Δ *acrAB*. The comparison to the genome of the parental strain *E. coli* C41(DE3) (GenBank ID: NZ_CP010585.1) (8) eliminated the possibility of other modifications apart from the desired deletions. Thus, the observed phenotypes in this study are solely due to the deletions of the outer membrane porin OmpF and the inner membrane complex of the tripartite efflux pump AcrAB-TolC.

We analysed the growth of the double deletion strain in comparison to C41(DE3) and the single deletion strain C41(DE3) Δ *ompF*. Our results demonstrate that under the tested condition the deletion of *ompF* from the genome results in growth to approximately 50 % higher ODs, while the additional deletion of *acrAB* does not further influence the growth behaviour (figure 1).

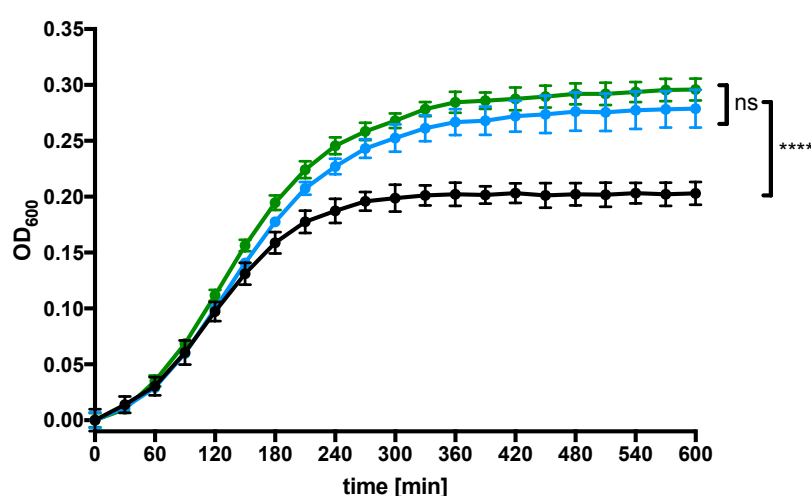


Figure 1: Growth curves of *E. coli* C41(DE3) (black line), *E. coli* C41(DE3) Δ *ompF* (blue line) and *E. coli* C41(DE3) Δ *ompF* Δ *acrAB* (green line). Measurements were performed in 2YT medium at 37°C over 10 hours. Error bars represent SD of two individual measurements. Ns: not significant, ****: $p < 0.0001$.

Overexpression of ABC transporters in *E. coli* C41(DE3), C41(DE3) Δ *ompF* and C41(DE3) Δ *ompF* Δ *acrAB*

In total, seven prokaryotic ABC transporters, both homologous and heterologous, were analysed. The total amounts of membrane-inserted target proteins were compared by SDS-PAGE. Equal amounts of total protein were loaded on the gels (Figure 2).

For five ABC transporters, expression was improved by using the OmpF-depleted strain, however, the additional deletion of *acrAB* had no further effect. One ABC transporter was only expressed in the double deleted strains in considerable amounts (Figure 2).

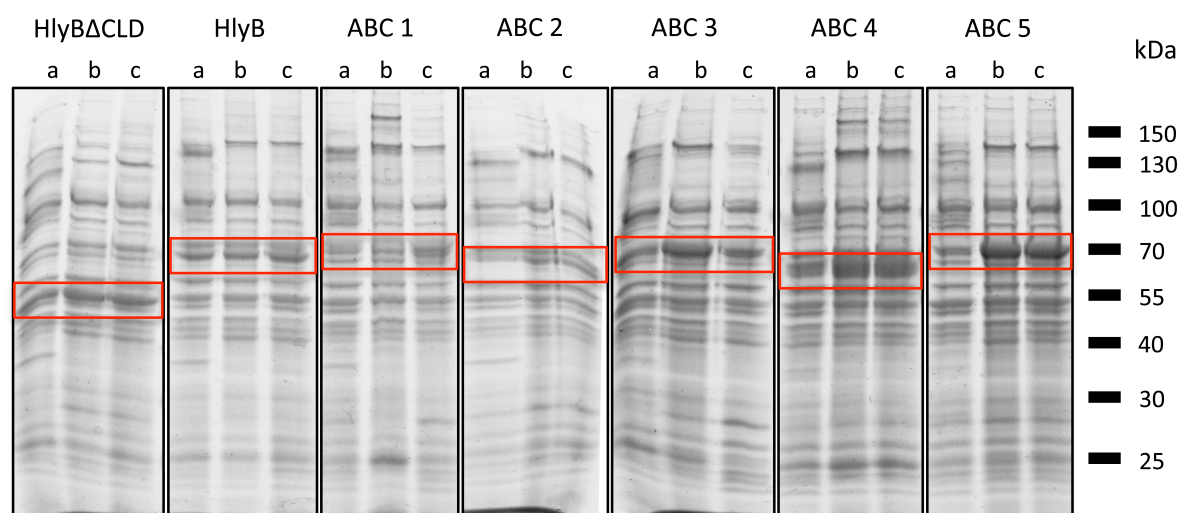


Figure 2: Overexpression of membrane proteins in *E. coli* C41(DE3) (a), C41(DE3) Δ *ompF* (b) and C41(DE3) Δ *ompF* Δ *acrAB* (c). Equal amounts of isolated membranes were loaded on 10 % SDS-PAGE and stained with Coomassie Brilliant Blue. Target proteins are marked by red boxes.

Comparing the solubilisation efficiency of different detergents using membranes from *E. coli* C41(DE3), C41(DE3) Δ *ompF* and C41(DE3) Δ *ompF* Δ *acrAB*

Based on the initial observation that very low amounts of fos-choline 14 (FC-14) were sufficient to extract close to 100 % of overexpressed HlyB from *E. coli* C41(DE3) Δ *ompF* Δ *acrAB* membranes (chapter IV), we tested a range of further commonly used detergents for solubilisation in membrane protein biochemistry. Notably, HlyB has been shown previously to be exclusively solubilised by fos-choline-derived detergents (25). We measured the efficiency of solubilisation by determining the turbidity of membrane samples after adding detergent at increasing concentrations. Obtained curves were normalised by setting the turbidity of completely solubilised membranes, which was accomplished by adding 5 % (w/v) SDS, to 0 %. This value was found to be equal for all membrane samples.

Overexpressing cells were grown under equal conditions and membranes were extracted using identical protocols. When using the zwitterionic detergent FC-14 the solubilisation of all membranes was similar. However, when expending the non-ionic detergents DDM or

LMNG, different solubilisation behaviour was observed as a consequence of the deletion of *ompF* and *acrAB* (figure 3). Thus, an improvement of overall membrane solubilisation, which results from the genomic deletion of the outer membrane porin OmpF and the inner membrane proteins AcrAB, was clearly observed.

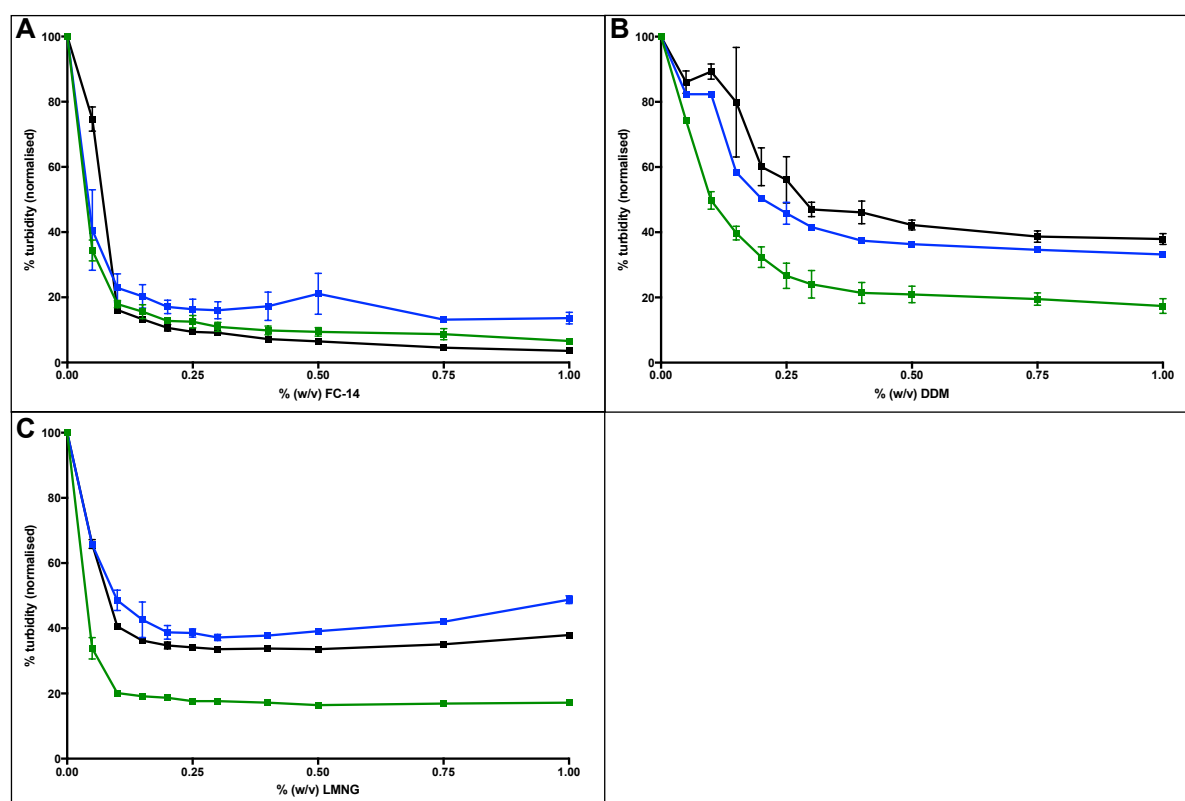


Figure 3: Visualisation of the solubilisation efficiency of the three detergents (A) FC-14, (B) DDM and (C) LMNG on HlyB-containing membranes from *E. coli* C41(DE3) (black line), C41(DE3)Δ*ompF* (blue line) and C41(DE3)Δ*ompF*Δ*acrAB* (green line).

Purification of membrane proteins from *E. coli* C41(DE3)Δ*ompF*Δ*acrAB*

The purification and subsequent biochemical characterisation of the ABC transporter HlyB has been previously published (25). Considering the results of the solubilisation assays we performed the purification of HlyB from C41(DE3)Δ*ompF*Δ*acrAB* membranes utilising the non-ionic detergents DDM and LMNG for extraction and subsequent purification steps. The original protocol published by Reimann *et al.* (25) that uses FC-14 for solubilisation, which is subsequently exchanged by LMNG while HlyB is immobilised on the IMAC column, yielded the largest amount of pure protein. However, in contrast to previous studies (25) the purification with non-ionic detergents yielded a substantial amount of HlyB with

comparable purity, confirming the improved extraction of HlyB from the membrane (Figure 4).

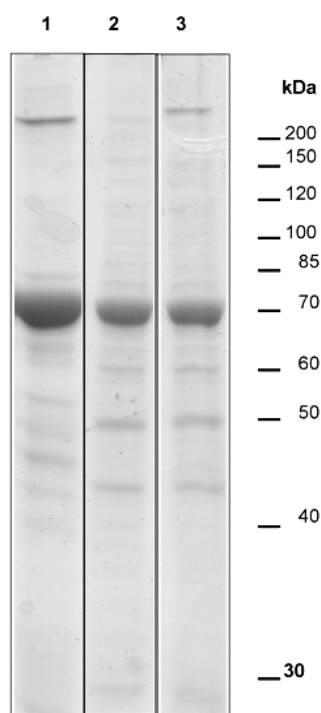


Figure 4: Coomassie Brilliant Blue stained SDS-PAGE of the purification of HlyB from *E. coli* C41(DE3) Δ *ompF* Δ *acrAB* employing different detergent-combinations for solubilisation (first detergent) and subsequent IMAC (second detergent). Shown are the pooled eluate fractions of equal volume. (1) Fos-choline 14 / LMNG, (2) DDM / DDM, (3) LMNG/ LMNG.

Purification of SecYEG and YidC from *E. coli* 41(DE3), C41(DE3) Δ *ompF* and C41(DE3) Δ *ompF* Δ *acrAB*

The protein conducting channel SecYEG and the insertase YidC are well-known and extensively studied *E. coli* membrane proteins, thus rendering them ideal candidates to perform test-purifications from C41(DE3), C41(DE3) Δ *ompF* and C41(DE3) Δ *ompF* Δ *acrAB*. For those, equal amounts of membranes were used and overall yield and purity were analysed by SDS-PAGE.

The protein translocase subunit SecY was found to be partially and nearly completely degraded in the membranes of C41(DE3) and C41(DE3) Δ *ompF*, respectively, which resulted in the purification of fragments termed SecY-N and SecY-C (figure 5). This degradation was unaffected by adding protease inhibitors to the membranes prior to purification, which indicates a proteolytic digest already during protein synthesis. However, using C41(DE3) Δ *ompF* Δ *acrAB* strongly reduced the degradation of SecY which resulted in a clear band for the full-length protein (figure 5). The other components of the protein conducting channel, SecE and SecG, were unaffected by the choice of expression strain.

For YidC, the effects of using C41(DE3) $\Delta ompF\Delta acrAB$ for the overexpression were less pronounced, however, a substantial increase in the yield of purified protein was observed, probably resulting from an increase in expression levels. This is reflected by a more intense band in the starting material (figure 5). We conclude that the use of C41(DE3) $\Delta ompF\Delta acrAB$ can lead to an increased yield of target protein, and furthermore, notably, can also improve its stability and provide a certain protection from degradation.

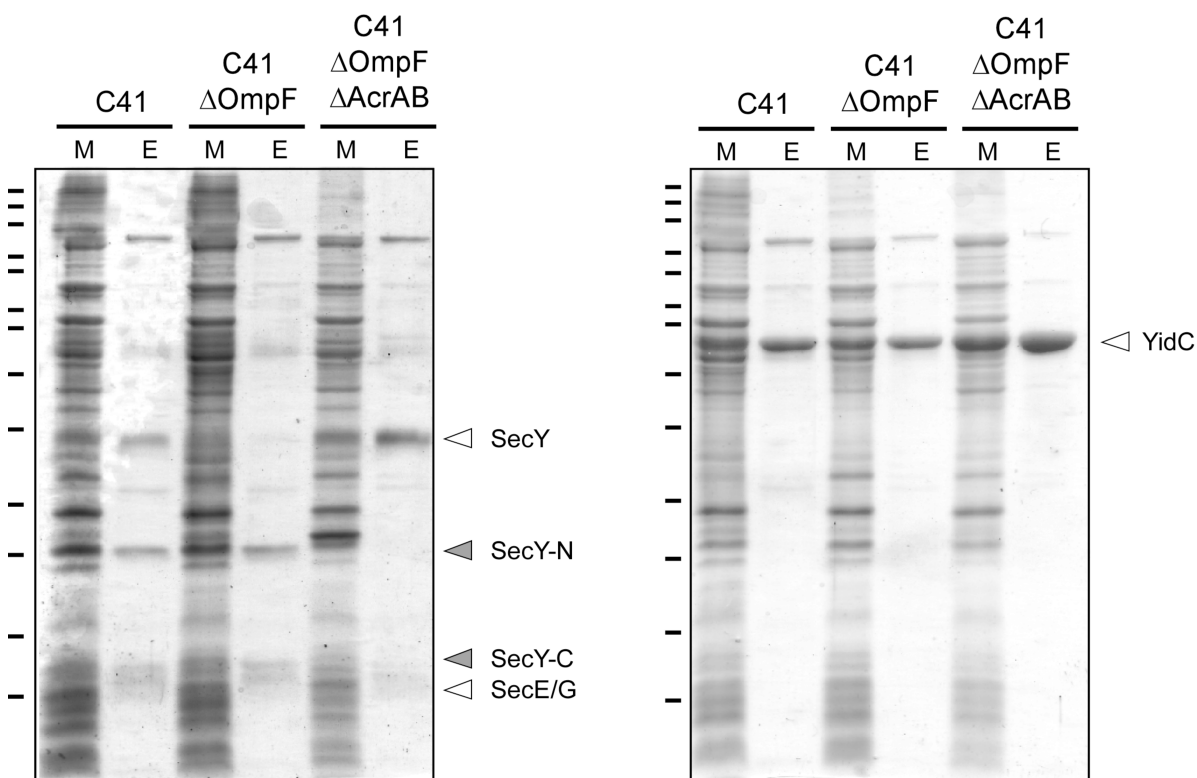


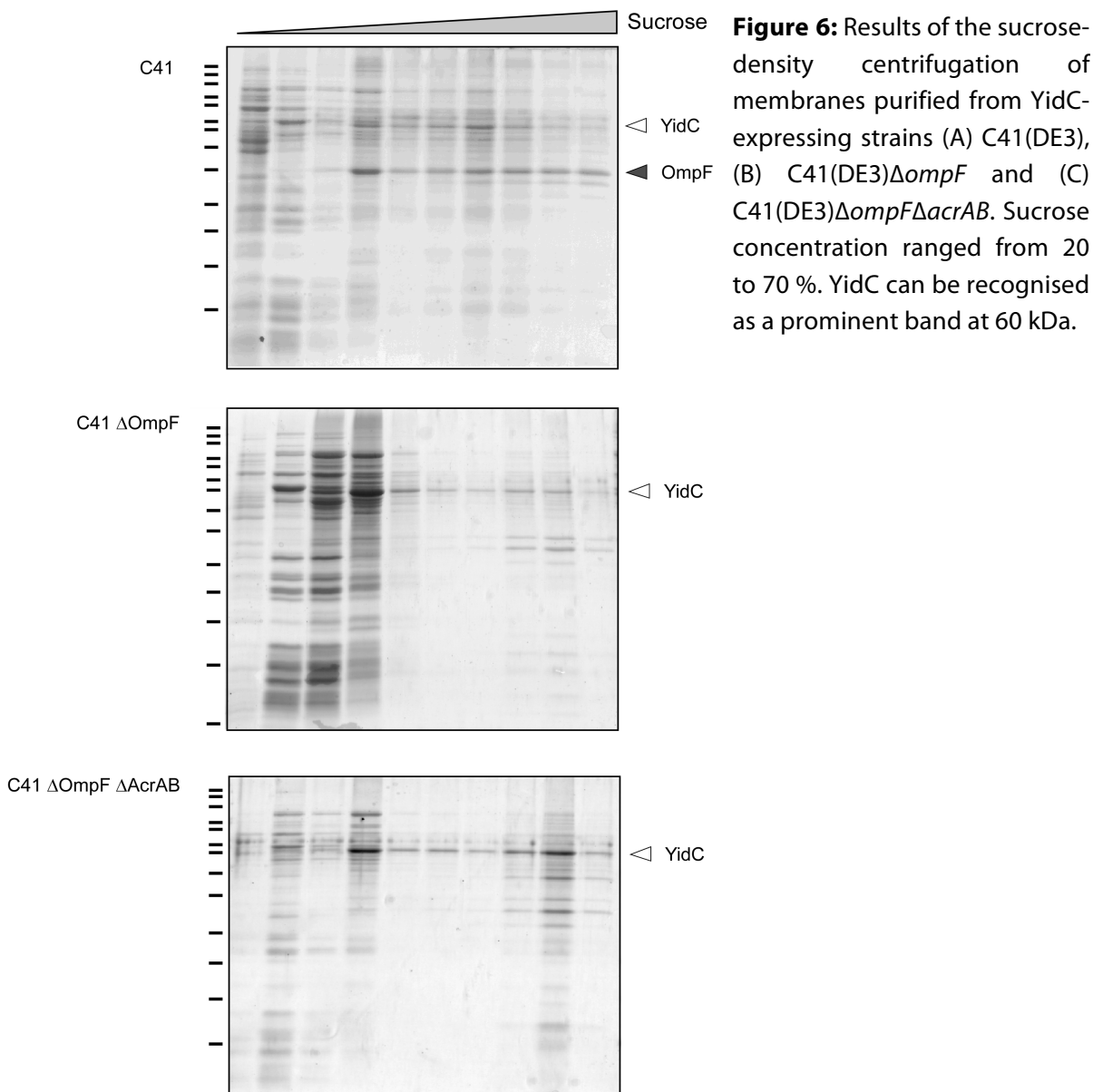
Figure 5: Purification of SecYEG and YidC from *E. coli* C41(DE3), C41(DE3) $\Delta ompF$ and C41(DE3) $\Delta ompF\Delta acrAB$. (A) Purification of SecYEG, M – starting material, E – eluted protein. Target protein and identified fragments are marked. (B) Purification of YidC, M – starting material, E – eluted protein. Target protein is marked.

Analysis of the membrane density by sucrose density gradient centrifugation

The YidC-containing membranes were fractionated and further analysed by sucrose density gradient centrifugation and SDS-PAGE. Early fractions (20 – 30 % sucrose) of all strains contained a large number of proteins and exhibited the characteristic pattern of ribosomes. Later fractions contained large amounts of YidC, however, its distribution varied between the three samples. In the parental strain, YidC is most prominent in fractions containing 30 – 50 % sucrose. The deletion of *ompF* resulted in a local concentration of YidC in fractions

containing approximately 30 % sucrose, but also in later fractions (50 – 70 % sucrose). The additional deletion of *acrAB* resulted in an even higher accumulation of YidC in these late fractions (figure 6). Our results suggest an alteration of the density of the membranes, which was further analysed by mass-spectrometric measurements of the lipidome.

Fractions of C41(DE3) also show a prominent band at approximately 40 kDa. Due to its absence from the other strains, this band very likely corresponds to OmpF and once more highlights the high abundance of this porin in *E. coli* membranes.



Analysis of the lipidomes by mass spectrometry

Mass spectrometry allows for detailed investigation of the lipidomes in respect to lipid head-groups, fatty acid tail lengths and overall lipid content. The main components of *E.coli* membranes are phosphatidylethanolamines (PE), phosphatidylglycerols (PG) and cardiolipins (CL). PE and PG contain two, CL four esterified fatty acid tails that can differ in length and / or saturation profile. In *E. coli* the main species of fatty acid tails are within the range of 16 to 18 carbon atoms (C16 – C18). For our analysis we chose cells overexpressing the ABC transporter HlyB, as here the most profound changes in the solubilisation of the membranes in different detergents were observed.

Phospholipids were extracted from the membrane samples applying the procedure of Bligh and Dyer (31) and the total amount of protein was determined by colorimetric assays. The quantification of total amounts of lipid and protein in membrane samples from C41(DE3), C41(DE3) $\Delta ompF$ and C41(DE3) $\Delta ompF \Delta acrAB$ revealed significant changes in the lipid to protein ratio. The deletion of *ompF* resulted in a 1.2-fold decrease in lipid content. Notably, the additional deletion of *acrAB* resulted in an overall 3.6-fold decline of total lipid (figure 7A).

Next, the membranes were analysed in respect to the phospholipid head group composition which was unaffected by both deletions (figure 7B).

To further investigate in detail the fatty acid composition of each subgroup (PE, PG, CL) all peaks of the chromatograms were assigned to the corresponding lipid molecules. A principle component analysis (PCA) was performed on the whole dataset of all phospholipid classes as a function of the fatty acids composition. The hierarchical clustering visualised three distinct groups of which each corresponded to one of the analysed strains. It attests differences in the lipidomes between the three strains and furthermore shows that C41(DE3) $\Delta ompF \Delta acrAB$ differs more from C41(DE3) than does C41(DE3) $\Delta ompF$ in terms of fatty acid composition (figure 7C).

The individual comparison of each identified lipid species between the three strains revealed a number of significant differences, which can overall be summarised as a decrease of C16 fatty acid tails in favour of C18 fatty acid tails (figure 7D). This effect is most pronounced in the CL and the PE subgroups. Furthermore, a slight increase of odd-numbered chains can be observed in the PE subgroup, however, this tendency was detected neither in the PG, nor in the CL subgroup (figure 7D).

In summary, the lipidomics data are in good agreement with the previously presented results and confirm an alteration of the cytosolic membrane composition as a result of the genomic deletions of *ompF* and *acrAB*.

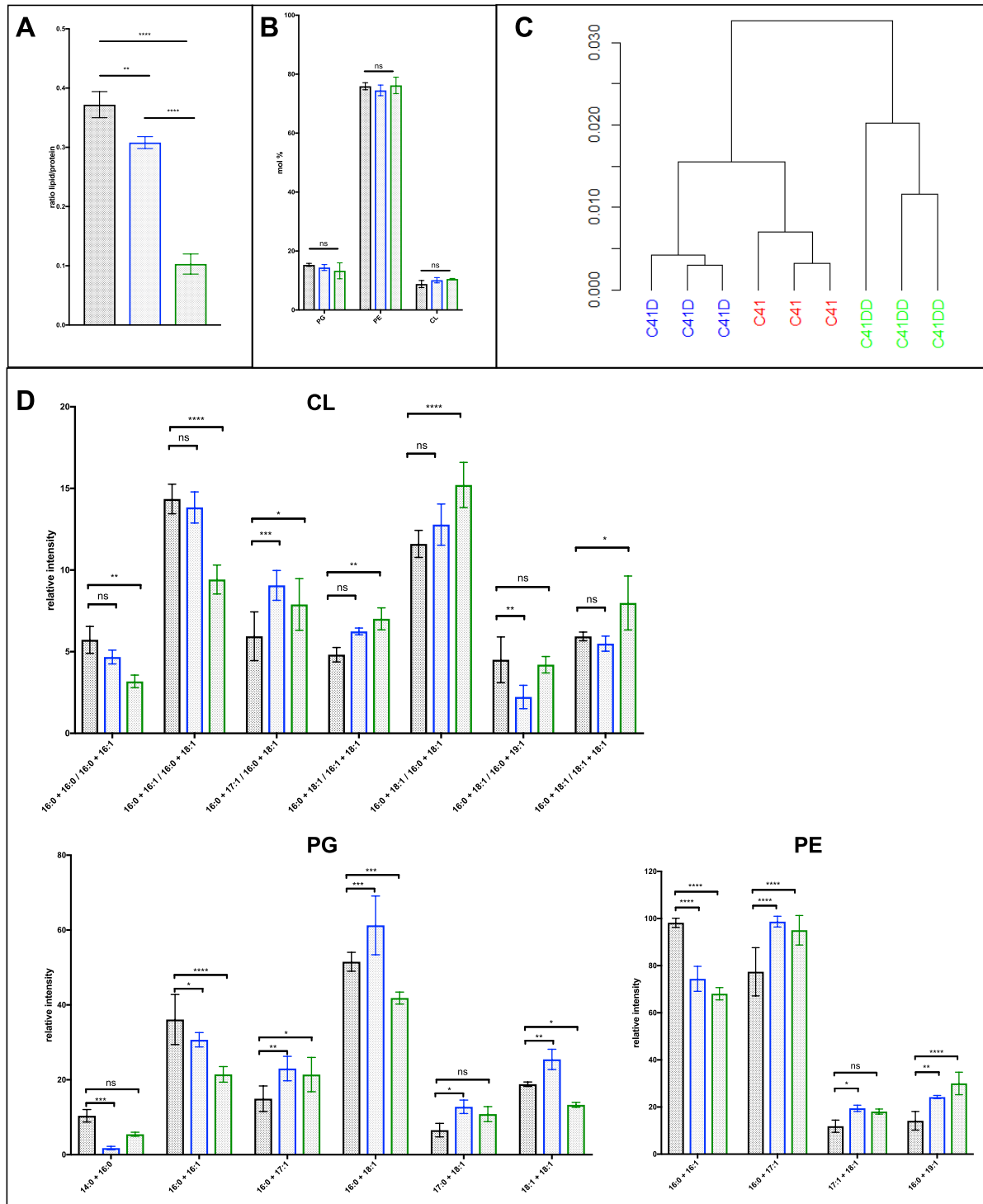


Figure 7: Analysis of the lipidomes of *E. coli* C41(DE3), C41(DE3) $\Delta ompF$ and C41(DE3) $\Delta ompF \Delta acrAB$, overexpressing the ABC transporter HlyB. (A) Lipid to protein ratio (w/w) in the membrane fractions of all three strains. P-values were calculated using a one-way ANOVA followed by a Tukey multiple comparisons test. Ns: not significant, *: $p < 0.0332$, **: $p < 0.0021$, ***: $p < 0.0002$. (B) Distribution of lipid head groups within the lipidomes of all three strains. No significant changes were detected. P-values were calculated using a two-way ANOVA followed by a Tukey multiple comparisons test. Ns: not significant. (C) Pearson-diagram visualising the results of PCA analysis of the whole MS dataset by hierarchical clustering as a function of fatty acid composition of the strains. (D) Diagrams summarising the statistically significant changes within

the subgroups (CL, PG, PE) of the lipidomes of all strains. The data was analysed by applying a two-way ANOVA followed by a Tukey multiple comparisons test to correct the P-values. Ns: not significant, *: $p < 0.0332$, **: $p < 0.0021$, ***: $p < 0.0002$, **** $p < 0.0001$ Due to the semi-quantitative nature of the method the height of the peaks does not reflect the abundance of the corresponding lipid in the membrane fraction.

Mass spectrometric analysis of the proteomes

The proteomes of C41(DE3), C41(DE3) $\Delta ompF$ C41(DE3) $\Delta ompF\Delta acrAB$ were analysed by mass spectrometry. The abundances of approximately 1400 different gene products were compared between the three strains.

The overall protein abundance patterns of C41(DE3) $\Delta ompF$ and C41(DE3) $\Delta ompF\Delta acrAB$ were found to be similar, as no clear abundance changes of single proteins were obvious except, as expected, for AcrA.

However, large differences became apparent when the single and double deletion strains were compared to the parental strain C41(DE3) (Figure 8). Beside the expected depletion of OmpF and additionally AcrA in C41(DE3) $\Delta ompF\Delta acrAB$, the two deletion strains show lower intensities of proteins targeted to the periplasmic space (p -value = $1 \text{ E-}6$ for $\Delta ompF$ and $6.2 \text{ E-}6$ for $\Delta ompF\Delta acrAB$) as well as higher abundances of plasma membrane associated proteins (p -value = 0.00029 for $\Delta ompF$ and 0.00098 for $\Delta ompF\Delta acrAB$). For example, the TMAO reductase TorT was found with high intensity in the parental strain samples but not in the deletion strains. Furthermore, periplasmic chaperones were significantly reduced whereas members of the outer membrane protein insertion complex (BAM, BamB and BamD) showed an increased abundance in the deletion strains.

Some differences were also found in proteins involved in LPS and lipid biosynthesis and/ or transport. The abundance of RfaQ, a heptosyltransferase involved in LPS biosynthesis (35), and the LPS-assembly protein LptD (36) were increased, while that of the LPS export LptA (37), which mediates the transport of LPS to the outer membrane, was decreased. Furthermore, the cyclopropane-fatty-acyl-phospholipid synthase (38) and the lysophospholipid lipase (39,40), both involved in the biogenesis of lipids, were reduced. Additionally, a decrease in the outer membrane protein MlaD was noted, which proved a direct link to the deletion of *ompF*. MlaD, as part of the MlaFEDB complex (41), is involved in the intermembrane phospholipid transport system, which maintains the asymmetry of the outer membrane. OmpF forms a complex with MlaA (41), which is thought to extract lipids

from the outer membrane and to pass it on to the MlaFEDB complex for subsequent translocation.

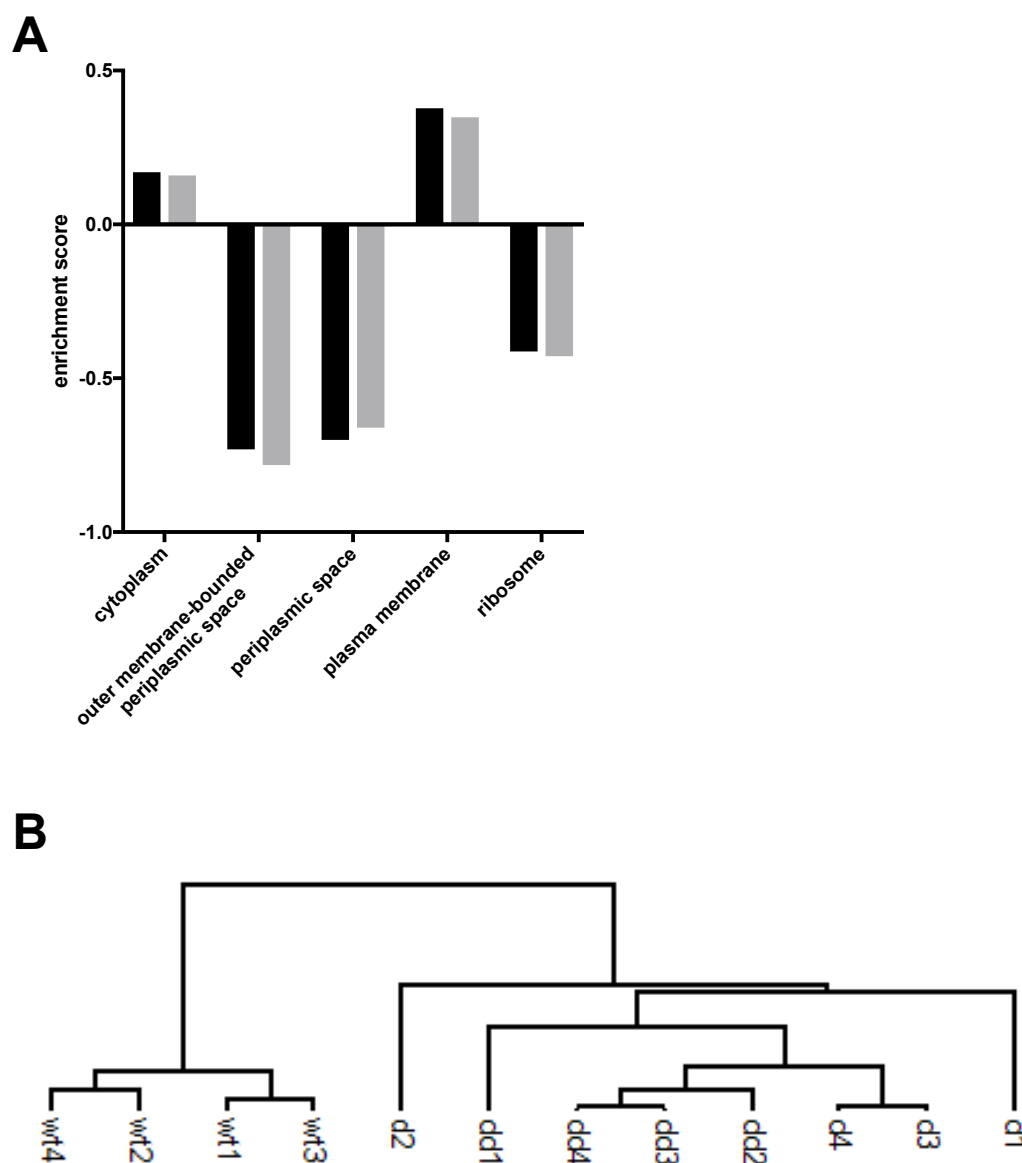


Figure 8: Summary of proteomics data. (A) – C41(DE3)ΔompF (black) and C41(DE)ΔompFΔacrAB (grey) compared to C41(DE3). Negative values mark a decrease, positive values an enrichment in protein in the corresponding cellular compartment. (B) – Cluster analysis of C41(DE3) (wt), C41(DE3)ΔompF (d) and C41(DE)ΔompFΔacrAB (dd).

In summary, the proteome analysis supports the previously described results and the theory of an altered lipid metabolism and/ or membrane biogenesis being responsible for the observed phenotypes in the *ompF* and *acrAB*-depleted strains.

Discussion

The purpose of this study was to construct an OmpF and AcrB depleted expression strain to improve the purity of membrane protein preparations. Whilst achieving this goal, we noted an overall increased overproduction of membrane proteins accompanied by altered membrane properties. Thus, we further characterised the new expression strain *E. coli* C41(DE3) Δ *ompF* Δ *acrAB*, which was confirmed to be largely advantageous for the overexpression and purification of a range of membrane proteins.

Sequencing of the genome revealed no differences to the parental strain C41(DE3) apart from the desired deletions, thus all effects observed result from the lack of OmpF and AcrAB in the membranes.

The strains revealed an improved growth to higher ODs upon the deletion of *ompF* while the additional deletion of *acrAB* had no further effect (figure 1).

We observed improved solubilisation efficiency with non-ionic detergents of a protein that was previously only extractable by using harsh zwitterionic detergents like FC-14 (figure 3, figure 4). Yield and purity of a number of proteins were largely improved, on one hand by the removal of OmpF and AcrB as impurities, but also due to decreased proteolytic degradation (SecYEG, figure 5), higher stability in a greater range of detergents (25) (figure 4) and, overall, a higher amount of incorporated target protein into the membrane (figure 2, figure 5).

A change in membrane characteristics was confirmed by sucrose density gradient centrifugation (figure 6) and detailed analysis of the lipidome by mass spectrometry (figure 6). We observed an altered membrane composition in terms of fatty acid tails in the individual lipid species, while the overall head group distribution was not affected. The lipid to protein ratio was significantly decreased and is coherent with the observed change in density (figure 6, figure 7). To complete our characterisation we analysed the proteomes, which revealed interesting changes in the protein content of the deletion strain (figure 8). Notably, we observed striking differences in the abundance of proteins related to or localised to the periplasm and the plasma membrane.

We conclude that the deletions of *ompF* and *acrAB* led to changes in the lipidome and thus, in the membrane characteristics. We hypothesise that the altered membrane properties facilitate the incorporation of detergent molecules, which subsequently results in improved

solubilisation of the membranes. Especially odd chain-lengths, which were found to be slightly increased, promote reduced densities of lipid bilayers.

Furthermore, OmpF was shown to be part of the Mla lipid transport machinery (41), which is maintaining the asymmetry of the outer membrane leaflets by shuttling lipids from the outer to the inner membrane leaflet. MlaA and OmpF, both located in the outer membrane, have been proposed to mediate the extraction of lipids and to subsequently pass them on to the MlaFEDB complex, which is located in the inner membrane where it mediates the transport (41,42). A defect in this transport system presumably leads to an increase of lipid molecules in the outer membrane and thus, changes the characteristics of the outer membrane of *E. coli*. A reduction of MalD was confirmed by the proteome analysis. It seems likely that the reduction of periplasmic proteins can be explained also by this change of membrane characteristics.

OmpF and AcrAB were both found to be involved in the fatty acid metabolism of *E. coli* by importing short chain fatty acids into the periplasm from the extracellular space and by exporting short-chain as well as long-chain fatty acids to the extracellular medium, respectively (19,20,43). Furthermore, the deletion of OmpF has been linked to an improved membrane integrity and tolerance towards certain substances and antibiotics by decreasing their influx, which provides a possible explanation for the improved growth of OmpF-depleted strains (43-45).

Our results characterise the new expression strains on lipid and protein level. Our findings link the observed phenotypes mainly to an alteration in membrane biogenesis. While previous studies to improve overexpression properties of a strain rather targeted the *lac*-promoter region (6,10,41) we present an entirely new approach by modifying the membrane environment instead, which we show to be a valid alternative to improve the membrane-incorporation, stability and subsequent downstream purification processes of overexpressed membrane proteins.

Acknowledgements

We would like to thank the members of the Institut de Biologie Physico-Chimique, Paris, France for the fruitful collaboration. Last, we would like to thank all members of the Institute of Biochemistry, especially Sander Smits, for stimulating discussions. This work was funded by the DFG through CRC1208 (project Z01 to K.S. and project A01 to L.S.).

References

1. Wallin, E., and von Heijne, G. (1998) Genome-wide analysis of integral membrane proteins from eubacterial, archaean, and eukaryotic organisms. *Protein Sci* **7**, 1029-1038
2. Lundstrom, K. (2007) Structural genomics and drug discovery. *J Cell Mol Med* **11**, 224-238
3. Wagner, S., Baars, L., Ytterberg, A. J., Klussmeier, A., Wagner, C. S., Nord, O., Nygren, P. A., van Wijk, K. J., and de Gier, J. W. (2007) Consequences of membrane protein overexpression in *Escherichia coli*. *Mol Cell Proteomics* **6**, 1527-1550
4. Studier, F. W., and Moffatt, B. A. (1986) Use of bacteriophage T7 RNA polymerase to direct selective high-level expression of cloned genes. *J Mol Biol* **189**, 113-130
5. Wagner, S., Klepsch, M. M., Schlegel, S., Appel, A., Draheim, R., Tarry, M., Hogbom, M., van Wijk, K. J., Slotboom, D. J., Persson, J. O., and de Gier, J. W. (2008) Tuning *Escherichia coli* for membrane protein overexpression. *Proc Natl Acad Sci U S A* **105**, 14371-14376
6. Miroux, B., and Walker, J. E. (1996) Over-production of proteins in *Escherichia coli*: mutant hosts that allow synthesis of some membrane proteins and globular proteins at high levels. *J Mol Biol* **260**, 289-298
7. Schlegel, S., Lofblom, J., Lee, C., Hjelm, A., Klepsch, M., Strous, M., Drew, D., Slotboom, D. J., and de Gier, J. W. (2012) Optimizing membrane protein overexpression in the *Escherichia coli* strain Lemo21(DE3). *J Mol Biol* **423**, 648-659
8. Kwon, S. K., Kim, S. K., Lee, D. H., and Kim, J. F. (2015) Comparative genomics and experimental evolution of *Escherichia coli* BL21(DE3) strains reveal the landscape of toxicity escape from membrane protein overproduction. *Sci Rep* **5**, 16076
9. Arechaga, I., Miroux, B., Karrasch, S., Huijbregts, R., de Kruijff, B., Runswick, M. J., and Walker, J. E. (2000) Characterisation of new intracellular membranes in *Escherichia coli* accompanying large scale over-production of the b subunit of F(1)F(o) ATP synthase. *FEBS Lett* **482**, 215-219
10. Angius, F., Illoaia, O., Amrani, A., Suisse, A., Rosset, L., Legrand, A., Abou-Hamdan, A., Uzan, M., Zito, F., and Miroux, B. (2018) A novel regulation mechanism of the T7 RNA polymerase based expression system improves overproduction and folding of membrane proteins. *Sci Rep* **8**, 8572
11. Seddon, A. M., Curnow, P., and Booth, P. J. (2004) Membrane proteins, lipids and detergents: not just a soap opera. *Biochim Biophys Acta* **1666**, 105-117
12. Arachea, B. T., Sun, Z., Potente, N., Malik, R., Isailovic, D., and Viola, R. E. (2012) Detergent selection for enhanced extraction of membrane proteins. *Protein Expr Purif* **86**, 12-20
13. Du, D., Wang, Z., James, N. R., Voss, J. E., Klimont, E., Ohene-Agyei, T., Venter, H., Chiu, W., and Luisi, B. F. (2014) Structure of the AcrAB-TolC multidrug efflux pump. *Nature* **509**, 512-515
14. Wiseman, B., Kilburg, A., Chaptal, V., Reyes-Mejia, G. C., Sarwan, J., Falson, P., and Jault, J. M. (2014) Stubborn contaminants: influence of detergents on the purity of the multidrug ABC transporter BmrA. *PLoS One* **9**, e114864
15. Veessler, D., Blangy, S., Cambillau, C., and Sciara, G. (2008) There is a baby in the bath water: AcrB contamination is a major problem in membrane-protein crystallization. *Acta Crystallogr Sect F Struct Biol Cryst Commun* **64**, 880-885

16. Kefala, G., Ahn, C., Krupa, M., Esquivies, L., Maslennikov, I., Kwiatkowski, W., and Choe, S. (2010) Structures of the OmpF porin crystallized in the presence of foscholine-12. *Protein Sci* **19**, 1117-1125
17. Chaptal, V., Kilburg, A., Flot, D., Wiseman, B., Aghajari, N., Jault, J. M., and Falson, P. (2016) Two different centered monoclinic crystals of the E. coli outer-membrane protein OmpF originate from the same building block. *Biochim Biophys Acta* **1858**, 326-332
18. Zhou, J., Wang, K., Xu, S., Wu, J., Liu, P., Du, G., Li, J., and Chen, J. (2015) Identification of membrane proteins associated with phenylpropanoid tolerance and transport in Escherichia coli BL21. *J Proteomics* **113**, 15-28
19. Lennen, R. M., Politz, M. G., Kruziki, M. A., and Pfleger, B. F. (2013) Identification of transport proteins involved in free fatty acid efflux in Escherichia coli. *J Bacteriol* **195**, 135-144
20. Rodriguez-Moya, M., and Gonzalez, R. (2015) Proteomic analysis of the response of Escherichia coli to short-chain fatty acids. *J Proteomics* **122**, 86-99
21. Baba, T., Ara, T., Hasegawa, M., Takai, Y., Okumura, Y., Baba, M., Datsenko, K. A., Tomita, M., Wanner, B. L., and Mori, H. (2006) Construction of Escherichia coli K-12 in-frame, single-gene knockout mutants: the Keio collection. *Mol Syst Biol* **2**, 2006 0008
22. Thomason, L. C., Costantino, N., and Court, D. L. (2007) E. coli genome manipulation by P1 transduction. *Curr Protoc Mol Biol* **Chapter 1**, Unit 1 17
23. Cherepanov, P. P., and Wackernagel, W. (1995) Gene disruption in Escherichia coli: TcR and KmR cassettes with the option of Flp-catalyzed excision of the antibiotic-resistance determinant. *Gene* **158**, 9-14
24. Datsenko, K. A., and Wanner, B. L. (2000) One-step inactivation of chromosomal genes in Escherichia coli K-12 using PCR products. *Proc Natl Acad Sci U S A* **97**, 6640-6645
25. Reimann, S., Poschmann, G., Kanonenberg, K., Stuhler, K., Smits, S. H., and Schmitt, L. (2016) Interdomain regulation of the ATPase activity of the ABC transporter haemolysin B from Escherichia coli. *Biochem J* **473**, 2471-2483
26. van der Sluis, E. O., Nouwen, N., and Driessen, A. J. (2002) SecY-SecY and SecY-SecG contacts revealed by site-specific crosslinking. *FEBS Lett* **527**, 159-165
27. Kedrov, A., Wickles, S., Crevenna, A. H., van der Sluis, E. O., Buschauer, R., Berninghausen, O., Lamb, D. C., and Beckmann, R. (2016) Structural Dynamics of the YidC:Ribosome Complex during Membrane Protein Biogenesis. *Cell Rep* **17**, 2943-2954
28. Kedrov, A., Kusters, I., Krasnikov, V. V., and Driessen, A. J. (2011) A single copy of SecYEG is sufficient for preprotein translocation. *EMBO J* **30**, 4387-4397
29. Grube, L., Dellen, R., Kruse, F., Schwender, H., Stuhler, K., and Poschmann, G. (2018) Mining the Secretome of C2C12 Muscle Cells: Data Dependent Experimental Approach To Analyze Protein Secretion Using Label-Free Quantification and Peptide Based Analysis. *J Proteome Res* **17**, 879-890
30. Vizcaino, J. A., Csordas, A., Del-Toro, N., Dianes, J. A., Griss, J., Lavidas, I., Mayer, G., Perez-Riverol, Y., Reisinger, F., Ternent, T., Xu, Q. W., Wang, R., and Hermjakob, H. (2016) 2016 update of the PRIDE database and its related tools. *Nucleic Acids Res* **44**, 11033
31. Bligh, E. G., and Dyer, W. J. (1959) A rapid method of total lipid extraction and purification. *Can J Biochem Physiol* **37**, 911-917

32. Ramos, R. G., Libong, D., Rakotomanga, M., Gaudin, K., Loiseau, P. M., and Chaminade, P. (2008) Comparison between charged aerosol detection and light scattering detection for the analysis of Leishmania membrane phospholipids. *J Chromatogr A* **1209**, 88-94
33. Pulfer, M., and Murphy, R. C. (2003) Electrospray mass spectrometry of phospholipids. *Mass Spectrom Rev* **22**, 332-364
34. Tyurin, V. A., Tyurina, Y. Y., Jung, M. Y., Tungekar, M. A., Wasserloos, K. J., Bayir, H., Greenberger, J. S., Kochanek, P. M., Shvedova, A. A., Pitt, B., and Kagan, V. E. (2009) Mass-spectrometric analysis of hydroperoxy- and hydroxy-derivatives of cardiolipin and phosphatidylserine in cells and tissues induced by pro-apoptotic and pro-inflammatory stimuli. *J Chromatogr B Analyt Technol Biomed Life Sci* **877**, 2863-2872
35. Mudapaka, J., and Taylor, E. A. (2015) Cloning and characterization of the Escherichia coli Heptosyltransferase III: Exploring substrate specificity in lipopolysaccharide core biosynthesis. *FEBS Lett* **589**, 1423-1429
36. Chng, S. S., Ruiz, N., Chimalakonda, G., Silhavy, T. J., and Kahne, D. (2010) Characterization of the two-protein complex in Escherichia coli responsible for lipopolysaccharide assembly at the outer membrane. *Proc Natl Acad Sci U S A* **107**, 5363-5368
37. Tran, A. X., Trent, M. S., and Whitfield, C. (2008) The LptA protein of Escherichia coli is a periplasmic lipid A-binding protein involved in the lipopolysaccharide export pathway. *J Biol Chem* **283**, 20342-20349
38. Guangqi, E., Lesage, D., and Ploux, O. (2010) Insight into the reaction mechanism of the Escherichia coli cyclopropane fatty acid synthase: isotope exchange and kinetic isotope effects. *Biochimie* **92**, 1454-1457
39. Cho, H., and Cronan, J. E., Jr. (1993) Escherichia coli thioesterase I, molecular cloning and sequencing of the structural gene and identification as a periplasmic enzyme. *J Biol Chem* **268**, 9238-9245
40. Cho, H., and Cronan, J. E., Jr. (1995) Defective export of a periplasmic enzyme disrupts regulation of fatty acid synthesis. *J Biol Chem* **270**, 4216-4219
41. Ekiert, D. C., Bhabha, G., Isom, G. L., Greenan, G., Ovchinnikov, S., Henderson, I. R., Cox, J. S., and Vale, R. D. (2017) Architectures of Lipid Transport Systems for the Bacterial Outer Membrane. *Cell* **169**, 273-285 e217
42. Lepore, B. W., Indic, M., Pham, H., Hearn, E. M., Patel, D. R., and van den Berg, B. (2011) Ligand-gated diffusion across the bacterial outer membrane. *Proc Natl Acad Sci U S A* **108**, 10121-10126
43. Tan, Z., Black, W., Yoon, J. M., Shanks, J. V., and Jarboe, L. R. (2017) Improving Escherichia coli membrane integrity and fatty acid production by expression tuning of FadL and OmpF. *Microb Cell Fact* **16**, 38
44. Moya-Torres, A., Mulvey, M. R., Kumar, A., Oresnik, I. J., and Brassinga, A. K. (2014) The lack of OmpF, but not OmpC, contributes to increased antibiotic resistance in Serratia marcescens. *Microbiology* **160**, 1882-1892
45. Kojima, S., and Nikaido, H. (2013) Permeation rates of penicillins indicate that Escherichia coli porins function principally as nonspecific channels. *Proc Natl Acad Sci U S A* **110**, E2629-2634

3.6 Chapter VI – Identifying a Secretion Signal in RTX Toxins

Title: **A Conserved Motif in the C-terminus of RTX Toxins is Essential for their Secretion via Type I Secretion Systems**

Authors: Kerstin Kanonenberg, Sandra Peherstorfer, Michael Lenders, Sander H. J. Smits, Lutz Schmitt

Published in: *to be submitted*

Impact Factor:

Own Work: 40 %
Bioinformatic analyses of RTX toxins
Designing mutants
Overexpression and purification of HlyA mutants
Writing of the manuscript

A Conserved Motif in the C-terminus of RTX Toxins is Essential for their Secretion via Type I Secretion Systems

Kerstin Kanonenberg, Sandra Peherstorfer, Michael HH Lenders, Sander HJ Smits, Lutz Schmitt

Institute of Biochemistry, Heinrich Heine University Düsseldorf, Germany

*: To whom correspondence should be addressed:

Lutz Schmitt, Institute of Biochemistry, Heinrich-Heine-University Düsseldorf,
Universitätsstr. 1, 40225 Düsseldorf, Germany

Phone: +49211-81-10773, Fax: 49211-81-15310, Email: lutz.schmitt@hhu.de

Abstract

Type I secretion systems are widespread across Gram-negative bacteria. Despite their relatively simple assembly they mediate the transport of a wide range of proteins of broad functional diversity and size. In general, the secretion signal has been located to the C-terminus and is not cleaved during secretion, however, no conserved motif has been identified so far that targets type I substrates to their dedicated transport system.

In this study, we have analysed the C-termini of RTX toxins by *in silico* methods and were able to identify a consensus motif approximately 30 amino acids upstream of the C-terminus. Subsequent *in vitro* studies confirm the importance of the motif for secretion and furthermore showed that the haemolytic activity of the activated toxin was not affected.

We suggest that RTX toxins are recognised by their transporter by this consensus sequence via a combination of a secondary structure and primary amino acid sequence motif within close proximity to the C-terminus.

Introduction

Secretion systems are a vital part of the proteomes of prokaryotic organisms and essential for their interaction with the extracellular environment. In Gram-negative bacteria, where secretion of (macro)molecules needs to take place across two membranes, a variety of complex secretion mechanisms have evolved. Some of these export machineries are able to translocate their substrates across both membranes in one step, without the occurrence of periplasmic intermediates. Namely, these are Type I, IV, V and VI secretion systems. Notably, more than 15 different types of secretion systems have been identified so far in Gram-negative organisms (1).

In this study, we focused on type I secretion systems. The secretory complex is built out of three membrane-localised proteins: an outer membrane porin (TolC-like, OMP) and an ABC transporter in complex with a membrane fusion protein (MFP) in the inner membrane (2,3). Upon recognition of its dedicated substrate in the cytosol, the three components form a tunnel-shaped complex that spans the periplasm, and the substrate is subsequently transported to the extracellular space (4,5).

The substrates of T1SS are of broad functional diversity and size. One small group comprises the class II microcins, a class of bacteriocins that are secreted by Gram-negative bacteria. They are only 5-6 kDa in size and contain an N-terminal secretion signal that is cleaved prior to secretion (6). However, the majority of T1SS substrates, which function as proteases, lipases, exotoxins or adhesins, possess a C-terminal secretion signal that is not cleaved during the secretion process (5,7,8).

One class of substrates comprises the family of so-called RTX (“repeats-in-toxin”) proteins. These proteins contain conserved aspartate and glycine-rich nonapeptide repeats (9,10) that bind calcium ions in the high macromolar range (11,12), which consequently induces the folding of the entire protein. As the cytosolic free calcium ion concentration is within the high nanomolar range (13), RTX proteins remain unfolded until they reach the extracellular space.

RTX proteins are secreted unfolded and C-terminus first, as it has been shown for the toxin HlyA from *Escherichia coli* and CyaA from *Bordetella pertussis* (14-16).

Many ABC transporters that are involved in type I secretion processes contain an additional domain to the canonical build of ABC transporters, located at the N-terminus (17,18). The

presence of these domains is essential for secretion. In class II microcin-T1SS, this domain is a C39-peptidase that cleaves the substrate prior to secretion (6). However, in many T1SS-ABC transporters these domains are catalytically non-functional, and thus called C39 peptidase like domains (CLD) (18). They have been shown to interact with the substrates, more precisely with the RTX domains (18), but their detailed function within the secretion process is still unknown.

Some T1SS-ABC transporters contain no additional domains, such as the HasA-secretion system from *Serratia marcescens*. Interestingly, the chaperone SecB is required for secretion in this particular T1SS (19), but whether this is linked to a missing CLD, suggesting a chaperone-like activity for CLDs, is not yet known.

A membrane fusion protein forms a complex with the ABC transporter in the inner membrane (20). It is thought to function as the major site of interaction between the inner-membrane complex and the OMP (20,21). MFPs sometimes contain a small cytosolic domain and in the case of HlyD, it was shown that this forms the hub from which assembly of the complex is initiated (21). However, it is still unknown which part of the substrate interacts with the cytosolic domain of the MFP.

To date, not much is known about the precise nature of the secretion signal of T1SS-substrates. However, considering the different types of substrates that are secreted by T1SS, a certain variation within the secretion signals would not be surprising. For HlyA it was found to be located within the last 50 to 60 amino acids of the polypeptide chain (5,8,18,22). Previous studies suggest minimum one further point of interaction with the ABC transporter that is located N-terminal to this area (18,23). In this study, we analyse the nature of the secretion signal of RTX proteins in greater detail by bioinformatic means and subsequent secretion experiments. Furthermore, we analysed the haemolytic activity of the mutants to assess a possible influence on the functionality of the protein.

Materials and Methods

Secretion assay of proHlyA-mutants

The secretion rate of the proHlyA mutants was determined as it was described before (24). Briefly, *E. coli* BL21(DE3) were transformed with pSU-HlyA plasmids and pK-184-HlyBD and selected on agar plates containing the appropriate antibiotics. Main cultures were inoculated to an OD₆₀₀ of 0.1 with overnight cultures grown from single colonies. Cultures were incubated at 37°C, 180 rpm until an OD₆₀₀ of 0.6. Protein expression was induced by adding IPTG to a final concentration of 1 mM. At the same time, Ca²⁺ was added to a final concentration of 10 mM. Cells were grown for a total of 4 h. Every hour, samples were taken and the supernatant was analysed by SDS-PAGE. ProHlyA as well as the secretion apparatus was subsequently quantified and the secretion rates were determined as amino acids per second and transporter as described in detail in Lenders et al. 2016 (24).

In vitro acylation assay and haemolytic activity of HlyA

To assess the activity of the secreted proHlyA mutants an *in vitro* acylation protocol was applied as described in Thomas et al. 2014 (25). Briefly, the proHlyA mutants were unfolded in 6 M urea and any divalent cations were removed by adding 10 mM EDTA. ProHlyA was mixed with HlyC and acyl-carrier protein (ACP) and the haemolysis-efficiency on erythrocytes was quantified by measuring the haemoglobin-release at 544 nm (25).

Overexpression and purification of proHlyA and mutants from inclusion bodies

E. coli BL21(DE3) cells were transformed with pSU-HlyA (25) and selected on LB-agar plates containing 100 µg/mL ampicillin. An overnight culture with 2YT medium and 100 µg/mL ampicillin was inoculated with a single colony and incubated for 15 h at 200 rpm, 37 °C. The main cultures were grown in 5 L-baffled flasks, containing 1 L of selective 2YT medium with 100 µg/mL ampicillin. Main cultures were inoculated from overnight cultures to OD₆₀₀ of 0.1 and grown at 37 °C, 200 rpm to OD₆₀₀ of 0.6. The expression of proHlyA was induced by adding IPTG to a final concentration of 1 mM. Incubation was continued for 4 h and cells were harvested by centrifugation (8000 xg, 10 min, 4 °C).

For the purification of proHlyA, cells were resuspended in buffer A (50 mM HEPES pH 7.4, 150 mM NaCl, 10 % (w/v) glycerol, 0.05 % (w/v) NaN₃) and lysed by passing three times through a cell disruptor at 1.5 kbar (Microfluidics). Inclusion bodies were collected by

centrifugation at 18,000 xg for 30 min. The pellets were washed and centrifuged successively in (1) buffer W1 (50 mM HEPES, pH 7.4, 50 mM EDTA, 1 % (w/v) Triton X-100, 0.05 % (w/v) NaN₃) and (2) buffer W2 (50 mM HEPES, pH 7.4, 1 mM EDTA, 1 M NaCl, 0.05 % (w/v) NaN₃). The pellet was solubilised overnight in buffer S (20 mM HEPES pH 7.4, 20 mM NaCl, 6 M urea). Insoluble material was removed by ultra-centrifugation (150,000 xg, 30 min, 4°C) and the urea-solubilised inclusion bodies were stored at -80°C.

Cloning of proHlyA mutants

Mutations were introduced to the proHlyA plasmid pSU-HlyA (25) by applying the quick-change PCR method using the primers listed in table 1.

Table 1: Primers used for quick-change PCRs

Mutant	Forward primer	Reverse primer
P975G	CAGGGTGATCTTAATGGATTAATTAA TGAAATCAGC	GCTGATTTCATTAATTAATCCATTAAGA TCACCCTG
N978G	GATCTTAATCCATTAATTGGTGAAAT CAGCAAAATC	GATTTTGCTGATTTCACCAATTAATGGA TTAAGATC
E979G	CCATTAATTAATGGAATCAGCAAAAT CATTTTCAGCTGC	GCAGCTGAAATGATTTTGCTGATTCCAT TAATTAATGG
E979P	CCATTAATTAATCCAATCAGCAAAAT CATTTTCAGCTGC	GCAGCTGAAATGATTTTGCTGATTGGAT TAATTAATGG
I980S	CCATTAATTAATGAATCCAGCAAAAT CATTTTCAGCTGC	GCAGCTGAAATGATTTTGCTGGATTCAT TAATTAATGG
I980P	CCATTAATTAATGAACCCAGCAAAAT CATTTTCAGCTGC	GCAGCTGAAATGATTTTGCTGGGTTTCAT TAATTAATGG
S981I	CATTAATTAATGAAATCATCAAAATC ATTTTCAGC	GCTGAAATGATTTTGATGATTTCATTAA TTAATG
S981P	CATTAATTAATGAAATCCCCAAAATC ATTTTCAGCTG	CAGCTGAAATGATTTTGGGGATTTCATT AATTAATG
K982T	CCATTAATTAATGAAATCAGCACAAT CATTTTCAGCTGC	GCAGCTGAAATGATTGTGCTGATTTCAT TAATTAATGG
K982P	CCATTAATTAATGAAATCAGCCCAAT CATTTTCAGCTGC	GCAGCTGAAATGATTGGGCTGATTTCAT TTAATTAATGG
S985A	CAGCAAAATCATTGCAGCTGCAGG	CCTGCAGCTGCAATGATTTTGCTG
S985P	CAGCAAAATCATTCCAGCTGCAGG	CCTGCAGCTGGAATGATTTTGCTG
F990P	CATTTTCAGCTGCAGGTAGCCCCGAT GTAAAGAGGAAAG	CTTTCCTCTTTAACATCGGGGCTACCTG CAGCTGAAATG
I984S	GAAATCAGCAAAATCAGCTCAGCTG CAGG	CCTGCAGCTGAGCTGATTTTGCTGATT C
I984P	GAAATCAGCAAAATCCCTTCAGCTG CAG	CTGCAGCTGAAGGGATTTTGCTGATTTC
I983S	GAAATCAGCAAAAGCATTTTCAGCTG	CTGCAGCTGAAATGCTTTTGCTGATTTC

	CAG	
I983P	GAAATCAGCAAACCCATTTTCAGCTG CAG	CTGCAGCTGAAATGGGTTTGCTGATTTC
A986P	GCAAATCATTTTCACCTGCAGGTAG C	GCTACCTGCAGGTGAAATGATTTTGC
E979G-I980S- K982T	CCATTAATTAATGGATCCAGCACAAAT CATTTTCAGCTGC	GCAGCTGAAATGATTGTGCTGGATCCA TTAATTAATGG
E979G-K982T	CCATTAATTAATGGAATCAGCACAAAT CATTTTCAGCTGC	GCAGCTGAAATGATTGTGCTGATTCCAT TAATTAATGG
E979P-I980P- K982P	CCATTAATTAATCCACCCAGCCCAAT CATTTTCAGCTGC	GCAGCTGAAATGATTGGGCTGGGTGGA TTAATTAATGG
E979G-I980S	CCATTAATTAATGGAAGCAGCAAAA TCATTTTCAGCTG	CAGCTGAAATGATTTTGCTGCTTCCATT AATTAATGG
I980S-K982T	CCATTAATTAATGAAAGCAGCACAA TCATTTTCAGCTGC	GCAGCTGAAATGATTGTGCTGCTTTCAT TAATTAATGG

In silico methods

To identify RTX proteins blastp was used (<https://blast.ncbi.nlm.nih.gov/Blast.cgi>).

Alignments were performed using MUSCLE (<https://www.ebi.ac.uk/Tools/msa/muscle>).

Alignments were coloured using Boxshade (https://embnet.vital-it.ch/software/BOX_form.html).

C-terminal fragments of defined length were extracted from fasta-sequences by using the newly developed python-derived tool “fasta-cutter”:

```
#!/usr/bin/env python
import sys
import re
from optparse import OptionParser, OptionGroup
import argparse
import os

def parse_args():
    error_list=[]
    parser = OptionParser()
    parser.set_defaults(infile=None, suffix="_out", cutoff=0)

    # Override the standard "-h" behaviour (see below)
    parser.remove_option("-h")
    parser.add_option("-h", "--help", action="store_true", dest="helpme", help="show
this message and exit")

    io = OptionGroup(parser,
    "=====\n input/output options")
    io.add_option("-i", "--input", action="callback", dest="infile",
callback=multiple_args,
help="Input in the form of one or multiple fasta
text files. (For multiple files use * or ? to select all files with one command:
"*.fasta") (Required)")
```

```

        io.add_option("-o", "--output", action="callback", dest="suffix",
callback=multiple_args,
                        help="Specify a suffix to be used to create the
output file. (Default: %default) ")
        io.add_option("-n", "--cutoff", metavar="NUMBER", dest="cutoff",
                        help="Provide the number of amino acids to select,
a positive number starts from N-terminus, a negative number starts from C-
terminus. (Required)")
        parser.add_option_group(io)

    (options, args) = parser.parse_args()

    # Present the same help text regardless of whether "-h",
    # "--help", or no arguments at all were invoked.
    if len(sys.argv) == 1: options.helpme = True
    if options.helpme:
        programInfo()
        parser.print_help()

    print("\n=====
=====\\n\\n")
        sys.exit(-1)

    if not os.path.isfile(options.infile[0]): error_list.append("Fasta file %s
does not exist.\\n" % options.infile)
    if options.cutoff==0:
        error_list.append("The cutoff value is not specified, please provide
a cutoff value using -n/--cutoff.")
    else:
        try:
            cutoff=int(options.cutoff)
        except:
            error_list.append("The cutoff value: %s is not a number. Please
provide a number." %(options.cutoff))

    if error_list:
        parser.error("Error(s) found in command line
parameters:\\n\\t%s"%(\\n\\t".join(error_list)))
        sys.exit(-1)

    return(options)

def multiple_args(option, opt_str, value, parser):
    value = []

    def floatable(str):
        try:
            float(str)
            return True
        except ValueError:
            return False

    for i,arg in enumerate(sys.argv):
        if i > sys.argv.index(opt_str):
            if arg[:2] == '--' and len(arg) > 2:
                break
            if arg[:1] == '-' and len(arg) > 1 and not floatable(arg):
                break
            if '*' in arg:
                value += glob.glob(arg)

```

```

        else:
            value.append(arg)

    setattr(parser.values, option.dest, value)

def programInfo():
    info=""=====
    =====\n
    This program selects a number of amino acids from a fasta sequence, either from
    the N or the C terminus.\n
    Written by: S.M.A. Hermans (susanne.hermans@hhu.de), December 2017\n
    =====
    =====\n\n""
    print info
    return()

def main():
    #print "python version:", sys.version
    #print "mpl version:", mpl.__version__
    options = parse_args()
    print "Input detected:\n"
    print "\tInput files: %s" %(options.infile)
    print "\tOutput suffix: %s" %(options.suffix)
    print "\tCutoff value: %s" %(options.cutoff)
    print "\nProcessing files now...\n"
    cutoff = int(options.cutoff)

    for infile in options.infile:
        print "Processing: %s" %(infile)
        fasta_in = open(infile,"r")
        outlist=infile.split(".")
        outlist[-2]=outlist[-2]+options.suffix
        outfile=".".join(outlist)
        out = open(outfile,"w")
        for line in fasta_in:
            new_line=""
            if ">" in line:
                new_line=line
                out.write(new_line)
            else:
                if len(line)<=cutoff:
                    print "This line %s is too short! please check
your input file. This line will be skipped in the output file." %(line)
                    new_line="### SKIPPED LINE ###"
                if cutoff>0:
                    new_line=line.strip()[:cutoff]
                elif cutoff<0:
                    new_line=line.strip()[cutoff:]
                out.write(new_line+"\n")
        fasta_in.close()
        out.close()
    print "\nFINISHED!\n\n"

#####
#####
if __name__=="__main__":
    main()

```

Results

Identifying a consensus sequence in the C-terminal region of RTX proteins

First alignments across all types of T1SS-substrates showed that no overall consensus sequence is present in their C-terminal moiety (not shown), recently summarised in a review (8). Thus, our analysis was reduced to the protein family of RTX toxins (10), of which the most prominent member is the *E. coli* exotoxin haemolysin A (HlyA). Related proteins were identified by pblast. As previous studies confirmed the presence of the secretion signal within the C-terminal 50 to 60 amino acids (7,22,26), we limited our analysis to the last 100 amino acids of the sequences. The large N-terminal parts of the proteins, which confer their functionality, are highly diverse also across the family of RTX-toxins and were thus excluded from the alignment studies.

First alignments were performed using a small subset of sequences, to which more sequences were added in a stepwise manner. A relatively conserved stretch of amino acid residues across all analysed substrates was identified approximately 30 residues upstream from the C-terminus (Figure 1). Based on the most prominent conserved residues, the identified region was consequently named “EISKIISS-motif”.

A secondary structure prediction tool (Jpred 4) was used to illustrate the secondary structure of the conserved residues, which revealed the potential presence of an amphipathic helix (Figure 1). The occurrence and correct prediction of this helical structure was further supported by the crystal structure of the adenylate cyclase CyaA from *Bordetella pertussis* (pdb entry 5CXL) (16). Here, the residues aligning to the previously mentioned EISKIISS-motif form an α -helical secondary structure at the extreme C-terminus of the protein. Consequently, we analysed the importance of this motif for the secretion and the haemolytic activity of HlyA as an exemplary RTX-toxin.

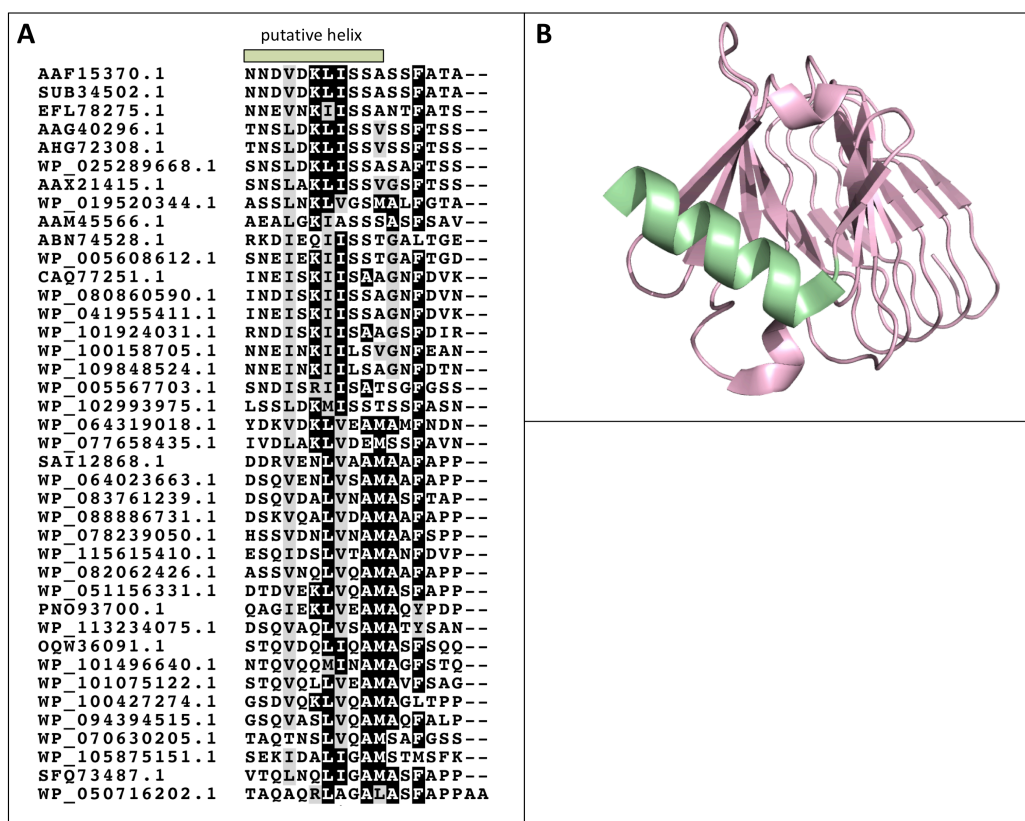


Figure 1: In silico analysis of the C-termini of RTX-toxins, comprising haemolysins, leukotoxins and adenylate cyclases. (A) Alignment of the conserved “EISKIIS-motif” in the C-termini of RTX toxins. Proteins are labelled with their accession codes. (B) Crystal structure of CyaA from *Bordetella pertussis* (pdb entry 5CXL). The C-terminal helix (residues 1664 – 1676) is highlighted in green.

Creation of proHlyA mutants and assessing their haemolytic activity

The identified consensus motif in the C-termini of RTX toxins and related proteins was further characterised by subsequent *in vitro* assays. For this, we chose to work with the well-characterised RTX toxin haemolysin A (HlyA) from *Escherichia coli*, whose overexpression and purification are well-established procedures (25,27). For our studies, we used the inactive form of HlyA, namely proHlyA, which lacks the activating lysine-acylations but is secreted at the same rate as the active toxin HlyA (24,25).

In an earlier publication a range of mutants of a shortened, C-terminal version of HlyA was characterised in terms of amounts of secreted protein, of which many were located in the EISKIIS-region (28).

Thus, we introduced the same mutations to proHlyA to address their effects on secretion and haemolytic activity. Furthermore, based on the theoretical helical structure of the EISKIIS region, we introduced a range of proline substitutions.

All proHlyA mutants were purified from inclusion bodies using the same protocols. The yields of all mutants were comparable to the wildtype.

First, we assessed the potential influence of the introduced mutations on the haemolytic activity of the toxin. To activate the haemolytic activity we employed the *in vitro* acylation assay that was developed by Thomas *et al.* (25). The lytic activity on sheep erythrocytes was quantified by absorption spectroscopy by measuring the release of haemoglobin upon cell lysis (Figure 2).

The results demonstrate that none of the introduced mutations affected the haemolytic activity of HlyA.

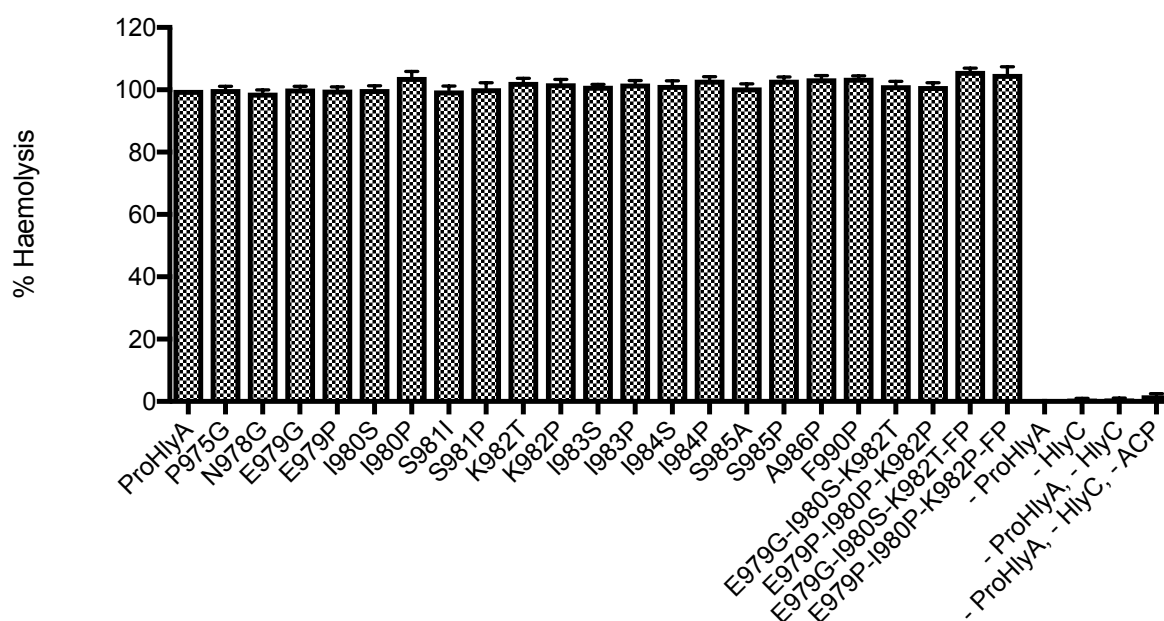


Figure 2: Haemolytic activity of HlyA mutants after *in vitro* acylation. The lysis of erythrocytes was quantified by measuring the consequent release of haemoglobin by absorption spectroscopy. Control measurements lacked proHlyA, HlyC, ACP, or combinations of these, in the assay.

Measuring the secretion rates of the proHlyA mutants

After confirming the functionality of all mutants by applying the *in vitro* acylation assay we quantified the influence of the mutations on the secretion rates, following the protocols published by Lenders *et al.* (24).

While the secretion of many mutants was unaffected we observed some substantial reductions of the secretion rates, mainly for the proline substitutions.

Interestingly, the triple mutant E979G-I980S-K982T shows a strong synergistic effect compared to the single mutants, where secretion rates were equal to the wildtype (Figure 3).

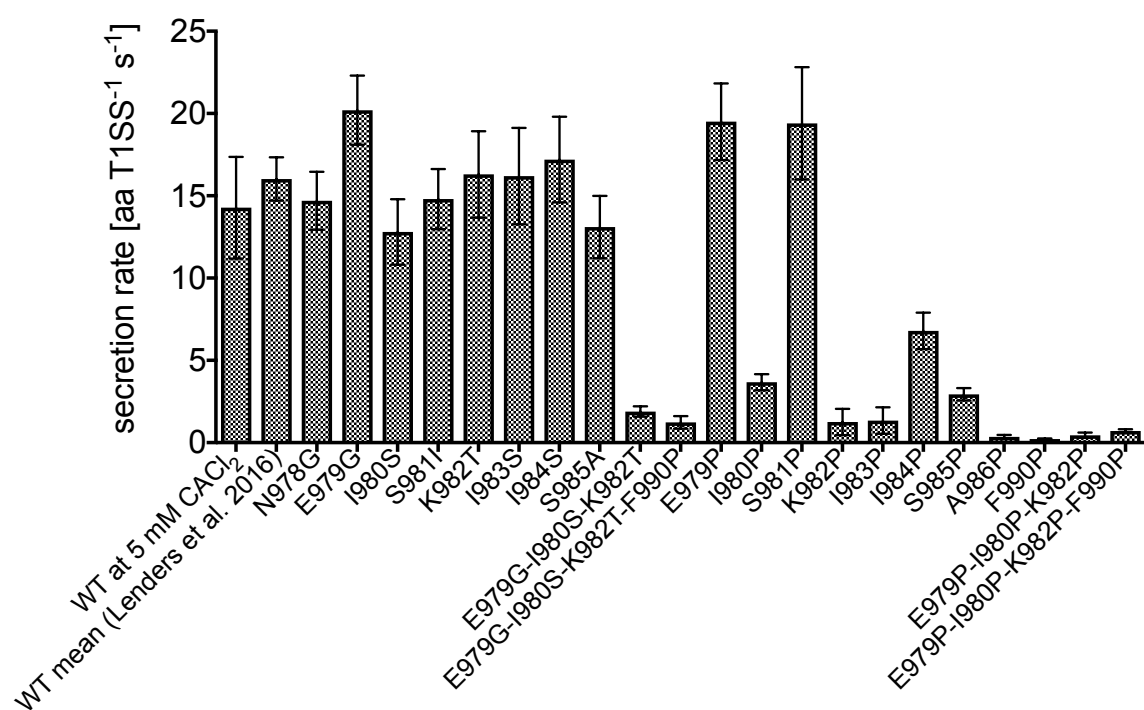


Figure 3: Secretion rates of proHlyA mutants and proHlyA wildtype (24). Substantial reduction of the secretion rates is mainly observed in the proline-substitution mutants.

Discussion

Type I secretion systems are ubiquitously present in Gram-negative bacteria, yet the targeting of the substrate to its dedicated transport system is still poorly understood, despite decades of research (8). For HlyA and related proteins, the secretion signal has been localised to the last 50 to 60 C-terminal amino acids (7,22,26), but its precise nature or a conserved feature was not identified.

The purpose of this current study was to examine the C-termini of RTX-toxins in greater detail by *in silico* methods in order to identify a common feature that might possibly be responsible for the targeting of the substrates to the translocons. For this, our analysis focused on the C-terminal 100 amino acids of each substrate. The *in silico* studies were complemented by *in vitro* studies with the *E. coli* exotoxin HlyA.

In this paper, we present for the first time the presence of a consensus sequence in the C-termini of RTX-toxins that we were able to link directly to their secretion. The motif itself, named “EISKIISS-motif”, a stretch of approximately 12 amino acids located about 30 amino acids upstream from the C-terminus, presumably forms a helical structure which is further supported by the crystal structure of the adenylate cyclase CyaA from *B. pertussis*. Prolines were introduced into the putative helical structure that largely affected the secretion rates, which further supported the importance of a secondary structural motif within the secretion process. However, the exchange of highly conserved residues outside the putative helical region such as F990 (HlyA) also greatly reduced the secretion rates.

Thus, from these results we conclude that a combination of the secondary structure and the primary amino acid sequence of the motif are involved in the secretion process. We hypothesise that this motif is involved in the recognition of the substrate by the transporter and might also play a role in triggering the assembly of the secretion complex.

A dual function of the C-terminus of HlyA has been previously suggested as being involved in secretion and correct folding of the protein (29). Thus, the *in vitro* haemolytic activity of all mutants was assessed (25), which confirmed the sole importance of the identified motif for the secretion of the toxin.

Taken together, these findings suggest a function of the secondary as well as of the primary structure for the secretion process. The insights gained from this study may be of assistance

in designing further experiments that investigate the detailed interactions of RTX-toxins with their dedicated transport systems.

Acknowledgements

We would like to express our gratitude towards Susanne Hermans, Institute of Pharmaceutical and Medical Chemistry, Heinrich Heine University Düsseldorf for providing us with the program “fasta cutter” which greatly facilitated the *in silico* work for the present study. Furthermore, we would like to thank the whole Institute of Biochemistry for stimulating discussions. This work was funded by CRC1208 (project A01 to L.S.).

References

1. Costa, T. R., Felisberto-Rodrigues, C., Meir, A., Prevost, M. S., Redzej, A., Trokter, M., and Waksman, G. (2015) Secretion systems in Gram-negative bacteria: structural and mechanistic insights. *Nat Rev Microbiol* **13**, 343-359
2. Felmler, T., Pellett, S., and Welch, R. A. (1985) Nucleotide sequence of an *Escherichia coli* chromosomal hemolysin. *J Bacteriol* **163**, 94-105
3. Wandersman, C., and Delepelaire, P. (1990) TolC, an *Escherichia coli* outer membrane protein required for hemolysin secretion. *Proc Natl Acad Sci U S A* **87**, 4776-4780
4. Noegel, A., Rdest, U., Springer, W., and Goebel, W. (1979) Plasmid cistrons controlling synthesis and excretion of the exotoxin alpha-haemolysin of *Escherichia coli*. *Mol Gen Genet* **175**, 343-350
5. Koronakis, V., Koronakis, E., and Hughes, C. (1989) Isolation and analysis of the C-terminal signal directing export of *Escherichia coli* hemolysin protein across both bacterial membranes. *EMBO J* **8**, 595-605
6. Hwang, J., Zhong, X., and Tai, P. C. (1997) Interactions of dedicated export membrane proteins of the colicin V secretion system: CvaA, a member of the membrane fusion protein family, interacts with CvaB and TolC. *J Bacteriol* **179**, 6264-6270
7. Gray, L., Mackman, N., Nicaud, J. M., and Holland, I. B. (1986) The carboxy-terminal region of haemolysin 2001 is required for secretion of the toxin from *Escherichia coli*. *Mol Gen Genet* **205**, 127-133
8. Holland, I. B., Peherstorfer, S., Kanonenberg, K., Lenders, M., Reimann, S., and Schmitt, L. (2016) Type I Protein Secretion-Deceptively Simple yet with a Wide Range of Mechanistic Variability across the Family. *EcoSal Plus* **7**
9. Welch, R. A. (1991) Pore-forming cytolysins of gram-negative bacteria. *Mol Microbiol* **5**, 521-528
10. Linhartova, I., Bumba, L., Masin, J., Basler, M., Osicka, R., Kamanova, J., Prochazkova, K., Adkins, I., Hejnova-Holubova, J., Sadilkova, L., Morova, J., and Sebo, P. (2010) RTX proteins: a highly diverse family secreted by a common mechanism. *FEMS Microbiol Rev* **34**, 1076-1112
11. Chenal, A., Guijarro, J. I., Raynal, B., Delepierre, M., and Ladant, D. (2009) RTX calcium binding motifs are intrinsically disordered in the absence of calcium: implication for protein secretion. *J Biol Chem* **284**, 1781-1789
12. Ostolaza, H., Soloaga, A., and Goni, F. M. (1995) The binding of divalent cations to *Escherichia coli* alpha-haemolysin. *Eur J Biochem* **228**, 39-44
13. Jones, H. E., Holland, I. B., Baker, H. L., and Campbell, A. K. (1999) Slow changes in cytosolic free Ca²⁺ in *Escherichia coli* highlight two putative influx mechanisms in response to changes in extracellular calcium. *Cell Calcium* **25**, 265-274
14. Lenders, M. H., Weidtkamp-Peters, S., Kleinschrodt, D., Jaeger, K. E., Smits, S. H., and Schmitt, L. (2015) Directionality of substrate translocation of the hemolysin A Type I secretion system. *Sci Rep* **5**, 12470
15. Bakkes, P. J., Jenewein, S., Smits, S. H., Holland, I. B., and Schmitt, L. (2010) The rate of folding dictates substrate secretion by the *Escherichia coli* hemolysin type 1 secretion system. *J Biol Chem* **285**, 40573-40580
16. Bumba, L., Masin, J., Macek, P., Wald, T., Motlova, L., Bibova, I., Klimova, N., Bednarova, L., Veverka, V., Kachala, M., Svergun, D. I., Barinka, C., and Sebo, P.

- (2016) Calcium-Driven Folding of RTX Domain beta-Rolls Ratchets Translocation of RTX Proteins through Type I Secretion Ducts. *Mol Cell* **62**, 47-62
17. Kanonenberg, K., Schwarz, C. K., and Schmitt, L. (2013) Type I secretion systems - a story of appendices. *Res Microbiol* **164**, 596-604
 18. Lecher, J., Schwarz, C. K., Stoldt, M., Smits, S. H., Willbold, D., and Schmitt, L. (2012) An RTX transporter tethers its unfolded substrate during secretion via a unique N-terminal domain. *Structure* **20**, 1778-1787
 19. Delepelaire, P., and Wandersman, C. (1998) The SecB chaperone is involved in the secretion of the *Serratia marcescens* HasA protein through an ABC transporter. *EMBO J* **17**, 936-944
 20. Thanabalu, T., Koronakis, E., Hughes, C., and Koronakis, V. (1998) Substrate-induced assembly of a contiguous channel for protein export from E.coli: reversible bridging of an inner-membrane translocase to an outer membrane exit pore. *EMBO J* **17**, 6487-6496
 21. Balakrishnan, L., Hughes, C., and Koronakis, V. (2001) Substrate-triggered recruitment of the TolC channel-tunnel during type I export of hemolysin by *Escherichia coli*. *J Mol Biol* **313**, 501-510
 22. Kenny, B., Chervaux, C., and Holland, I. B. (1994) Evidence that residues -15 to -46 of the haemolysin secretion signal are involved in early steps in secretion, leading to recognition of the translocator. *Mol Microbiol* **11**, 99-109
 23. Reimann, S., Poschmann, G., Kanonenberg, K., Stuhler, K., Smits, S. H., and Schmitt, L. (2016) Interdomain regulation of the ATPase activity of the ABC transporter haemolysin B from *Escherichia coli*. *Biochem J* **473**, 2471-2483
 24. Lenders, M. H., Beer, T., Smits, S. H., and Schmitt, L. (2016) In vivo quantification of the secretion rates of the hemolysin A Type I secretion system. *Sci Rep* **6**, 33275
 25. Thomas, S., Smits, S. H., and Schmitt, L. (2014) A simple in vitro acylation assay based on optimized HlyA and HlyC purification. *Anal Biochem* **464**, 17-23
 26. Jarchau, T., Chakraborty, T., Garcia, F., and Goebel, W. (1994) Selection for transport competence of C-terminal polypeptides derived from *Escherichia coli* hemolysin: the shortest peptide capable of autonomous HlyB/HlyD-dependent secretion comprises the C-terminal 62 amino acids of HlyA. *Mol Gen Genet* **245**, 53-60
 27. Thomas, S., Bakkes, P. J., Smits, S. H., and Schmitt, L. (2014) Equilibrium folding of pro-HlyA from *Escherichia coli* reveals a stable calcium ion dependent folding intermediate. *Biochim Biophys Acta* **1844**, 1500-1510
 28. Chervaux, C., and Holland, I. B. (1996) Random and directed mutagenesis to elucidate the functional importance of helix II and F-989 in the C-terminal secretion signal of *Escherichia coli* hemolysin. *J Bacteriol* **178**, 1232-1236
 29. Jumpertz, T., Chervaux, C., Racher, K., Zouhair, M., Blight, M. A., Holland, I. B., and Schmitt, L. (2010) Mutations affecting the extreme C terminus of *Escherichia coli* haemolysin A reduce haemolytic activity by altering the folding of the toxin. *Microbiology* **156**, 2495-2505

3.7 Chapter VII – Studying the Assembled Inner Membrane Complex of the HlyA-T1SS

Title: Functional Purification and Initial Structural Studies of the Haemolysin A Type I Secretion System Inner Membrane Complex from *Escherichia coli*

Authors: Kerstin Kanonenberg, Lutz Schmitt

Published in: *to be submitted*

Impact Factor:

Own Work: 70 %
Fed-batch fermentation
Purification of HlyBD
Data evaluation
Writing of the manuscript

Functional purification and Initial Structural Studies of the Haemolysin A Type I Secretion System Inner Membrane Complex from *Escherichia coli*

Kerstin Kanonenberg, Lutz Schmitt*

Institute of Biochemistry, Heinrich Heine University Duesseldorf, Universitaetsstrasse 1, 40225 Duesseldorf, Germany

* To whom correspondence should be addressed:

Lutz Schmitt, Institute of Biochemistry, Heinrich-Heine-University Duesseldorf, Universitaetsstr. 1, 40225 Duesseldorf, Germany

Phone: +49211-81-10773, Fax: 49211-81-15310, Email: lutz.schmitt@hhu.de

Abstract

The study of protein complexes has always been a challenging task, especially in the field of membrane protein biochemistry. The inner membrane complex of the haemolysin A type I secretion system is composed of an ABC transporter and a membrane fusion protein and *in vitro*, only its individual components but never the assembled complex have been studied. Previous studies suggest a trimeric, as well as a hexameric assembly of the membrane fusion protein around the dimeric ABC transporter.

The present study describes the overexpression of assembled HlyB/HlyD complex by fed-batch fermentation employing a two-plasmid expression system. We were able to successfully overexpress and purify the assembled HlyB/HlyD complex. We provide first negative-stain electron microscopy images of the assembled complex and based on our data obtained by multi angle light scattering, we suggest a 2 : 6 stoichiometry for the HlyB/HlyD inner membrane complex of the HlyA type I secretion system.

Introduction

Type I secretion systems (T1SS) are widespread secretory complexes in Gram-negative organisms that deliver their dedicated substrates, proteins of large functional variety, to the extracellular space without the occurrence of periplasmic intermediates (1-3) (reviewed recently in Kanonenberg et al. 2018 (4)).

T1SS display a relatively simple assembly of an inner membrane complex, composed of an ABC transporter and a membrane fusion protein (MFP), and a TolC-like outer membrane protein (OMP) (4-7). In the case of one of the most prominent and extensively studied T1SS, the haemolysin A (HlyA)-T1SS from *Escherichia coli*, these are HlyB, HlyD and TolC, respectively (8,9). HlyA is a haemolytically active exotoxin that is secreted by uropathogenic *E. coli* strains (10). It is exported in one step, C-terminus first, across both membranes (11). Subsequently, its folding is initiated in the extracellular space by the binding of calcium ions to specific RTX-domains (12-14). HlyB and HlyD have been shown to reside assembled in the inner membrane while TolC is recruited only upon substrate recognition in the cytosol, presumably by a small cytosolic domain of the MFP HlyD (15,16).

Additionally to the canonical domains of ABC transporters, namely two transmembrane domains (TMD) and two nucleotide-binding domains (NBD), HlyB comprises a so-called C39-peptidase-like domain (CLD) at its N-terminus, localised on the cytosolic side of the membrane. The term CLD was coined upon its structural resemblance to C39-peptidases (17), yet the catalytically active triad is disrupted and renders the domain inactive in terms of proteolytic activity (18). However, the domain was shown to be essential for secretion and interacts with the unfolded substrate (18,19), but its detailed function in the secretion process is not yet fully understood.

Recent studies on the HlyA-T1SS focussed on the ABC transporter HlyB and its biochemical characterisation in detergent solution (19) as well as reconstituted in saposin A-derived nanoparticles (Chapter IV). As these studies do not include the membrane fusion protein HlyD, they do not reflect the entire *in vivo* situation of the inner membrane complex. However, these studies confirm an interaction of the substrate with the ABC transporter and assign an important role to the CLD in the secretion process.

Functional studies on the assembled inner membrane complex of the HlyA-T1SS have been exclusively performed *in vivo*, which resulted in the determination of the secretion rate of 16 amino acids per second and transporter (20) and provided direct proof for the C-terminal

directionality of substrate-transport (11). Despite these great advances in the characterisation of T1SS, the *in vivo* system lacks the possibility to analyse detailed interactions of the particular components on a molecular level.

Studying purified complexes *in vitro* offers the great advantage of performing biochemical assays under tightly controlled conditions, which allows for the characterisation of functional details and interactions. Furthermore, purified protein complexes are amenable for structural studies, e.g. by x-ray crystallography or cryo-electron microscopy (cryo-EM) (21,22).

The isolation of functional protein complexes states a particular challenge in the field of (membrane) protein biochemistry. The assembly of complexes can be initiated *in vitro* after separate purification of the individual components or accomplished by co-expression *in vivo* (23).

An individual problem in the case of the HlyA-T1SS is the unclear stoichiometry of the assembled inner membrane complex, for which a trimeric as well as a hexameric state of the membrane fusion proteins has been suggested (15,24).

The AcrAB-TolC tripartite efflux pump that comprises a similar assembly as T1SS was successfully purified by creating a fusion construct of the inner membrane components (25). Other secretion complexes, such as the type IV secretion core complex, have been purified in an assembled manner for biochemical and structural characterisation (26).

The objective of this study was to establish an overexpression and purification protocol for the assembled inner membrane complex of the HlyA-T1SS from *E. coli* and to unravel its still unclear stoichiometry. First structural studies were attempted in order to provide first biochemical data of the assembled complex.

Materials and Methods

Overexpression of HlyB/HlyD complex by fed-batch fermentation

To overexpress the T1SS inner membrane complex, *E. coli* cells (strain defined in the results-section) were transformed with the HlyB and HlyD expression plasmids pBADHisHlyB (19) and pET28-HisTEV-HlyD (27), respectively. Positive clones were selected on LB-agar plates containing 100 µg/mL ampicillin and 30 µg/mL kanamycin. A first pre-culture, inoculated with a single colony, was grown in 2YT-medium containing the appropriate antibiotics for 15 h at 37 °C, 200 rpm in an orbital shaker. A second pre-culture was inoculated to an OD₆₀₀ of 0.05 with the first pre-culture and grown at identical conditions until the exponential growth phase, characterised by an OD₆₀₀ of approximately 1. Cells were spun down (4000 xg, 10 min) and used to inoculate the bioreactor to an OD₆₀₀ of approximately 0.1.

For fed-batch fermentation, a 15 L fermenter (Applikon Biotechnology BV, Delft, The Netherlands) was filled with 7 L of minimal medium (15 g/L KH₂PO₄, 20 g/L glycerol, 5 g/L (NH₄)₂SO₄, 3 g/L MgSO₄ · 7 H₂O, 0.015 g/L CaCl₂, 0.15 g/L FeSO₄ · 7 H₂O, 0.1 g/L ZnCl₂, C₆H₅Na₃O₇ · 2 H₂O, 1.5 mL/L thiamine solution (5 g/L stock solution), 1.5 mL/L trace elements solution (2 g/L Al₂(SO₄)₃ · 18 H₂O, 0.75 g/L CoSO₄ · 7 H₂O, 2.5 g/L CuSO₄ · 5 H₂O, 0.5 g/L H₃BO₃, 24 g/L MnSO₄ · H₂O, 3 g/L Na₂MoO₄, 25 g/L NiSO₄ · 6 H₂O, 15 g/L ZnSO₄ · 7 H₂O, 2 mL/L 30 % H₂SO₄). The pH was kept constant at 6.8 and was constantly adjusted by 100 mM H₂SO₄ and 10 % (v/v) ammonia solution. Temperature was set to 36 °C and a constant stirring at 1000 rpm was used. Additional aeration was activated at O₂ concentration below 30 %. Growth was followed by monitoring the oxygen saturation in the culture. A sudden rise indicated the depletion of the initially added glycerol and feeding was started by adding feeding solution (50 % (w/v) glycerol, supplemented with 1 mL/L trace elements solution) via an externally connected peristaltic pump. Feeding was slowly increased in a stepwise manner, until OD₆₀₀ was ≥ 45. The expression of HlyB and HlyD was induced by sequentially adding arabinose and IPTG to final concentrations of 10 mM and 1 mM, respectively, with a delay of 1 h. Expression was continued at constant feeding for another 60 – 90 min, depending on cell viability. Cells were harvested by centrifugation (8000 xg, 15 min, 4 °C) and stored at -80 °C (long term) or -20 °C (short term).

Purification of the HlyB/HlyD complex from *E. coli* cells

Cells were resuspended in buffer A (50 mM NaH₂PO₄ pH 8, 300 mM NaCl) and lysed by passing three times through a cell disruptor at 1.5 kbar (Microfluidics). Undisrupted cells and cell debris were removed by a low-spin centrifugation step (18,000 xg, 30 min, 4 °C), followed by an ultra-centrifugation step to pellet the membranes (150,000 xg, 90 min, 4 °C). Membranes were homogenised in buffer A and 10 % (v/v) glycerol were added prior to storage at -80 °C.

For solubilisation, membranes were diluted to a protein concentration of 10 mg/ mL using buffer A and solubilised by adding 0.3 % (w/v) fos-choline 16 (FC-16). Membranes were stirred for 1 h at 8 °C. Unsolubilised material was removed by ultracentrifugation (150,000 xg, 30 min, 4 °C) and solubilised membranes were diluted three-fold by adding buffer A. Imidazole was added to a final concentration of 2 mM and membranes were loaded on two 5 mL HiTrap IMAC HP columns charged with Ni²⁺ (GE Healthcare) at a maximum flow-rate of 1.2 mL/min. Subsequently, the columns were washed with 2 column volumes (CV) buffer A, supplemented with 2 mM imidazole and 0.003 % (w/v) LMNG, 0.015 % (w/v) DDM or 0.003 % (w/v) PCC. The imidazole-concentration was increased in a stepwise manner. 3 CV were washed with 12.5 mM, followed by 3 CV 25 mM, 3 CV 37.5 mM, 3 CV 50 mM and 6 CV 62.5 mM of imidazole to remove non-specifically bound material and to complete the detergent exchange. HlyB/HlyD complex was eluted with buffer A supplemented with 250 mM imidazole and 0.003 % (w/v) LMNG, 0.015 % (w/v) DDM or 0.003 % PCC. Eluted protein was concentrated to a final volume of 1 mL and subjected to size exclusion chromatography (SEC) on a Superose 6 Increase 10/300 GL column (GE Healthcare), equilibrated in buffer B (100 mM HEPES pH 8, 250 mM NaCl) supplemented with 0.003 % (w/v) LMNG, 0.015 % (w/v) DDM or 0.003 % PCC. The column was operated at a flow-rate of 0.5 mL/min and the protein was collected in fractions of 0.5 mL.

Multi-angle light scattering of purified HlyB/HlyD complex

To assess the monodispersity, the molecular weight and the oligomeric assembly of the purified HlyB/HlyD complex we applied high-pressure liquid chromatography coupled to multi angle light scattering (HPLC-MALS). A superose 6 Increase 10/300 GL column was equilibrated with buffer B supplemented with 0.003 % (w/v) LMNG. For MALS analysis, an Agilent Technologies system connected to a triple-angle light scattering detector (miniDAWN TREOS, Wyatt Technology Europe GmbH, Dernbach, Germany) followed by

a differential refractive index detection system (Optilab t-rEX, Wyatt Technology) was used. Typically, 250 μ L of purified HlyB/HlyD complex (1.5 – 2 mg/mL) were loaded onto the column. The obtained data was analysed using the ASTRA software package (Wyatt Technology).

Negative-stain electron microscopy

Purified HlyB/HlyD complex was concentrated to approximately 1 mg/mL (centricon, MWCO = 100 kDa). Protein samples were stained using 0.75 % uranyl-formate stain. 4 μ L of protein sample were applied on a glow-discharged carbon-coated copper grid and let to absorb for 1 min. The grids were washed with water and subsequently with staining solution. Grids were incubated in staining solution for 1 min and air-dried before analysed under the electron microscope (Joel-1400, running at 120 kV, LaB6 cathode, normal magnification 25,000-fold, defocus of 1.5 μ m for 60,000-fold magnification, detector: 4k x 4k CCD camera, exposure time: 1 s).

Results

Fed-batch fermentation to overexpress HlyB/HlyD complex

Overexpression of HlyB/HlyD complex was achieved by using an expression system composed of two individual plasmids, of which each encoded for one of the inner membrane complex components. While the expression of HlyB was controlled by an arabinose-inducible pBAD-promoter, the HlyD-encoding plasmid contained an IPTG-inducible lac-promoter. This allowed a separate, consecutive induction of both proteins. Both expression constructs contained an N-terminal poly-histidine-tag for downstream purification processes.

The overexpression of HlyB/HlyD was found to be impossible in flask-cultivation. Thus, a fed-batch fermentation approach was established to optimise the oxygen saturation of the culture and ensure constant supply of nutrients. A minimal medium, supplemented with trace elements and glycerol, was found to be most suitable combined with a step-wise increase of feeding and ensured stable growth until high ODs (Figure 1). During feeding, a linear growth of approximately $10 \text{ OD}_{600} / \text{h}$ was targeted. Growth was followed by online-monitoring of the oxygen-saturation in the culture and measuring the OD_{600} (Figure 1).

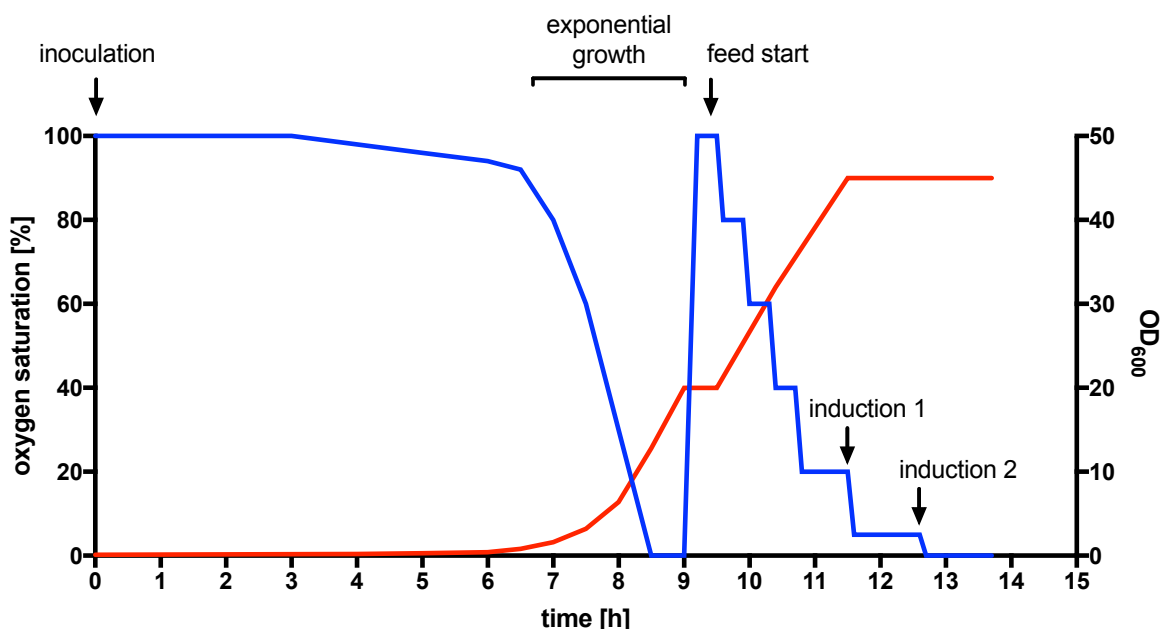


Figure 1: Schematic representation of a typical fed-batch fermentation of HlyB/HlyD complex. Blue line: oxygen saturation, red line: OD_{600} .

Two expression strains were successfully used for fed-batch fermentation: An *acrAB*-deficient C43(DE3)-strain (C43(DE3) Δ *acrAB*) and an *ompF*-deleted C41(DE3) strain (C41(DE3) Δ *ompF*). The growth of both strains in the bioreactor was similar and only displayed differences in the length of the lag-phase after inoculation, which was found to be prolonged in the C41(DE3)-derived strain. Overall, approximately 100 g of wet cells were obtained per litre of fed-batch fermentation culture.

Purification of the HlyB/HlyD complex from *E. coli* membranes

For the purification of the complex, membranes were isolated from *E. coli* cells and solubilised using 0.3 % (w/v) FC-16. His-tagged proteins were subsequently immobilised on a Ni²⁺-charged IMAC column. Step-wise washing from 2 to 62.5 mM imidazole ensured the removal of non-specifically bound protein and, at concentrations above 50 mM, of non-assembled HlyB (Figure 2).

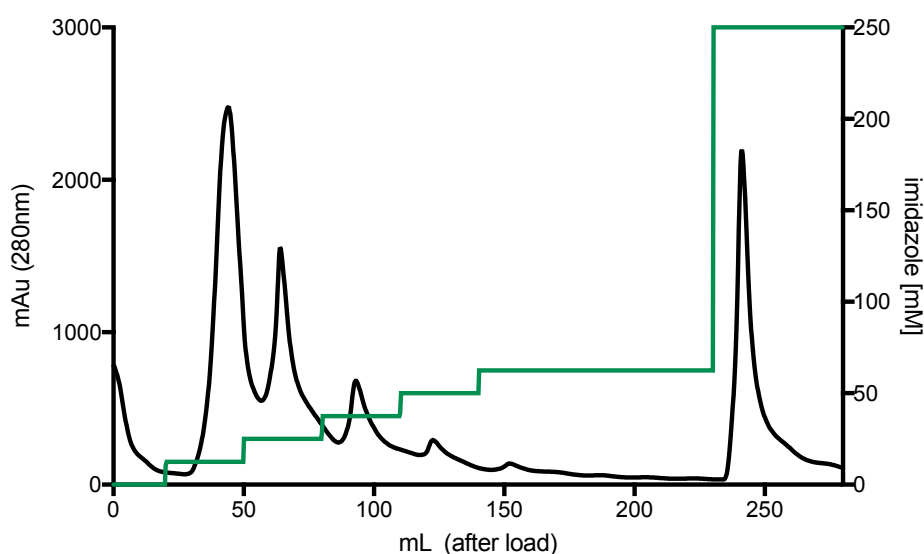


Figure 2: Typical IMAC-purification chromatogram of HlyB/HlyD complex from solubilised *E. coli* membranes. Load of the sample is not shown. Black line – mAu (280 nm), green line – imidazole concentration in buffers.

Purity of the protein was assessed by SDS-PAGE (Figure 3). For further purification and to assess the homogeneity the purified protein SEC was performed (Figure 4). The analysis revealed differences depending on the detergent that was used for purification. In PCC, the overall homogeneity of the sample was reduced. However, the main protein species always eluted at a retention volume of approximately 10 – 12 mL from the column (Figure 4).

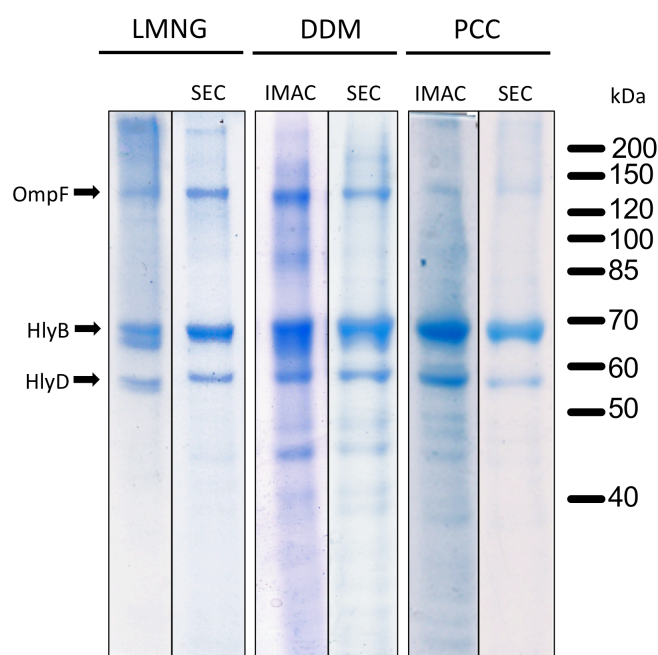


Figure 3: SDS-PAGE of IMAC- and SEC-purified HlyB/HlyD complex from C43(DE3) Δ acrAB in different detergents. OmpF as the most prominent impurity is visible on all gels. HlyB typically migrates at approximately 70 kDa (19) and is visible as a double band without DTT in the sample buffer. HlyD is visible just below 60 kDa. The impurity OmpF runs typically at approximately 150 kDa.

A prominent impurity band running at approximately 150 kDa is visible on SDS-PAGE. Later analysis by electron microscopy identified it as the outer membrane porin OmpF. Overall, the choice of detergent did not have a large impact on the purity of the protein samples (Figure 3).

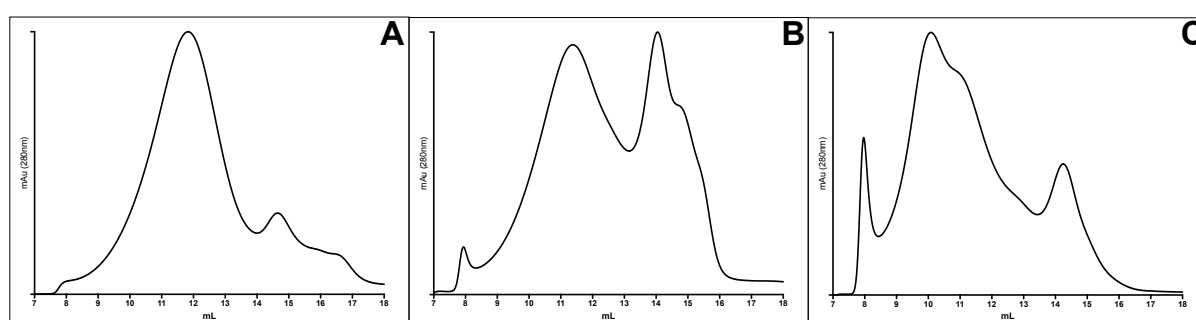


Figure 4: SEC of HlyB/HlyD complex purified from C43(DE3) Δ acrAB in different detergents, using a Superose 6 Increase 10/300 GL column. (A) LMNG, (B) DDM, (C) PCC.

To improve the purity of the protein samples, purification was additionally performed from the expression strain C41(DE3) Δ ompF (Figure 5) following identical protocols, resulting in a removal of OmpF from the preparation and thus the disappearance of its band on SDS-PAGE at approximately 150 kDa (Figure 5). The protein samples displayed a low homogeneity on SEC that could not be improved by using different detergents for

purification (Figure 5). Thus, further experiments were only performed with protein purified from C43(DE3) Δ *acrAB*.

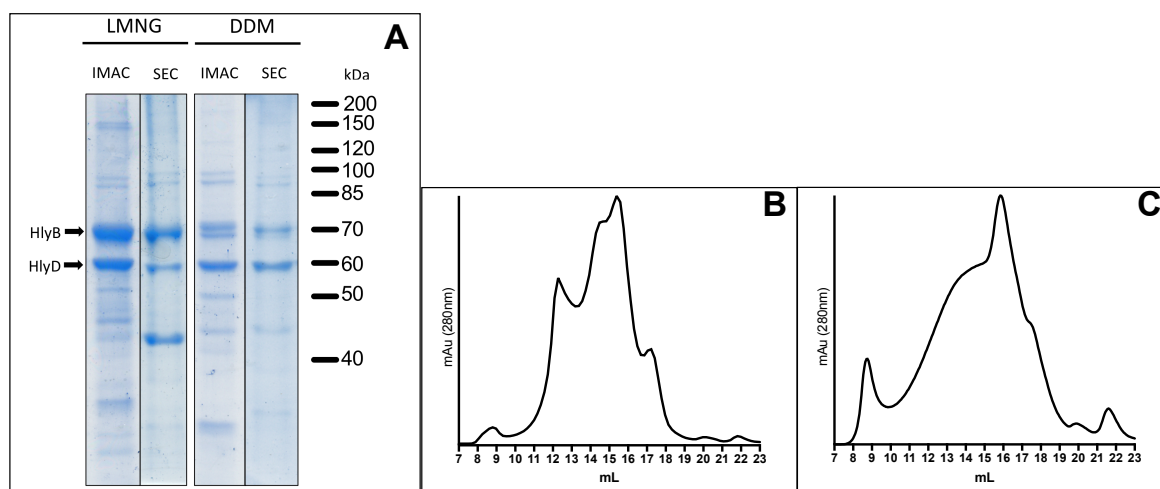


Figure 5: Purification of HlyB/HlyD complex from C41(DE3) Δ *ompF*. (A) SDS-PAGE of LMNG- and DDM-purified protein, (B) SEC in LMNG, (C) SEC in DDM.

Assessing the stoichiometry of the HlyB/HlyD complex by multi-angle light scattering

To analyse the molecular weight and dispersity of the purified HlyB/HlyD complex, high-pressure liquid chromatography, coupled to multi-angle light scattering (HPLC-MALS), was used. The setup with a Superose 6 Increase 10/300 GL column allows for precise determination of the molecular weight of the protein as well as the detergent belt surrounding it. For this, a conjugate analysis was performed, for which the extinction coefficient of the protein was calculated from the primary amino acid sequence. The computational analysis calculates the amount of protein in the whole particle, which consequently also determines the number of detergent molecules bound to the protein complex (28).

For HPLC-MALS, protein purified by IMAC and SEC was used. The main peak from 10–12 mL retention volume was concentrated to 1.2 – 1.8 mg/mL prior to injection.

The measurements of HlyB/HlyD complex in LMNG resulted in a molecular weight of approximately 500 kDa. Similar results were obtained for measurements in DDM and PCC (Figure 6, Table 1).

The calculated molecular weight points towards a hexameric arrangement of HlyD in the inner membrane complex. However, large amounts of OmpF were present in the measured protein samples (Figure 6), which might falsify the obtained results. Thus, it was aimed to

repeat the experiments with protein purified from the OmpF-deficient expression strain; however, the results could not be reproduced.

All results from HPLC-MALS are summarised in table 1. The theoretical number of detergent molecules arranged around the protein complex was calculated from the difference of total molecular weight and the protein-containing fraction.

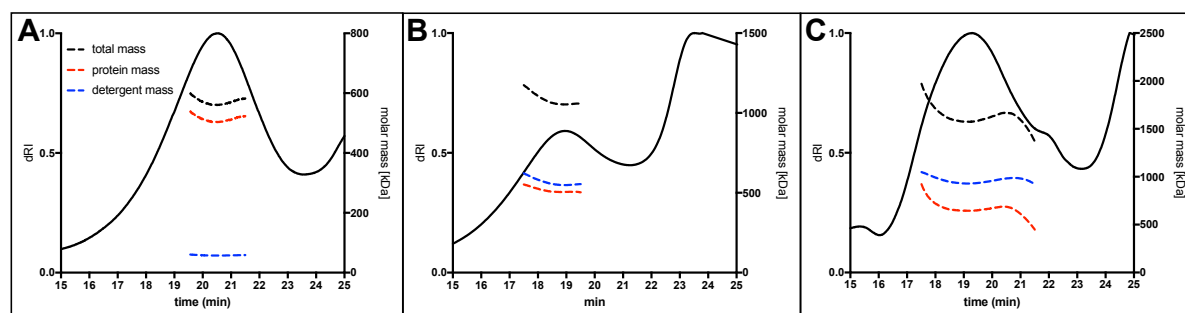


Figure 6: HPCL-MALS of purified HlyB/D complex in (A) LMNG, (B) DDM and (C) PCC. Black line: differential refractive index (dRI, left y-axis), black dashed line: total molar mass, red dashed line: protein molar mass, blue dashed line: detergent molar mass.

Table 1: MALS results of purified HlyB/HlyD complex from C43(DE3) Δ *acrAB* in different detergents.

Detergent	Total mass [kDa]	Protein mass [kDa]	Detergent mass [kDa]	Number of detergent molecules
LMNG	553	495	58	58
DDM	1066	505	561	1100
PCC	1600	657	94	171

Structural studies of the HlyB/HlyD complex by electron microscopy

Negative-stain electron microscopy was used to perform initial structural studies on the inner-membrane complex of the HlyA-T1SS.

For the alignment of the obtained small dataset, a total of 123 images were recorded and 140400 particles were picked semiautomatically. An initial classification of the observed specimen yielded a large, tunnel-shaped protein complex, which was presumably assembled HlyB/HlyD complex. However, large amounts of a structure with a trimeric symmetry were observed, which, after comparison to its electron density map derived from its crystal structure, were identified as OmpF (Figure 7).

No sample purified from the OmpF-deficient strain met the criteria to be analysed by electron microscopy. Further research needs to be performed to increase the yield of pure and assembled HlyB/HlyD complex without the impurity OmpF to pursue further structural studies.

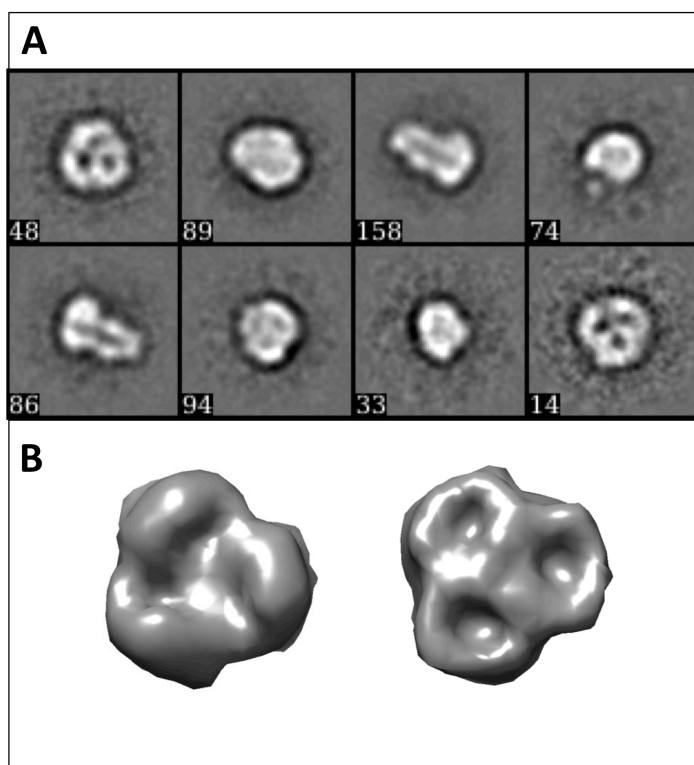


Figure 7: Negative-stain electron microscopy of HlyB/HlyD complex. (A) Results of classification, yielding two classes of tunnel-shaped particles and several classes of proteins of trimeric assembly. (B) Electron density map of OmpF at 20 Å (pdb: 3NSG). Images were taken at the Max-Planck-Institute of molecular physiology, Dortmund, Germany (Prof. Dr. Stefan Raunser) and provided by Dr. Anne Kuhlee.

Discussion

Studying assembled membrane complexes is of crucial importance to fundamentally understand their functional properties and interactions. The overexpression of the inner membrane complex of the HlyA-T1SS from *E. coli* has to date not been published. In the present study, we provide overexpression protocols for assembled complex by fed-batch fermentation and purification protocols for substantial amounts of assembled protein. We performed initial studies to determine the stoichiometry of the protein complex and provide preliminary structural studies by negative-stain electron microscopy.

Overexpression in flask-cultivation was not successful, thus a fed-batch fermentation protocol for a bioreactor was developed to optimise growth conditions and permit the feeding of the cultures during growth and expression. Best results were obtained using a defined minimal medium based on phosphate buffer and supplemented with salts and trace elements. These largely improved conditions in a fermenter facilitated the growth to high cell-densities compared to flask-cultivation. We performed the overexpression of HlyB/HlyD complex in two different expression strains, C43(DE3) Δ *acrAB* and C41(DE3) Δ *ompF*. Both strains showed similar growth behaviour with the developed protocol (Figure 1).

A main issue in fed-batch fermentation is the production of acetate that has detrimental effects on growth and viability of the cell culture (29,30). However, the formation of acetate can be significantly decreased by keeping the growth rate below a critical value and using glycerol instead of glucose for feeding (29,30). As a consequence of the lower rate of transport of glycerol into the cells the overall growth rate is reduced, which allowed for easier control of the bioreactor due to a lower oxygen demand and reduced emission of metabolic heat (29). Furthermore, glycerol has been shown to have beneficial effects on the viability of cells and protein production in a bioreactor (31).

As a feeding strategy, increased stepwise feeding with indirect, manually controlled feedback control was used via the concentration of dissolved oxygen in the culture. In a batch culture, the growth rate continually decreases when higher ODs are reached due to the limited availability of nutrients. A stepwise increase of feed can compensate this decrease in the growth rate and achieve a linear increase of cell mass. The growth was monitored by evaluating the dissolved oxygen (DO) in the fed-batch culture. A rise in DO indicated a nutrient-depletion and thus a demand for external feeding.

However, growth and expression of the cultures can be further optimised by an on-line feedback control of nutrient supply to avoid phases of depletion and to better and faster respond to changes in the growth rate. Here, the DO marks only an indirect measurement for growth while CO₂-emission or optical density allow for the direct monitoring of growth and precise calculations of the growth rates.

The purification of the HlyB/HlyD complex was achieved by affinity chromatography via the poly-histidine tags present on both proteins (Figure 2). The purification of assembled complex with only the ABC transporter carrying a his-tag did not work (not shown). We suspect that the affinity to the column matrix was not sufficient, perhaps due to a certain shielding of the his-tags by HlyD. Thus, the removal of complex-fragments that carry less his-tags and thus have a lower affinity for the IMAC resin was achieved by washing with imidazole concentrations up to 62.5 mM. Subsequent SEC separated the different protein specimen by size, which also enabled us to primarily isolate assembled complexes (Figure 3, Figure 4).

However, we observed remarkable differences when purifying from the two expression strains C43(DE3) Δ *acrAB* and C41(DE3) Δ *ompF*. Overall, the protein purified from the *OmpF*-deficient strain was of higher purity, most strikingly characterised by the absence of the prominent band of *OmpF* at approximately 150 kDa (Figure 3, Figure 5). However, the removal of *ompF* from the genome appeared to have a negative impact on the *in vivo* assembly of the complex, as more complex-fragments were present in the samples represented by SEC-peaks at higher retention volumes (Figure 4, Figure 5).

In samples purified from C43(DE3) Δ *acrAB* the main protein peak eluted at 10 – 12 mL from the SEC column. Upon the change of the expression strain, this peak largely disappeared and instead, smaller species were present eluting at 13 – 16 mL from the same column. Furthermore, the samples displayed an overall decrease in homogeneity, which was found to be disadvantageous for further characterisation. These effects could not be reduced by employing different detergents for purification (Figure 5).

In previous research we were able to show that the deletion of *ompF* has substantial influences on the proteome and lipidome of *E. coli* cells. We hypothesise that these changes influence the *in vivo* assembly of HlyB/HlyD complex in the membrane and consequently, changes the outcome of all downstream purification processes.

The purification process was optimised by employing a range of different detergents. All detergents were exchanged during IMAC and subsequently used for all downstream experiments, such as SEC, HPLC-MALS or structural studies.

Three detergents were successfully employed in the purification and yielded assembled protein complex, namely LMNG, DDM and PCC. In PCC, however, samples were less homogeneous than in LMNG or DDM, rendering the detergent less suitable for HlyB/HlyD complex purification (Figure 4). The main protein species had a retention volume of 10 – 12 mL on SEC and to determine its precise molecular weight and to assess its dispersity, samples were collected and reinjected on HPLC-MALS (Figure 6).

Judging from the obtained curves, best results were obtained from the LMNG-purified sample as it displayed the most constant mass distribution across the protein peak.

To date, the stoichiometry of the inner membrane complex of T1SS is under debate. Early studies suggested a trimeric assembly of the MFP (15), however, these results are not supported by the multiplicity of the complex (TolC – trimer, HlyB – dimer) and a homology model based on known assemblies of MFPs also strongly supports the idea of a hexameric state (24).

The calculated mass of the assembled HlyB/HlyD complex derived from our expression constructs is 512 kDa. The MALS-measurements yielded masses between 495 and 657 kDa, which point towards a hexameric assembly of HlyD. These masses were obtained by performing a conjugate analysis with the obtained data. For this, the precise extinction coefficient of the analysed protein is needed, which can be determined from the primary amino acid sequence (28). Additionally, the analysis provided insights to the molecular mass of the detergent bound to the protein complex, which, together with the precise molar mass of the detergent used, permits the calculation of the number of detergent molecules forming the detergent belt (Figure 6, Table 1).

Here, pronounced differences can be observed between the three detergents used. Only low amounts of LMNG, in total around 60 molecules, are sufficient to keep the protein complex in solution. In contrast, twice as many DDM molecules are needed and nearly 19-fold more detergent molecules form the belt of PCC (Table 1).

To summarise, our HPLC-MALS experiments support the hypothesis of a hexameric state of HlyD and would be in good agreement with the stoichiometry of other export machineries of similar assembly, for example the AcrAB-TolC tripartite efflux pump (25), yet further experiments need to be performed to deliver final proof.

For structural studies, negative-stain electron microscopy was chosen as the elevated size of the protein complex makes it a suitable target for this method. Negative-stain images showed a tunnel-shaped structure that was hypothesised to be the HlyB/HlyD complex. However, large amounts of OmpF in the preparation prevented further analysis of the samples by methods possibly leading to higher resolution images, such as cryo electron microscopy.

In summary, our studies open the possibility for the purification of the assembled inner membrane complex of the HlyA-T1SS. Both proteins were obtained in large amounts and were shown to be assembled into a complex. However, the stoichiometry of both was not determined with high confidence although our preliminary results suggest a hexameric assembly of HlyD. Initial structural studies show a large, tunnel-shaped molecule.

Further studies will focus on an improved purification of pure but assembled inner membrane complex and subsequent structural and functional studies. Biochemical assays in the presence of the substrate HlyA might shed further light on the roles of the cytosolic appendices of both proteins. Combining purified inner membrane complex with TolC might also offer the possibility of assembling the whole secretion complex *in vitro* across two artificial membrane systems. This would further enable studies to provide a detailed functional understanding and would even more comprise an interesting target for profound structural studies by cryo electron microscopy.

Acknowledgements

We would like to thank Dr. Anne Kuhlee (formerly MPI Dortmund) and Prof. Dr. Stefan Raunser (MPI Dortmund) for providing the first negative-stain images of the HlyB/HlyD complex. Further, we would like to thank the whole Institute of Biochemistry for stimulation discussions. This project was funded by CRC 1208 to L.S.

References

1. Koronakis, V., Koronakis, E., and Hughes, C. (1989) Isolation and analysis of the C-terminal signal directing export of Escherichia coli hemolysin protein across both bacterial membranes. *EMBO J* **8**, 595-605
2. Gray, L., Baker, K., Kenny, B., Mackman, N., Haigh, R., and Holland, I. B. (1989) A novel C-terminal signal sequence targets Escherichia coli haemolysin directly to the medium. *J Cell Sci Suppl* **11**, 45-57
3. Chervaux, C., Sauvonnnet, N., Le Clainche, A., Kenny, B., Hung, A. L., Broome-Smith, J. K., and Holland, I. B. (1995) Secretion of active beta-lactamase to the medium mediated by the Escherichia coli haemolysin transport pathway. *Mol Gen Genet* **249**, 237-245
4. Kanonenberg, K., Spitz, O., Erenburg, I. N., Beer, T., and Schmitt, L. (2018) Type I secretion system-it takes three and a substrate. *FEMS Microbiol Lett* **365**
5. Delepelaire, P. (2004) Type I secretion in gram-negative bacteria. *Biochim Biophys Acta* **1694**, 149-161
6. Kanonenberg, K., Schwarz, C. K., and Schmitt, L. (2013) Type I secretion systems - a story of appendices. *Res Microbiol* **164**, 596-604
7. Holland, I. B., Peherstorfer, S., Kanonenberg, K., Lenders, M., Reimann, S., and Schmitt, L. (2016) Type I Protein Secretion-Deceptively Simple yet with a Wide Range of Mechanistic Variability across the Family. *EcoSal Plus* **7**
8. Felmlee, T., Pellett, S., and Welch, R. A. (1985) Nucleotide sequence of an Escherichia coli chromosomal hemolysin. *J Bacteriol* **163**, 94-105
9. Wandersman, C., and Delepelaire, P. (1990) TolC, an Escherichia coli outer membrane protein required for hemolysin secretion. *Proc Natl Acad Sci U S A* **87**, 4776-4780
10. Noegel, A., Rdest, U., Springer, W., and Goebel, W. (1979) Plasmid cistrons controlling synthesis and excretion of the exotoxin alpha-haemolysin of Escherichia coli. *Mol Gen Genet* **175**, 343-350
11. Lenders, M. H., Weidtkamp-Peters, S., Kleinschrodt, D., Jaeger, K. E., Smits, S. H., and Schmitt, L. (2015) Directionality of substrate translocation of the hemolysin A Type I secretion system. *Sci Rep* **5**, 12470
12. Welch, R. A. (1991) Pore-forming cytolysins of gram-negative bacteria. *Mol Microbiol* **5**, 521-528
13. Baumann, U., Wu, S., Flaherty, K. M., and McKay, D. B. (1993) Three-dimensional structure of the alkaline protease of Pseudomonas aeruginosa: a two-domain protein with a calcium binding parallel beta roll motif. *EMBO J* **12**, 3357-3364
14. Thomas, S., Smits, S. H., and Schmitt, L. (2014) A simple in vitro acylation assay based on optimized HlyA and HlyC purification. *Anal Biochem* **464**, 17-23
15. Thanabalu, T., Koronakis, E., Hughes, C., and Koronakis, V. (1998) Substrate-induced assembly of a contiguous channel for protein export from E.coli: reversible bridging of an inner-membrane translocase to an outer membrane exit pore. *EMBO J* **17**, 6487-6496
16. Balakrishnan, L., Hughes, C., and Koronakis, V. (2001) Substrate-triggered recruitment of the TolC channel-tunnel during type I export of hemolysin by Escherichia coli. *J Mol Biol* **313**, 501-510
17. Ishii, S., Yano, T., Ebihara, A., Okamoto, A., Manzoku, M., and Hayashi, H. (2010) Crystal structure of the peptidase domain of Streptococcus ComA, a bifunctional ATP-binding cassette transporter involved in the quorum-sensing pathway. *J Biol Chem* **285**, 10777-10785
18. Lecher, J., Schwarz, C. K., Stoldt, M., Smits, S. H., Willbold, D., and Schmitt, L. (2012) An RTX transporter tethers its unfolded substrate during secretion via a unique N-terminal domain. *Structure* **20**, 1778-1787

19. Reimann, S., Poschmann, G., Kanonenberg, K., Stuhler, K., Smits, S. H., and Schmitt, L. (2016) Interdomain regulation of the ATPase activity of the ABC transporter haemolysin B from *Escherichia coli*. *Biochem J* **473**, 2471-2483
20. Lenders, M. H., Beer, T., Smits, S. H., and Schmitt, L. (2016) In vivo quantification of the secretion rates of the hemolysin A Type I secretion system. *Sci Rep* **6**, 33275
21. Costa, T. R. D., Ignatiou, A., and Orlova, E. V. (2017) Structural Analysis of Protein Complexes by Cryo Electron Microscopy. *Methods Mol Biol* **1615**, 377-413
22. Murata, K., and Wolf, M. (2018) Cryo-electron microscopy for structural analysis of dynamic biological macromolecules. *Biochim Biophys Acta Gen Subj* **1862**, 324-334
23. Vincentelli, R., and Romier, C. (2016) Complex Reconstitution and Characterization by Combining Co-expression Techniques in *Escherichia coli* with High-Throughput. *Adv Exp Med Biol* **896**, 43-58
24. Kim, J. S., Song, S., Lee, M., Lee, S., Lee, K., and Ha, N. C. (2016) Crystal Structure of a Soluble Fragment of the Membrane Fusion Protein HlyD in a Type I Secretion System of Gram-Negative Bacteria. *Structure* **24**, 477-485
25. Du, D., Wang, Z., James, N. R., Voss, J. E., Klimont, E., Ohene-Agyei, T., Venter, H., Chiu, W., and Luisi, B. F. (2014) Structure of the AcrAB-TolC multidrug efflux pump. *Nature* **509**, 512-515
26. Fronzes, R., Schafer, E., Wang, L., Saibil, H. R., Orlova, E. V., and Waksman, G. (2009) Structure of a type IV secretion system core complex. *Science* **323**, 266-268
27. Lenders, M. H. (2016) Mechanisms of hemolysin A Type 1 secretion in *Escherichia coli*. *Heinrich Heine Universität Düsseldorf*, doctoral thesis
28. Slotboom, D. J., Duurkens, R. H., Olieman, K., and Erkens, G. B. (2008) Static light scattering to characterize membrane proteins in detergent solution. *Methods* **46**, 73-82
29. Lee, S. Y. (1996) High cell-density culture of *Escherichia coli*. *Trends Biotechnol* **14**, 98-105
30. Korz, D. J., Rinas, U., Hellmuth, K., Sanders, E. A., and Deckwer, W. D. (1995) Simple fed-batch technique for high cell density cultivation of *Escherichia coli*. *J Biotechnol* **39**, 59-65
31. Kopp, J., Slouka, C., Ulonska, S., Kager, J., Fricke, J., Spadiut, O., and Herwig, C. (2017) Impact of Glycerol as Carbon Source onto Specific Sugar and Inducer Uptake Rates and Inclusion Body Productivity in *E. coli* BL21(DE3). *Bioengineering (Basel)* **5**

4. Discussion

The description of the first secreted peptide dates back as far as 1925, when the bacteriocin MvvC was discovered as a bactericidal product of *E. coli* and hence named “colicin” (113). The first large secreted protein was discovered in 1979 (92), when the exotoxin haemolysin A, due to its ability to lyse erythrocytes, was identified. The detailed analysis of both operons revealed similar types of translocons, consisting of an ABC transporter and a membrane fusion protein (MFP) in the inner membrane (85,94,114). Later on, TolC was identified as the outer membrane component of both secretion systems (85,115). The secretion apparatus was named type I secretion system and to date, the HlyA-T1SS serves as a paradigm to generally describe functionality and mechanistic details of T1SS.

T1SS are widespread in Gram-negative bacteria. Interestingly, many of their substrates are virulence factors and promote the pathogenicity of their host organism. For example, the toxin HlyA is secreted by uropathogenic *E. coli* strains and was shown to lyse urothelial cells (116). *Bordetella pertussis*, the causative agent of whooping cough, secretes an adenylate cyclase as the major essential virulence factor, which has both invasive, cytotoxic and haemolytic, pore-forming activity (117-120). Many *Pseudomonas sp.* strains secrete large adhesins, which are crucial for biofilm formation and protect the organism against antimicrobial agents (121). SiiE, another adhesin and secreted by *Salmonella sp.*, mediates the first contact to a host cell, which subsequently results in bacterial internalisation and cell invasion (122-124).

The vast variety in function and size of substrates is also reflected by different types of T1SS. They all share a common, basic assembly out of three proteins: an ABC transporter and a membrane fusion protein as a complex in the inner membrane and a TolC-like outer membrane porin. The translocons mediate the secretion to the extracellular space without periplasmic intermediates but overall, differ largely in their accessory domains, proteins or operon organisation. Thus, an initial classification of T1SS was attempted based on the presence or absence of an N-terminal accessory domain on the ABC transporters (11) (Chapter I). However, this analysis did not go beyond the ABC transporter subunit of the secretion complex. To provide a more detailed classification of T1SS various other aspects have subsequently been taken into account, which are described in further detail in the following paragraphs.

The presence of two membranes in Gram-negative bacteria imposes a specific challenge to secrete proteins and peptides, but also other substances, to the extracellular space. To enable the transport of polypeptide chains, a range of secretion systems has evolved that perform the transport applying a number of different mechanisms and comprising a range of translocon structures (21).

This thesis focuses on the type I secretion system, more precisely on the HlyA-T1SS from *Escherichia coli*, which was the first T1SS to be identified (92,94,115). For the HlyA-T1SS, the secretion rate was determined to be 16 amino acids per second and transporter (104). Early on, the secretion signal was located to the C-terminal moiety of the substrate (64,65) and finally, after a long debate within the field of study about the directionality of transport, it was directly proven that HlyA-secretion indeed takes place C-terminus first (103).

Another well-studied T1SS is the haemophore HasA-secreting system from *Serratia marcescens* (43). To date, it is the only T1SS where a chaperone, in this particular case SecB, is involved in the export process by keeping the substrate unfolded in the cytosol until secretion is initiated by the C-terminal secretion signal (74,125).

Although T1SS secrete a vast variety of proteins that goes well beyond RTX toxins, haemophores or proteases, general rules for operon organisation or mechanisms of transport have been formulated based only on a few examples, although remarkable differences are already well apparent between them.

This chapter deals in detail with the different operon-organisations that can be found amongst T1SS, the differences in the ABC transporters, membrane fusion proteins, substrates and accessory proteins, and suggests a classification of the different T1SS that can be found across Gram-negative organisms.

4.1 Bacteriocin-Secreting T1SS

Notwithstanding the often stated general rule that T1SS substrates contain a C-terminal secretion signal, which is not cleaved during the secretion process, there is a small yet somewhat neglected subgroup of T1SS where the substrates differ remarkably from both the latter statements (126).

These T1SS secrete small bacteriocins from the subclass of class II microcins (126). Bacteriocins are small antimicrobial peptides that display bactericidal activity. The class II

microcins can be divided into the two distinct subgroups class IIa and class IIb. Both subgroups are secreted by type I secretion systems but differ largely in their operon organisation (126,127).

Class IIa microcins are not post-translationally modified. One of the most prominent members of the class IIa is MccV (formerly colicin V) from *E. coli* that kills bacterial cells by disrupting their membrane potential once it gains access to their periplasmic space (128). Interestingly, it states the first T1SS-substrate to be described in literature, as early as 1925 (129). However, it took another 62 years until the cognate secretion system was discovered and subsequently, analysed in greater detail (85,114,130).

The operons of class IIa-secreting T1SS are composed of only four genes: an ABC transporter, a membrane fusion protein, the substrate and an immunity protein conferring resistance against the bactericidal activity of own bacteriocin (85,114,126,130). The typical organisation is depicted in Figure 11.

Class IIb microcins are generally extensively post-translationally modified. Thus, their coding regions are very complex and can harbour up to ten different genes (131), which are, besides the four components also present in the operons of class IIa microcins, mostly required for post-translational modifications, but also for export (Figure 11) (132-134). One secretion system is mediating the export of up to three microcins that can vary in their localisations within the coding region (Figure 11).

The operons of bacteriocin-T1SS do not contain an outer membrane protein. Instead, a polyvalent OMP (TolC or equivalent) is employed for the secretion process (44). The different components of the bacteriocin T1SS are described in further detail below, highlighting their unique features amongst T1SS.

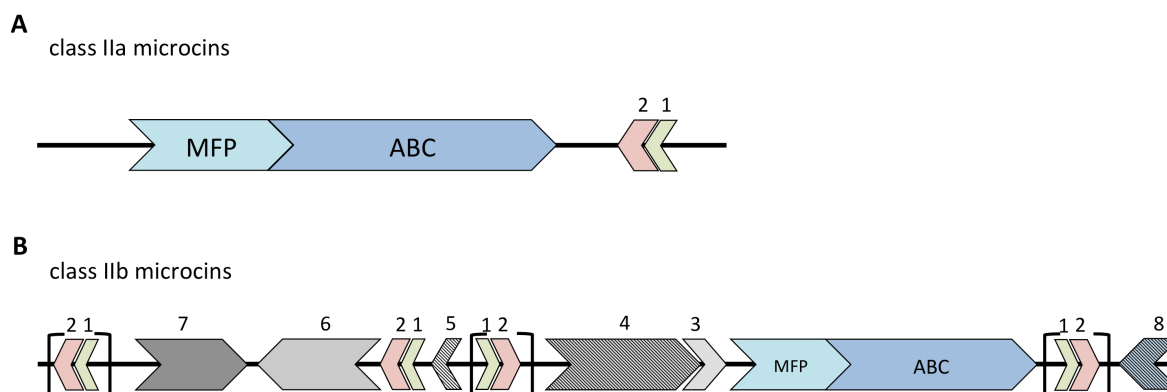


Figure 11: Schematic overview of the coding regions of class II microcin-secreting T1SS. ABC – ABC transporter, MFP – membrane fusion protein, 1 – self-immunity protein, 2 – substrate, 3 – lysine acyltransferase, 4 – unknown function in post-translational modification, 5 – unknown function, 6 – enterobactin esterase, 7 – glycosyltransferase, 8 – unknown function in export. (A) Class IIa microcin operons are composed of only four genes. (B) Class IIb coding regions contain up to ten different genes of which most are required for post-translational modifications. Genes in brackets [] mark their possible locations.

4.1.1 The Bacteriocin-T1SS ABC Transporter

T1SS-ABC transporters often comprise accessory domains at their N-termini (11). ABC transporters that are part of bacteriocin-T1SS contain a C39 peptidase-domain that is located in the cytosol and cleaves an N-terminal signal peptide from the substrate prior to secretion (44,69,135). ABC transporters with C39 peptidase domains are widespread in Gram-positive bacteria where they mediate the secretion of related antimicrobial peptides (69).

The three-dimensional structures of an isolated C39 peptidase domain (70) as well as of an ABC transporter from a Gram-positive bacterium (68) are available. C39 peptidases as accessory domains are, amongst Gram-negative bacteria, a unique feature of bacteriocin-T1SS.

4.1.2 The Substrates of Bacteriocin-T1SS

Bacteriocins are small (< 10 kDa), antimicrobial peptides that are secreted by many bacteria. However, they can mainly be found in Gram-positive bacteria whereas in Gram-negative organisms, only members of the *Enterobacteriaceae* secrete bacteriocins from the subgroup of class II microcins (126). They cause cell-lysis of closely related cells, either by disrupting

the membrane potential upon entering the periplasmic space (class IIa) (136) or by presumably forming pores in the plasma membranes (class IIb) (132-134). Class IIa microcins are activated by a disulphide-bond formation in the periplasm of the target cell (137-139) while Class IIb microcins experience substantial post-translational modifications that finally yield the bactericidal peptide (126,132-134).

Class II microcins contain an N-terminal secretion signal that is cleaved upon a typical “GG-motif” by the N-terminal C39 peptidase domain of the ABC transporter prior to secretion (137). This secretion signal is highly conserved amongst bacteriocins from Gram-negative and Gram-positive bacteria, while their C-terminal moieties that confer the bactericidal properties are of greater variability (Figure 12) (126,137).

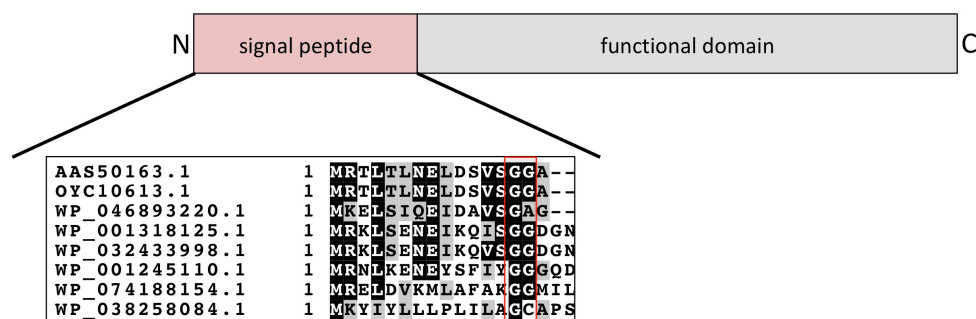


Figure 12: Alignment of the N-termini of selected T1SS-secreted bacteriocins. The conserved “GG-motif” is highlighted by a red box.

4.2 Large RTX Toxin-T1SS

Over the years, especially the T1SS secreting large RTX toxins have received much attention and many T1SS-paradigms are based on experimental investigations on the *E. coli* haemolysin A T1SS.

The operons of RTX toxin-T1SS contain an ABC transporter, a MFP, the substrate and often an accessory protein that is responsible for toxin-activation via post-translational modifications, like acylations, prior to secretion (Figure 13) (67,96,115,140). The operon sometimes contains a TolC-like outer membrane protein but otherwise, TolC, encoded elsewhere on the chromosome, functions as the outer membrane component (115).

RTX toxins are large substrates with sizes typically ranging from 700 to more than 2500 amino acids. Normally, only one substrate is present per operon (Figure 13).

4.2.1 The Substrates of Large RTX Toxin-T1SS

The group of RTX toxins comprises exotoxins such as leukotoxins (141), haemolysins (38,142) and adenylate cyclases (143) but also some proteins of unknown functions. RTX toxins are normally virulence factors and confer pathogenicity to their host organisms. They all contain a common motif in their C-termini, which has been named the EISKIIS-motif (Chapter VI) and linked directly to secretion. Just upstream from the secretion signal a variable number of RTX-domains are located, which trigger the folding of the substrate upon binding of calcium ions in the extracellular space. Interestingly, it has been shown that the secretion of HlyA is independent of the extracellular calcium ion concentration (104) while that of the adenylate cyclase CyaA is not and for which a ratchet-like mechanism was suggested that depends on the subsequent “pulling” of the substrate from the translocator (107). In *Neisseria meningitidis*, the folding of the RTX domains results in autocatalytic processing of the secreted substrate (144,145).

The secretion signal of RTX-toxins has been located to the approximately 50 – 60 C-terminal amino acids, which also comprises the EISKIIS-motif about 30 residues upstream from the extreme C-terminus (Chapter VI).

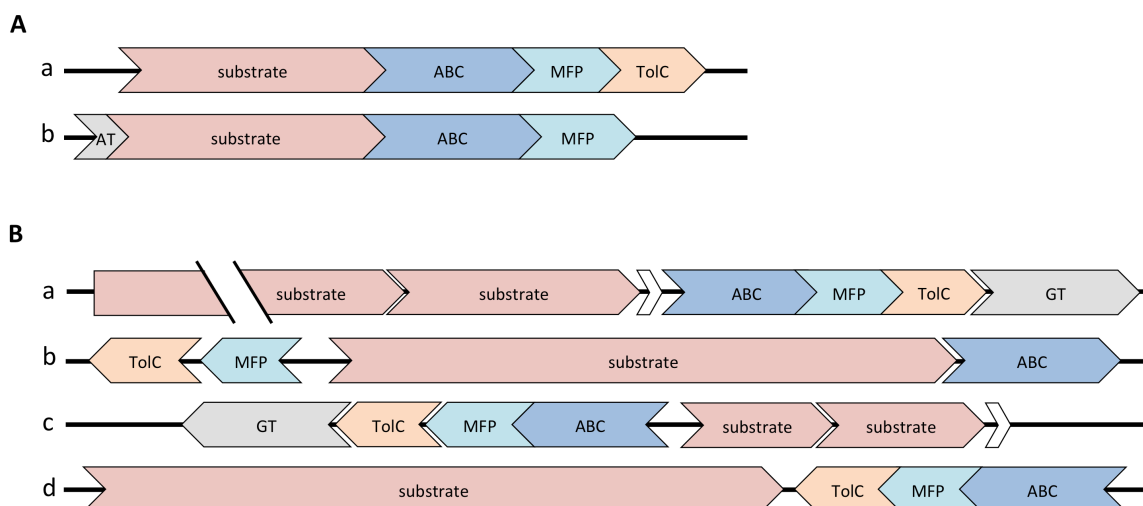


Figure 13: Variable operon organisation of large RTX toxin-T1SS. ABC – ABC transporter, MFP – membrane fusion protein, TolC – TolC-like outer membrane protein, AT – acyltransferase, GT – glucuronosyltransferase. White genes represent genes of unknown functions. (A) Most common operon organisations of large RTX-toxin-T1SS represented by (a) adenylate cyclases and (b) haemolysins. (B) Examples of uncommon operon arrangements, containing (a, c) two substrates or (b-d) unusual arrangements of substrates, translocon subunits and/ or accessory proteins on complement strands.

4.2.2 ABC Transporters of Large RTX Toxin-T1SS

The ABC transporters of large RTX toxin-T1SS always comprise an accessory domain at their N-terminus, a C39 peptidase-like domain (CLD) (6). Its catalytical triad is corrupted, leaving the domain with no proteolytic activity; however, its presence is essential for secretion and, in the case of the HlyA-T1SS, it was shown to interact with the substrate via the unfolded RTX domains (6). In functional assays, its importance during the secretion process was further emphasised, as its presence strongly changes the biochemical response of the transporter to the substrate (71) (Chapter IV).

The ABC transporters of RTX toxin-T1SS are thought to follow a unique translocation mechanism, as the commonly accepted alternating access model cannot be applied due to the sheer length of the transported substrate (11,22,38).

4.2.3 Large RTX Toxin-T1SS Membrane Fusion Proteins

Membrane fusion proteins of RTX toxin-T1SS comprise a unique appendix, a small N-terminal domain that is located in the cytosol. The importance of this domain has been assessed for the HlyA-T1SS and was shown to function as a hub, where, via an interaction with the substrate, the outer membrane component is recruited into the secretion complex (41,42).

This domain is highly conserved across the MFPs of RTX toxin-T1SS (Figure 14). Its absence in all other T1SS accounts for a unique function in the mechanism of transport, which has not yet been investigated in greater detail.

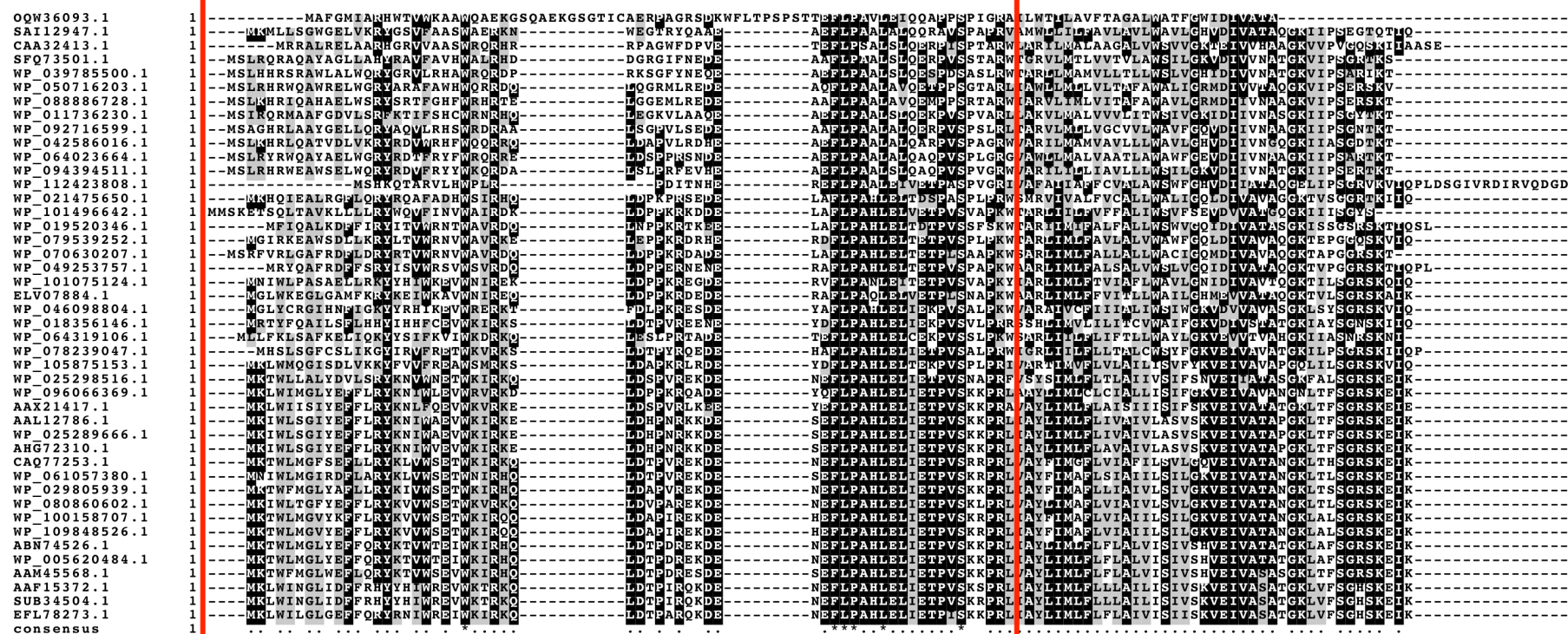


Figure 14: Alignment of the N-terminal domain of MFPs from RTX-toxin T1SS, represented by their accession numbers (RefSeq, DDBJ/EMBL/GenBank). The red box indicates the complete N-terminal domain, comprising approximately residues 1 to 60. The consensus is shown at the bottom, * indicates 100 % identity across all sequences. Alignment was performed with MUSCLE (146,147), the figure was created using Boxshade (https://embnet.vital-it.ch/software/BOX_form.html).

4.3 Small RTX Protein-T1SS

The small RTX protein-T1SS transport mainly metalloproteases (“serralyins”) (148), but also lipases (149), haemophores (150), haem peroxidases (151) or surface layer proteins (S-layer proteins) (152). Despite their functional variance, they comprise very similar operon organisations, which differ in the presence of distinct accessory proteins (Figure 15).

The overall common feature of all small RTX-T1SS is the absence of N-terminal domains on the ABC transporter as well as the MFP. Apart from few exceptions, a TolC-like protein is present in the operon just upstream of the ABC transporter and the MFP. Interestingly, up to five substrates with similar functions were found in one single operon in different locations (Figure 15). Only one example was found where two substrates with different functions were encoded in the same operon, a lipase (TliA) and protease (PrtA) secreting T1SS from *Pseudomonas fluorescens* (47). The size of the substrates is diverse and ranges from about 220 amino acids (haemophores) to a length of 2000 residues (haem peroxidases) but most are within the range of 400 to 650 amino acids. Not all, but most substrates contain RTX domains. Although there was no conserved motif identified in the C-termini of the substrates, a region of high similarity, approximately 10-15 amino acids upstream from the C-terminus, can be observed (Figure 16). Whether this comprises a secretion signal or interaction site with the translocon requires further functional analysis.

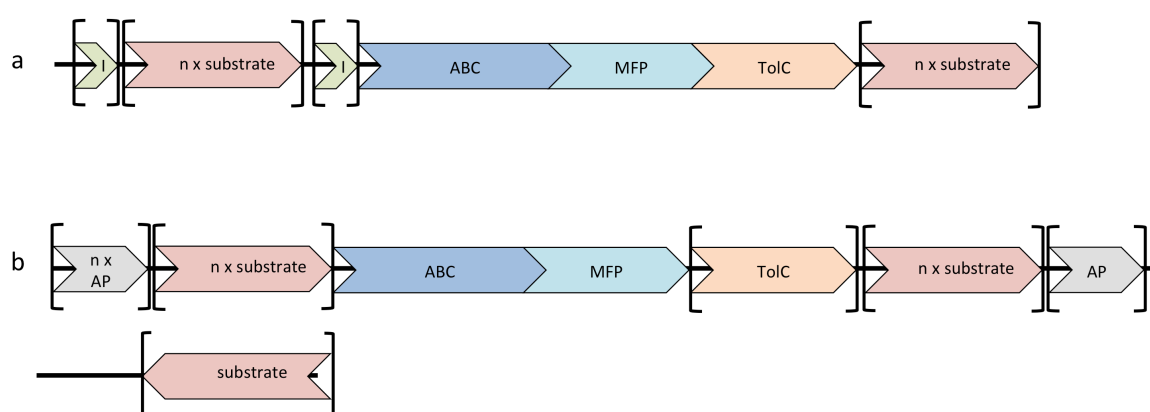


Figure 15: Possible operon organisations of “serralyisin-like” T1SS. (a) Serralyisin-encoding operons. I – inhibitor, ABC – ABC transporter, MFP – membrane fusion protein. n – one to five substrates were found to be encoded in one operon. Genes in brackets [] show their possible locations. (b) Haemophore/ surface layer protein / lipidase/ haem peroxidase encoding T1SS. AP – accessory protein (diverse functions, further details in text). The substrates of some haem peroxidases were found to be encoded on the complementary strand.

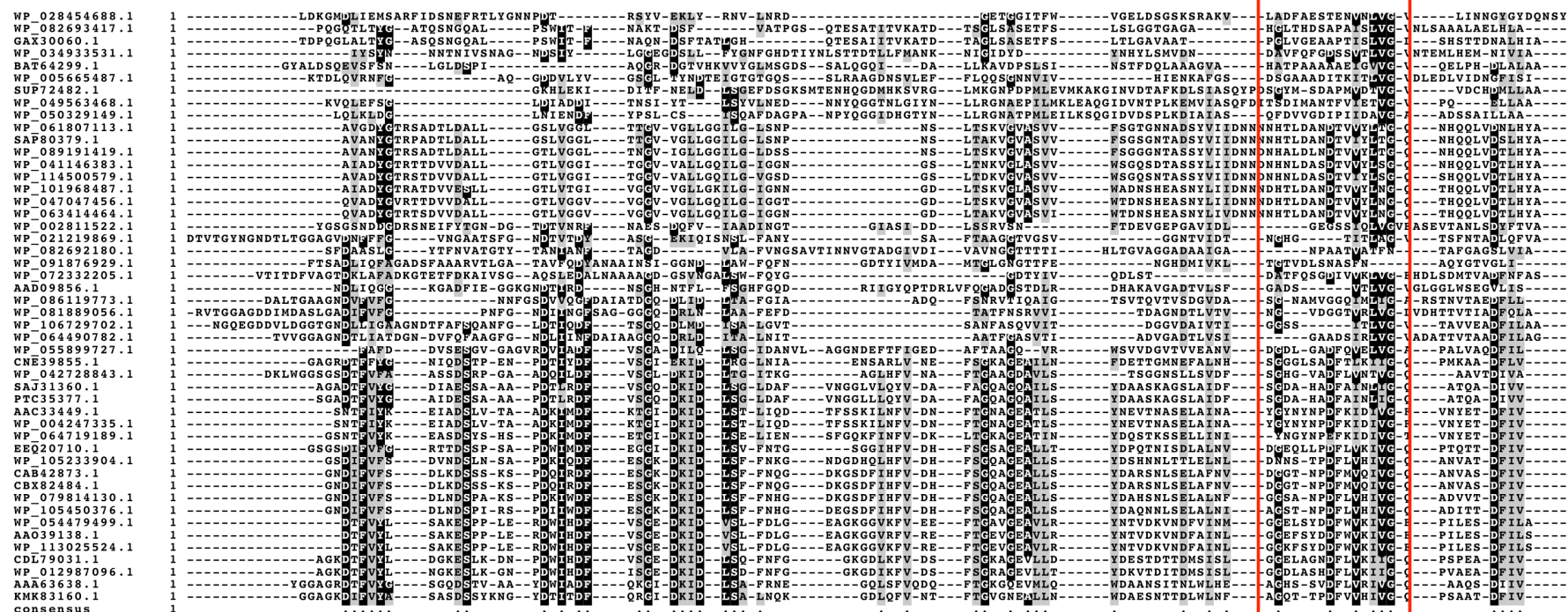


Figure 16: Alignment of the C-terminal 100 amino acids using MUSCLE (146,147) of small RTX proteins. The region of highest similarity, approximately 10-15 amino acids upstream from the C-terminus, is highlighted by the red box. The figure was created using Boxshade (https://embnet.vital-it.ch/software/BOX_form.html).

4.3.1 The Small RTX Protein Substrates – Serralysins, Proteases

Serralysins are zinc-dependent metalloproteases that function as virulence factors and are secreted by Gram-negative bacteria (148,153). First discovered in the supernatants of *Erwinia chrysanthemi* (154), they have been identified in large numbers of Gram-negative genomes. They contain RTX domains, which, just as in most RTX toxins, trigger the folding of the substrate in the extracellular space and confer high chemical and thermal stability to the protein (155). They belong to the zinc-dependent metazincin superfamily, which is defined by its conserved zinc-binding active site (156,157). The secretion signal of serralysins has been located to the C-terminus of the proteins (154,158). However, studies concerning the detailed secretion mechanism of serralysins and related proteases are lacking.

Serralysin-operons always contain a periplasmic inhibitor that confers resistance against the secreted metalloprotease (159-161). The operons sometimes contain up to five substrates (Figure 15).

4.3.2 The Small RTX Protein Substrates – Haemophores

Haemophores, or iron-scavenger proteins, are involved in supplying the host-cell with iron by mediating the uptake of haem from the extracellular space (162-164). They are secreted into the extracellular space where they collect haem and shuttle it to specific receptors located on the cell surface (HasR) (163-166). Thus, the haemophore-T1SS are often implemented into a whole genomic region of iron-responding proteins. Accessory proteins are for example the outer membrane haem receptor HasR or TonB, which is involved in siderophore (ferric chelates) transport (167). With a length of approximately 220 amino acids, haemophores are amongst the smallest T1SS substrates that contain a C-terminal secretion signal. Interestingly, they do not contain RTX domains. The operons sometimes contain several copies of HasA proteins (Figure 15).

4.3.3 The Small RTX Protein Substrates – Lipases

Lipase-secreting T1SS operons are of simple organisation and do not contain any accessory proteins (Figure 15). In total, only a few T1SS-secreted lipases have been identified, mainly in *Pseudomonas sp.* (149). They contain RTX domains and catalyse the hydrolysis of lipid molecules. Interestingly, operons from *Pseudomonas sp.* sometimes contain a lipase as well as a protease, which are both secreted via the same translocon (47).

4.3.4 The Small RTX Protein Substrates – Surface Layer Proteins

One group amongst the variety of small RTX T1SS substrates are the surface layer proteins (S-layer proteins). They form a porous, lattice-like layer of high symmetry that completely covers the cell surface (168). They are thought to be involved in adhesion, but also in protective or enzymatic functions. A known member is SapA from *Campylobacter sp.* (169). The substrate is often located on the opposite strand than the rest of the T1SS. The operon only contains the inner- and outer membrane components of the translocon and the substrate, but no accessory proteins. A pblast analysis revealed that S-layer proteins often contain the domain of unknown function 4214 (DUF4214).

4.3.5 The Small RTX Protein Substrates – Haem Peroxidases

Despite their length of up to 2000 amino acids the haem peroxidases fit best into the class of small RTX proteins. Their physiological function is not well understood. They contain several RTX domains just upstream from the C-terminal secretion signal (151).

4.4 “LapA-like” T1SS

To date, the biochemical data available on LapA- and related proteins and their cognate secretion systems is still limited. However, a number of very unique features have been identified that differ strongly from all other T1SS described so far (170).

LapA and related proteins belong to the class of adhesins, which are responsible for biofilm formation (171-173). They are anchored to the cell surface via their cognate T1SS and

mediate the attachment of cells to a variety of surfaces (66). Adhesins are probably the largest T1SS substrates with sizes ranging between 2500 and 8300 residues, which, like many other T1SS substrates, contain calcium-binding RTX domains. LapA-like adhesins typically contain many repetitive Ig-like domains (174). The C-terminal moieties of different substrates are similar in terms of amino acids sequence, but no clear conserved motif could be identified.

While the extreme C-terminus contains the putative secretion signal, a specific domain at the N-terminus anchors the protein inside the translocation tunnel to retain it to the cell surface (170). To detach and subsequently release the adhesin into the extracellular space, this domain is proteolytically cleavable by a periplasmic protease, LapG (175,176), also encoded within the operon. Thus, unlike other T1SS, the secretion apparatus remains (partially) assembled for an extended period of time.

The protease LapG is under the control of the membrane receptor LapD. Upon decrease in cyclic-di-GMP, LapG is released and cleaves LapA upstream from the anchor region, which results in the release of the protein into the extracellular space (175,177-179).

The operon arrangement of LapA-like T1SS is highly conserved. The substrate, together with a small protein of unknown function, is encoded on the complement strand, while the accessory proteins and the secretion apparatus are encoded in the opposite direction (Figure 17).



Figure 17: Operon organisation of LapA-like T1SS. 1- protein of unknown function, TolC- TolC-like outer membrane protein, ABC – ABC transporter, MFP – membrane fusion protein, LapG/ LapD – proteins homologous to LapG and LapD, respectively, substrate – 2500 – 8000 amino acids, LapA-like

Interestingly, in LapA-like operons the outer membrane proteins are always encoded in front of the ABC transporter and the MFP (Figure 17). All operons contain a small protein of unknown function, approximately 120 amino acids in length, after the dedicated substrates (Figure 17). Although it has not been analysed in any of the performed studies, its conserved presence and location indicates an important function during the secretion or adhesion process. Considering the degree of variability in the operon organisation of other T1SS, it

can be hypothesised that this arrangement has a certain importance in the functionality of the system.

4.4.1 The LapA-like T1SS ABC Transporter

The ABC transporters (LapB-like) of LapA-T1SS contain a CLD that differs in its conserved residues from RTX-toxin CLDs, as the characteristic H22 and Y23 are missing. It was hypothesised that this accounts for an altered interaction with the substrate, but experimental proof is missing (170). A structural prediction of the CLD indicates a diverging fold to the CLD of HlyB (pdb: 3ZUA) but a very similar fold to the CLD of an ABC transporter from *Vibrio parahaemolyticus* (pdb 3B79) (Figure 18). However, the genome reveals no potential substrate in close proximity of this ABC transporter, but given the overall high sequence similarity to LapB-CLD we suspect it to be involved also in adhesin-secretion.

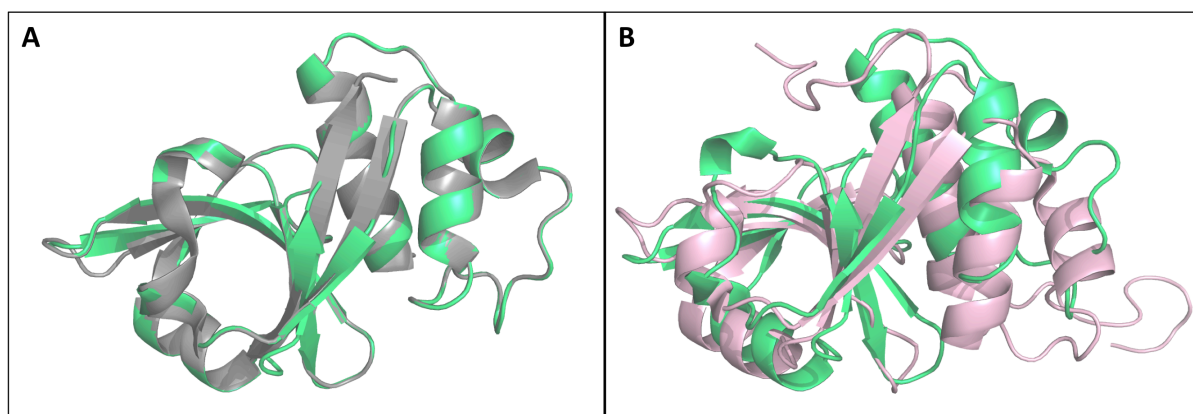


Figure 18: (A) Homology models created with Swissmodel (180,181) of a LapB-like CLD (residues 1-140, green) with a CLD from *Vibrio parahaemolyticus* (grey, pdb 3B79) as a template. The GMQE and QMEAN-scores were 0.63 and -0.89 , respectively, which accounts for a high accuracy and reliability of the model. (B) Alignment of the LapB-like CLD model (green) based on 3B79 to HlyB-CLD (light pink, pdb 3ZUA), which shows differences in the overall fold. Figures were created using PyMOL (The PyMOL Molecular Graphics System, Version 2.0 Schrödinger, LLC).

4.5 SiiE-like T1SS

SiiE-like proteins belong to the group of non-fimbrial adhesins and, just like LapA-like adhesins, are retained to the cell surface by their cognate T1SS, yet by a completely differing retention mechanism. This is reflected also by a diverging operon organisation and a different set of accessory proteins.

Two proteins homologous to MotA and MotB, respectively, utilise the proton motive force (PMF) across the bacterial membrane for SiiE retention (124). However, the exact mechanism is not yet understood. MotA and MotB form a complex of unknown stoichiometry and have been shown to interact with the translocon (124).

SiiE-like proteins are equally involved in biofilm formation, surface and host-cell adhesion and typically, contain Ig-like domains and RTX domains (122,123,182). Like LapA-like proteins they can be of remarkable size and up to 5000 amino acids in length. The secretion signal is located in the extreme C-terminus (182), which does not show any apparent similarity between different substrates. No anchor domain is present in the N-terminal moiety.

Interestingly, in SiiE-like operons the ABC transporter (SiiF) and the MFP are separated (Figure 19).



Figure 19: Operon organisation of SiiE-like operons. MFP – membrane fusion protein, ABC – ABC transporter, MotB, MotA – proteins homologues of MotB and MotA, respectively.

Sequence alignments of the CLDs show that it differs completely from RTX-toxin ABC transporter CLDs (Figure 20).

```

HlyB      1  SCHKID-VGLYA---LEILAQYHNVSVN--PEETKRRF-----DTDGTGLGLTSWLPAAK
SiiF      1  MDKKLEPVYLSAETALSIVSKKFNIKIDIKEDDNLRFKKYDRNNTDDSIQMKNFQ---

HlyB     50  STEPKVKQV--KKTIDRLN-----FIFLPAVWR---EDGRHFITTKIS-----
SiiF     58  SLGSLQDILFNNGEDLNEPMPILLTPEMKMMVCVSGCQIKLVNARGELCYVEIEDE

HlyB     89  --KEVNRYLIFDIEQRNPRVLEQSEFEALYQGHILI-----
SiiF    118  YLKELSAFSLPLN----KVVDNISRVKNIKNSLSMNKIFYTKY

```

Figure 20: Sequence alignment of HlyB-CLD and SiiF-like CLD by MUSCLE (146,147). Figure was created using Boxshade (https://embnet.vital-it.ch/software/BOX_form.html).

A structural modelling of the CLD was attempted with Swissmodel, but no templates were found when applying automated searching. Thus, The HlyB-CLD was chosen manually as a model, which resulted in a similar three-dimensional fold of the SiiF-CLD (Figure 21). The low scores of the model question its reliability and accuracy. For detailed structural studies, experimental investigation is inevitable.

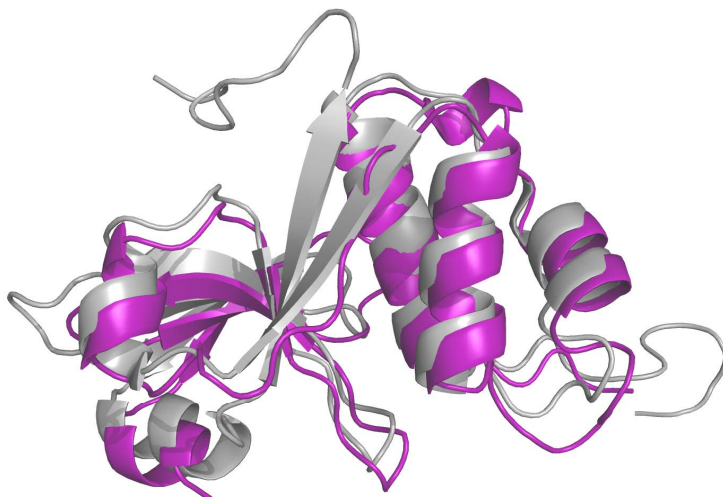


Figure 21: Structural alignment by Swissmodel (180,181) of a SiiF-like CLD (residues 1-157, pink) with HlyB CLD (grey, pdb 3ZUA) as a template. The GMQE and QMEAN-scores were 0.35 and -3.02, respectively, which accounts for a rather low accuracy and reliability of the model. The figure was created using PyMOL.

4.6 Summary

The large variety in operon organisation, functional differences and also different domain organisations of the individual T1SS translocon proteins demonstrate that T1SS show a basic common assembly of the transporting unit, yet vary in terms of secretion mechanisms and function. Different accessory proteins of diverse functions complete specific T1SS. In a few cases, distinct secretion signals or conserved regions have been identified but there is no general feature that is present in all substrates.

Also, the presence or absence of a CLD on the ABC transporter is neither linked to the presence of RTX domains in the substrate nor to a certain substrate size. In total, three different CLDs were identified but no data is available yet on functional differences.

The membrane fusion proteins contain largely conserved domains, however, the N-termini are of high variability and, in the case of RTX toxin-T1SS MFPs, comprise a unique cytosolic domain that is actively involved in the secretion process.

We conclude that a classification of T1SS cannot only be based on one individual member of the transport machinery or the substrate. Rather, the ensemble of the operon, the C-termini of the substrates, the accessory proteins and domains have to be all taken into account, which resulted in an overall classification into five distinct T1SS subgroups (Table 1). Notably, CLD domains are widespread in T1SS but it remains questionable whether they fulfil identical functions in the secretion process as they diverge in structural and sequential alignments.

Table 1: Classification of T1SS based on their operons and accessory domains and proteins.

Class	ABC	MFP	ToIC-like	Accessory proteins	substrate	Features	Ref.
bacteriocin	C39 peptidase domain	No cytosolic (?) domain	no	self-immunity protein	N-terminal signal peptides, cleavage, 1 – 3 substrates per operon		(11,44,68- 70,85,114,1 26-139)
RTX-toxin	CLD (HlyB- like)	N-terminal, cytosolic (?) domain	variable	acyltransferases	EISKIIS-motif, 1 substrate per operon, RTX domains		(6,11,22,38, 41,42,67,71, 94,96,104,1 07,115,140- 145)
Serralyisin	no domain	no cytosolic (?) domain	yes (with a few exceptions)	depends on function of substrate	large variety in function and size, ± RTX domains, common motif in C- terminus, 1- 5 substrates per operon	large variations in operon organisations	(47,148- 157,159- 167,183)
LapA-like adhesins	LapB-CLD	no cytosolic (?) domain	yes, always	LapG/ LapD	large adhesins, 2500 – 5000 aa, N- terminal anchor domain	retained to cell surface by N- terminal anchor domain	(66,170- 172,174- 179)
SiiE-like adhesins	SiiF-CLD	no cytosolic (?) domain	yes, always	MotA/ MotB	large adhesins up to 8000 aa	retained to cell surface by MotA/ MotB, probably pmf involved	(122- 124,182)

4.7 Exceptions and “Incomplete” Operons

Despite thorough examination, some T1SS did not fit into one of the five classes defined above. One clearly is the well-studied HasA secretion system from *Serratia marcescens*. The C-terminus of this haemophore does not align to any of the other substrates of small RTX nor to any other class. Furthermore, it is still the only T1SS where the chaperone SecB has been proven to be involved in the secretion process (74).

Other exceptions are T1SS operons in Gram-negative genomes that only include an ABC transporter and a membrane fusion protein, with no substrate in close proximity. We speculate that the substrates of these T1SS are localised elsewhere in the genome and thus cannot be identified based only on the sequences of the inner membrane complex. For a further characterisation of these systems, *in vitro* studies are required.

Another group that was not classified are T1SS secreting BapA-like adhesins (184-186). The substrates are similar to SiiE or LapA-related proteins and contain a C-terminal secretion signal but the operons do not contain accessory proteins. The ABC transporters are sometimes similar to LapB-like ABC transporters but no general similarity was found. The operons may contain several substrates and the localisation of the translocon subunits varies. To date, only little data is available on these T1SS and a further characterisation is necessary to classify these T1SS into one of the groups stated above or into an additional class of T1SS.

4.8 Characterisation of the Haemolysin A T1SS from *Escherichia coli*

The major part of this thesis dealt with the HlyA-T1SS from *E. coli*. A main goal was to establish the functional reconstitution of the ABC transporter HlyB and subsequently of the assembled inner membrane complex, composed of HlyB and HlyD. The latter was subjected also to initial structural characterisation by negative-stain electron microscopy; however, the purifications did not meet the criteria of high purity and homogeneity due to large amounts of the outer membrane porin OmpF in all preparations. As all strategies to reduce the impurities failed, a new expression strain lacking not only OmpF but also the inner membrane part of the tripartite efflux pump, AcrA and AcrB as in other studies, AcrB was shown to be equally problematic as OmpF (187).

The genomic deletions of the three genes not only resulted in protein samples of substantially increased purity, but led also to a range of interesting and advantageous features, which are discussed in the following chapter.

4.8.1 Improving Membrane Protein Overexpression by Modifying the Membrane Environment

Hitherto, new expression strains to improve membrane protein production were developed by targeting the promoter region, thus to allow for better control of overexpression and subsequent membrane insertion of the target protein in the plasma membrane (188,189). The first strains to be developed were the so-called Walker strains, namely C41(DE3) and C43(DE3), both derived from BL21(DE3) (190). Ever since, both strains have been widely used in (membrane) protein overproduction.

A first genomic analysis revealed mutations in the *lacUV5* promoter region of both strains, which weakened the T7 RNA polymerase activity (191). However, as present in both strains, these findings did not explain the differences in the behaviour of C41(DE3) and C43(DE3) and a further genome-wide analysis identified a mutation in *lacI*, which was shown to help C43(DE3) to overcome the toxicity of certain membrane proteins (192).

C43(DE3) additionally contains two large deletions of 21 kb and 37 kb, respectively, whose influence on the overexpression and toxicity was not further analysed (192).

Targeted genomic modifications resulted in the development of the Lemo-strain (188,189). A rhamnose-inducible promoter was introduced into the genome, which allowed for adjusted activity of the T7 repressor T7 lysozyme (188). A second, more recent approach introduced a novel regulator system for the T7 RNA polymerase, which substantially improved the overexpression of a range of bacterial and even eukaryotic membrane proteins (193).

Initially, the deletions of *ompF* and *acrAB* in C41(DE3) were performed with the intention of developing a strain that permits the preparation of membrane protein samples, especially for structural studies, free of these widespread and largely described impurities (187,194,195). Their ability to crystallise from only traces in protein samples led to numerous entries of AcrB and OmpF in the protein database.

Also in the course of this thesis, AcrB crystals were obtained during crystallisation trials with the ABC transporter HlyB (figure 22), and OmpF was found as an omnipresent impurity in samples of the assembled T1SS inner membrane complex used for negative-stain electron microscopy (Chapter VII).

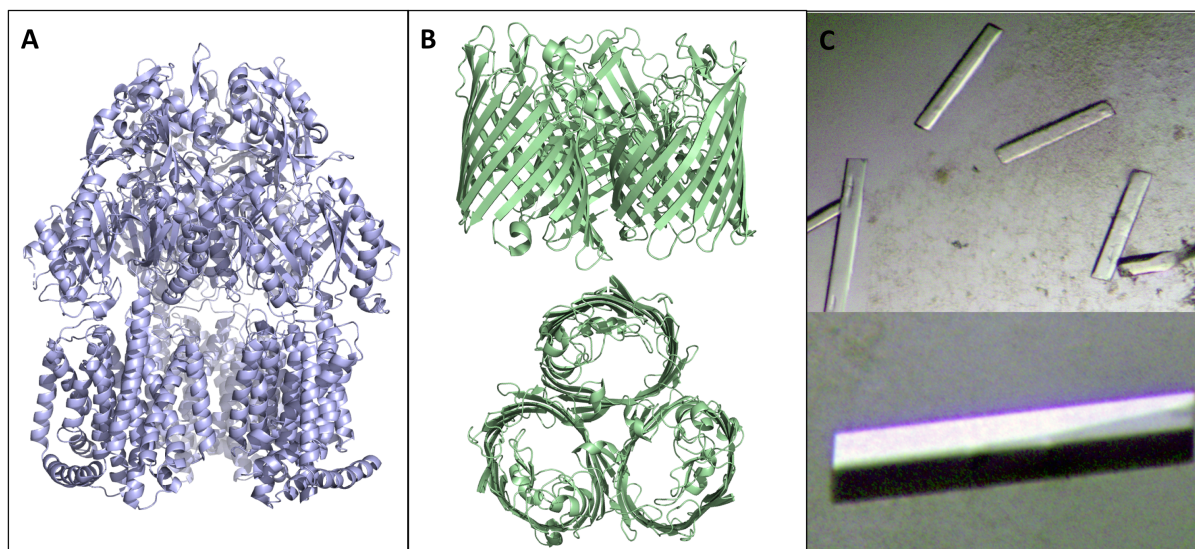


Figure 22: Crystal Structures of (A) AcrB (pdb: 1IWG (196)) and (B) OmpF (pdb: 3K19 (195)). (C) AcrB crystals obtained during the course of this study.

As no purification strategy was proven successful to remove the contaminants, both proteins were consequently removed from the genome of C41(DE3). It was expected to yield samples of higher purity that would be suitable for extended structural studies.

OmpF and AcrAB were deleted by P1 transduction (197) and the lambda-red recombinase system (198), respectively. The deletion of both proteins led to significant changes within the lipidome and the proteome, which overall resulted in an improved expression strain especially for integral membrane proteins such as ABC transporters. The improvements ranged from increased yields to a higher protein stability and, most notably, protection from proteolytic degradation within the cell (Chapter V).

How these effects are caused by the two genomic deletions cannot be explained in detail with the provided analysis. Notably, OmpF is involved in the MlaFEDB transport machinery that maintains the asymmetry between the inner and the outer membrane (199,200). AcrAB and OmpF are also both involved in the fatty acid transport of *E. coli* (201-203). Nevertheless, it remains speculative how the physiological functions of both proteins are linked to the observed phenotypes.

To combine the fruitful outcome of this study with the superior behaviour of C43(DE3) in overexpressing certain, in C41(DE3) toxic, membrane proteins, both mutations were equally introduced to C43(DE3) following the same protocols as described in Chapter V.

Initial test expressions show a similar behaviour as known from C41(DE3) but most interestingly, additionally to integrating high amounts of protein into the plasma membrane the cells produced large amounts of inclusion bodies of most of the overexpressed membrane proteins (Figure 23).

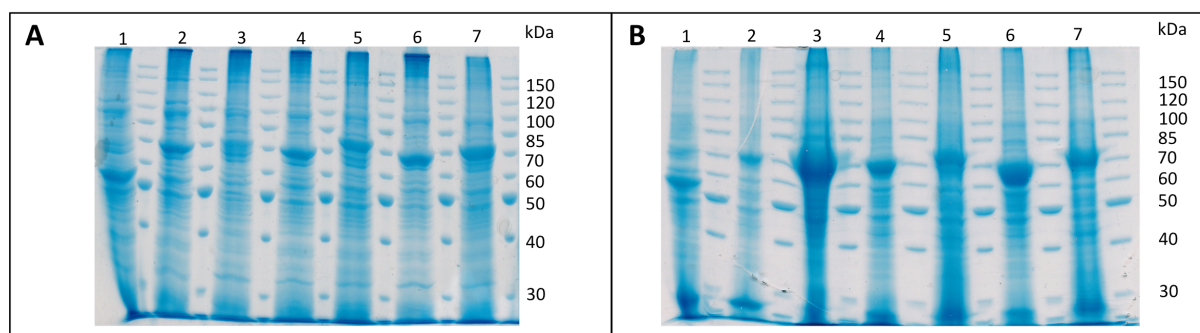


Figure 23: Overexpression of ABC transporters in C43(DE3) Δ ompF Δ acrAB. 1 – HlyB Δ CLD, 2 – HlyB, 3-7 – prokaryotic ABC transporters (A) SDS-PAGE of isolated plasma membranes. (B) SDS-PAGE of isolated inclusion bodies.

Given the overall different properties of C43(DE3) it would be worthwhile to further characterise this second new strain in comparison to C41(DE) Δ ompF Δ acrAB in order to extend the availability of expression hosts for integral membrane proteins.

In summary, the development of new expression strains in this thesis follows a completely new approach by modifying the membrane environment to improve the overexpression, integration and stability of membrane proteins. Furthermore, the possible preparation of protein samples free of OmpF and AcrAB make them an excellent choice for future structural, but also functional studies on membrane proteins.

4.8.2 Functional Reconstitution of HlyB and the Detrimental Effects of Free Detergent Micelles

A primary goal of this thesis was the functional reconstitution of T1SS components and their biochemical characterisation in a more native-like environment than detergent micelles can offer. Detergents are known to influence the stability (204) and functional properties (205) of

membrane proteins, especially by binding to soluble domains outside the transmembrane region (204,206-208).

The reconstitution of HlyB was not successful when the protein was purified from other strains than C41(DE3) $\Delta ompF\Delta acrAB$. The incorporation into saposin-A derived nanoparticles was finally successful, but functional modulation in the presence of substrate was only observed when producing nanoparticles with lysolipids (Chapter IV).

Lysolipids form micelles in aqueous solution, solubilise phospholipid bilayers and occur in low concentrations also in natural membranes (209,210). They contain the same head groups as phospholipids but carry only one fatty acid tail. This arrangement results in an “inverted-cone” shaped room occupancy compared to phospholipids, which results in reduced membrane rigidity (Figure 24) (211,212).

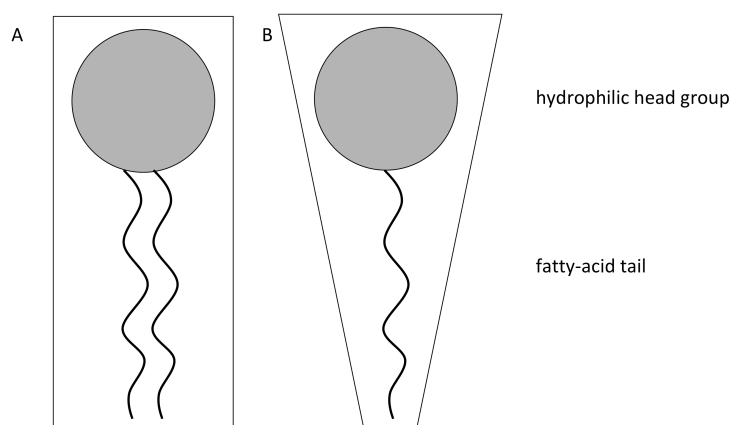


Figure 24: Room occupancy of lysolipids and lipids. (A) Cylindrical shape of phospholipid with two fatty-acid tails. (B) Inverted-cone shape of lysolipid with one fatty-acid tail.

The ATPase activity of HlyB was restored once it was incorporated in nanoparticles, even when they were formed with detergent-like molecules like lysolipids. This demonstrates clearly that in the case of HlyB only free detergent molecules affect the functionality of the protein, probably by binding to regions of the protein outside the transmembrane domains.

While the basal ATPase activity of wildtype HlyB is ten-fold reduced in detergent compared to HlyB Δ CLD (71), the level of activity is equal in saposin-A nanoparticles and within the range of HlyB Δ CLD in detergent solution.

These results demonstrate the importance of not necessarily working in detergent-free, but at least in micelle-free environments. They show that it is not the detergent *per se* which causes detrimental effects but rather an excess of free detergent molecules that can cause undesired interactions with the protein of interest.

4.8.3 Studying the Assembled Inner Membrane Complex

As part of this thesis, the possibilities of studying the assembled inner membrane complex of the HlyA-T1SS composed of HlyB and HlyD were examined (Chapter VII). Previous studies showed that both proteins reside assembled in the inner membrane also in the absence of substrate (41,42). Thus, it was attempted to purify the assembled overexpressed complex rather than performing complex-assembly *in vitro*.

The overexpression of the inner membrane complex was established by fed-batch fermentation. Expression in flasks in orbital shakers did not produce any inner membrane complex, thus fermentation was chosen to optimise oxygen and nutrient supply during growth and, at the same time, maximise the yield of biomass by growing cultures to ODs between 50 and 60. The optimal growth environment in a bioreactor allows for good and stable growth even in minimal media, which offer the possibility of tightly controlling all growth conditions and makes fed-batch fermentations highly reproducible.

Initial purifications of HlyB/ HlyD complex were highly contaminated by the outer membrane porin OmpF. This was even more apparent in initial structural studies by negative-stain EM, where nearly equal numbers of assembled inner membrane complex and OmpF molecules were found. Although several approaches were taken to optimise the purification, optimal conditions could not be identified. The use of OmpF-deficient strains resulted in the presence of disassembled complex or partially assembled fragments (Chapter VII).

Overall, the yield of assembled HlyB/ HlyD complex needs to be further improved to assess the to date unclear stoichiometry of the complex. First MALS measurements point towards a hexameric state of HlyD, which is in good agreement with other studies on related export systems (35) and homology models (78) but contradicts crosslinking studies performed *in vivo* on the HlyA-T1SS, which showed a trimeric assembly of the MFP (41,42).

5. References

1. Albers, R. W. (1967) Biochemical aspects of active transport. *Annu Rev Biochem* **36**, 727-756
2. Wilbrandt, W., and Rosenberg, T. (1961) The concept of carrier transport and its corollaries in pharmacology. *Pharmacol Rev* **13**, 109-183
3. Welch, R. A., Forestier, C., Lobo, A., Pellett, S., Thomas, W., Jr., and Rowe, G. (1992) The synthesis and function of the Escherichia coli hemolysin and related RTX exotoxins. *FEMS Microbiol Immunol* **5**, 29-36
4. Rees, D. C., Johnson, E., and Lewinson, O. (2009) ABC transporters: the power to change. *Nat Rev Mol Cell Biol* **10**, 218-227
5. Biemans-Oldehinkel, E., Doeven, M. K., and Poolman, B. (2006) ABC transporter architecture and regulatory roles of accessory domains. *FEBS Lett* **580**, 1023-1035
6. Lecher, J., Schwarz, C. K., Stoldt, M., Smits, S. H., Willbold, D., and Schmitt, L. (2012) An RTX transporter tethers its unfolded substrate during secretion via a unique N-terminal domain. *Structure* **20**, 1778-1787
7. Jardetzky, O. (1966) Simple allosteric model for membrane pumps. *Nature* **211**, 969-970
8. ter Beek, J., Guskov, A., and Slotboom, D. J. (2014) Structural diversity of ABC transporters. *J Gen Physiol* **143**, 419-435
9. Chen, S., Oldham, M. L., Davidson, A. L., and Chen, J. (2013) Carbon catabolite repression of the maltose transporter revealed by X-ray crystallography. *Nature* **499**, 364-368
10. Fitzpatrick, A. W. P., Llabres, S., Neuberger, A., Blaza, J. N., Bai, X. C., Okada, U., Murakami, S., van Veen, H. W., Zachariae, U., Scheres, S. H. W., Luisi, B. F., and Du, D. (2017) Structure of the MacAB-TolC ABC-type tripartite multidrug efflux pump. *Nat Microbiol* **2**, 17070
11. Kanonenberg, K., Schwarz, C. K., and Schmitt, L. (2013) Type I secretion systems - a story of appendices. *Res Microbiol* **164**, 596-604
12. Higgins, C. F., and Linton, K. J. (2004) The ATP switch model for ABC transporters. *Nat Struct Mol Biol* **11**, 918-926
13. Jones, P. M., and George, A. M. (2009) Opening of the ADP-bound active site in the ABC transporter ATPase dimer: evidence for a constant contact, alternating sites model for the catalytic cycle. *Proteins* **75**, 387-396
14. Linton, K. J., and Higgins, C. F. (2007) Structure and function of ABC transporters: the ATP switch provides flexible control. *Pflugers Arch* **453**, 555-567
15. Verhalen, B., Dastvan, R., Thangapandian, S., Peskova, Y., Koteiche, H. A., Nakamoto, R. K., Tajkhorshid, E., and McHaourab, H. S. (2017) Energy transduction and alternating access of the mammalian ABC transporter P-glycoprotein. *Nature* **543**, 738-741
16. Timachi, M. H., Hutter, C. A., Hohl, M., Assafa, T., Bohm, S., Mittal, A., Seeger, M. A., and Bordignon, E. (2017) Exploring conformational equilibria of a heterodimeric ABC transporter. *Elife* **6**
17. Hellmich, U. A., Lyubenova, S., Kaltenborn, E., Doshi, R., van Veen, H. W., Prisner, T. F., and Glaubitz, C. (2012) Probing the ATP hydrolysis cycle of the ABC multidrug transporter LmrA by pulsed EPR spectroscopy. *J Am Chem Soc* **134**, 5857-5862

18. George, A. M., and Jones, P. M. (2012) Perspectives on the structure-function of ABC transporters: the Switch and Constant Contact models. *Prog Biophys Mol Biol* **109**, 95-107
19. Damas, J. M., Oliveira, A. S., Baptista, A. M., and Soares, C. M. (2011) Structural consequences of ATP hydrolysis on the ABC transporter NBD dimer: molecular dynamics studies of HlyB. *Protein Sci* **20**, 1220-1230
20. Hohl, M., Briand, C., Grutter, M. G., and Seeger, M. A. (2012) Crystal structure of a heterodimeric ABC transporter in its inward-facing conformation. *Nat Struct Mol Biol* **19**, 395-402
21. Costa, T. R., Felisberto-Rodrigues, C., Meir, A., Prevost, M. S., Redzej, A., Trokter, M., and Waksman, G. (2015) Secretion systems in Gram-negative bacteria: structural and mechanistic insights. *Nat Rev Microbiol* **13**, 343-359
22. Kanonenberg, K., Spitz, O., Erenburg, I. N., Beer, T., and Schmitt, L. (2018) Type I secretion system-it takes three and a substrate. *FEMS Microbiol Lett* **365**
23. Economou, A., and Dalbey, R. E. (2014) Preface to special issue on protein trafficking and secretion in bacteria. *Biochim Biophys Acta* **1843**, 1427
24. Hu, B., Morado, D. R., Margolin, W., Rohde, J. R., Arizmendi, O., Picking, W. L., Picking, W. D., and Liu, J. (2015) Visualization of the type III secretion sorting platform of *Shigella flexneri*. *Proc Natl Acad Sci U S A* **112**, 1047-1052
25. Galan, J. E., and Wolf-Watz, H. (2006) Protein delivery into eukaryotic cells by type III secretion machines. *Nature* **444**, 567-573
26. Alvarez-Martinez, C. E., and Christie, P. J. (2009) Biological diversity of prokaryotic type IV secretion systems. *Microbiol Mol Biol Rev* **73**, 775-808
27. Bradley, D. E. (1980) Morphological and serological relationships of conjugative pili. *Plasmid* **4**, 155-169
28. Durrenberger, M. B., Villiger, W., and Bachi, T. (1991) Conjugational junctions: morphology of specific contacts in conjugating *Escherichia coli* bacteria. *J Struct Biol* **107**, 146-156
29. Russell, A. B., Peterson, S. B., and Mougous, J. D. (2014) Type VI secretion system effectors: poisons with a purpose. *Nat Rev Microbiol* **12**, 137-148
30. Hood, R. D., Singh, P., Hsu, F., Guvener, T., Carl, M. A., Trinidad, R. R., Silverman, J. M., Ohlson, B. B., Hicks, K. G., Plemel, R. L., Li, M., Schwarz, S., Wang, W. Y., Merz, A. J., Goodlett, D. R., and Mougous, J. D. (2010) A type VI secretion system of *Pseudomonas aeruginosa* targets a toxin to bacteria. *Cell Host Microbe* **7**, 25-37
31. Russell, A. B., Hood, R. D., Bui, N. K., LeRoux, M., Vollmer, W., and Mougous, J. D. (2011) Type VI secretion delivers bacteriolytic effectors to target cells. *Nature* **475**, 343-347
32. Basler, M., Pilhofer, M., Henderson, G. P., Jensen, G. J., and Mekalanos, J. J. (2012) Type VI secretion requires a dynamic contractile phage tail-like structure. *Nature* **483**, 182-186
33. Gallique, M., Bouteiller, M., and Merieau, A. (2017) The Type VI Secretion System: A Dynamic System for Bacterial Communication? *Front Microbiol* **8**, 1454
34. Wang, Z., Fan, G., Hryc, C. F., Blaza, J. N., Serysheva, II, Schmid, M. F., Chiu, W., Luisi, B. F., and Du, D. (2017) An allosteric transport mechanism for the AcrAB-TolC multidrug efflux pump. *Elife* **6**
35. Du, D., Wang, Z., James, N. R., Voss, J. E., Klimont, E., Ohene-Agyei, T., Venter, H., Chiu, W., and Luisi, B. F. (2014) Structure of the AcrAB-TolC multidrug efflux pump. *Nature* **509**, 512-515

36. Nehme, D., Li, X. Z., Elliot, R., and Poole, K. (2004) Assembly of the MexAB-OprM multidrug efflux system of *Pseudomonas aeruginosa*: identification and characterization of mutations in mexA compromising MexA multimerization and interaction with MexB. *J Bacteriol* **186**, 2973-2983
37. Lopez, C. A., Travers, T., Pos, K. M., Zgurskaya, H. I., and Gnanakaran, S. (2017) Dynamics of Intact MexAB-OprM Efflux Pump: Focusing on the MexA-OprM Interface. *Sci Rep* **7**, 16521
38. Holland, I. B., Peherstorfer, S., Kanonenberg, K., Lenders, M., Reimann, S., and Schmitt, L. (2016) Type I Protein Secretion-Deceptively Simple yet with a Wide Range of Mechanistic Variability across the Family. *EcoSal Plus* **7**
39. Thomas, S., Holland, I. B., and Schmitt, L. (2014) The Type 1 secretion pathway - the hemolysin system and beyond. *Biochim Biophys Acta* **1843**, 1629-1641
40. Delepelaire, P. (2004) Type I secretion in gram-negative bacteria. *Biochim Biophys Acta* **1694**, 149-161
41. Thanabalu, T., Koronakis, E., Hughes, C., and Koronakis, V. (1998) Substrate-induced assembly of a contiguous channel for protein export from E.coli: reversible bridging of an inner-membrane translocase to an outer membrane exit pore. *EMBO J* **17**, 6487-6496
42. Balakrishnan, L., Hughes, C., and Koronakis, V. (2001) Substrate-triggered recruitment of the TolC channel-tunnel during type I export of hemolysin by *Escherichia coli*. *J Mol Biol* **313**, 501-510
43. Letoffe, S., Ghigo, J. M., and Wandersman, C. (1994) Secretion of the *Serratia marcescens* HasA protein by an ABC transporter. *J Bacteriol* **176**, 5372-5377
44. Hwang, J., Zhong, X., and Tai, P. C. (1997) Interactions of dedicated export membrane proteins of the colicin V secretion system: CvaA, a member of the membrane fusion protein family, interacts with CvaB and TolC. *J Bacteriol* **179**, 6264-6270
45. Chabeaud, P., de Groot, A., Bitter, W., Tommassen, J., Heulin, T., and Achouak, W. (2001) Phase-variable expression of an operon encoding extracellular alkaline protease, a serine protease homolog, and lipase in *Pseudomonas brassicacearum*. *J Bacteriol* **183**, 2117-2120
46. Chung, G. H., Lee, Y. P., Jeohn, G. H., Yoo, O. J., and Rhee, J. S. (1991) Cloning and nucleotide sequence of thermostable lipase gene from *Pseudomonas fluorescens* SIK W1. *Agric Biol Chem* **55**, 2359-2365
47. Ahn, J. H., Pan, J. G., and Rhee, J. S. (1999) Identification of the tliDEF ABC transporter specific for lipase in *Pseudomonas fluorescens* SIK W1. *J Bacteriol* **181**, 1847-1852
48. Zhang, L., Conway, J. F., and Thibodeau, P. H. (2012) Calcium-induced folding and stabilization of the *Pseudomonas aeruginosa* alkaline protease. *J Biol Chem* **287**, 4311-4322
49. Wandersman, C., Delepelaire, P., Letoffe, S., and Schwartz, M. (1987) Characterization of *Erwinia chrysanthemi* extracellular proteases: cloning and expression of the protease genes in *Escherichia coli*. *J Bacteriol* **169**, 5046-5053
50. Guzzo, J., Pages, J. M., Duong, F., Lazdunski, A., and Murgier, M. (1991) *Pseudomonas aeruginosa* alkaline protease: evidence for secretion genes and study of secretion mechanism. *J Bacteriol* **173**, 5290-5297
51. Goebel, W., and Hedgpeth, J. (1982) Cloning and functional characterization of the plasmid-encoded hemolysin determinant of *Escherichia coli*. *J Bacteriol* **151**, 1290-1298

52. Lo, R. Y., Strathdee, C. A., and Shewen, P. E. (1987) Nucleotide sequence of the leukotoxin genes of *Pasteurella haemolytica* A1. *Infect Immun* **55**, 1987-1996
53. Chenal, A., Karst, J. C., Sotomayor Perez, A. C., Wozniak, A. K., Baron, B., England, P., and Ladant, D. (2010) Calcium-induced folding and stabilization of the intrinsically disordered RTX domain of the CyaA toxin. *Biophys J* **99**, 3744-3753
54. Griessl, M. H., Schmid, B., Kassler, K., Braunsmann, C., Ritter, R., Barlag, B., Stierhof, Y. D., Sturm, K. U., Danzer, C., Wagner, C., Schaffer, T. E., Sticht, H., Hensel, M., and Muller, Y. A. (2013) Structural insight into the giant Ca(2)(+)-binding adhesin SiiE: implications for the adhesion of *Salmonella enterica* to polarized epithelial cells. *Structure* **21**, 741-752
55. Welch, R. A. (2001) RTX toxin structure and function: a story of numerous anomalies and few analogies in toxin biology. *Curr Top Microbiol Immunol* **257**, 85-111
56. Linhartova, I., Bumba, L., Masin, J., Basler, M., Osicka, R., Kamanova, J., Prochazkova, K., Adkins, I., Hejnova-Holubova, J., Sadilkova, L., Morova, J., and Sebo, P. (2010) RTX proteins: a highly diverse family secreted by a common mechanism. *FEMS Microbiol Rev* **34**, 1076-1112
57. Welch, R. A. (1991) Pore-forming cytolysins of gram-negative bacteria. *Mol Microbiol* **5**, 521-528
58. Chenal, A., Guijarro, J. I., Raynal, B., Delepierre, M., and Ladant, D. (2009) RTX calcium binding motifs are intrinsically disordered in the absence of calcium: implication for protein secretion. *J Biol Chem* **284**, 1781-1789
59. Sotomayor Perez, A. C., Karst, J. C., Davi, M., Guijarro, J. I., Ladant, D., and Chenal, A. (2010) Characterization of the regions involved in the calcium-induced folding of the intrinsically disordered RTX motifs from the bordetella pertussis adenylate cyclase toxin. *J Mol Biol* **397**, 534-549
60. Ostolaza, H., Soloaga, A., and Goni, F. M. (1995) The binding of divalent cations to *Escherichia coli* alpha-haemolysin. *Eur J Biochem* **228**, 39-44
61. Sanchez-Magraner, L., Viguera, A. R., Garcia-Pacios, M., Garcillan, M. P., Arrondo, J. L., de la Cruz, F., Goni, F. M., and Ostolaza, H. (2007) The calcium-binding C-terminal domain of *Escherichia coli* alpha-hemolysin is a major determinant in the surface-active properties of the protein. *J Biol Chem* **282**, 11827-11835
62. Thomas, S., Bakkes, P. J., Smits, S. H., and Schmitt, L. (2014) Equilibrium folding of pro-HlyA from *Escherichia coli* reveals a stable calcium ion dependent folding intermediate. *Biochim Biophys Acta* **1844**, 1500-1510
63. Jones, H. E., Holland, I. B., Baker, H. L., and Campbell, A. K. (1999) Slow changes in cytosolic free Ca²⁺ in *Escherichia coli* highlight two putative influx mechanisms in response to changes in extracellular calcium. *Cell Calcium* **25**, 265-274
64. Gray, L., Mackman, N., Nicaud, J. M., and Holland, I. B. (1986) The carboxy-terminal region of haemolysin 2001 is required for secretion of the toxin from *Escherichia coli*. *Mol Gen Genet* **205**, 127-133
65. Koronakis, V., Koronakis, E., and Hughes, C. (1989) Isolation and analysis of the C-terminal signal directing export of *Escherichia coli* hemolysin protein across both bacterial membranes. *EMBO J* **8**, 595-605
66. Hinsä, S. M., Espinosa-Urgel, M., Ramos, J. L., and O'Toole, G. A. (2003) Transition from reversible to irreversible attachment during biofilm formation by *Pseudomonas fluorescens* WCS365 requires an ABC transporter and a large secreted protein. *Mol Microbiol* **49**, 905-918

67. Felmlee, T., Pellett, S., Lee, E. Y., and Welch, R. A. (1985) Escherichia coli hemolysin is released extracellularly without cleavage of a signal peptide. *J Bacteriol* **163**, 88-93
68. Lin, D. Y., Huang, S., and Chen, J. (2015) Crystal structures of a polypeptide processing and secretion transporter. *Nature* **523**, 425-430
69. Havarstein, L. S., Diep, D. B., and Nes, I. F. (1995) A family of bacteriocin ABC transporters carry out proteolytic processing of their substrates concomitant with export. *Mol Microbiol* **16**, 229-240
70. Ishii, S., Yano, T., Ebihara, A., Okamoto, A., Manzoku, M., and Hayashi, H. (2010) Crystal structure of the peptidase domain of Streptococcus ComA, a bifunctional ATP-binding cassette transporter involved in the quorum-sensing pathway. *J Biol Chem* **285**, 10777-10785
71. Reimann, S., Poschmann, G., Kanonenberg, K., Stuhler, K., Smits, S. H., and Schmitt, L. (2016) Interdomain regulation of the ATPase activity of the ABC transporter haemolysin B from Escherichia coli. *Biochem J* **473**, 2471-2483
72. Morgan, J. L. W., Acheson, J. F., and Zimmer, J. (2017) Structure of a Type-1 Secretion System ABC Transporter. *Structure* **25**, 522-529
73. Letoffe, S., Delepelaire, P., and Wandersman, C. (1990) Protease secretion by Erwinia chrysanthemi: the specific secretion functions are analogous to those of Escherichia coli alpha-haemolysin. *EMBO J* **9**, 1375-1382
74. Sapriel, G., Wandersman, C., and Delepelaire, P. (2002) The N terminus of the HasA protein and the SecB chaperone cooperate in the efficient targeting and secretion of HasA via the ATP-binding cassette transporter. *J Biol Chem* **277**, 6726-6732
75. Zgurskaya, H. I., Yamada, Y., Tikhonova, E. B., Ge, Q., and Krishnamoorthy, G. (2009) Structural and functional diversity of bacterial membrane fusion proteins. *Biochim Biophys Acta* **1794**, 794-807
76. Pimenta, A. L., Racher, K., Jamieson, L., Blight, M. A., and Holland, I. B. (2005) Mutations in HlyD, part of the type 1 translocator for hemolysin secretion, affect the folding of the secreted toxin. *J Bacteriol* **187**, 7471-7480
77. Murata, D., Okano, H., Angkawidjaja, C., Akutsu, M., Tanaka, S. I., Kitahara, K., Yoshizawa, T., Matsumura, H., Kado, Y., Mizohata, E., Inoue, T., Sano, S., Koga, Y., Kanaya, S., and Takano, K. (2017) Structural Basis for the Serratia marcescens Lipase Secretion System: Crystal Structures of the Membrane Fusion Protein and Nucleotide-Binding Domain. *Biochemistry* **56**, 6281-6291
78. Kim, J. S., Song, S., Lee, M., Lee, S., Lee, K., and Ha, N. C. (2016) Crystal Structure of a Soluble Fragment of the Membrane Fusion Protein HlyD in a Type I Secretion System of Gram-Negative Bacteria. *Structure* **24**, 477-485
79. Kim, H. M., Xu, Y., Lee, M., Piao, S., Sim, S. H., Ha, N. C., and Lee, K. (2010) Functional relationships between the AcrA hairpin tip region and the TolC aperture tip region for the formation of the bacterial tripartite efflux pump AcrAB-TolC. *J Bacteriol* **192**, 4498-4503
80. Lee, M., Jun, S. Y., Yoon, B. Y., Song, S., Lee, K., and Ha, N. C. (2012) Membrane fusion proteins of type I secretion system and tripartite efflux pumps share a binding motif for TolC in gram-negative bacteria. *PLoS One* **7**, e40460
81. Symmons, M. F., Bokma, E., Koronakis, E., Hughes, C., and Koronakis, V. (2009) The assembled structure of a complete tripartite bacterial multidrug efflux pump. *Proc Natl Acad Sci U S A* **106**, 7173-7178
82. Staron, P., Forchhammer, K., and Maldener, I. (2014) Structure-function analysis of the ATP-driven glycolipid efflux pump DevBCA reveals complex organization with TolC/HgdD. *FEBS Lett* **588**, 395-400

83. Koronakis, V., Sharff, A., Koronakis, E., Luisi, B., and Hughes, C. (2000) Crystal structure of the bacterial membrane protein TolC central to multidrug efflux and protein export. *Nature* **405**, 914-919
84. Pei, X. Y., Hinchliffe, P., Symmons, M. F., Koronakis, E., Benz, R., Hughes, C., and Koronakis, V. (2011) Structures of sequential open states in a symmetrical opening transition of the TolC exit duct. *Proc Natl Acad Sci U S A* **108**, 2112-2117
85. Gilson, L., Mahanty, H. K., and Kolter, R. (1990) Genetic analysis of an MDR-like export system: the secretion of colicin V. *EMBO J* **9**, 3875-3884
86. Koronakis, V., Eswaran, J., and Hughes, C. (2004) Structure and function of TolC: the bacterial exit duct for proteins and drugs. *Annu Rev Biochem* **73**, 467-489
87. Eswaran, J., Hughes, C., and Koronakis, V. (2003) Locking TolC entrance helices to prevent protein translocation by the bacterial type I export apparatus. *J Mol Biol* **327**, 309-315
88. Letoffe, S., Delepelaire, P., and Wandersman, C. (1996) Protein secretion in gram-negative bacteria: assembly of the three components of ABC protein-mediated exporters is ordered and promoted by substrate binding. *EMBO J* **15**, 5804-5811
89. Bavro, V. N., Pietras, Z., Furnham, N., Perez-Cano, L., Fernandez-Recio, J., Pei, X. Y., Misra, R., and Luisi, B. (2008) Assembly and channel opening in a bacterial drug efflux machine. *Mol Cell* **30**, 114-121
90. Vakharia, H., German, G. J., and Misra, R. (2001) Isolation and characterization of *Escherichia coli* tolC mutants defective in secreting enzymatically active alpha-hemolysin. *J Bacteriol* **183**, 6908-6916
91. Lenders, M. H., Reimann, S., Smits, S. H., and Schmitt, L. (2013) Molecular insights into type I secretion systems. *Biol Chem* **394**, 1371-1384
92. Noegel, A., Rdest, U., Springer, W., and Goebel, W. (1979) Plasmid cistrons controlling synthesis and excretion of the exotoxin alpha-haemolysin of *Escherichia coli*. *Mol Gen Genet* **175**, 343-350
93. Ludwig, A., Schmid, A., Benz, R., and Goebel, W. (1991) Mutations affecting pore formation by haemolysin from *Escherichia coli*. *Mol Gen Genet* **226**, 198-208
94. Felmlee, T., Pellett, S., and Welch, R. A. (1985) Nucleotide sequence of an *Escherichia coli* chromosomal hemolysin. *J Bacteriol* **163**, 94-105
95. Nicaud, J. M., Mackman, N., Gray, L., and Holland, I. B. (1985) Regulation of haemolysin synthesis in *E. coli* determined by HLY genes of human origin. *Mol Gen Genet* **199**, 111-116
96. Issartel, J. P., Koronakis, V., and Hughes, C. (1991) Activation of *Escherichia coli* prohaemolysin to the mature toxin by acyl carrier protein-dependent fatty acylation. *Nature* **351**, 759-761
97. Stanley, P., Hyland, C., Koronakis, V., and Hughes, C. (1999) An ordered reaction mechanism for bacterial toxin acylation by the specialized acyltransferase HlyC: formation of a ternary complex with acylACP and protoxin substrates. *Mol Microbiol* **34**, 887-901
98. Stanley, P., Packman, L. C., Koronakis, V., and Hughes, C. (1994) Fatty acylation of two internal lysine residues required for the toxic activity of *Escherichia coli* hemolysin. *Science* **266**, 1992-1996
99. Thomas, S., Smits, S. H., and Schmitt, L. (2014) A simple in vitro acylation assay based on optimized HlyA and HlyC purification. *Anal Biochem* **464**, 17-23
100. Zaitseva, J., Jenewein, S., Jumpertz, T., Holland, I. B., and Schmitt, L. (2005) H662 is the linchpin of ATP hydrolysis in the nucleotide-binding domain of the ABC transporter HlyB. *EMBO J* **24**, 1901-1910

101. Kelley, L. A., Mezulis, S., Yates, C. M., Wass, M. N., and Sternberg, M. J. (2015) The Phyre2 web portal for protein modeling, prediction and analysis. *Nat Protoc* **10**, 845-858
102. Schmitt, L., Benabdelhak, H., Blight, M. A., Holland, I. B., and Stubbs, M. T. (2003) Crystal structure of the nucleotide-binding domain of the ABC-transporter haemolysin B: identification of a variable region within ABC helical domains. *J Mol Biol* **330**, 333-342
103. Lenders, M. H., Weidtkamp-Peters, S., Kleinschrodt, D., Jaeger, K. E., Smits, S. H., and Schmitt, L. (2015) Directionality of substrate translocation of the hemolysin A Type I secretion system. *Sci Rep* **5**, 12470
104. Lenders, M. H., Beer, T., Smits, S. H., and Schmitt, L. (2016) In vivo quantification of the secretion rates of the hemolysin A Type I secretion system. *Sci Rep* **6**, 33275
105. Young, R., and Bremer, H. (1976) Polypeptide-chain-elongation rate in *Escherichia coli* B/r as a function of growth rate. *Biochem J* **160**, 185-194
106. Uchida, K., Mori, H., and Mizushima, S. (1995) Stepwise movement of preproteins in the process of translocation across the cytoplasmic membrane of *Escherichia coli*. *J Biol Chem* **270**, 30862-30868
107. Bumba, L., Masin, J., Macek, P., Wald, T., Motlova, L., Bibova, I., Klimova, N., Bednarova, L., Veverka, V., Kachala, M., Svergun, D. I., Barinka, C., and Sebo, P. (2016) Calcium-Driven Folding of RTX Domain beta-Rolls Ratchets Translocation of RTX Proteins through Type I Secretion Ducts. *Mol Cell* **62**, 47-62
108. Zaitseva, J., Jenewein, S., Oswald, C., Jumpertz, T., Holland, I. B., and Schmitt, L. (2005) A molecular understanding of the catalytic cycle of the nucleotide-binding domain of the ABC transporter HlyB. *Biochem Soc Trans* **33**, 990-995
109. Zaitseva, J., Oswald, C., Jumpertz, T., Jenewein, S., Wiedenmann, A., Holland, I. B., and Schmitt, L. (2006) A structural analysis of asymmetry required for catalytic activity of an ABC-ATPase domain dimer. *EMBO J* **25**, 3432-3443
110. Benabdelhak, H., Kiontke, S., Horn, C., Ernst, R., Blight, M. A., Holland, I. B., and Schmitt, L. (2003) A specific interaction between the NBD of the ABC-transporter HlyB and a C-terminal fragment of its transport substrate haemolysin A. *J Mol Biol* **327**, 1169-1179
111. Frauenfeld, J., Loving, R., Armache, J. P., Sonnen, A. F., Guettou, F., Moberg, P., Zhu, L., Jegerschold, C., Flayhan, A., Briggs, J. A., Garoff, H., Low, C., Cheng, Y., and Nordlund, P. (2016) A saposin-lipoprotein nanoparticle system for membrane proteins. *Nat Methods* **13**, 345-351
112. Denisov, I. G., Grinkova, Y. V., Lazarides, A. A., and Sligar, S. G. (2004) Directed self-assembly of monodisperse phospholipid bilayer Nanodiscs with controlled size. *J Am Chem Soc* **126**, 3477-3487
113. Gratia, A. (1925) Sur un remarquable exemple d'antagonisme entre deux souches de colibacille. *C. R. Soc. Biol. (Paris)*, 1040-1041
114. Gilson, L., Mahanty, H. K., and Kolter, R. (1987) Four plasmid genes are required for colicin V synthesis, export, and immunity. *J Bacteriol* **169**, 2466-2470
115. Wandersman, C., and Delepelaire, P. (1990) TolC, an *Escherichia coli* outer membrane protein required for hemolysin secretion. *Proc Natl Acad Sci U S A* **87**, 4776-4780
116. Nagamatsu, K., Hannan, T. J., Guest, R. L., Kostakioti, M., Hadjifrangiskou, M., Binkley, J., Dodson, K., Raivio, T. L., and Hultgren, S. J. (2015) Dysregulation of *Escherichia coli* alpha-hemolysin expression alters the course of acute and persistent urinary tract infection. *Proc Natl Acad Sci U S A* **112**, E871-880

117. Benz, R., Maier, E., Ladant, D., Ullmann, A., and Sebo, P. (1994) Adenylate cyclase toxin (CyaA) of *Bordetella pertussis*. Evidence for the formation of small ion-permeable channels and comparison with HlyA of *Escherichia coli*. *J Biol Chem* **269**, 27231-27239
118. Barry, E. M., Weiss, A. A., Ehrmann, I. E., Gray, M. C., Hewlett, E. L., and Goodwin, M. S. (1991) *Bordetella pertussis* adenylate cyclase toxin and hemolytic activities require a second gene, *cyaC*, for activation. *J Bacteriol* **173**, 720-726
119. Sebo, P., Glaser, P., Sakamoto, H., and Ullmann, A. (1991) High-level synthesis of active adenylate cyclase toxin of *Bordetella pertussis* in a reconstructed *Escherichia coli* system. *Gene* **104**, 19-24
120. Goodwin, M. S., and Weiss, A. A. (1990) Adenylate cyclase toxin is critical for colonization and pertussis toxin is critical for lethal infection by *Bordetella pertussis* in infant mice. *Infect Immun* **58**, 3445-3447
121. Davey, M. E., and O'Toole G, A. (2000) Microbial biofilms: from ecology to molecular genetics. *Microbiol Mol Biol Rev* **64**, 847-867
122. Morgan, E., Bowen, A. J., Carnell, S. C., Wallis, T. S., and Stevens, M. P. (2007) SiiE is secreted by the *Salmonella enterica* serovar Typhimurium pathogenicity island 4-encoded secretion system and contributes to intestinal colonization in cattle. *Infect Immun* **75**, 1524-1533
123. Barlag, B., and Hensel, M. (2015) The giant adhesin SiiE of *Salmonella enterica*. *Molecules* **20**, 1134-1150
124. Wille, T., Wagner, C., Mittelstadt, W., Blank, K., Sommer, E., Malengo, G., Dohler, D., Lange, A., Sourjik, V., Hensel, M., and Gerlach, R. G. (2014) SiiA and SiiB are novel type I secretion system subunits controlling SPI4-mediated adhesion of *Salmonella enterica*. *Cell Microbiol* **16**, 161-178
125. Izadi-Pruneyre, N., Wolff, N., Redeker, V., Wandersman, C., Delepierre, M., and Lecroisey, A. (1999) NMR studies of the C-terminal secretion signal of the haem-binding protein, HasA. *Eur J Biochem* **261**, 562-568
126. Vassiliadis, G., Destoumieux-Garzón, D., and Peduzzi, J. (2011) Class II Microcins. in *Prokaryotic Antimicrobial Peptides*. pp 309-332
127. Vassiliadis, G., Destoumieux-Garzon, D., Lombard, C., Rebuffat, S., and Peduzzi, J. (2010) Isolation and characterization of two members of the siderophore-microcin family, microcins M and H47. *Antimicrob Agents Chemother* **54**, 288-297
128. Gerard, F., Pradel, N., and Wu, L. F. (2005) Bactericidal activity of colicin V is mediated by an inner membrane protein, SdaC, of *Escherichia coli*. *J Bacteriol* **187**, 1945-1950
129. Gratia, A. (1925) Sur un remarquable exemple d'antagonisme entre deux souches de colibacille. *C R Soc Biol*, 1041-1042
130. Pons, A. M., Delalande, F., Duarte, M., Benoit, S., Lanneluc, I., Sable, S., Van Dorsselaer, A., and Cottenceau, G. (2004) Genetic analysis and complete primary structure of microcin L. *Antimicrob Agents Chemother* **48**, 505-513
131. Lagos, R., Baeza, M., Corsini, G., Hetz, C., Strahsburger, E., Castillo, J. A., Vergara, C., and Monasterio, O. (2001) Structure, organization and characterization of the gene cluster involved in the production of microcin E492, a channel-forming bacteriocin. *Mol Microbiol* **42**, 229-243
132. Nolan, E. M., Fischbach, M. A., Koglin, A., and Walsh, C. T. (2007) Biosynthetic tailoring of microcin E492m: post-translational modification affords an antibacterial siderophore-peptide conjugate. *J Am Chem Soc* **129**, 14336-14347

133. Nolan, E. M., and Walsh, C. T. (2008) Investigations of the MceIJ-catalyzed posttranslational modification of the microcin E492 C-terminus: linkage of ribosomal and nonribosomal peptides to form "trojan horse" antibiotics. *Biochemistry* **47**, 9289-9299
134. Vassiliadis, G., Peduzzi, J., Zirah, S., Thomas, X., Rebuffat, S., and Destoumieux-Garzon, D. (2007) Insight into siderophore-carrying peptide biosynthesis: enterobactin is a precursor for microcin E492 posttranslational modification. *Antimicrob Agents Chemother* **51**, 3546-3553
135. Wu, K. H., and Tai, P. C. (2004) Cys32 and His105 are the critical residues for the calcium-dependent cysteine proteolytic activity of CvaB, an ATP-binding cassette transporter. *J Biol Chem* **279**, 901-909
136. Yang, C. C., and Konisky, J. (1984) Colicin V-treated *Escherichia coli* does not generate membrane potential. *J Bacteriol* **158**, 757-759
137. Havarstein, L. S., Holo, H., and Nes, I. F. (1994) The leader peptide of colicin V shares consensus sequences with leader peptides that are common among peptide bacteriocins produced by gram-positive bacteria. *Microbiology* **140** (Pt 9), 2383-2389
138. Zhang, L. H., Fath, M. J., Mahanty, H. K., Tai, P. C., and Kolter, R. (1995) Genetic analysis of the colicin V secretion pathway. *Genetics* **141**, 25-32
139. Ize, B., Gerard, F., Zhang, M., Chanal, A., Voulhoux, R., Palmer, T., Filloux, A., and Wu, L. F. (2002) In vivo dissection of the Tat translocation pathway in *Escherichia coli*. *J Mol Biol* **317**, 327-335
140. Hardie, K. R., Issartel, J. P., Koronakis, E., Hughes, C., and Koronakis, V. (1991) In vitro activation of *Escherichia coli* prohaemolysin to the mature membrane-targeted toxin requires HlyC and a low molecular-weight cytosolic polypeptide. *Mol Microbiol* **5**, 1669-1679
141. Narayanan, S. K., Nagaraja, T. G., Chengappa, M. M., and Stewart, G. C. (2002) Leukotoxins of gram-negative bacteria. *Vet Microbiol* **84**, 337-356
142. Braun, V., Schonherr, R., and Hobbie, S. (1993) Enterobacterial hemolysins: activation, secretion and pore formation. *Trends Microbiol* **1**, 211-216
143. Carbonetti, N. H. (2010) Pertussis toxin and adenylate cyclase toxin: key virulence factors of *Bordetella pertussis* and cell biology tools. *Future Microbiol* **5**, 455-469
144. Sviridova, E., Rezacova, P., Bondar, A., Veverka, V., Novak, P., Schenk, G., Svergun, D. I., Kuta Smatanova, I., and Bumba, L. (2017) Structural basis of the interaction between the putative adhesion-involved and iron-regulated FrpD and FrpC proteins of *Neisseria meningitidis*. *Sci Rep* **7**, 40408
145. Osicka, R., Kalmusova, J., Krizova, P., and Sebo, P. (2001) *Neisseria meningitidis* RTX protein FrpC induces high levels of serum antibodies during invasive disease: polymorphism of frpC alleles and purification of recombinant FrpC. *Infect Immun* **69**, 5509-5519
146. Edgar, R. C. (2004) MUSCLE: a multiple sequence alignment method with reduced time and space complexity. *BMC Bioinformatics* **5**, 113
147. Edgar, R. C. (2004) MUSCLE: multiple sequence alignment with high accuracy and high throughput. *Nucleic Acids Res* **32**, 1792-1797
148. Baumann, U. (2004) 152 - Serralyisin and related enzymes. in *Handbook of Proteolytic Enzymes (Second Edition)* (Barrett, A. J., Rawlings, N. D., and Woessner, J. F. eds.), Academic Press, London. pp 579-581
149. Angkawidjaja, C., and Kanaya, S. (2006) Family I.3 lipase: bacterial lipases secreted by the type I secretion system. *Cell Mol Life Sci* **63**, 2804-2817

150. Ascenzi, P., di Masi, A., Leboffe, L., Frangipani, E., Nardini, M., Verde, C., and Visca, P. (2015) Structural Biology of Bacterial Haemophores. *Adv Microb Physiol* **67**, 127-176
151. Santamaria-Hernando, S., Krell, T., and Ramos-Gonzalez, M. I. (2012) Identification of a novel calcium binding motif based on the detection of sequence insertions in the animal peroxidase domain of bacterial proteins. *PLoS One* **7**, e40698
152. Fernandez, L. A., and Berenguer, J. (2000) Secretion and assembly of regular surface structures in Gram-negative bacteria. *FEMS Microbiol Rev* **24**, 21-44
153. Gomis-Ruth, F. X. (2009) Catalytic domain architecture of metzincin metalloproteases. *J Biol Chem* **284**, 15353-15357
154. Delepelaire, P., and Wandersman, C. (1989) Protease secretion by *Erwinia chrysanthemi*. Proteases B and C are synthesized and secreted as zymogens without a signal peptide. *J Biol Chem* **264**, 9083-9089
155. Zhang, L., Morrison, A. J., and Thibodeau, P. H. (2015) Interdomain Contacts and the Stability of Serralyisin Protease from *Serratia marcescens*. *PLoS One* **10**, e0138419
156. Balaban, N. P., Rudakova, N. L., and Sharipova, M. R. (2012) Structural and functional characteristics and properties of metzincins. *Biochemistry (Mosc)* **77**, 119-127
157. Hase, C. C., and Finkelstein, R. A. (1993) Bacterial extracellular zinc-containing metalloproteases. *Microbiol Rev* **57**, 823-837
158. Ghigo, J. M., and Wandersman, C. (1992) Cloning, nucleotide sequence and characterization of the gene encoding the *Erwinia chrysanthemi* B374 PrtA metalloprotease: a third metalloprotease secreted via a C-terminal secretion signal. *Mol Gen Genet* **236**, 135-144
159. Letoffe, S., Delepelaire, P., and Wandersman, C. (1989) Characterization of a protein inhibitor of extracellular proteases produced by *Erwinia chrysanthemi*. *Mol Microbiol* **3**, 79-86
160. Duong, F., Lazdunski, A., Cami, B., and Murgier, M. (1992) Sequence of a cluster of genes controlling synthesis and secretion of alkaline protease in *Pseudomonas aeruginosa*: relationships to other secretory pathways. *Gene* **121**, 47-54
161. Hege, T., Feltzer, R. E., Gray, R. D., and Baumann, U. (2001) Crystal structure of a complex between *Pseudomonas aeruginosa* alkaline protease and its cognate inhibitor: inhibition by a zinc-NH₂ coordinative bond. *J Biol Chem* **276**, 35087-35092
162. Wandersman, C., and Delepelaire, P. (2012) Haemophore functions revisited. *Mol Microbiol* **85**, 618-631
163. Ghigo, J. M., Letoffe, S., and Wandersman, C. (1997) A new type of hemophore-dependent heme acquisition system of *Serratia marcescens* reconstituted in *Escherichia coli*. *J Bacteriol* **179**, 3572-3579
164. Letoffe, S., Redeker, V., and Wandersman, C. (1998) Isolation and characterization of an extracellular haem-binding protein from *Pseudomonas aeruginosa* that shares function and sequence similarities with the *Serratia marcescens* HasA haemophore. *Mol Microbiol* **28**, 1223-1234
165. Letoffe, S., Nato, F., Goldberg, M. E., and Wandersman, C. (1999) Interactions of HasA, a bacterial haemophore, with haemoglobin and with its outer membrane receptor HasR. *Mol Microbiol* **33**, 546-555
166. Letoffe, S., Debarbieux, L., Izadi, N., Delepelaire, P., and Wandersman, C. (2003) Ligand delivery by haem carrier proteins: the binding of *Serratia marcescens* haemophore to its outer membrane receptor is mediated by two distinct peptide regions. *Mol Microbiol* **50**, 77-88

167. Noinaj, N., Guillier, M., Barnard, T. J., and Buchanan, S. K. (2010) TonB-dependent transporters: regulation, structure, and function. *Annu Rev Microbiol* **64**, 43-60
168. Madhurantakam, C., Howorka, S., and Remaut, H. (2014) S-layer Structure in Bacteria and Archaea. in *Nanomicrobiology: Physiological and Environmental Characteristics* (Barton, L. L., Bazylnski, D. A., and Xu, H. eds.), Springer New York, New York, NY. pp 11-37
169. Thompson, S. A., Shedd, O. L., Ray, K. C., Beins, M. H., Jorgensen, J. P., and Blaser, M. J. (1998) Campylobacter fetus surface layer proteins are transported by a type I secretion system. *J Bacteriol* **180**, 6450-6458
170. Smith, T. J., Font, M. E., Kelly, C. M., Sondermann, H., and O'Toole, G. A. (2018) An N-terminal Retention Module Anchors the Giant Adhesin LapA of *Pseudomonas fluorescens* at the Cell Surface: A Novel Sub-family of Type I Secretion Systems. *J Bacteriol*
171. Ivanov, I. E., Boyd, C. D., Newell, P. D., Schwartz, M. E., Turnbull, L., Johnson, M. S., Whitchurch, C. B., O'Toole, G. A., and Camesano, T. A. (2012) Atomic force and super-resolution microscopy support a role for LapA as a cell-surface biofilm adhesin of *Pseudomonas fluorescens*. *Res Microbiol* **163**, 685-691
172. El-Kirat-Chatel, S., Beaussart, A., Boyd, C. D., O'Toole, G. A., and Dufrene, Y. F. (2014) Single-cell and single-molecule analysis deciphers the localization, adhesion, and mechanics of the biofilm adhesin LapA. *ACS Chem Biol* **9**, 485-494
173. El-Kirat-Chatel, S., Boyd, C. D., O'Toole, G. A., and Dufrene, Y. F. (2014) Single-molecule analysis of *Pseudomonas fluorescens* footprints. *ACS Nano* **8**, 1690-1698
174. Vance, T. D., Olijve, L. L., Campbell, R. L., Voets, I. K., Davies, P. L., and Guo, S. (2014) Ca²⁺-stabilized adhesin helps an Antarctic bacterium reach out and bind ice. *Biosci Rep* **34**
175. Newell, P. D., Boyd, C. D., Sondermann, H., and O'Toole, G. A. (2011) A c-di-GMP effector system controls cell adhesion by inside-out signaling and surface protein cleavage. *PLoS Biol* **9**, e1000587
176. Boyd, C. D., Chatterjee, D., Sondermann, H., and O'Toole, G. A. (2012) LapG, required for modulating biofilm formation by *Pseudomonas fluorescens* Pf0-1, is a calcium-dependent protease. *J Bacteriol* **194**, 4406-4414
177. Navarro, M. V., Newell, P. D., Krasteva, P. V., Chatterjee, D., Madden, D. R., O'Toole, G. A., and Sondermann, H. (2011) Structural basis for c-di-GMP-mediated inside-out signaling controlling periplasmic proteolysis. *PLoS Biol* **9**, e1000588
178. Newell, P. D., Monds, R. D., and O'Toole, G. A. (2009) LapD is a bis-(3',5')-cyclic dimeric GMP-binding protein that regulates surface attachment by *Pseudomonas fluorescens* Pf0-1. *Proc Natl Acad Sci U S A* **106**, 3461-3466
179. Boyd, C. D., Smith, T. J., El-Kirat-Chatel, S., Newell, P. D., Dufrene, Y. F., and O'Toole, G. A. (2014) Structural features of the *Pseudomonas fluorescens* biofilm adhesin LapA required for LapG-dependent cleavage, biofilm formation, and cell surface localization. *J Bacteriol* **196**, 2775-2788
180. Bienert, S., Waterhouse, A., de Beer, T. A., Tauriello, G., Studer, G., Bordoli, L., and Schwede, T. (2017) The SWISS-MODEL Repository-new features and functionality. *Nucleic Acids Res* **45**, D313-D319
181. Waterhouse, A., Bertoni, M., Bienert, S., Studer, G., Tauriello, G., Gumienny, R., Heer, F. T., de Beer, T. A. P., Rempfer, C., Bordoli, L., Lepore, R., and Schwede, T. (2018) SWISS-MODEL: homology modelling of protein structures and complexes. *Nucleic Acids Res* **46**, W296-W303

182. Wagner, C., Polke, M., Gerlach, R. G., Linke, D., Stierhof, Y. D., Schwarz, H., and Hensel, M. (2011) Functional dissection of SiiE, a giant non-fimbrial adhesin of *Salmonella enterica*. *Cell Microbiol* **13**, 1286-1301
183. Ghigo, J. M., and Wandersman, C. (1992) A fourth metalloprotease gene in *Erwinia chrysanthemi*. *Res Microbiol* **143**, 857-867
184. Fong, J. N. C., and Yildiz, F. H. (2015) Biofilm Matrix Proteins. *Microbiol Spectr* **3**
185. Latasa, C., Roux, A., Toledo-Arana, A., Ghigo, J. M., Gamazo, C., Penades, J. R., and Lasa, I. (2005) BapA, a large secreted protein required for biofilm formation and host colonization of *Salmonella enterica* serovar Enteritidis. *Mol Microbiol* **58**, 1322-1339
186. Yoshida, K., Toyofuku, M., Obana, N., and Nomura, N. (2017) Biofilm formation by *Paracoccus denitrificans* requires a type I secretion system-dependent adhesin BapA. *FEMS Microbiol Lett* **364**
187. Wiseman, B., Kilburg, A., Chaptal, V., Reyes-Mejia, G. C., Sarwan, J., Falson, P., and Jault, J. M. (2014) Stubborn contaminants: influence of detergents on the purity of the multidrug ABC transporter BmrA. *PLoS One* **9**, e114864
188. Wagner, S., Klepsch, M. M., Schlegel, S., Appel, A., Draheim, R., Tarry, M., Høgbom, M., van Wijk, K. J., Slotboom, D. J., Persson, J. O., and de Gier, J. W. (2008) Tuning *Escherichia coli* for membrane protein overexpression. *Proc Natl Acad Sci U S A* **105**, 14371-14376
189. Schlegel, S., Lofblom, J., Lee, C., Hjelm, A., Klepsch, M., Strous, M., Drew, D., Slotboom, D. J., and de Gier, J. W. (2012) Optimizing membrane protein overexpression in the *Escherichia coli* strain Lemo21(DE3). *J Mol Biol* **423**, 648-659
190. Miroux, B., and Walker, J. E. (1996) Over-production of proteins in *Escherichia coli*: mutant hosts that allow synthesis of some membrane proteins and globular proteins at high levels. *J Mol Biol* **260**, 289-298
191. Schlegel, S., Genevaux, P., and de Gier, J. W. (2015) De-convoluting the Genetic Adaptations of *E. coli* C41(DE3) in Real Time Reveals How Alleviating Protein Production Stress Improves Yields. *Cell Rep*
192. Kwon, S. K., Kim, S. K., Lee, D. H., and Kim, J. F. (2015) Comparative genomics and experimental evolution of *Escherichia coli* BL21(DE3) strains reveal the landscape of toxicity escape from membrane protein overproduction. *Sci Rep* **5**, 16076
193. Angius, F., Iliaia, O., Amrani, A., Suisse, A., Rosset, L., Legrand, A., Abou-Hamdan, A., Uzan, M., Zito, F., and Miroux, B. (2018) A novel regulation mechanism of the T7 RNA polymerase based expression system improves overproduction and folding of membrane proteins. *Sci Rep* **8**, 8572
194. Veisler, D., Blangy, S., Cambillau, C., and Sciara, G. (2008) There is a baby in the bath water: AcrB contamination is a major problem in membrane-protein crystallization. *Acta Crystallogr Sect F Struct Biol Cryst Commun* **64**, 880-885
195. Kefala, G., Ahn, C., Krupa, M., Esquivies, L., Maslennikov, I., Kwiatkowski, W., and Choe, S. (2010) Structures of the OmpF porin crystallized in the presence of foscholine-12. *Protein Sci* **19**, 1117-1125
196. Murakami, S., Nakashima, R., Yamashita, E., and Yamaguchi, A. (2002) Crystal structure of bacterial multidrug efflux transporter AcrB. *Nature* **419**, 587-593
197. Thomason, L. C., Costantino, N., and Court, D. L. (2007) *E. coli* genome manipulation by P1 transduction. *Curr Protoc Mol Biol* **Chapter 1**, Unit 1 17
198. Datsenko, K. A., and Wanner, B. L. (2000) One-step inactivation of chromosomal genes in *Escherichia coli* K-12 using PCR products. *Proc Natl Acad Sci U S A* **97**, 6640-6645

199. Ekiert, D. C., Bhabha, G., Isom, G. L., Greenan, G., Ovchinnikov, S., Henderson, I. R., Cox, J. S., and Vale, R. D. (2017) Architectures of Lipid Transport Systems for the Bacterial Outer Membrane. *Cell* **169**, 273-285 e217
200. Lepore, B. W., Indic, M., Pham, H., Hearn, E. M., Patel, D. R., and van den Berg, B. (2011) Ligand-gated diffusion across the bacterial outer membrane. *Proc Natl Acad Sci U S A* **108**, 10121-10126
201. Lennen, R. M., Politz, M. G., Kruziki, M. A., and Pfleger, B. F. (2013) Identification of transport proteins involved in free fatty acid efflux in Escherichia coli. *J Bacteriol* **195**, 135-144
202. Rodriguez-Moya, M., and Gonzalez, R. (2015) Proteomic analysis of the response of Escherichia coli to short-chain fatty acids. *J Proteomics* **122**, 86-99
203. Tan, Z., Black, W., Yoon, J. M., Shanks, J. V., and Jarboe, L. R. (2017) Improving Escherichia coli membrane integrity and fatty acid production by expression tuning of FadL and OmpF. *Microb Cell Fact* **16**, 38
204. Yang, Z., Wang, C., Zhou, Q., An, J., Hildebrandt, E., Aleksandrov, L. A., Kappes, J. C., DeLucas, L. J., Riordan, J. R., Urbatsch, I. L., Hunt, J. F., and Brouillette, C. G. (2014) Membrane protein stability can be compromised by detergent interactions with the extramembranous soluble domains. *Protein Sci* **23**, 769-789
205. White, J. F., and Grisshammer, R. (2010) Stability of the neurotensin receptor NTS1 free in detergent solution and immobilized to affinity resin. *PLoS One* **5**, e12579
206. Zhou, H. X., and Cross, T. A. (2013) Influences of membrane mimetic environments on membrane protein structures. *Annu Rev Biophys* **42**, 361-392
207. Murray, D. T., Griffin, J., and Cross, T. A. (2014) Detergent optimized membrane protein reconstitution in liposomes for solid state NMR. *Biochemistry* **53**, 2454-2463
208. Zoonens, M., Comer, J., Masscheleyn, S., Pebay-Peyroula, E., Chipot, C., Miroux, B., and Dehez, F. (2013) Dangerous liaisons between detergents and membrane proteins. The case of mitochondrial uncoupling protein 2. *J Am Chem Soc* **135**, 15174-15182
209. Fuller, N., and Rand, R. P. (2001) The influence of lysolipids on the spontaneous curvature and bending elasticity of phospholipid membranes. *Biophys J* **81**, 243-254
210. Henriksen, J. R., Andresen, T. L., Feldborg, L. N., Duelund, L., and Ipsen, J. H. (2010) Understanding detergent effects on lipid membranes: a model study of lysolipids. *Biophys J* **98**, 2199-2205
211. Stiasny, K., and Heinz, F. X. (2004) Effect of membrane curvature-modifying lipids on membrane fusion by tick-borne encephalitis virus. *J Virol* **78**, 8536-8542
212. Chernomordik, L. V., Vogel, S. S., Sokoloff, A., Onaran, H. O., Leikina, E. A., and Zimmerberg, J. (1993) Lysolipids reversibly inhibit Ca(2+)-, GTP- and pH-dependent fusion of biological membranes. *FEBS Lett* **318**, 71-76

5. Curriculum Vitae

Personal Data

Name	Kerstin Kanonenberg
Date of birth	30 March 1988
Place of birth	Cologne, Germany

University Education

10/2012 – 11/2018	Doctorate Heinrich-Heine-Universität Düsseldorf, Institute of Biochemistry, Prof. Dr. Lutz Schmitt. „Functional Characterisation of the Haemolysin A type I secretion system from <i>Escherichia coli</i> “.
10/2010 – 09/2012	Master of Science Biochemistry (grade 1.6) Heinrich-Heine-Universität Düsseldorf, Institute of Biochemistry, Prof. Dr. Lutz Schmitt. „Functional Reconstitution of a Type I Secretion System“ (grade 1.0).
07/2011 – 12/2011	Biomedical Sciences, Victoria University Wellington, New Zealand (Master courses).
10/2007 – 09/2010	Bachelor of Science Biochemistry (grade 1.8) Heinrich-Heine-University Düsseldorf, Institute of Plant Biochemistry, Prof. Dr. Andreas P.M. Weber „Functional characterisation of novel plant proteins“ (grade 1.0).

School Education

08/1998 – 06/2007	General qualification for university entrance (Abitur), grade 1.3 Heinrich-Heine-Gymnasium, Cologne
07/2004 – 06/2005	St. Catherine's College, Wellington, New Zealand

Awards and Scholarships

2018	Poster Prize GBM Transport Colloquium, Rauischholzhausen, Germany
2015	The FEBS Journal Poster Prize, 40 th FEBS Congress Berlin, Germany
2014	ABC2014 Student Fellowship, 5 th FEBS Special Meeting on ATP-Binding Cassette (ABC) Proteins, Innsbruck, Austria

Conferences Attended

2018	11 th Transporter Colloquium, Rauischholzhausen, Germany (poster presentation)
2017	Gordon Research Seminar and Conference: Mechanisms of Membrane Transport, New London, NH, United States (poster presentation)
2016	6 th Special Meeting on ATP-Binding Cassette (ABC) Proteins, Innsbruck, Austria (poster presentation)
2015	40 th FEBS Congress “The Biochemical Basis of Life“, Berlin, Germany (oral and poster presentation)
2014	5 th Special Meeting on ATP-Binding Cassette (ABC) Proteins, Innsbruck, Austria (oral and poster presentation)
2013	Molecular Life Science 2013 – Herbsttagung der GBM, Frankfurt, Germany (poster presentation)

List of Publications

Kanonenberg, K., Spitz, O., Erenburg, I. N., Beer, T., and Schmitt, L. (2018) Type I secretion system-it takes three and a substrate. *FEMS Microbiol Lett* 365

Holland, I. B., Peherstorfer, S., Kanonenberg, K., Lenders, M., Reimann, S., and Schmitt, L. (2016) Type I Protein Secretion-Deceptively Simple yet with a Wide Range of Mechanistic Variability across the Family. *EcoSal Plus* 7

Reimann, S., Poschmann, G., Kanonenberg, K., Stuhler, K., Smits, S. H., and Schmitt, L. (2016) Interdomain regulation of the ATPase activity of the ABC transporter haemolysin B from *Escherichia coli*. *Biochem J* 473, 2471-2483

Kanonenberg, K., Schwarz, C. K., and Schmitt, L. (2013) Type I secretion systems - a story of appendices. *Res Microbiol* 164, 596-604

Rosar, C., Kanonenberg, K., Nanda, A. M., Mielewczik, M., Brautigam, A., Novak, O., Strnad, M., Walter, A., and Weber, A. P. (2012) The leaf reticulate mutant *dov1* is impaired in the first step of purine metabolism. *Mol Plant* 5, 1227-1241

6. Acknowledgements

Mein höchster und besonderer Dank gilt Prof. Dr. Lutz Schmitt. Vielen Dank, dass Du mir die Möglichkeit gegeben hast, meine Masterarbeit und die anschließende Promotion in Deinem Institut durchzuführen. Danke, dass Du mich in dieser Zeit stets unterstützt hast und ideale Voraussetzungen geschaffen hast, mich selbst in meiner Arbeit zu verwirklichen. Die Möglichkeit, unzählige Konferenzen und Seminare im In- und Ausland zu besuchen und der daraus resultierende rege wissenschaftliche Austausch haben mich sehr in meinem Beschluss bestärkt in der akademischen Forschung zu bleiben. Mein ganz besonderer Dank für Deinen unerschütterlichen Optimismus, selbst bei wirklich grenzwertig schlechter Datenlage, ohne den ich wohl so einige Male aufgegeben hätte. Danke für die zusätzliche Unterstützung in der Endphase meiner Promotion und beim Schreiben meines ersten "richtigen" Antrags. Danke für die fundierte Ausbildung in so vielen Teilbereichen der Biochemie, mit der ich mich gut gerüstet fühle nun eigene Wege zu gehen. Lutz, ich danke Dir für diese unvergessliche Zeit!

Ebenso danken möchte ich Dr. Sander Smits. Auch wenn man sie nicht unbedingt immer gerne hört, ist fundierte Kritik doch ebenso wichtig für das Weiterkommen wie Optimismus und Zuversicht. Ich möchte Dir von Herzen dafür danken mir (zugegebenermaßen, manchmal doch recht schonungslos) die Schwachstellen in meine Daten und Argumentationen aufgezeigt zu haben. Dies regte nicht nur viele Male zum Nachdenken an, sondern half auch sehr bei der persönlichen Weiterentwicklung und Lösungsfindung. Vielen Dank für deine Unterstützung und Hilfe, das Ziel nicht aus den Augen zu verlieren. Danke für die vielen Korrekturen und Feedbacks, die ich sehr geschätzt habe!

Großer Dank gebührt auch PD Dr. Ulrich Schulte. Vom „gefürchteten Herrn Schulte“ während meiner Bachelor- und Masterzeit zum „Uli“ der Promotionszeit – Du hast mich während meines gesamten Studiums in Düsseldorf begleitet. Vielen Dank für Deine Gelassenheit und unkompliziert Art Probleme anzugehen und zu lösen.

Mein besonderer Dank gilt Prof. Dr. Andreas Weber zum einen für die Übernahme des Korreferats dieser Arbeit, zum anderen für die Möglichkeit, schon früh während meines

Studiums erste wissenschaftliche Erfahrungen als HiWi, sowie während der anschließenden Bachelorarbeit in Ihrem Institut sammeln zu können.

Ein riesiger Dank geht an Frau Blum, „the one and only“, wenn es um Formulare, Anfragen, Rechnungen und anderen lästigen Papierkram geht. Ihre Hilfe hat mich sehr viel Zeit und Nerven gespart.

Bedanken möchte ich mich besonders bei Jens Reiners, der mir über die Jahre als Kollege ein lieber Freund geworden ist. Vielen Dank für die ungezählten Kaffeepausen und das Teilen einer großen Leidenschaft: essen in der Schweinemensa! Vielen Dank, dass du immer für mich da warst, für die vielen technischen Tipps und Kniffe. Für die abendlichen Burgersessions. Für die spätabendliche Pizza im Institut, wenn die Experimente mal wieder ungeplant länger dauerten. Für das Nachhausefahren, wenn der letzte Zug schon weg war, für die tiefsinnigen und manchmal weniger tiefsinnigen Gespräche.. die Liste könnte ich noch ewig so weiterführen! Vielen Dank für alles, bleib so wie du bist – und HA! Ich bin doch vor dir fertig.

Vielen Dank an die ehemaligen und jetzigen „Leidensgenossen“ auf dem Typ I Sekretionsprojekt. Dr. Michael Lenders, Dr. Sven Reimann, Tobias Beer, Olivia Spitz, Isabell Ehrenburg – vielen Dank für die anregenden und konstruktiven Diskussionen und wissenschaftliches Feedback. Für euren weiteren wissenschaftlichen Werdegang wünsche ich euch alles Gute und viel Erfolg.

Dr. Sakshi Khosa, thank you for sharing so many late-night working sessions with me. Thanks for helping me with anything concerning crystallisation trials and introducing me to the magic of hanging drops – I'll never forget your phone call when you told me about my first crystals! I wish you all the best for the future and your scientific career, I know you'll do great!

I would like to thank the latest members of the institute, the AG Kedrov: Jun.-Prof. Dr. Alexej Kedrov, Athanasios (aka Anasthasius) Papadopoulos, Michael Kamel and Maryna Löwe. Thank you for the short but nice company and stimulating discussions. Alexej, many thanks for the data for our superbugs paper, this was really much appreciated!

Danken möchte ich Dr. Diana Kleinschrodt und Iris Fey für die “DNA-magic” und sämtliche Hilfestellungen für alles, was mit DNA zu tun hat. Ihr habt es einfach drauf, danke!

Ich möchte mich ganz herzlich bei Dr. Alexander Minges bedanken: für einige epische Synchrotontrips und die interessante Erfahrung, was 42 Stunden Wachsein so alles bewirkt („Das ist Schinken, ich wollte Käse.“ „Aber du hast Schinken bestellt..?“ „Echt? Aber Käse gedacht!“). Vielen Dank für die Hilfestellung bei meinen ersten Gehversuchen im Bereich der Fed-Batch Fermentation und das legendäre PAN-Rezept!

Bedanken möchte ich mich auch besonders bei Martina Wesemann, die den Laden hier so gut im Griff hat und ohne die einfach nichts funktionieren würde. Vielen Dank für alles!

Meinen besonderen Dank möchte ich Dr. Nils Hanekop aussprechen, für die Betreuung während meiner Masterarbeit und dafür, dass du mich zum Bleiben bewegt hast. Zudem möchte ich Dr. Christian Schwarz für viele anregende wissenschaftliche Diskussionen danken.

Bedanken möchte ich mich bei meinen Bürokolleginnen Kalpana Shanmugarajah, Katharina Gräfe, Zohreh Pourhassan Najafabadi, Silke Mavaro und bei allen anderen Institutskollegen und –Kolleginnen: Marcel Lagedroste, Tim Kroll, Julia Zäschke-Kriesche, Martin Prescher, Katja Döhl – vielen Dank für die angenehme Arbeitsatmosphäre und zahlreichen anregenden Diskussionen. Ich wünsche euch weiterhin viel Erfolg und Durchhaltevermögen!

Bedanken möchte ich mich beim SFB1208 für die finanzielle Unterstützung und zahlreiche interessante Veranstaltungen und Vorträge. Hierbei ist besonders Dr. Cordula Kruse zu erwähnen – danke für die tolle Organisation!

Zum Schluss möchte ich in ganz besonderem Maße meinen Freunden und meiner Familie danken, die mich in der ganzen Zeit so toll unterstützt haben. Danke für die bedingungslose Unterstützung und für den Rückhalt während meiner Promotionszeit.

Le plus grand merci à mon époux Jean-François. Merci pour ton support, ton amour et de m'avoir apprivoisé. Passer sa vie avec une scientifique passionnée, ce n'est pas toujours facile.. Merci!

7. Declaration

Ich versichere an Eides Statt, dass die Dissertation von mir selbständig und ohne unzulässige fremde Hilfe unter Beachtung der „Grundsätze zur Sicherung guter wissenschaftlicher Praxis an der Heinrich-Heine-Universität Düsseldorf“ erstellt worden ist. Die Dissertation wurde in der vorgelegten oder in ähnlicher Form noch bei keiner anderen Fakultät eingereicht. Ich habe bisher keine erfolglosen und erfolgreichen Promotionsversuche unternommen.

(Ort, Datum)

(Kerstin Kanonenberg)